UNIVERSITA' DEGLI STUDI DI PADOVA

Dipartimento di Scienze Biomediche Sperimentali

Dottorato di ricerca in
BIOSCIENZE, indirizzo NEUROBIOLOGIA
CICLO XX

OPA1, a mitochondrial pro-fusion protein, regulates the *cristae* remodelling pathway during apoptosis

Direttore della Scuola : Ch.mo Prof. Tullio Pozzan
Supervisore: Dott. Luca Scorrano

Dottorando: Christian Frezza

31 Gennaio 2008

Table of contents

1 Riassunto dell'attività svolta

I mitocondri sono organelli essenziali per la vita della cellula essendo la principale fonte di ATP, molecola chiave per moltissime reazioni endoergoniche.
Recentemente è stato dimostrato che i mitocondri hanno un ruolo cruciale in molti processi cellulari, dalla regolazione delle vie di segnale del calcio alla morte cellulare programmata.
In seguito ad uno stimolo apoptotico i mitocondri rilasciano citocromo *c* e altre proteine solubili nello spazio intermembrana che sono necessarie, nel citoplasma, per l'attivazione e l'amplificazione della cascata di segnale che porta al disassemblamento della cellula.
Il rilascio di citocromo *c* è un evento precoce nel processo apoptotico completo e veloce, ed *in vivo* non è associato a rigonfiamento mitocondriale (swelling). Grazie ai notevoli sviluppi della microscopia elettronica associata a ricostruzione tridimensionale il modello di ultrastruttura dei mitocondri è stato recentemente rivoluzionato; le *cristae*, dapprima identificate come semplici invaginazioni della membrana mitocondriale interna (IMM) (Palade, 1952), risultano essere compartimenti distinti di IMM, separati dallo spazio intermembrana da giunzioni tubulari strette definite *cristae junctions* (Mannella et al., 1994). La maggior parte del citocromo *c* e dei componenti della fosforilazione ossidativa sono localizzati all'interno delle *cristae*. Per garantire un completo rilascio di citocromo *c* indipendente da swelling mitocondriale le singole *cristae* si fondono tra di loro e le giunzioni tubulari strette si allargano: questo processo, noto con il nome di *cristae* remodelling, è associato alla mobilizzazione del citocromo *c* dal compartimento intra-cristale allo spazio intermembrana, evento necessario per il suo successivo rilascio attraverso la membrana mitocondriale esterna (OMM) (Scorrano et al., 2002). Il meccanismo molecolare alla base di questo processo non è attualmente noto e nel laboratorio dove ho svolto la mia tesi di dottorato è stato ipotizzato che OPA1, l'unica proteina appartenente alla famiglia delle dinamine localizzata nella IMM attualmente conosciuta (Alexander et al., 2000; Delettre et al., 2000) potesse partecipare al controllo del rimodellamento delle *cristae*. La famiglia delle proteine simili a dinamine è costituita da un numero crescente di proteine che regolano la morfologia del reticolo mitocondriale, controllando l'equilibrio tra eventi di fissione e fusione dell'organello. A questa famiglia appartengono le mitofusine (MFN) 1 e 2 nella membrana esterna e OPA1 nella membrana mitocondriale interna. OPA1 è una GTPasi ad alto peso molecolare ancorata alla membrana mitocondriale interna ed affacciata allo spazio intermembrana (Olichon et al., 2002; Satoh et al., 2003). Studi effettuati in lievito hanno evidenziato che il suo ortologo Mgm1p è necessario per il mantenimento della fusione mitocondriale, attraverso la cooperazione con una proteina dinamina-simile localizzata nella OMM e chiamata Fzo1p; studi condotti nel nostro laboratorio hanno osservato che in mammifero OPA1 promuove la fusione del reticolo mitocondriale mediante una dei due

ortologhi in mammifero di Fzo1p MFN1. Nel 2000 in due laboratori distinti è stato osservato che mutazioni nel gene codificante per OPA1 sono la causa di una malattia neurodegenerativa della retina, l'atrofia ottica dominante (ADOA) caratterizzata dalla morte selettiva di una sottopopolazione cellulare retinica, le cellule gangliari (RGC). Il fatto che mutazioni in una proteina mitocondriale coinvolta nella regolazione della dinamica mitocondriale causassero morte cellulare ha aperto un nuovo scenario che corrobora la posizione centrale del mitocondrio nel controllare la risposta apoptotica. Scopo della mia tesi di dottorato è stato quello di analizzare il ruolo di OPA1 nella via mitocondriale di morte cellulare. Abbiamo iniziato il nostro studio con un approccio diretto al problema: abbiamo sovraespresso OPA1 in modo transiente in una linea cellulare, i fibroblasti embrionali di topo (MEFs) e misurato la vitalità cellulare in seguito all'incubazione con stimoli proapototici intrinseci, che reclutano la via mitocondriale di morte. La sovraespressione transiente di OPA1, ma non di mutanti nel sito GTPasico OPA1^{K301A} o privi della parte C-terminale della proteina OPA1^{R905*} è in grado di proteggere da morte indotta da perossido di idrogeno, staurosporina, etoposide e sovraespressione di BID, una proteina proapoptotica della famiglia di Bcl-2 che induce rimodellamento delle *cristae*. Per confermare che la sovraespressione di OPA1 si estrinsecasse a livello mitocondriale abbiamo analizzato due aspetti della disfunzione mitocondriale: il rilascio di citocromo *c* e la caduta di potenziale mitocondriale.

A questo scopo abbiamo sovraespresso una proteina rossa localizzata ai mitocondri (mtRFP) come marcatore del reticolo mitocondriale ed in seguito eseguito un saggio di immunofluorescenza per evidenziare la distribuzione del citocromo *c*; la sovraespressione di OPA1 è in grado di prevenire il rilascio di citocromo *c* indotto da stimoli intrinseci, al contrario della sovraespressione del mutante inattivo OPA1^{K301A} che addirittura accelera la cinetica di rilascio. Abbiamo quindi analizzato un altro aspetto della disfunzione mitocondriale e cioè la perdita del potenziale mitocondriale $\Delta\psi_m$, utilizzando la sonda potenziometrica tetrametil rodamina metilestere (TMRM) la cui fluorescenza mitocondriale è proporzionale al potenziale mitocondriale. La sovraespressione di OPA1, ma non del suo mutante K301A, è in grado di prevenire la depolarizzazione mitocondriale indotta da stimoli intrinseci, confermando che OPA1 previene la morte cellulare a livello mitocondriale, riducendo il rilascio di citocromo *c* e prevenendo la caduta di $\Delta\psi_m$. Come può una proteina che regola la morfologia del reticolo mitocondriale proteggere da apoptosi? Mentre conducevamo i nostri studi, stava emergendo l'ipotesi che in corso di apoptosi il reticolo mitocondriale si frammentasse in modo irreversibile e che questo evento, tanto quanto il processo di *cristae* remodeling, fosse necessario per un rilascio completo di rilascio di citocromo *c*. In linea di principio OPA1 può regolare l'apoptosi ad entrambi questi livelli: stimolando la fusione mitocondriale e quindi controbilanciando l'incipiente frammentazione, oppure regolando il processo di *cristae* remodeling indipendentemente dalla sua azione sulla fusione organellare.

Per capire a che livello OPA1 manifestasse la sua attività antiapoptotica abbiamo utilizzato un approccio genetico, sovraesprimendo OPA1 in cellule *Mfn1*-/-, in cui OPA1 non è in grado di indurre la fusione del reticolo mitocondriale. La sovraespressione di OPA1 in questo genotipo protegge da apoptosi indotta da stimoli intrinseci; poiché una residua attività profusogena poteva essere mediata da MFN2, abbiamo ripetuto lo stesso esperimento in cellule in cui erano state ablate entrambe le mitofusine (DMF). Anche in queste condizioni, la sovraespressione di OPA1 protegge da apoptosi a livello mitocondriale, rallentando la cinetica di rilascio di citocromo *c.* OPA1, quindi, ha un'attività antiapoptotica indipendente dalla sua attività profusogena del reticolo mitocondriale.

A questo punto ci siamo chiesti se OPA1 avesse un ruolo nel processo di rimodellamento delle *cristae* durante apoptosi. Abbiamo quindi generato delle linee cellulari che sovraesprimessero in modo stabile OPA1 ed il suo mutante $OPA1^{K301A}$ e una linea stabile in cui i livelli di OPA1 fossero stati ridotti mediante short hairpin RNA interference (shOPA1). Abbiamo isolato i mitocondri e misurato le cinetiche di rilascio di citocromo *c* indotto da BID ricombinante tagliato da caspasi 8 (cBID) mediante un saggio ELISA specifico. La sovraespressione stabile di OPA1 è in grado di rallentare il rilascio di citocromo *c* in modo indipendente da MFN1, mentre il suo silenziamento causa una notevole accelerazione della cinetica di rilascio. Utilizzando un saggio specifico, abbiamo osservato che OPA1 è in grado di prevenire la mobilizzazione di citocromo *c* dalle *cristae* in modo indipendente da MFN. Questi risultati sono stati confermati dal fatto che la sovraespressione del mutante $OPA1^{K301A}$ provoca un incremento di mobilizzazione, quasi totale quando i livelli di OPA1 vengono ridotti. Un'approfondita analisi morfometrica di mitocondri isolati da queste linee stabili, associata ad uno studio tomografico con ricostruzione tridimensionale ha rivelato che OPA1 è controlla la morfologia delle *cristae* e previene l'apertura delle giunzioni tubulari strette in risposta a cBID.

Per cercare di comprendere il meccanismo molecolare attraverso il quale OPA1 regola la morfologia delle *cristae* ed il diametro delle giunzioni tubolari strette, ci siamo basati sulla possibile analogia con i processi di vescicolazione mediati dalla dinamina citosolica, che partecipa per esempio alla produzione delle vescicole endocitotiche oligomerizzando sul collo della vescicola nascente. L'attività GTPasica della dinamina porta poi alla costrizione meccanoenzimatica del collo della vescicola. D'altra parte, OPA1, a differenza della dinamina, non si trova all'esterno della membrana biologica che deve tubulare, ma al suo interno, ponendo quindi un problema fondamentale a questo possibile modello di funzionamento di OPA1. Abbiamo quindi cercato innanzitutto di analizzare le caratteristiche biochimiche di OPA1. Studi di gel filtrazione hanno evidenziato che OPA1 si trova in frazioni ad alto peso molecolare (>600 KDa) e che in seguito all'incubazione con cBID, scompare dalle frazioni a più alto peso molecolare. Studi paralleli effettuati nel nostro laboratorio hanno inoltre evidenziato che OPA1 può essere processata da una proteasi romboide, nota come PARL, per dare origine ad una forma solubile nello spazio intermembrana, responsabile dalla funzione antiapoptotica ma non

della funzione profusogena di OPA1. Abbiamo quindi ipotizzato che OPA1 si potesse organizzare in oligomeri formati sia dalla proteina legata alla IMM che da quella solubile generata da PARL. Per confermare questa ipotesi abbiamo eseguito un esperimento di crosslinking, grazie al quale abbiamo confermato la presenza di una banda immunoreattiva per OPA1 ad alto peso molecolare che scompare quando la struttura delle *cristae* viene persa a seguito di rigonfiamento osmotico dei mitocondri. Questo oligomero stabilizzato dal crosslinkante contiene tanto la forma solubile, quanto quella legata alla IMM di OPA1, come confermato dalla sua immuoreattività per entrambe le forme di OPA1 opportunamente marcate e co-espresse.
L'oligomero immumoreattivo per OPA1 viene distrutto da cBID in modo dipendente dal tempo e la sovraespressione di OPA1 lo stabilizza. Possiamo quindi concludere che OPA1 controlla la mobilizzazione di citocromo *c* e il rimodellamento delle *cristae* in corso di apoptosi. Questa funzione di OPA1 è indipendente dal suo ruolo profusogeno ed è correlata alla stabilità di complessi ad alto peso molecolare contenenti OPA1 legata alla membrana e solubile nello spazio intermembrana.

I nostri dati sulla funzione antiapoptotica di OPA1 nel rimodellamento delle *cristae* pongono tutta una serie di domande. Innanzitutto, non è assolutamente chiara la natura e la composizione dei complessi contenti OPA1, in mitocondri normali e apoptotici. Per questo abbiamo messo a punto una serie di approcci biochimici volti a identificare i complessi contenenti OPA1 in mitocondri normali ed apoptotici isolati da cellule con diverso background genetico. L'analisi proteomica delle molecole rinvenute in complesso con OPA1 ci consentirà di comprendere regolazione e funzione dei complessi, prima e dopo l'induzione di morte.
In secondo luogo, visto che OPA1 sembra rivestire un ruolo cardine nel processo apoptotico e che OPA1 è significativamente sovraespressa in alcune forme di tumore del polmone (Dean Fennel, comunicazione personale), ci siamo chiesti se OPA1 potesse essere un bersaglio per nuovi farmaci che possono aumentare la morte cellulare programmata in cellule tumorali.. A questo scopo, in collaborazione con il professor Stefano Moro del dipartimento di Chimica Farmaceutica dell'Università di Padova, stiamo testando una libreria di possibili inibitori di OPA1 generata in seguito ad uno screening *in silico* di composti indirizzati alla tasca GTPasica di OPA1 ottenuta per *homology modeling* usando come *template* il dominio GTPasico di dynamin A di *Dyctiostelyum Discoideum*.

In conclusione, i dati presentati in questa tesi di dottorato dimostrano che la proteina mitocondriale OPA1 partecipa alla regolazione della mobilizzazione di citocromo *c* e al rimodellamento delle *cristae* in corso di apoptosi. Abbiamo dimostrato che OPA1 forma complessi oligomerici ad alto peso molecolare la cui distruzione correla con il rimodellamento delle *cristae*. Questa funzione può essere distinta dal ruolo di OPA1 nel controllo della fusione

mitocondriale, lasciando intuire una specializzazione di questa proteina simile a dinamina nel corso dell’evoluzione.

2 Summary

Mitochondria are essential organelles for the life of the cells since it is the major source of ATP, key molecule for many endoergonic reaction.

Recently it has been demonstrated that mitochondrial play a key role in many other cellular processes like Ca^{2+} signaling and programmed cell death.

Following an apoptotic insult mitochondria release cytochrome *c* and other proteins required in the cytosol for the activation of the effector caspases required for cell demise.

What is remarkable about cytochrome *c* release is that is fast, complete and usually is not associated with mitochondrial swelling. Thanks to the advances in 3D electron microscopy it has been demonstrated that *cristae* are not just invagination of the inner mitochondrial membrane (IMM) as previously depicted by Palade (Palade, 1952) but rather distinct compartments of it, separated from the inter membrane space (IMS) by tubular narrow *cristae* junctions. The majority of cytochrome *c* and the other respiratory chain components are restricted in this compartment. To reach a complete cytochrome *c* release in the absence of mitochondrial swelling mitochondria remodel their internal structure: individual *cristae* fuse and tubular narrow *cristae* junctions widen; this process, defined *cristae* remodeling is associated with the mobilization of cytochrome *c* towards the IMS for its subsequent release across the outer mitochondrial membrane (OMM) (Scorrano et al., 2002). The molecular mechanism beyond this dynamic process is not well understood and in the laboratory where I did my doctoral Thesis it has been hypothesized that OPA1, the only dynamin related protein of the IMM (Alexander et al., 2000; Delettre et al., 2000) could control *cristae* remodeling. Dynamin related proteins are regulators of mitochondrial morphology promoting mitochondrial fusion and fission. To this family belong Mitofusins (MFN) 1 and 2 in the OMM and OPA1 that resides in the IMM. OPA1 is a large GTPase anchored in the IMM, facing the IMS (Olichon et al., 2002; Satoh et al., 2003); it has been shown that in yeast, its orhologue Mgm1p is required for fusion competent mitochondria by the cooperation with a protein of the same family on the OMM called Fzo1p. In our laboratory it has been demonstrated that in mammalian cells OPA1 promotes mitochondrial fusion through one of the two mammaliam orthologue of Fzo1p called MFN1.

In 2000 two distinct laboratories demonstrated that mutations in OPA1 gene are the cause of dominant optic atrophy (ADOA), the leading case of inherited blindness in human, characterized by selective death of retinal ganglion cell (RGC) (Alexander et al., 2000; Delettre et al., 2000). The fact the mutation in a mitochondrial protein involved in mitochondrial morphology caused cell death opened a new scenario that corroborates the central position of mitochondria in regulating apoptotic signaling.

The aim of my thesis was to analyze the role of OPA1 in mitochondria-dependent apoptosis.

We started with a brute force approach by overexpressing OPA1 in murine embryonic fibroblasts (MEFs) and measuring cells viability in response to intrinsic apoptotic stimuli that specifically trigger apoptosis through the mitochondrial pathway.

Overexpression of wt OPA1 but not of mutant in the GTPase domain ($OPA1^{K301A}$) or a truncated mutant in the coiled coil domain (OPA^{R905*}) is able to prevent from apoptosis induced by hydrogen peroxide, staurosporine, etoposide and overexpression of tBID, a BH3 only protein of the Bcl-2 family that promotes *cristae* remodeling. To confirm that OPA1 antiapoptotic activity was exerted at the mitochondrial level we analyzed two aspects of the mitochondrial dysfunction: cytochrome *c* release and mitochondrial depolarization.

To this aim we overexpressed a mitochondrially targeted red fluorescent protein (mtRFP) as marker of the mitochondrial network and then we immunodecorated cytochrome *c* with a FITC-conjugated secondary antibody. OPA1 overexpression prevented cytochrome *c* release in response to intrinsic stimuli while its inactive mutant OPA^{K301A} aggravated cytochrome *c* release kinetic.

We then analyzed another aspect of the mitochondrial dysfunction: mitochondrial depolarization, taking advantage of the potentiometric probe tetramethylrhodamine-methyl ester (TMRM) which mitochondrial fluorescence is proportional to mitochondrial potential. Overexpression of OPA1, but not of its inactive K301A mutant, prevented mitochondrial depolarization induced by intrinsic stimuli, confirming that OPA may prevent from apoptosis at the mitochondrial level by reducing cytochrome *c* release and mitochondrial depolarization. How can a dynamin related protein prevent from apoptosis? We asked this because when our study was ongoing an intriguing hypotesys emerged: during apoptosis mitochondrial network undergoes irreversible massive fragmentation; this event and apoptotic *cristae* remodeling are required for complete cytochrome *c* release. In principle, OPA1 could prevent apoptosis at both of these levels either counteracting mitochondrial fragmentation thanks to its pro-fusion activity or by the regulation of *cristae* remodeling. To understand at which of these levels OPA1 was exerting its antiapototic activity, we started a genetic approach, overexpressing OPA1 in *Mfn1*-/-, where OPA1 pro-fusion activity was prejudiced.

Overexpression of OPA1 in these cells prevented from apoptosis induced by intrinsic stimuli; in view of the fact that a residual pro-fusion activity of OPA1 could be mediated by the presence of MFN2 we repeated the same experiments in cells in which both mitofusins were ablated (DMF). Also in this conditions OPA1 prevented from apoptosis at the mitochondrial level, slowing down cytochrome *c* release kinetic. OPA1 has an antiapoptotica function that is independent of its pro-fusion activity on the mitochondrial network.

At this point we asked whether OPA1 may have a role on apoptotic *cristae* remodeling. We generated stable cell lines that stably overexpressed OPA1 and its K301A mutant both in wt and in *Mfn1*-/- cells and a cell line depleted of OPA1 by short hairpin RNA interference (shOPA1RNAi). We then isolated mitochondria and measured cytochrome *c* release induced by

recombinant caspase 8 cleaved BID (cBID) using a specific ELISA immunoassay. Stable overexpression of OPA1 is able to prevent cytochrome *c* relase independently of MFN1 while its downregulation dramatically increases its release. Using a specific assay we observed that OPA1 is also able to prevent cytochrome *c* mobilization from the *cristae* independently of MFN. These results were confirmed by the fact that overexpression of the $OPA1^{K301A}$ mutant increased cytochrome *c* mobilization that was almost complete when OPA1 levels were depleted by RNAi. A thorough morphometric analysis of isolated mitochondria from these cell lines, associated with 3D reconstruction of electron microscopy tomography, showed that OPA1 controls *cristae* morphology and prevents *cristae* junction widening in response to cBID. To better understand the molecular mechanism through which OPA1 controls *cristae* remodeling and *cristae* junctions diameter we based our hypothesis on the possible analogy with vesciculation processes regulated by cytosolic dynamin, where GTPase activity of it mediated mechanoenzimatic constriction of the vesicle collar. Despite this analogy, we should mention that OPA1, unlike dynamin, is located on the inner side of the membrane to be constricted and not on the outside as dynamin complicating the model. First, we analyzed biochemical characteristic of OPA1: gel filtration studies showed that OPA1 is eluted at very high molecular weight fractions (>600 KDa) and in response to cBID incubation it is retrieved in low molecular weight fractions. Parallel studies in our laboratory demonstrated that OPA1 is processed by a rhomboid protease, PARL, into a short form found soluble in the IMS that is responsible for the antiapototic but not of the pro-fusion activity of OPA1. We therefore reasoned that OPA1 could organize into high molecular weight complexes made up at least by the PARL generated soluble form and the membrane bound form of OPA1. To confirm this hypothesis we crosslinked this complex and confirmed the presence of a high molecular weight immunoreactive band for OPA1 that disappear following the mechanical expansion of the *cristae* induced by osmotic swelling. These crosslinker-stabilized oligomers contain both the soluble and the membrane bound forms of OPA1 as demonstrated by their immunoreactivity for properly tagged and co-expressed forms.

The OPA1-containing oligomers is targeted by cBID in a time dependent manner and OPA1 overexpression stabilizes these complexes. We can conclude that OPA1 controls cytochrome *c* mobilization and *cristae* remodeling that occurs during apoptosis. This function of OPA1 is independent of MFNs and is correlated to the formation of high molecular weight complexes.

The data collected so far on OPA1 antiapoptotic function open a new scenario. First we need to investigate on the molecular composition of these complexes in normal and apoptotic conditions. To this aim we started a biochemical study on OPA1-containing complexes in mitochondria isolated from different genetic background in normal and apoptotic conditions. The proteomic analysis of the proteins eventually found in complex with OPA1 will allow us to

comprehend the function and regulation of OPA1 oligomers before and after cell death induction.

OPA1 appears as a crucial protein in the apoptotic process; as a confirmation of this, it has been found that OPA1 is highly overexpressed in some lung cancer (Dean Fennel, personal communication); we then asked whether OPA1 could be a target for the development of new drugs that enhance apoptosis in tumor cells. To this aim, we started a collaboration with Stefano Moro from the Department of Medicinal Chemistry of the University of Padova, to generate a library of candidate inhibitors of OPA1 performing a virtual screening of compounds targeted to the GTPase pocket of OPA1 obtained following an *homology modeling* on the *Dyctiostelium Discoideum* GTPase domain of Dynamin A.

In conclusion, the data presented in this doctoral thesis show that mitochondrial protein OPA1 participates in the regulation of cytochrome *c* mobilization and *cristae* remodeling during apoptosis. We demonstrated that OPA1 organizes into high molecular weight complexes which disruption correlates with *cristae* junction widening. This function is distinct from its role in mitochondrial morphology and this suggest a bifurcation and specialization of OPA1 function during evolution.

3 Introduction

The term ‘apoptosis’ was first introduced in 1972 by John Kerr to designate common morphological features of programmed cell death (Kerr et al., 1972). In multicellular organisms, apoptosis ensures the precise and orderly elimination of surplus or damaged cells. Cell death during embryonic development is essential for successful organogenesis and crafting of complex multicellular tissues; during adulthood it ensures the maintenance of normal cellular homeostasis.

Mitochondria acquired a central position in the field of programmed cell death when the group of S. Korsmeyer demonstrated that the protein product of the antiapoptotic proto-oncogene Bcl-2 localizes to mitochondria. A few years later, X. Wang and colleagues demonstrated that a protein of the respiratory chain, cytochrome *c*, is crucial in the cytosol to activate the effector caspases (Liu et al., 1996). The same year, several groups demonstrated that Bcl-2 in fact prevents the release of cytochrome *c* and therefore blocks the recruitment of mitochondria in the apoptotic cascade.

Mitochondrial shape is extremely complex, with the organelle bound by two distinct membranes; an higher degree of complexity is found in the ultrastructure of mitochondria where the inner membrane (IMM) is organized in distinct compartments, the peripheral inner membrane and the *cristae* (Frey and Mannella, 2000), defined by several lines of evidence the active site of oxidative phosphorilation (D'Herde et al., 2001; Perotti et al., 1983; Vogel et al., 2006) , separated from the peripheral inner membrane by narrow tubular junctions.

Our laboratory demonstrated that to grant complete cytochrome *c* release, this component of the respiratory chain must relocate from the *cristae* compartment, thanks to the fusion of individual *cristae* and to the widening of the narrow tubular *cristae* junctions (Scorrano et al., 2002).

In the cytosol, mitochondria acquire specialized shape, undergo change in number and intracellular distribution and often reorganize their morphology in response to metabolic needs; mitochondrial morphology is finely regulated by a set of proteins that regulate the balance between fusion and fission of the organelle (Dimmer and Scorrano, 2006). In addition to the ultrastructural changes that participate in the complete release of cytochrome *c,* massive mitochondrial fragmentation appears to be another morphological change that allows the progression of the apoptic cascade (Frank et al., 2001).

In conclusion, *cristae* remodeling and mitochondrial fragmentation seem to be two tightly linked morphological events required for cytochrome *c* release and apoptosis. How these events are linked and regulated during apoptosis, and in particular the molecular mechanisms controlling the remodeling of the *cristae* were largely unknown when we started this Thesis. Our aim has

therefore been to investigate the role of mitochondria-shaping proteins and of OPA1 in particular, in the regulation of *cristae* remodeling.

3.1 Mitochondria at the dawn of the new millennium

Mitochondria are cellular organelles bordered by two distinct membranes. They hold about one tenth of the cellular proteins and, on a weight basis, convert between 10,000 and 50,000 times more energy per second than the sun (Schatz, 2007). The Swiss anatomist Rudolf Albrecht von Koelliker first described them in 1857, calling them sarcosomes; few years later, in 1890, the German pathologist Richard Altman proposed that they were intracellular parasites and eight years later the German microbiologist Carl Benda gave them the name “mitochondria”. In the first half of the last century, the Belgian biochemist Albert Claude isolated them by centrifugation from disrupted cells and showed that they catalyzed respiration: since then mitochondria have been defined as the power plant of the cell. In the following two decades, biochemists tracked down the different parts of this power plant and characterized them, until they mapped the circuit of electrons from NADH and reduced flavins to molecular oxygen in remarkable detail. Peter Mitchell’s chemiosmotic theory (Mitchell and Moyle, 1965) was the compelling fruit of these very intense decades of insight into mitochondrial bioenergetics and granted him the Nobel Prize in Chemistry in 1978.

For two decades thereafter, bioenergetics, in general, and “mitochondriology”, stagnated until an increasing number of evidences showed that mitochondria are highly dynamic players in regulating cell physiology and interestingly, they appeared pivotal in one of the most critical step in cell life: the cell suicide.

3.2 Mitochondrial shape and dynamics

Mitochondrial shape in living cells is very heterogeneous and can range from small spheres to interconnected tubules (Bereiter-Hahn and Voth, 1994). For example, the mitochondria of rat cardiac muscle and diaphragm skeletal muscle appear as isolated ellipses or tubules in embryonic stages but then reorganize into reticular networks in the adult (Bakeeva et al., 1978). The different shapes of mitochondria were already noticed in early times by cytologists who observed this organelle under the light microscope. Noticing that mitochondrial morphology was heterogeneous, they accordingly christened this organelle ‘mitochondrion’, a combination of the Greek words for ‘thread” and “grain’.

The morphological plasticity of mitochondria results from the ability of this organelle to undergo fusion and fission. Real-time imaging reveals that individual mitochondrial tubules continually move back and forth along their long axes on radial tracks. Occasionally, two mitochondrial tubules encounter each other and fuse, end to end or head to side (Bereiter-Hahn and Voth, 1994; Chen et al., 2003). On the other hand, tubules can also undergo fission events, giving rise

to two or more mitochondrial units. It is important to note that mitochondrial fusion and fission are complicated processes, being mitochondria bound by two membranes. Thus, any mechanism of fusion and fission should take into account that the coordinate fusion division of four lipid bilayers is required to complete the process.

3.2.1 Mitochondria-shaping proteins

3.2.1.1 Proteins involved in mitochondrial fusion

3.2.1.1.1 Fzo/Mitofusin-1,-2

Proteins involved in mitochondrial morphology have been discovered in the recent years (Figure 1). The first mediator of mitochondrial fusion to be identified was the *D. melanogaster* Fuzzy onions 1 protein (Fzo1), a large transmembrane (TM) guanosine triphosphatase (GTPase)

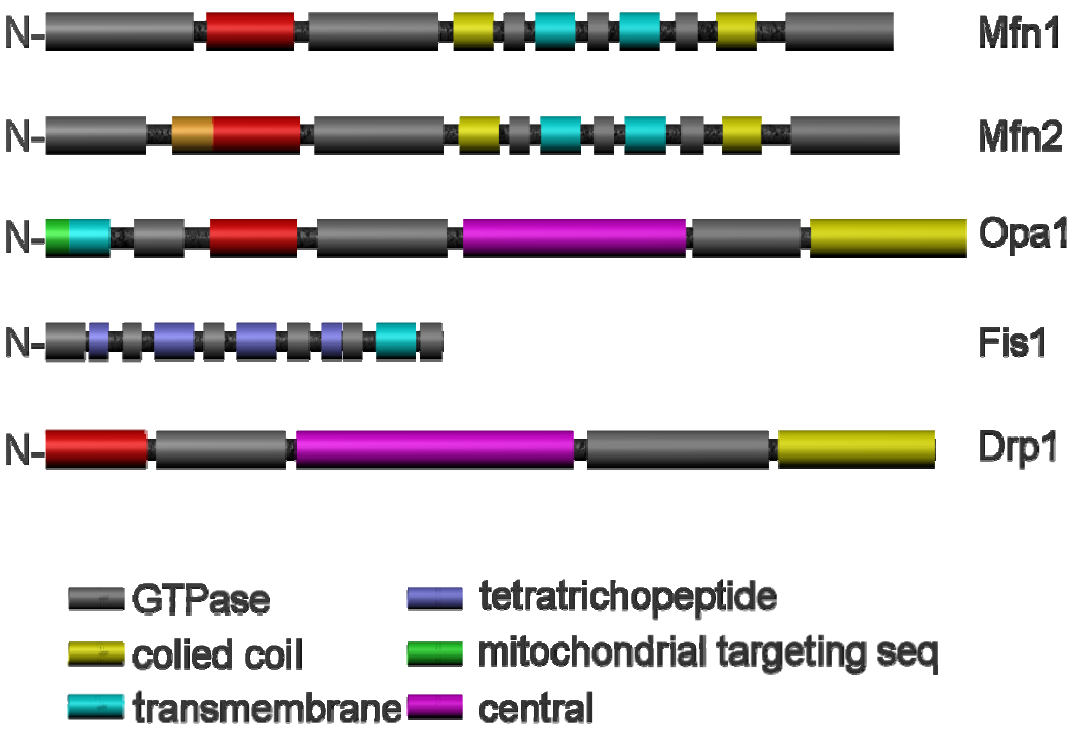

Figure 1 "Core" mammalian mitochondria-shaping proteins.
The figure depicts the individual domains identified in the core components of the pathway regulating mammalian mitochondrial shape. Note that the regulators highlighted in the text are not represented for the sake of clarity.

required for the formation of the giant mitochondrial derivative during spermatogenesis (Hales and Fuller, 1997). The *S. cerevisae* ortholog of Fzo1, called Fzo1p, mediates mitochondrial fusion events during mitotic growth and mating and is required for long-term maintenance of mitochondrial deoxyribonucleic acid (mtDNA) (Hermann et al., 1998). In mammals, two Fzo1p homologues Mitofusin (MFN)-1 and -2, were discovered, both widely expressed in many tissues (Eura et al., 2003; Rojo et al., 2002; Santel et al., 2003); MFN1 and -2 display high (81%) identity, similar topologies and both reside in the OMM (Chen et al., 2003; Legros et al., 2002;

Rojo et al., 2002; Santel et al., 2003; Santel and Fuller, 2001). They also possess a GTPase domain and a coiled coil domain located at the N-terminus of the proteins, protruding towards the cytosol. Two TM regions form a U-shaped membrane anchor, ending in a cytosolic, C-terminal coiled coil motif (Rojo et al., 2002; Koshiba et al., 2004; Santel, 2006). The coiled coil is a widespread helical structural motif functioning as oligomerization domain (Oakley and Hollenbeck, 2001). In the case of MFNs, two molecules on opposing membranes can bind in *trans* to bridge mitochondria, maintaining a distance of 95 Å between the two membranes (Koshiba et al., 2004). Moreover, MFN2 possesses a p21ras-binding domain at its N-terminal, which is not retrieved in MFN1 (Chen et al., 2004). *In silico* analysis of MFN2 reveals that this protein also has a proline-rich-domain between aminoacids 576 and 590 which is poorly conserved in MFN1 and Fzo1p. Proline-rich domains are involved in the binding to other proteins (Kay et al., 2000).

It has been recently reported that MFN2 forms high molecular weight complexes with stomatin-like protein 2 (Stoml2), a novel protein associated to the IM, facing the IMS. The function of this protein remains still unknown, however the protein does not seem to have a role in regulating mitochondrial morphology (Hajek et al., 2007).

The two mitofusins seem to play differential roles during mitochondrial fusion. Direct measurement of mitochondrial fusion rates in *Mfn1*-/- and *Mfn2*-/- cells showed that cells containing only MFN1 retain more fusion activity than those that contain only MFN2 (Chen et al., 2003). A number of other experimental evidences strengthened this experimental observation: MFN1 mediates GTP-dependent tethering of mitochondria more efficiently than MFN2 and its GTPase activity is higher than that of MFN2, even if MFN2 has a greater affinity for GTP (Ishihara et al., 2004; Neuspiel et al., 2005). Finally, MFN1 but not MFN2 is essential for OPA1-mediated mitochondrial fusion (Cipolat et al., 2004). Extending these cell biological observations, genetic ablation of the two genes in the mouse does not result in the same phenotype: *Mfn1*-/- mice die in midgestation, while *Mfn2*-/- embryos display deficient placentation. Overall, these observations suggest that if MFNs can obviously share a common role in mitochondrial fusion, they appear to probably regulate this process in different manners and to have additional functions. In particular, increasing experimental evidence is mounting on the role of MFN2 in different pathological and physiological conditions, ranging from diabetes (Bach et al., 2003; Bach et al., 2005), to vascular proliferative diseases (Chen et al., 2004).

3.2.1.1.2 Mgm1p/Msp1p/OPA1

Optic atrophy 1 (OPA1) is a dynamin-related protein located in the IMM. Mgm1p, the yeast homologue of OPA1, has been identified in a genetic screen for nuclear genes required for the maintenance of mtDNA in the budding yeast *S. Cerevisae* (Jones and Fangman, 1992). Years later, Pelloquin and colleagues isolated Msp1p, the *S. Pombe* orthologue (Pelloquin et al., 1999). The human gene OPA1 was identified in 2000 by two independent groups (Alexander et

al., 2000; Delettre et al., 2000). A more detailed analysis showed that Mgm1p, Msp1p and OPA1 are localized in the IMS, tightly associated with the IMM (Cortopassi and Wong, 1999; Sesaki et al., 2003; Wong et al., 2003). These proteins, albeit they display a sequence identity of approximately 20%, maintain a highly conserved secondary structure, consisting of two predicted coiled coils, one N-terminal to the GTPase domain and the other at the C-terminus. The C-terminal coiled coil domain of OPA1 may function as a GTPase effector domain (GED) (for a schematic of OPA1 topology see Figure 1). On its N-terminal, OPA1 possesses a mitochondrial targeting sequence that targets the protein to mitochondria (Satoh et al., 2003). Studies in yeast show that MTS of Mgm1p is cleaved by the mitochondrial processing peptidase (MPP) upon import (Satoh et al., 2003). The functional analysis of Mgm1p and Msp1p reveals that both proteins are required for the maintenance of fusion-competent mitochondria in *S. cerevisae* and *pombe*. Mgm1p forms a complex together with Fzo1p which participates in the coordinated fusion of the IMM and OMM (Wong et al., 2003). The high degree of secondary structure conservation suggests that the function of OPA1 is conserved in mammals. On the other hand, it was less clear whether OPA1 played a role in fission, or in fusion of mitochondria, since high levels of OPA1 can drive fragmentation of the mitochondrial reticulum (Griparic et al., 2004; Misaka et al., 2002; Olichon et al., 2003). However in our laboratory we unequivocally showed that a linear relationship between OPA1 levels and mitochondrial fusion exists, as overexpression of OPA1 enhances fusion, while its downregulation by siRNA represses it in mouse embryonic fibroblasts (Cipolat et al., 2004).

We will discuss in detailed and separated chapters the role of OPA1 in disease (3.3.1), the regulation of OPA1 function by processing (3.2.2.4.5) and the role of OPA1 in mitochondria dependent apoptosis (3.4.4.3.4).

3.2.1.2 Proteins involved in mitochondrial fission

3.2.1.2.1 Dnm1p/DLP1/DRP1

The two proteins FIS1 and DRP1 (Figure 1) are required for mitochondrial fission in mammals. Dynamin is a large GTPase that participates in membrane scission in multiple endocytic and secretory organelles (Praefcke and McMahon, 2004). The dynamin-like-proteins Dlp1p in yeast, DRP-1 in *C. elegans*, and DLP1/DRP1 in mammals are homologues. DRP1 exists largely in a cytosolic pool, but a fraction is found in spots on mitochondria at sites of constriction (Labrousse et al., 1999; Smirnova et al., 2001). DRP1 contains a dynamin-like-central domain and a C-terminal GTPase effector domain (GED), in addition to its N-terminal GTPase. Intramolecular interaction between the GTPase and GED regions appear to be required for full GTPase activities at fission sites (Zhu et al., 2004). DRP1 can oligomerize, *in vitro*, into ring-like structures and intermolecular oligomerization is observed at membrane constriction sites. Given

these similarities with dynamin, DRP1 has been proposed to couple GTP hydrolysis with mitochondrial membrane constriction and fission (Hinshaw, 1999; Smirnova et al., 2001).

3.2.1.2.2 Fis1p/hFis1

FIS1 is an outer membrane protein evenly distributed on the surface of mitochondria (James et al., 2003). Its N-terminal domain is exposed to the cytoplasm and forms a tetratricopeptide (TPR)-like fold (Suzuki et al., 2003). The C-terminal domain of FIS1 possesses a predicted TM domain and a short stretch of aminoacids facing the IMS (Figure 1). FIS1 is thought to recruit DRP1 to punctuate structures on mitochondria during mitochondrial fusion. It is therefore considered the limiting factor in the fission reaction (Stojanovski et al., 2004). During assembly of the yeast mitochondrial fission complex, the outer membrane protein Fis1 recruits the dynamin-related GTPase Dnm1p to mitochondria. Despite being earlier controversial, this direct physical interaction has been recently confirmed (Wells et al., 2007); in addition, genetic and biochemical studies indicate that both binding interfaces of the TPR of Fis1p are important for binding of two adaptors Mdv1p and Caf4p to Fis1p and for mitochondrial fission activity *in vivo* ((Zhang and Chan, 2007). Moreover, it has been shown that the N-terminal Fis1p arm acts in an autoinhibitory manner to regulate access to a binding pocket that is evolutionarily conserved for binding the dynamin-like GTPase Dnm1p (Wells et al., 2007). It can be speculated that this autoinhibitory function of the Fis1p arm is conserved also in mammalian cells and regulate binding of Fis1 with Drp1

3.2.1.2.3 Endophilin B1

Endophilin B1 has recently been reported to be required for the maintenance of mitochondrial morphology in mammalian cells, especially for the remodelling of the OMM (Karbowski et al., 2004b). Endophilin B1 partially colocalizes and cofractionates with mitochondria and its downregulation by siRNA leads to changes in mitochondrial shape, as well as the formation of OMM-bound structures resembling those formed by vesicles in neuronal terminals after inactivation of endophilin 1. Members of the endophilin family, which are all bin-amphiphysin-rvs(BAR)-domain proteins (like for example amphiphysin and endophilin 1), are supposed to participate in the regulation of membrane curvature, a process required for membrane scission during dynamin mediated endocytosis (Gallop et al., 2006). However the mechanism by which BAR-domain proteins and related components regulate membrane scission has recently been questioned. First, it has been proposed that BAR-domain proteins have an acyl transferase activity that promotes membrane fission. Acyl transferases add a fatty acyl chain (inverted-cone shaped lipid) to a lyso-glycerolipid (cone shaped lipid), thereby altering membrane curvature from positive to negative (Schmidt et al., 1999). Later studies by the laboratory of H. McMahon demonstrated that BAR-domain proteins have no fatty acyl transferase activity as previously believed (Gallop et al., 2005). The amphipathic helices of BAR domains alter membrane

curvature by inserting into the phospholipids bilayers and not by displaying a fatty acyl transferase activity (Gallop et al., 2006; Gallop and McMahon, 2005). Similarly, endophilin B1 seems to participate in the control of the morphology of OMM by altering membrane curvature. Whether this is a direct effect, or requires the recruitment of other proteins, such as phospholipase D and/or other mitochondria-shaping proteins, remains to be elucidated.

3.2.1.2.4 MTP18

MTP18, a nuclear-encoded mitochondrial membrane protein, is also suggested to be a novel component required for mitochondrial fission in mammalian cells (Tondera et al., 2004; Tondera et al., 2005). MTP18 is supposed to be an intramitochondrial protein exposed to the IMS, however it is still not clear whether MTP18 is an OMM or IMM protein. Interestingly MTP18 is a downstream effector of phosphatidyl-inositol 3-kinase (PI3-K) signalling. It has been reported that overexpression of MTP18 leads to mitochondrial fragmentation and downregulation of MTP18 levels by siRNA induces mitochondrial elongation. Thus, MTP18 could be a regulator of mitochondrial shape that responds to activation of PI3-K, coupling morphology of the reticulum to cellular cues.

3.2.2 Mechanisms of mitochondrial fusion and fission

3.2.2.1 Fission

Mitochondrial fission in mammalian cells seems to follow the same mechanism described in yeast. Like in yeast, it has been shown that DRP1 is recruited to spots on mitochondria and it seems that constriction of the membranes takes place via interaction with FIS1, since it has been shown that recombinant DRP1 and recombinant FIS1 can interact *in vitro* (Yoon et al., 2003). However, this association has never been shown *in vivo* and reduction of FIS1 levels by siRNA does not disrupt DRP1 localization to mitochondria (Lee et al., 2004). While this could argue against the possibility that Fis1 acts as the mitochondrial receptor for DRP1, it should be considered that the residual level of FIS1 could still be sufficient to recruit DRP1 to mitochondria. It is unclear which are the signals that induce the recruitment of DRP1 to mitochondria. On the other hand, it has been recently discovered that its turnover is controlled by the equilibrium between ubiquitination and sumoylation, as well as by its phosphorylation/dephosphorylation.

3.2.2.2 Regulation of mitochondrial fission

3.2.2.2.1 Phosphorylation of DRP1

Mitochondrial division is coordinated with the cell cycle in higher eukaryotes. Recent experiments using cultured human cells showed that mitochondrial scission is induced at the

onset of mitosis, leading to partial fragmentation of mitochondria (Taguchi et al., 2007). Revealing a direct link between the cell-cycle and the mitochondrial-division machinery, this burst of mitochondrial division is correlated with the cyclinB–cyclin-dependant kinase (CDK1-dependent) phosphorylation of DRP1. This is the first demonstration that the addition of a phosphate moiety to DRP1 regulates its activity and *in vitro* assays using purified proteins coupled with cell-culture experiments indicate that the most potent mitotic phosphorilation event occurs on a serine residue in the carboxyl-terminal GTPase-effector domain (GED) of DRP1. Another recent study showed that cyclic-AMP-kinase-dependent phosphorilation of a different serine in the GED can decrease the GTPase activity of DRP1 by inhibiting the intramolecular interactions known to increase the GTPase activity of DRP1 (Chang and Blackstone, 2007). Although these initial studies indicate that DRP1 phosphorylation can modulate the frequency of mitochondrial division, it remains to be determined if fission competent DRP1 is always phosphorylated or if this is a mechanism exploited only during the cell cycle.

Recently Cribbs and Strack (Cribbs and Strack, 2007) identified a crucial phosphorylation site that is conserved in all metazoan DRP1 orthologues. Ser 656 is phosphorylated by cyclic AMP-dependent protein kinase and dephosphorylated by calcineurin, and its phosphorylation state is controlled by sympathetic tone, calcium levels and cell viability. Thus, DRP1 phosphorylation at Ser 656 provides a mechanism for the integration of cAMP and calcium signals in the control of mitochondrial shape, apoptosis and other aspects of mitochondrial function.

3.2.2.2.2 Sumoylation of DRP1

The small ubiquitin-like modifier (SUMO) is highly conserved from yeast to humans and can be conjugated to a wide variety of proteins in a manner similar to ubiquitin. Unlike ubiquitinylation, which often leads to degradation of substrates, sumoylation usually alters the subcellular localization of target proteins or protects them from ubiquitin-mediated destruction. DRP1 pull-down experiments identified SUMO-1 and its conjugating enzyme Ubc9 as DRP1-binding partners (Harder et al., 2004). Confirming that these two proteins form a functional complex that binds and modifies DRP1, sumoylated Drp1 has been isolated from mammalian cells (Harder et al., 2004). Consistent with the idea that sumoylated DRP1 promotes mitochondrial division, overexpressing SUMO1or silencing sentrin/SUMO-specific protease (SENP5), the protease that removes SUMO from DRP1, yields cells with many small mitochondria (Zunino et al., 2007). Interestingly, SENP5 is also a key player in cell-cycle progression (Di and Gill, 2006) and, similar to the cyclinB–CDK1 dependent phosphorylation of DRP1, the interactions among DRP1, SUMO and SENP5 might help progression into mitosis.

3.2.2.2.3 Ubiquitinylation of DRP1 and MFNs: MARCH-V

The regulation of mitochondrial fusion is poorly understood. However, two recent discoveries point to a role for ubiquitinylation in this process. Membrane-associated ‘really-interesting-new-

gene-'cystein/histidine (RING-CH) V (MARCH)-V is a novel ubiquitin ligase integrated in the OMM. MARCH-V is a E3 ubiquitin ligase and catalyses polyubiquitinylation in the presence of the E2 enzymes UbcH6 or UbcH5 (Nakamura et al., 2006). MARCH-V interacts with MFN2 and promotes mitochondrial elongation in a MFN2-dependent manner. On the other side, MARCH-V promotes ubiquitinylation of DRP1.

The most recent work suggests that MARCH-V ubiquitinylates DRP1 but does not control the stability of DRP1. Instead, DRP1 ubiquitinylation seems to regulate the kinetics of DRP1 binding to the mitochondrial surface. In this instance, ubiquitin conjugation might regulate subcellular trafficking and assembly of DRP1 and eventually influence the rate of mitochondrial division. Altogether, it seems that MARCH-V controls mitochondrial morphology by regulating the activity of mitochondria-shaping proteins.

3.2.2.3 Fusion

Fusion of mammalian mitochondria is thought to occur in a similar way as in yeast. The mammalian orthologues of Fzo1p, MFN1 and MFN2, are believed to dock two juxtaposed mitochondria *via* their coiled coil domains (Koshiba et al., 2004). However, MFN2 seems to have a different role from MFN1. First, it has been shown that MFN1 has a higher GTPase activity than MFN2, although its affinity for GTP is lower (Ishihara et al., 2004). In agreement with this, MFN1 exhibits a higher capacity in inducing fusion. But how is OMM fusion coordinated with IMM fusion? In yeast a multimolecular complex of Mgm1p, Ugo1p and Fzo1p apparently coordinates fusion of the two membranes. On the other hand, a mammalian orthologue of Ugo1p has not yet been identified and it is unclear whether OPA1 and MFN1 directly interact to promote mitochondrial fusion.

Studies in intact cells showed that in higher eukaryotes an intact IMM potential is required for mitochondrial fusion, which conversely appears to be independent of a functional cytoskeleton (Legros et al., 2002; Mattenberger et al., 2003). Taking advantage of the yeast model, mitochondrial fusion has been recently recapitulated *in vitro.* This approach dissected the fusion process into two mechanistically distinct, resolvable steps: OMM fusion and IMM fusion. OMM fusion requires homotypic *trans* interactions of the Fzo1p, the proton-gradient component of the inner membrane electrical potential, and low levels of GTP hydrolysis. Fusion of IMM requires the electrical component of the inner membrane potential and high levels of GTP hydrolysis. However, time-lapse analysis of mitochondrial fusion in yeast and mammalian cells, *in vivo*, clearly shows that fusion of the OMM and IMM is temporally linked. These observations indicate that individual fusion machineries exist in each membrane and that they can communicate *in vivo*, resulting in coupled outer and inner membrane fusion (Meeusen et al., 2004).

Regulation of mitochondrial fusion is likely to involve transcriptional regulation in mammalian cells as well as post-traductional variation in the level of fusion proteins in a given cell.

Furthermore, slight changes in the mitochondrial membrane potential may also serve to fine-tune fusion rates.

3.2.2.4 Regulation of mitochondrial fusion

3.2.2.4.1 Phospholipase D

Recent work reported the involvement of a novel phospholipase D isoform (mitoPLD), possessing a MTS that directs it to the external face of mitochondria, in fusion of the organelle. This lipid-modifying enzyme participates in mitochondrial fusion by hydrolyzing cardiolipin to generate phosphatidic acid (Choi et al., 2006). Phosphatidic acid facilitates vesicular fusion driven by specialized SNARE-complexes. This indicates for the first time the existence of a common mechanism between SNARE-mediate vesicle fusion and MFN-mediated mitochondrial fusion.

3.2.2.4.2 Mitofusin Binding Protein

Mitofusin-binding protein (MIB) regulates mitochondrial morphology via its interaction with MFN1 (Eura et al., 2006). MIB is a member of the medium-chain dehydrogenase/reductase protein superfamily and has a conserved coenzyme binding domain (CBD). MIB needs an intact CBD domain to interact with MFN1, this interaction results in inhibition of MFN1 function and mitochondrial fragmentation. The subcellular localization of MIB is not very clear, since only ~50% of the cellular protein associates with mitochondria; the rest is in the cytosol or seems to be associated with microsomes. However the association of MIB with other membranes does not seem to affect their morphology. Whether MIB regulates morphology in response to the supply of fatty acids to mitochondria remains an intriguing possibility that waits experimental testing.

3.2.2.4.3 Degradation of Fzo1p/MFN

Modulation of the amount of MFNs regulates the extent of mitochondrial fusion. For example, in wild-type yeast cells, Fzo1p is turned-over and degraded rapidly by at least two distinct mechanisms (Fritz et al., 2003; Neutzner and Youle, 2005). During vegetative growth, Fzo1p stability is influenced by the OMM F-box-containing protein, Mdm30p. F-boxes are present in subunits of a subset of E3 ubiquitin ligases and are often required for the ubiquitin-conjugating activity of these proteins. Cells expressing a F-box-mutant version of Mdm30p accumulate Fzo1p, contain fragmented mitochondria and exhibit reduced mitochondrial fusion (Fritz et al., 2003), further substantiating the discovery of Fzo1p as ubiquitinated in a genome-wide analysis (Hitchcock et al., 2003). Surprisingly, constitutive Fzo1p turn-over does not require known ubiquitin or proteasome machinery, suggesting that Mdm30p-mediated degradation can occur independently of the proteasome (Durr et al., 2006; Escobar-Henriques et al., 2006). Perhaps

yeast cells use autophagy or mitochondrial proteases, such as the AAA proteases, to degrade Fzo1p. Proteasome-mediated degradation of yeast Fzo1p could favor organelle fragmentation during cell death, which appears similar to the fragmentation of mitochondria seen in mammalian apoptosis (Cereghetti and Scorrano, 2006). To date, no studies are available that have examined the half-life of MFNs or determined if MFNs are ubiquitinylated. Therefore, it will be interesting to test whether the same rules that govern Fzo1p turn-over impact the function of MFNs in healthy and apoptotic mammalian cells.

3.2.2.4.4 BAX and BAK and mitochondrial morphogenesis

The proapoptotic BCL-2 family members BAX and BAK seem to play an additional role during life of the cell in controlling mitochondrial fusion. They are retrieved in a high-molecular weight complex with MFN2 and their ablation reduces the rate of mitochondrial fusion, implying these multidomain proapoptotics also in the control of mitochondrial morphology (Karbowski et al., 2006).

3.2.2.4.5 Processing of OPA1: a busy pathway

A further and perhaps even more crucial level of control is exerted by the proteolytic cleavage of Mgm1p/OPA1. In yeast, Mgm1p can be cleaved by the rhomboid proteases Pcp1p (Herlan et al., 2003; McQuibban et al., 2003; Sesaki et al., 2003) to produce a short (s-), soluble and a long (l-), membrane anchored form of Mgm1p with different function.
The regulation of OPA1 processing in mammalian cells is matter of intense studies: this field is complicated by the fact that in human cells OPA1 is present in 8 isoforms (Delettre et al., 2001), each of them probably differentially regulated by post-traductional processing. A number of evidence involved proteases other than Parl, the orthologue of Pcp1p, in the processing of OPA1.

Interestingly, Ishihara et al. found that different isoforms of long (-L) OPA1 can be processed into two different short forms, according to the exons present, by paraplegin, a matrix facing AAA protease (m-AAA); dissipation of membrane potential, expression of paraplegin, or induction of apoptosis stimulated this processing along with mitochondrial fragmentation. These results indicated that the L-isoforms are the fusion-active species of OPA1 (Ishihara et al., 2006). The group of Reichert confirmed that mitochondrial depolarization induces OPA1

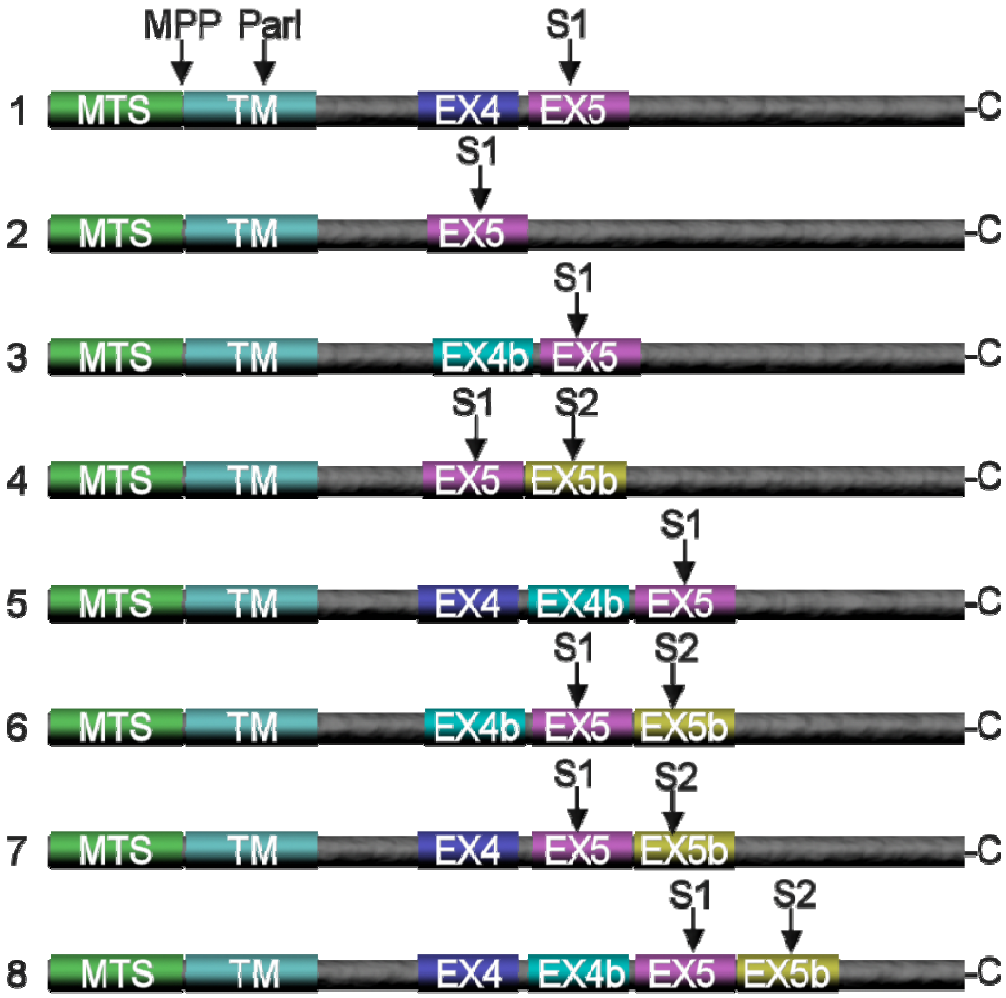

Figure 2 **OPA1 mRNA splice forms and putative site of cleaveage**
(A) Schematic of the eight *OPA1* mRNA splice forms. The mRNA splice forms differ in the presence or absence of exons 4, 4b, and 5b. Cleavage of the mitochondrial targeting sequence (MTS) by MPP leads to the long isoforms. Additional cleavage at sites S1 (exon 5) or S2 (exon 5b) leads to the short isoforms. TM, transmembrane. (B) Processing of polypeptides encoded by individual OPA1 mRNA splice forms.

cleavage which in turn causes fragmentation of mitochondrial network, as a consequence of the imbalance between fusion and fission. (Duvezin-Caubet et al., 2006). On the other hand, they challenged the role of paraplegin in the processing of OPA1, by showing that AFG3L2, another component of the m-AAA protease complex, is involved in the $\Delta\psi_m$-dependent processing of this mitochondria-shaping protein (Duvezin-Caubet et al., 2006). A mass spectrometric characterization of OPA1 isoforms in HeLa cells not only revealed their formation by alternative

splicing and proteolytic processing, but also that OPA1 is recognized and cleaved by *m*-AAA protease isozymes complexes composed of murine Afg3l1, Afg3l2, or human AFG3L2 subunits (Duvezin-Caubet et al., 2007). On the other hand, it was recently shown that an AAA protease acting in the intermembrane space (i-AAA) can process OPA1 in a $\Delta\Psi_m$-independent fashion: isoforms of OPA1 containing exon 4b and 5b seem to present an additional cleavage site for the i-AAA Yme1L; in addition, a combination of long and Yme1L-processed OPA1 isoforms is important for mitochondrial fusion activity (Griparic et al., 2007; Song et al., 2007). A similar processing was confirmed recently by another group (Guillery et al., 2007). This suggests that the exact cleavage sites may not be important in terms of protein function, but that Yme1L-dependent processing could compete with or precede the $\Delta\psi_m$-dependent m-AAA one. The presence of multiple sites could increase the flexibility of OPA1 processing, as confirmed by the involvement of distinct proteases and by the differential regulation by membrane potential. For a cartoon of OPA1 isoforms and demonstrated cleaveage see Figure 2 .

In this picture, the role of Parl is completely unclear. In this Thesis we used a genetic approach to explore the fate of OPA1 in *Parl*-/- tissues and cells. Our results indicate a role for Parl in OPA1 processing, albeit this is not related to the prototypical function of this protein in fusion, but to its role in apoptosis. Interestingly, Baricault and colleagues demonstrated that apoptosis induction and PTP opening, as well as $\Delta\psi_m$ dissipation induce cleavage of OPA1. Moreover, they suggest that decreased mitochondrial ATP levels, either generated by apoptosis induction, depolarization or inhibition of ATP synthase, is the common and crucial stimulus that controls OPA1 processing (Baricault et al., 2007). Thus, cleavage and processing of OPA1 appear to be regulated in a tight manner during life and death of a cell. The precise functional significance of this regulation is unclear at the moment and requires further studies.

3.3 Mitochondria-shaping proteins in health and disease

In the past years, mitochondrial defects have been implicated in a number of degenerative diseases, aging and cancer. Mitochondrial diseases involve mainly tissues with high energetic demands, such as muscle, heart, endocrine and renal systems. More recently, mutations in genes coding for pro-fusion proteins have been associated with genetic disorders.

3.3.1 OPA1 in disease: autosomal dominant optic atrophy.

Mutations in OPA1 are associated with autosomal dominant optic atrophy (ADOA), also known as type I Kjer disease, affecting mainly retinal ganglion cells and causing progressive blindness due to their progressive loss (Alexander et al., 2000; Delettre et al., 2000).

3.3.1.1 Clinical features

The typical presentation in ADOA is characterized by a slowly progressive, roughly bilaterally symmetrical visual loss in childhood, accompanied by temporal pallor of the optic discs. Classic ADOA usually begins before 10 years of age, with a large variability in the severity of clinical phenotype, which may range from non-penetrant unaffected cases up to very severe, early onset cases, even within the same family carrying the same molecular defect (Cohn et al., 2007; Delettre et al., 2002). The patient is often unaware of a vision defect, and the disease is recognized by chance during routine vision testing (school eye screenings).

Examination also demonstrates centrocaecal scotomas and impairments of color vision (tritanopia). Peripheral vision is usually spared, and a central, paracentral, or cecocentral scotoma is typical. Variability of clinical expression is reflected by the extent of optic atrophy reached by different patients.

Despite the remarkable difference of the clinical evolution, the endpoint of the pathological process in Kjer's is clinically indistinguishable from another type of neuropathy, the Leber's hereditary optic neuropathy (LHON). For differential diagnosis a frequent feature of ADOA's end-stage fundus examination is optic disc excavation (Votruba et al., 2003). Such excavation is also frequently reported in LHON (Carelli et al., 2004) and specifically characterizes the optic neuropathy in normal tension glaucoma (NTG) (Buono et al., 2002). A recent detailed study of optic disc morphology in ADOA patients with Opa1 mutations showed optic disc excavation with enlarged cup to disc ratio, frequent peripapillary atrophy, and temporal gray crescent, most of which are features also seen in glaucomatous optic neuropathy (Votruba et al., 2003). Optic disc pallor, prevalent on the temporal side, is typically seen in ADOA patients.

Most of the mutations associated with ADOA cluster in the GTPase and in the coiled coil domain of Opa1 (Ferre et al., 2005). Almost 50% of mutations in the OPA1 gene described to date are predicted to lead to a truncated protein and suggest that haploinsufficiency is the cause of the disease (Marchbank et al., 2002; Pesch et al., 2001). Nearly 40% of mutations occurs in the GTPase domain and may cause a dominant negative effect, impairing the mechanoenzymatic activity of the protein complexes. This possibility is reinforced by the fact that two mouse models of *Opa1* mutation (a GTPase missense and a nonsense, truncative mutation) display minimal retinal defects in the heterozygous status (Alavi et al., 2007; Davies et al., 2007).

The mitochondrial dysfunction in ADOA seems predispose the neuronal cells to apoptotic death: drops in the mitochondrial membrane potential and cellular respiration occur in cells where OPA1 expression has been downregulated (Chen et al., 2005; Olichon et al., 2003). Interestingly, recent results obtained from primary cultures from type 1-ADOA patients (Amati-Bonneau et al., 2005) fit with the *in vivo* data obtained using ^{31}P magnetic resonance spectroscopy that demonstrate defective ATP synthesis in skeletal muscle from these patients

(Lodi et al., 2004). Nevertheless, in ADOA the primary defect would be attributed to the role of OPA1 in mitochondrial dynamics and/or the structural organization of the *cristae*, since many studies demonstrated the involvement of OPA1 mutations in controlling apoptosis in different cellular models (Arnoult et al., 2005; Griparic et al., 2004; Lee et al., 2004; Olichon et al., 2003). The objective of this Thesis has therefore been the elucidation of the role of Opa1 in apoptosis and in the pathway of *cristae* remodelling.

3.3.1.2 OPA1 expression in mammalian tissues

Despite that *OPA1* is ubiquitously expressed, the tissue specificity of ADOA is surprising. While most abundant in the retina, OPA1 mRNA is widely expressed in mammalian tissues (Alexander et al., 2000; Delettre et al., 2000; Pesch et al., 2001); OPA1 protein is also present in many tissues (Aijaz et al., 2004; Olichon et al., 2003) and is expressed not only in the RGC layer but also in other different layers of the retina. (Ju et al., 2005; Kamei et al., 2005; Pesch et al., 2004). Despite many studies focused on OPA1 localization, some uncertainties remain: Pesch et al. (Pesch et al., 2004) found that OPA1 was absent from mitochondria-rich nerve fibers and optic nerve in the adult rat, while Aijaz et al (Aijaz et al., 2004) recently reported that OPA1 is expressed in the adult mouse and human optic nerve only in myelinated regions. On the other hand, Ju and colleagues (Ju et al., 2005) showed that OPA1 was not found in glial cells, such as astrocytes, oligodendrocytes, and microglial cells in the normal rat optic nerve; but OPA1 immunoreactivity was present in the axonal mitochondria, concluding that OPA1 function in the optic nerve depends on axonal mitochondria of the RGCs.

3.3.1.3 Are only RGCs selectively killed?

Since OPA1 is widely expressed in many tissues the reason why RGC are primarily affected by OPA1 mutation remains a conundrum. What makes the optic nerve so vulnerable to mitochondrial dysfunction? One common hypothesis is that neurons have a high demand for energy in regions that may be at a considerable distance from the cell body, where the biogenesis of the mitochondria occurs. Bioenergetic defects may be deleterious for the conduction of action potentials, as well as for mitochondrial transport, and may thus result in nonfunctional synapses, axonal degeneration and ultimately cell death. Due to the high energy demand required for the conduction of electrical impulses through the anterior unmyelinated portion of the axons, and the long course of the axons, the RGC may be a bioenergetically weak element of the central nervous system.

A plausible hypothesis as to why these neurons may be more vulnerable to OPA1 inactivation could be a particular susceptibility to mitochondrial membrane disorders inducing mitochondrial dysfunction or mislocalization. While the former point is in agreement with reports that describe altered mitochondrial ATP synthesis and respiration in OPA1-inactivated cells (Amati-Bonneau et al., 2005; Chen et al., 2005), the latter may relate to the particular distribution of the

mitochondria in RGC. These show an accumulation of mitochondria in the cell bodies and in the intraretinal unmyelinated axons, where they accumulate in the varicosities, and a relative scarcity of mitochondria in the myelinated parts of axons (Andrews et al., 1999; Bristow et al., 2002; Wang et al., 2003). A better understanding of the role of mitochondrial dynamics in mitochondrial and cellular function is essential to evaluate the physiological and physiopathological impact of these processes. As a matter of fact, despite OPA1 has a well established role in mitochondria-dependent apoptosis it can be argued that defects in mitochondrial dynamics can cause added deficits in mitochondrial respiration, morphology and motility. Moreover, mutations in another mitochondria pro-fusion gene, Mitofusin-2, lead to Charcot-Marie-Tooth type 2A, a peripheral neuropathy. Perhaps it is the strict spatial and functional requirements for mitochondria in neurons that cause defects in mitochondrial fusion to manifest primarily as neurodegenerative diseases.

3.3.1.4 A syndromic form of optic neuropathy

It should be noted that most of the mutations are invariably associated with a non-syndromic, slowly progressive form of optic neuropathy, as originally described by Kjer in 1959.(Kjer, 1959) However, there is at least one clear example standing out of this paradigm. This is a mutation in the *OPA1* gene, *i.e.* the c.1334G4A leading to R445H amino acid change, being associated with a syndromic form of optic neuropathy and sensorineural deafness (Amati-Bonneau et al., 2005), and in some of the reported cases with chronic progressive external ophthalmoplegia (CPEO), ptosis and myopathy. This scenario can argue against the hypothesis of a selective effect of Opa1 mutations in RGC and hypothesize a role of Opa1 in mtDNA maintainance that, if impaired, leads to a specific damage to skeletal muscle (Amati-Bonneau et al., 2007; Hudson et al., 2007; mati-Bonneau et al., 2007).

Despite the putative pathogenesis of *OPA1* mutations in ADOA, it is still not clear how a mitochondrial dynamin-related protein could impact so deeply on mitochondrial physiology; for this reason we need to clarify and discuss in detail the role of mitochondria in apoptosis

3.4 Apoptosis: one way to die

The word apoptosis (“apo” stands for from and “ptosis” for falling) is of Greek origin and was introduced by Kerr and colleagues (Kerr et al., 1972) to describe a specific form of cell death. It was chosen because it means “falling of leaves,” a necessary part of the life cycle of trees.

Programmed cell death (Lockshin and Williams, 1965) and its morphologic manifestation of apoptosis is a conserved pathway that in its basic tenets appears operative in all metazoans. Multiple rounds of cell death during embryonic development are essential for successful organogenesis and the crafting of complex multicellular tissues. The evolutionary advent of differentiated cell types may have required controlling death as well death as division in order to keep neighboring cells interdependent and insure the proper balance of each cell lineage.

Apoptosis also operates in adult organisms to maintain normal cellular homeostasis. This is especially critical in long-lived mammals that must integrate multiple physiological as well as pathological death signals, including the response to infectious agents. Gain- and loss-of-function models in the core apoptotic pathway indicate that the violation of cellular homeostasis can be a primary pathogenic event that results in disease (Danial and Korsmeyer, 2004).

Mitochondrial are not innocent bystander in PCD: interestingly, the discovery by Korsmeyer and coworkers that the antiapoptotic oncogene BCL-2 targets its product to mitochondria (Hockenbery et al., 1990) strongly suggested that they were involved in controlling cell death.

A few years later cytochrome *c,* the only soluble component of the respiratory chain, was found to be required in the cytosol to activate downstream apoptosis signals (Liu et al., 1996). After that, many soluble proteins of the intermembrane space have been found to amplify the apoptotic machinery: among them Smac/DIABLO and Omi/HtrA2 enhance caspase activation through the neutralization of inhibitors of apoptosis proteins (Du et al., 2000; Verhagen et al., 2000), although the role of these two proteins in apoptosis is controversial (Martins et al., 2004). Other mitochondrial proteins that are released during apoptosis have been suggested to play other roles in cell death. Endonuclease G (Li et al., 2001), apoptosis-inducing factor (AIF) (Susin et al., 1999), and Omi/Htra2 (van et al., 2002) each have been proposed to function in caspase-independent cell death.

Once released, cytosolic cytochrome *c* binds to APAF-1, increasing its affinity for dATP/ADP. The complex composed by APAF-1, cytochrome *c*, dATP and ADP forms the apoptosome. The apoptosome is able to recruit procaspase-9, facilitate its auto-activation and subsequently lead to the activation of downstream executioner caspases, cysteine proteases, that effect cell demise (Thornberry and Lazebnik, 1998; Zou et al., 1997). Executioner caspases then cleave other intracellular substrates leading to the characteristic morphological changes in apoptosis such as chromatin condensation, nucloesomal DNA fragmentation, nuclear membrane breakdown, externalization of phosphatidylserine (PS) and formation of apoptotic bodies (Hengartner, 2000).

In 1972 Wojtczak and Sottocasa (Wojtczak et al., 1972) demonstrated that the OMM is impermeable to cytochrome c; thus in order for this protein to be released in the cytosol to activate the apoptosome the OMM should change its permeability properties, but the precise mechanism of this event is highly debated. This process could explain the egress of cytochrome *c* from mitochondria but a complete understanding of this is event seems far; however, it appears clear that the BCL-2 family proteins are sentinels of the mitochondrial integrity. In addition to permeabilization of the outer membrane, at least two other morphological changes must occour for complete cytochrome *c* release: *cristae* remodeling and mitochondrial fragmentation.

3.4.1 Mitochondrial morphology and apoptosis

A growing body of evidence suggests that mitochondria- shaping proteins participate in cell death. Dnm1p, the yeast ortholog of DRP-1, mediates mitochondrial fragmentation and apoptosis-like death in *S. cerevisiae* (Fannjiang et al., 2004). Blocking Drp-1 in C. elegans inhibits apoptotic mitochondrial fragmentation and results in the accumulation of supernumerary cells during development (Jagasia et al., 2005). In mammalian cells, death by mitochondria utilizing intrinsic stimuli is accompanied by mitochondrial fragmentation and blunted by dominant negative DRP-1 (Frank et al., 2001).

Similarly, expression of hFis1 results in cytochrome *c* release and death (James et al., 2003) and its downregulation by RNA interference prevents apoptosis to a greater extent than DRP-1 silencing (Lee et al., 2004). In our laboratory it has been shown that mitochondrial fission induced by hFis1 is genetically distinct from classical, BAX and, BAK dependent apoptosis. Death by hFis1 relies on the other hand on the ER gateway of apoptosis: hFis1 did not directly activate BAX and BAK, but induced Ca^{2+}-dependent mitochondrial dysfunction. Thus, hFis1 is a bifunctional protein that independently regulates mitochondrial fragmentation and ER-mediated apoptosis (Alirol et al., 2006).

Of note, it was recently demonstrated by two separate groups that inhibiting DRP1-mediated mitochondrial fission by RNA interference (Estaquier and Arnoult, 2007; Parone et al., 2006) delayed but not prevented apoptosis and cell death: a likely explanation is that inhibition of DRP1-mediated mitochondrial fission partially prevents cytochrome *c* release but has no effect on the release of Smac/DIABLO, Omi/HtrA2, Adenilate Kinase and DDP/TIMM8a that can still mediate apoptosis. These data support the hypothesis that DRP1 has a relevant function in regulating cytochrome *c* egress trough OMM probably by impacting on ultrastructure of IMM.

Further analysis revealed that early in the course of cell death, MFN1 dependent mitochondrial fusion is largely inhibited (Karbowski et al., 2004a) and combined overexpression of MFN1 and MFN2 protects from death by intrinsic stimuli like etoposide and BID (Sugioka et al., 2004). Loss of function of OPA1, in analogy to Mgm1p deficiency in yeast, leads to mitochondrial fragmentation. *In vitro*, RNAi-mediated knockdown of OPA1 causes extreme cellular sensitization toward exogenous apoptosis induction as well as spontaneous apoptotic cell death (Lee et al., 2004).

These data seem to establish a linear correlation between fragmentation, blocking of fusion and apoptosis, but the picture is probably not so simple. First, fission does not always promote apoptosis, as confirmed by the ability of overexpressed DRP-1 to inhibit death by ceramide (Szabadkai et al., 2004). In this case, DRP-1 appears to protect by blunting the mitochondrial Ca^{2+} waves that transmit ceramide-mediated apoptotic signal (Pacher and Hajnoczky, 2001). Second, inhibiting mitochondrial fission (even if we assume that complete knock out rather than

silencing is obtained for each protein studied) does not lead to a complete inhibition of cytochrome *c* release. There are two possible explanations to this: mitochondrial fission could be seen as a positive feedback to amplify permeabilization of the outer membrane and the release of cytochrome *c.* The amount of cytochrome *c* that is initially released, before recruitment of proteins of the fission machinery and mitochondrial fission, would be, in most cells, sufficient to trigger the formation of the apoptosome and caspase activation. Inhibiting mitochondrial fission would only slow down the kinetics of cell death. Alternatively, activation of fission could result in inner mitochondrial changes that are required to amplify the release of cytochrome *c,* such as the *cristae* remodelling observed by G. Shore and coworkers (Germain et al., 2005).

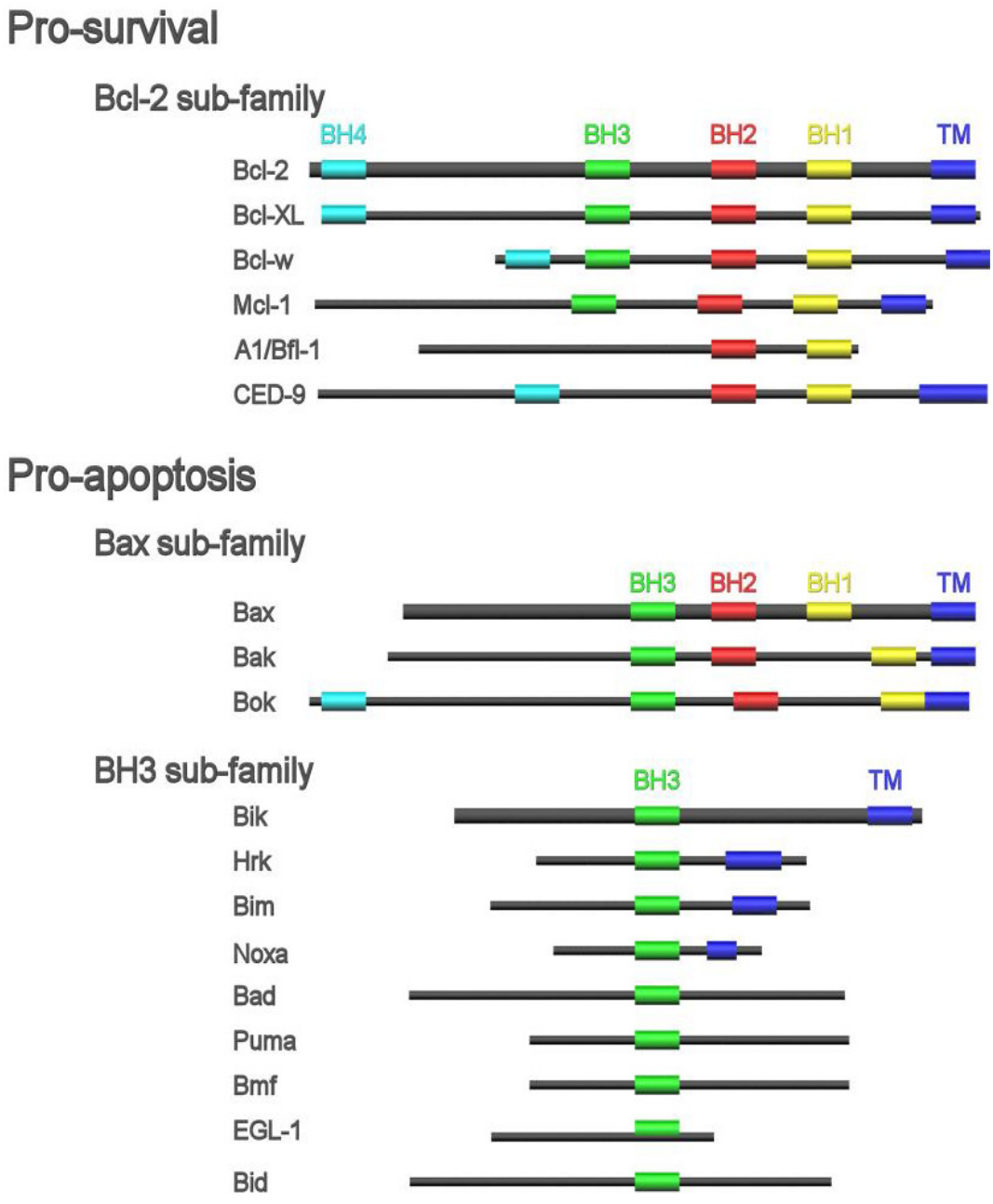

Figure 3 **Summary of anti- and proapoptotic BCL-2 family members. BCL-2 homology domains are highlighted**.

3.4.2 The riddle of the Outer Mitochondrial Membrane Permeabilization: the BCL-2 family

The BCL-2 family proteins are critical death regulators that reside immediately upstream of mitochondria and consist of both anti- and proapoptotic members. BCL-2 family members possess conserved α-helices with sequence conservation clustered in BCL-2 homology (BH) domains. Antiapoptotic members exhibit the homology in all segments BH1 to 4, while proapoptotic molecules lack stringent sequence conservation of the first α-helical BH4 domain and can be further subdivided into ‘‘multidomain’’ and ‘‘BH3-only’’ proteins (Figure 3). Multidomain proapoptotic members such as BAX and BAK display sequence conservation in BH1-3 domains. BH3-only members display sequence conservation only in the amphipathic α-helical BH3 region (Scorrano and Korsmeyer, 2003). The BH3-only proteins studied to date reside upstream in the pathway. Death signals trigger their activation by transcriptional regulation or post-translational modification to connect proximal signals with the core apoptotic pathway (Gross et al., 1999). For example, after activation of CD95 (Fas) or TNFR1 death receptors, BID is cleaved and activated to p15 tBID (Luo et al., 1998) by caspase 8. The efficiency of the translocation process at the OMM surface can be enhanced by modifications such as the N-terminal myristoylation of tBID that follows its cleavage by caspase-8 (Zha et al., 2000).

The mechanism by which activated BH3-only proteins interact with the proapoptotic members of the BCL-2 family is highly debated and two major hypothesis are considered (Adams and Cory, 2007):

In the **direct activation model** (Figure 4), a subgroup of BH3-only proteins, termed activators, are proposed to bind directly to BAX and BAK to promote their activation (Letai et al., 2002). These putative activators include BIM and tBID, and perhaps also Puma, although this has been disputed. In this model, the remaining BH3-only proteins, termed sensitizers, function by binding to the pro-survival proteins and freeing any bound BIM or tBID to directly activate BAX and BAK.

The **indirect activation model** (Figure 4) instead proposes that all BH3-only proteins function solely by binding to their pro-survival relatives, thereby preventing those guardians of cell survival from inhibiting BAX and BAK. In this model, BIM, tBID, and PUMA are the most potent BH3-only proteins simply because they can engage all the pro-survival proteins.

In vitro data from liposome disruption (Walensky et al., 2006) and from some mutant proteins (Kim et al., 2006) argue that certain BH3-only proteins, such as tBID, can directly activate BAX/BAK (Figure 4).

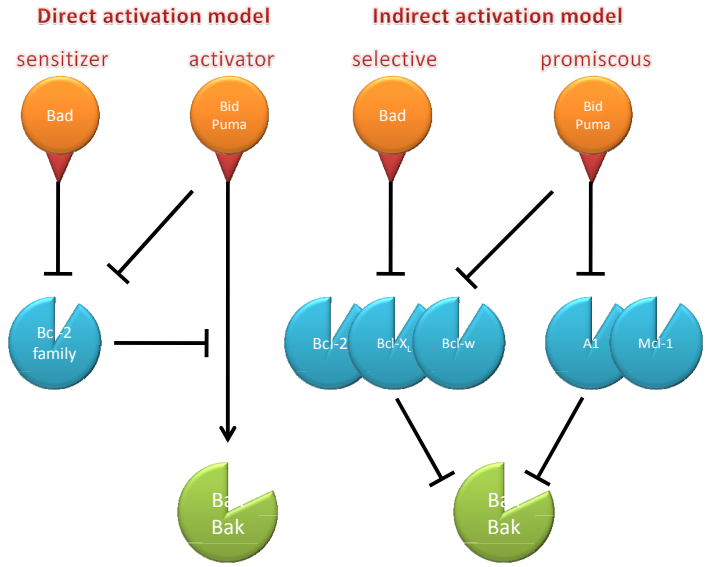

Figure 4 **Two models for how BH3-only proteins activate BAX and BAK**.
In the direct activation model, the indicated activator BH3-only proteins, via their BH3 domain (red triangle), directly engage BAX and BAK and activate them, whereas sensitizer BH3-only proteins (e.g. BAD or NOXA), which can only bind the pro-survival proteins, serve only to displace activators from the pro-survival proteins. In the indirect activation model the BH3-only proteins only bind the pro-survival proteins. Because the promiscuous binders (BIM, tBID, and PUMA) can neutralize all pro-survival proteins, each can readily trigger BAX/BAK activation, whereas any selective binder (e.g. BAD) must be co-expressed with a complementary binder (e.g. NOXA) to do so.

While considerable detail regarding reciprocal interactions between Bcl-2 members has been revealed, uncertainties still exist concerning the precise mechanism(s) by which proapoptotic BCL-2 family members regulate the release of cytochrome *c* from mitochondria.

3.4.3 BAX and BAK oligomerization is a prerequisite for cytochrome c release.

The prodeath function of BH3-only proteins relies on the presence of BAX and BAK (Lindsten et al., 2000; Wei et al., 2000; Wei et al., 2001) Korsmeyer and colleagues demonstrated that the mechanism underlying this requirement was the oligomerization of these proteins, which was required for the permeabilization of the mitochondrial outer membrane that was required for cytochrome *c* release (Wei et al., 2000). While BAX has the ability to form pores that could in principle permit the egress of cytochrome *c*, the precise composition of the cytochrome *c* release pore is still not completely resolved (Saito et al., 2000). There are indications, however, that BAX and BAK may indeed make up an important part of it.

A major question is how oligomerized multidomain BAX, BAK effect the release of proapoptotic activators from mitochondria. Current models include:

(i) BAX, BAK oligomers generate a pore in the outer mitochondrial membrane permeable to cytochrome *c* and possibly to other proapoptotic proteins.

(ii) interactions between BAX and resident mitochondrial proteins such as VDAC (Shimizu et al., 1999) or ANT (Marzo et al., 1998) which are proposed to release cytochrome *c* directly or trigger the mitochondrial permeability transition (PT);

(iii) a global effect on the permeability of the OM, this includes a number of possibilities, including a concept of ‘‘lipid’’ channels in the bilayer (Kluck et al., 1999; Kuwana et al., 2002).

3.4.3.1 BAX and BAK pores in the OMM

Activated BAX, BAK may form pores in the OMM that directly or indirectly allow the efflux of cytochrome *c* and perhaps of the other IMS proteins that drive death effectors pathways.

The initial insight leading to the pore model was that the structure of Bcl-xL (Muchmore et al., 1996) had a distinct similarity to that of the translocation domain of diphtheria toxin (DTT) a domain that can form pores in artificial lipid bilayers and chaperones another toxin subunit across cellular membranes (Antignani and Youle, 2006).

The organization of the BCL-x_L and BAX α-helices resembles that of the T domain of diphtheria toxin (Suzuki et al., 2000) and topology analyses of the membrane-inserted conformation of the DTT domain (Wang et al., 2006b; Wang et al., 2006a), BCL-2 (Kim et al., 2004), Bcl-XL (Garcia-Saez et al., 2004) and BAX (Annis et al., 2005) yield similar models, with the long hairpin helices inserted across the membrane and most of the amphipathic helices adhering to the *cis* side of the membrane.

Recombinant BAX forms homo-oligomeric pores in liposomes which in a concentration dependent fashion will release cytochrome *c* from them. A Hill plot of the kinetics of release indicates a slope that progresses from 2 to 4 participating molecules of BAX. Release through a putative pore at a BAX molecularity of 4 can be competed by blocking molecules that size the pore at 22 Å, slightly bigger than soluble cytochrome *c* (Saito et al., 2000).

Electrophysiological analysis of outer mitochondrial membrane patches isolated from apoptotic cells has reported novel, high conductance channels. Their properties are comparable to channels recorded in yeast mitochondria after treatment with recombinant BAX. Interestingly, these channels were also noted in mitochondria from VDAC defined strains, suggesting that this intrinsic OMM protein is not required (Pavlov et al., 2001). Further studies showed that this channel is typically voltage-independent [for a review see (Dejean et al., 2006)] and slightly cation-selective, which is consistent with its putative role in releasing the cationic protein cytochrome *c*. The polymer exclusion method indicates that channels of this "family" with conductances between 1.5 and 5 nS have pore sizes of 2.9–7.6 nm, which should be large enough to allow the passage of 3 nm cytochrome *c.* In particular, it was determined that this channel is, at least in part, composed of BAX and/or BAK and that BCL-2 blocks its formation.

It has been suggested that the oligomerization of BAX mediated by tBID is dependent on one or more non-mitochondrial proteins (Roucou et al., 2002): this cytosolic factor called BAF (BAX activating factor) seems to be required for a proper oligomerization of BAX in response to tBID in synthetic liposomes. Although oligomeric BAX has been shown to be a component of MAC, no endogenous proteins resident in the OMM are clearly implicated in its structure.

A development if the field is presently given by the fresh attention in mitochondrial dynamics: mitochondria typically fragment during apoptosis and inhibition of fission blocks cell death (Frank et al., 2001). In this respect, it has been shown by confocal and electron microscopy that

BAX and Bak coalesce into only 2–10 extremely large clusters on the surface of mitochondria during apoptosis constituting a possible pore through which cytochrome *c* is released. Interestingly, these BAX/BAK foci colocalize with mitochondrial fission sites and dynamin family GTPases, DRP1 and MFN2, suggesting links to mitochondrial morphogenesis (Karbowski et al., 2002; Karbowski et al., 2006; Youle and Karbowski, 2005).

3.4.3.2 The permeability transition and cytochrome c *release: a cause or a related effect?*

The mitochondrial permeability transition (PT) is an increase of IMM permeability to solutes with molecular masses up to 1500 Da. Under the conditions used in most *in vitro* studies, PT is accompanied by depolarization, matrix swelling, depletion of matrix pyridine nucleotides (PN), OMM rupture and release of IMM proteins, including cytochrome *c* (Bernardi, 1999) and could thus be the general trigger of apoptosis

This hypothesis has by many been viewed as implausible. Among other objections, mitochondrial matrix swelling is not normally seen in apoptosis (Kerr et al., 1979) and therefore seems to be limited to some special circumstances rather than applying to the core events of mitochondrial apoptosis. Despite this, the interaction of multidomain proapoptotics with VDAC and ANT, proposed components of the PT pore (PTP) has been pursued. Unfortunately, to date, none of the candidate pore components stood rigorous genetic testing [for a review (Bernardi et al., 2006)]. Contrasting results emerged from studies that attempted to measure evidence of PT, such as mitochondrial swelling and depolarization in response to activated BAX. While under some experimental conditions active BAX (and BAK) was noted to induce PT (Marzo et al., 1998; Narita et al., 1998; Pastorino et al., 1998), others reported that BAX was unable to promote it (Eskes et al., 1998; Jurgensmeier et al., 1998). Some of this discrepancy may reflect first that studies in isolated mitochondria do not completely reproduce what occurs in situ, where the cellular milieu and the complexity of mitochondrial architecture differs and importantly many of the techniques used in isolated mitochondria lack sensitivity and are not able to measure ‘‘transient’’ PT.

3.4.3.3 The innocent bystander scenario hyphothesis

As recently reviewed by Green and colleagues (Chipuk et al., 2006) there are some evidences that cytochrome *c* release occurs without direct decision made by mitochondria but is dictated by some interaction between cytoplasmic effectors and OMM: in this so called “innocent bystander scenario” the commitment to die or rather the commitment step that results in induction of cytochrome *c* release rests entirely with the BCL-2 family of proteins and their regulators. The authors suggest that is not that the OMM or IMM do not participate in the induction of cytochrome *c* release, but that, if they do, they do so in a manner that always depends on the activities of the BH3-only or multidomain BCL-2 proteins in the cytosol. In this

context, an injure acts first damaging mitochondria; the decision to undergo apoptosis, rather than necrosis, for instance, is made through some amplificatory loops (probably mediated by ROS) that in the cytosol activate Bcl-2 members to promote cytochrome *c* release.

This scenario differs from classical view since Bcl-2 proapoptotic members are not seen as causative events of a damage to mitochondria but rather decision makers on promoting cytochrome *c* release and hence apoptosis.

3.4.4 Permeabilization of the outer membrane is not sufficient for complete cytochrome *c* release

Irrespective of the exact mechanism by which active BAX, BAK release cytochrome *c*, it appears clear that these multidomain proapoptotics act as the essential gateway to the mitochondria.

Recent data indicate that while this step is requisite, there are additional pathways downstream of the BH3-only proteins that ensure complete release of cytochrome c: they include remodeling of the *cristae* characterized by fusion of individual *cristae* and opening of the *cristae* junctions (Scorrano et al., 2002) and fragmentation of the mitochondrial network (Frank et al., 2001) that we discussed earlier in 3.4.1.

Any model of cytochrome *c* release must account for the rapid kinetics and complete extent of cytochrome *c* release (Goldstein et al., 2000). Discrete levels of cytochrome *c* are required in the cytosol to activate the death response (Zhivotovsky et al., 1998) and in certain cells the amount of cytochrome *c* released is critical to overcoming protection by the IAP caspase inhibitors (Deveraux et al., 1998). In this respect, the complete release of cytochrome *c* must be put into the context of our current understanding of mitochondrial ultrastructure.

Thanks to the advance in electron microscopy, it has been shown that *cristae* are not simple invagination of the IMM as depicted by Palade (Palade, 1952) but rather they are distinct compartment of it. High-voltage electron microscopic (HVEM) tomography of mitochondria revealed that the IMS is very narrow, as the average distance between the OMM and IMM boundary membranes is only about 20 nm (Frey and Mannella, 2000), consistent with functional estimates that only 15%–20% of total cytochrome *c* is available in the IMS (Bernardi and Azzone, 1981). The pleomorphic, tubular *cristae* constitute highly sequestered compartments, where the majority of oxidative phosphorilation complexes (D'Herde et al., 2001; Perotti et al., 1983; Vogel et al., 2006) and cytochrome *c* is separated from the IMS by narrow *cristae* junctions (Figure 5B).

Computer models indicate that this subcompartmentalization has a functional counterpart in the generation of ion and ADP diffusion gradients across the narrow *cristae* junctions (Mannella et al., 2001; Moraru, 2000).

Interestingly, Attardi and coworkers noted that only cells primed for apoptosis by Fas activation released all stores of cytochrome *c* upon selective permeabilization of the OMM by digitonin

(Hajek et al., 2001). Increased accessibility of cytochrome *c* to the OMM was previously noted following Ca^{2+}-induced mitochondrial swelling (Bernardi and Azzone, 1981).

We therefore need to explain how the stores of cytochrome *c* that appear to be so heavily subcompartmentalized can be fully released in the absence of mitochondrial swelling, as is frequently observed in the course of apoptosis.

3.4.4.1 Apoptotic cristae remodeling

A turning point was the demonstration that following several death stimuli, including the BH3-only proteins BID (Scorrano et al., 2002) and BIK (Germain et al., 2005) or after Fas pathway activation (Mootha et al., 2001), mitochondria remodel their internal structure: individual *cristae* fuse and *cristae* junctions widen, to allow cytochrome *c* mobilization from its intra-*cristae* compartment toward the IMS for its subsequent release across the OMM according to the efflux pathway described in the previous section (Figure 5C).

While tBID did not induce large amplitude mitochondrial swelling, it did induce transient openings of the PTP. Transient openings have been noted in isolated mitochondria and intact cells, and are not associated with swelling or $\Delta\psi_m$ collapse (Huser et al., 1998; Petronilli et al., 1999). This transient PT was coordinated with *cristae* remodeling and cytochrome *c* mobilization as both proved BH3 independent, BAK independent, yet CsA inhibitable. This parallel regulation suggests a common mechanism or a shared component. It has been suggested that components of the PTP reside at contact points between the IMM and OMM (Zoratti and Szabo, 1995). While the mobilization of cytochrome *c* would have no obvious need to involve such contact points, the striking remodeling of *cristae* strongly suggests that tBID has an effect on the IMM.

The capacity of CsA to block this process suggests that its mitochondrial target, cyclophilin D (Nicolli et al., 1996), could be a functional component of this remodeling process. Alternatively, a CsA/cyclophilin D complex might affect another mitochondrial protein by analogy with the mechanism by which CsA inhibits cytosolic calcineurin (Clipstone and Crabtree, 1992).

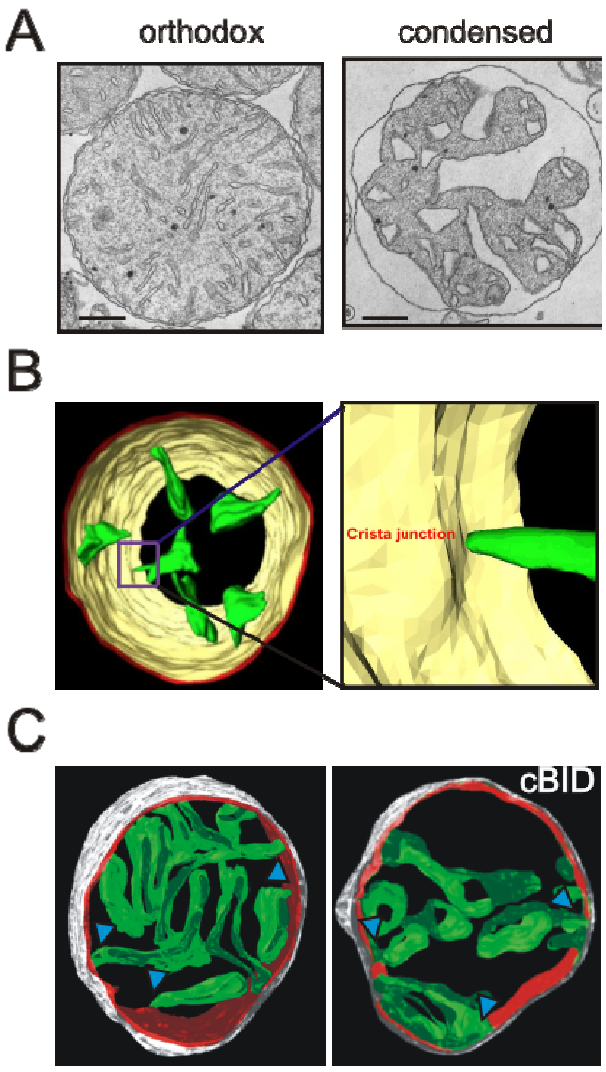

Figure 5 Ultrastructure of mitochondria and cristae remodeling
(A) The condensed conformation and the orthodox conformation. The spatial folding of the electron-transport membrane is random. The volume of the matrix is approximately 50% of the total mitochondrial volume. X 110,000. (taken from (Hackenbrock, 1966)). (B). The 3d of mitochondria with a magnification to indicate the cristae compartments and tubular narrow cristae junction (taken from (Mannella et al., 2001)). (C) Apoptotic cristae remodeling: Surface-rendered views of tomographic reconstructions; the OMM is depicted in green, the inner boundary membrane in red, and the cristae in green. On the right typical enlargement of cristae junction and increase in cristae complexity is clearly visible

It has been proposed that tBid promotes negative curvature of membranes and as a result it destabilizes the IMM (Epand et al., 2002). Conversely, CsA induces positive membrane curvature, counteracting tBID effects (Epand et al., 2002). The possibility that intrinsic membrane curvature plays a crucial role in regulating *cristae* remodeling is an attractive idea.

Finally, it is tempting to argue that tBID, with its recently discovered lipid transferase activity (Esposti et al., 2001) might be involved in changing intrinsic curvature by altering lipid composition.

Recently, the group of Terry Frey (Sun et al., 2007) identified remodeling of the inner mitochondrial membrane into many separate vesicular matrix compartments using a correlated three-dimensional light and electron microscopy. However, despite this remodeling accompanied release of IMS proteins, they suggested that it was not required for efficient release of cytochrome *c* and that it resulted as a “byproduct” of caspase activation. In addition, the authors took advantage of a mathematical model and hypothesize that *cristae* junctions should not prevent release of intra-*cristae* cytochrome *c* within 1–2 minutes, the time required for apoptotic cytochrome *c* release. These results suggest that mitochondrial remodelling might be an effect, rather than a proximate cause of apoptosis; but at the same the authors justify this apparent incongruity saying that under other conditions apoptosis may proceed by a different mechanism.

A number of discrepancies arouse between this study and the previous conducted in our laboratory. First, remodelling of the *cristae* has been observed in isolated mitochondria devoid of caspases. Furthermore, it was not sensitive to the pan-caspase inhibitor zVAD-fmk, it was reported to occur in Bak-deficient mouse liver mitochondria (that do not release cytochrome *c*)

as well as in DKO cells, where the activation of caspases is prevented by the lack of cytochrome *c* release. Second, the correlative studies performed by Frey and colleagues rely on tagged cytochrome *c* molecules, whose intramitochondrial cytochrome *c* distribution is unknown (it is conceivable that this overexpressed cytochrome *c* does not localize to the *cristae* compartment as the native one). Third, no analysis is performed by Frey and colleagues on the effect of caspase inhibition on the diameter of the *cristae* junction in the subpopulation of mitochondria from where the tagged cytochrome *c* has not been released. In conclusion, in our view, remodeling of mitochondrial ultrastructure remains a crucial commitment step during apoptosis.

It must be noted that changes in matrix conformation are not only an apoptotic hallmark but may have also a physiological relevance. In fact, more than 40 years ago, Hackenbrock described a reversible folding of the *cristae* compartments tightly linked to the metabolic state of isolated mitochondria (Hackenbrock, 1966) (Figure 5A). This ultrastructural flexibility was characterized by a change of matrix configuration from an orthodox state, in non stimulated respiration, to a condensed state reached after ADP addition; of note, the volume of isolated mitochondria is not changing during this transition.

The condensed conformation has two major characteristics which distinguish it from the orthodox conformation (Figure 5A):

(a) randomly folded inner membrane with very little suggestion of organized mitochondrial *cristae*;

(b) decreased matrix volume.

As a consequence of the volume decrease in the matrix compartment, there is a volume increase in the outer compartment-intra*cristae* space which is presumably a sucrose-accessible space.

In the EM analysis, increased opacity of the matrix resulted from increased diffraction of electrons, making the matrix appear darker in the image. Therefore, the more condensed the matrix, the more electrons it diffracts and the darker it appears on the micrograph.

Taking advantage of three-dimensional analysis, Mannella and colleagues studied and confirmed the morphological changes observed by Hackenbrock and suggested that the interconversion between these states can only be achieved by a dynamic fusion and fission of the IMM (Mannella et al., 2001).

Many efforts have been made to understand whether apoptotic *cristae* remodeling and O/C transition are the same phenomenon, with dramatically different biochemical results. An interesting link between mitochondrial dysfunction and matrix configuration changes was given by the group of Thompson, who demonstrated that a decrease in $\Delta\psi_m$ leads to matrix condensation and exposure of cytochrome *c* to the intermembrane space, facilitating cytochrome *c* release and cell death following an apoptotic insult (Gottlieb et al., 2003).

Thus, it is tempting to speculate that both in apoptotic *cristae* remodeling and O/C transition cytochrome *c* is mobilized to the IMS and the different outcome is established by the activation of the upstream pathway of apoptosis: the oligomerization of BAX and BAK. On the other hand it is believed that another process must occours in order to mobilize cytochrome *c* from the IMM once *cristae* remodeling occurred.

3.4.4.2 Cytochrome c mobilization:

Orrenius and colleagues demonstrated that cytochrome *c* detachment from its high affinity cardiolipin binding sites on the inner mitochondrial membrane is crucial (Ott et al., 2002) for a complete cytochrome *c* release.

Cytochrome *c* is present as loosely and tightly bound pools attached to the inner membrane by its association with cardiolipin. In order to release cytochrome *c,* this interaction must first be disrupted to generate a soluble pool of the protein, as substantiated by the fact that neither disrupting the interaction of cytochrome *c* with cardiolipin, nor permeabilizing the outer membrane with BAX, alone, was sufficient to trigger this protein's release.

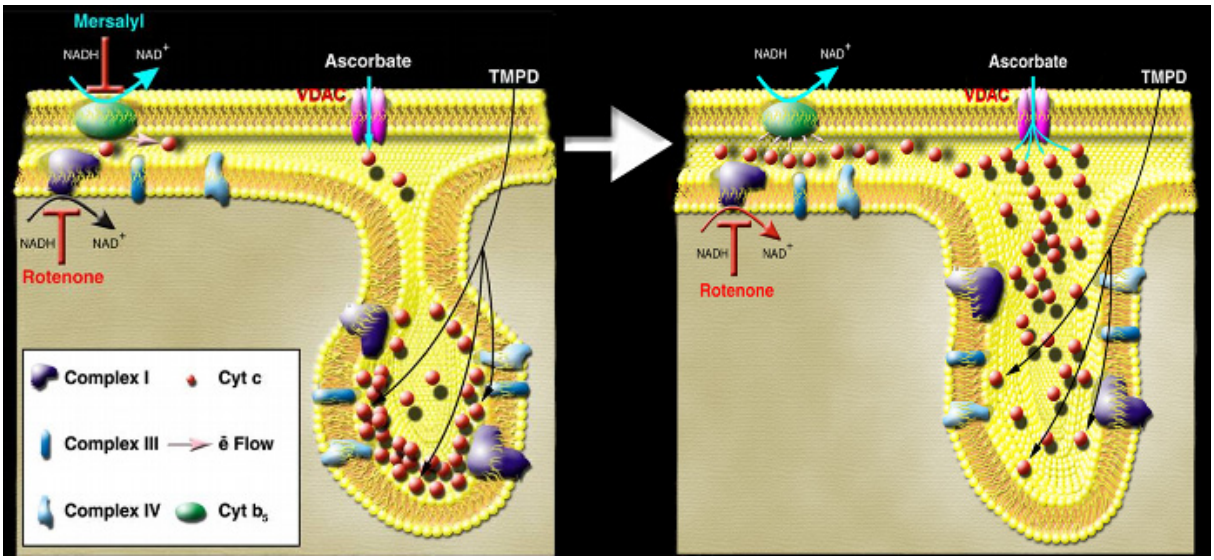

Figure 6 Schematic of different intramitochondrial cytochrome *c* pools and their accessibility by cytochrome *b5* or ascorbate. Symbols used are detailed in the cartoon legend. Taken from (Scorrano et al., 2002)

3.4.4.2.1 Cytochrome *c* binding to cardiolipin

Cytochrome *c* is a water-soluble basic protein that is bound to the mitochondrial inner membrane by its association with the phospholipid cardiolipin (CL). This association facilitates electron transport between complexes III and IV of the respiratory chain. The binding of cytochrome *c* to CL is specific and stoichiometric (Tuominen et al., 2002), thus under normal physiological conditions, CL anchors the protein to the inner mitochondrial membrane to participate in electron transport thereby ensuring a limited soluble pool of the hemoprotein. CL is an anionic phospholipid found exclusively in the inner mitochondrial membrane of eukaryotic

cells (Schlame et al., 1993). Its unique structure among phospholipids confers fluidity and stability to the mitochondrial membrane, as well as contact sites between the inner and outer mitochondrial membranes (Grijalba et al., 1998). Due to its intracellular distribution CL has been postulated, and more recently demonstrated, to be an essential component in many mitochondrial processes, such as electron transport, ADP/ATP translocation, ion permeability, and protein transport. Furthermore, many of the inner membrane respiratory enzymes, such as cytochrome *c* oxidase, have a specific association with CL and their activities are dependent on the presence of CL, and not on other phospholipids (Zhang et al., 2002).

3.4.4.2.2 Physicochemical properties of bounded cytochrome *c*

Cytochrome *c* bears a net positive charge of +8 and binds avidly to model membranes containing acidic phospholipids. Yet, the interaction of cytochrome *c* with acidic phospholipids involves more than electrostatic attraction.

It is well known, since the early study of Jacobs and Sanadi (Jacobs and Sanadi, 1960), that increase of ionic strength and osmotic swelling depress the binding of cytochrome *c* to the inner mitochondrial membrane. Ferguson Miller and colleagues (Ferguson-Miller et al., 1976) reported that increase of ionic strength, and more specifically physiological concentrations of ATP, decrease the affinity of this binding to the point that interaction of cytochrome *c* with numerous mitochondrial phospholipids sites can competitively remove cytochrome *c* from the oxidase. It is suggested that this effect of ATP represents a possible mechanism for the control of electron flow to the oxidase.

Two different types of interaction have been characterized for the membrane binding of cytochrome *c* and have been shown to be due to distinct sites, named the A-site and the C-site, respectively (Rytomaa and Kinnunen, 1995). More specifically, negative surface charge density of the membranes, pH, and ionic strength together determine whether cytochrome *c* is bound electrostatically via its A-site or by hydrogen bonding and hydrophobic interaction via its C-site (Rytomaa and Kinnunen, 1995). The hydrophobic component of C-site-mediated interaction of cytochrome *c* with an acidic phospholipid has been suggested to be due to the so-called extended lipid anchorage, a general mechanism for peripheral membrane protein-lipid interaction (Kinnunen et al., 1994).

In a similar fashion, Hackenbrock showed that membrane binding of cytochrome *c* under ionic conditions that are physiological for the IMS (125 mM KCl) renders a complex mixture of membrane-bound forms that differ in intrinsic electron transfer (ET) activity (Cortese et al., 1998).

3.4.4.2.3 Breaching cytochrome *c* binding to the IMM

The hypothesis proposed by S. Orrenius that the electrostatic and/or hydrophobic interactions between CL and cytochrome *c* must be ‘‘breached’’ in order for cytochrome *c* to leave

mitochondria (Ott et al., 2002) is also supported by previous studies demonstrating that the peroxidation of CL virtually abolishes this interaction (Shidoji et al., 2002). CL oxidation designates an important stage of the execution of apoptotic program because oxidized CL in contrast to non-oxidized CL does not effectively bind cytochrome *c* (Petrosillo et al., 2003; Petrosillo et al., 2004).

In addition, the group of Kagan demonstrated that cytochrome *c* may act as the direct source of peroxidation of CL: the role of cytochrome *c* changes from mostly an electron-carrier in normal mitochondria to mostly a CL-specific peroxidase during apoptosis. The switch between these two functions is due to cytochrome *c* association with CL, whose availability at the sites of location of cytochrome *c* sets the limit for peroxidase activity: it is likely that migration of CL early in apoptosis and its interaction with cytochrome *c* regulates itself the peroxidase activity of cytochrome *c* in a self regulating system [for a review see (Bayir et al., 2006)].

To emphasize the role of CL in the apoptotic process it should be considered that in cellular models in which CL synthesis is lacking, cytochrome *c* in the IMS is increased and can be prognostic of an increased apoptosis and on the other hand stabilization of CL levels might protect against apoptosis (Choi et al., 2007).

3.4.4.3 Factors that affect the shape of cristae

It is clear that *cristae* shape has more than a single physiological role and that the topology of the IMM is a complex function of spontaneous curvature, dynamic physical interaction between IMM and OMM, and probably the action of mitochondria-shaping proteins: for example the extension of the *cristae* can be likely regulated by the volume restriction dictated by the OMM or, on the other hand, the protein-rich matrix can set the minum volume below which the space bounded by the IMM and OMM can collapse. Besides these kinds of intrinsic factors, new findings implicate several mitochondrial components as regulators of this membrane topology.

3.4.4.3.1 ANT and tBID interactions

As noted above, tBid triggers a remodeling of mouse liver mitochondria, involving reversal of curvature of the crista membranes. Epand et al. have observed that tBid induces reversed curvature in cardiolipin-containing membrane phases (Epand et al., 2002), suggesting that the remodeling of the cardiolipin-rich mitochondrial inner membrane might be lipid-mediated, i.e., a direct effect of tBid on the organization of lipids in these membranes. Further evidence in support of this hypothesis has been provided by studies involving the adenine nucleotide translocator (ANT), the inner membrane carrier protein which binds cardiolipin and requires it for activity (Hoffmann et al., 1994). Gonzalvez et al. recently have reported that tBid inhibits ANT activity of yeast mitochondria in a cardiolipin-dependent manner, consistent with this inhibition being an indirect effect of tBid on cardiolipin organization (Gonzalvez et al., 2005). Interestingly, Klingenberg and co-workers reported three decades earlier that ANT ligands, such as the

inhibitor atractyloside (ATR), induce a morphological change in beef heart mitochondria that, in retrospect, appears similar to the tBid induced remodeling of mitochondria. Klingenberg et al. recognized the change in inner membrane shape as a reversal in membrane curvature and attributed it to a ligand-induced “re-orientation” of a mobile carrier protein to the matrix side of the membrane. However, Klingenberg later questioned whether the stoichiometry of ANT could be sufficient to cause so dramatic a change in inner membrane structure (Klingenberg, 1973; Klingenberg, 1976; Klingenberg, 1992). Alternative explanations include that: (i) ligand-induced conformational changes in ANT cause a reorganization of the cardiolipin in the inner membrane, which, in turn, triggers the inner membrane remodeling; (ii) atractyloside acts by inducing the PT, which is associated with the remodelling of the *cristae*; (iii) tBid (like ATR) directly interacts with ANT and the reversal of curvature that both induce in the mitochondrial inner membrane is protein-mediated, *i.e.* due to a conformational change in the carrier protein.

3.4.4.3.2 ATP synthase

In yeast, the mitochondrial F_1F_0-ATP synthase complex has been strongly implicated in contributing to the curvature of the inner membrane as a result of its oligomerization. Allen showed that F1 complexes are arranged as a double row of particles along the full length of the helically shaped tubular *cristae* in *Paramecium multimicronucleatum* (Allen et al., 1989). Based on these observations, he proposed that the double-cone shape of ATP synthase dimers offers the potential to form a rigid arc, which leads to an inner membrane protrusion that is then amplified to form tubules upon association of additional complexes during mitochondrial biogenesis. Interestingly, Paumard et al. have shown that mutations in ATP synthase subunit e (also called Atp21p and, formerly, Tim11p) inhibit formation of the ATP synthase dimer (the first step in formation of larger oligomers) and results in appearance of concentric onion-like *cristae* (Paumard et al., 2002).

More recently, single-particle electron microscopic studies from two laboratories (Minauro-Sanmiguel et al., 2005) and (Dudkina et al., 2005) have revealed the likely basis for the membrane bending ability of ATP synthase. Since the lateral dimension of the membrane-embedded F_0 domain (at which dimer binding occurs) is considerably less than that of the extra-bilayer F_1 domain, lateral close-packing causes the complexes to be tilted with respect to each other and so imparts a local bend to the membrane of 40° in the case of beef heart ATP synthase and 70° for the algal complex.

A mitochondrial DNA mutation in the gene encoding subunit 6 (F_0 domain) of the ATP synthase recently has been described in *Drosophila* (Celotto et al., 2006). This mutation (ATP6^1) causes marked reduction in ATP production in neuronal mitochondria and very unusual inner membrane topology: rounded crista compartments contiguous with flattened lamellar regions of the same membrane. A possible explanation for this highly unusual topological transition is that ATP synthase dimerization is normally inhibited in flat, lamellar *cristae* and that the ATP6^1

mutation somehow weakens the inhibition, allowing complex dimerization and, consequently, increased membrane curvature.

The major criticism of this experimental approach is that the few mitochondrial ATP synthase mutants isolated were often genetically unstable, giving rise to *petites*, *i.e.* cells bearing large deletions in the mtDNA (ρ^- or totally lacking mtDNA (ρ^0). To avoid dramatic consequences on mitochondrial bioenergetics following mutation of ATP synthase genes, Rak and colleagues generated an elegant model for investigating the consequences of a specific lack of *ATP6* obtaining only a moderate mtDNA instability (Rak et al., 2007). In these conditions they showed that *cristae*-like structures were clearly discernible in the *atp6* mutant indicating that neither Atp6p nor the ATP synthase activity is crucial for *cristae* generation. A corollary, according to Allen's model, would be that absence of Atp6p should not prevent the formation of the double-cone shape of ATP synthase dimers presumed to be responsible for *cristae* formation.

3.4.4.3.3 Mitofilin

Mitofilin, also known as heart muscle protein, is a 90-kDa inner-membrane protein, with predicted membrane anchor and coiled-coil domains with an amino-terminal transmembrane domain with the majority of the protein is extruding into the intermembrane space (Gieffers et al., 1997). John et al. recently have reported that down-regulation of mitofilin in HeLa cells by siRNA results in the formation of concentric onion-like inner mitochondrial membranes (John et al., 2005). The mitofilin-deficient mitochondria tend to form progressively larger membrane swirls, which were analyzed by electron tomography. The larger IMM structures were found to be composed of a complex, interconnected network of membranes totally lacking tubular connections to each other or to the peripheral inner membrane. John et al. have proposed that mitofilin's physiological role is to maintain normal *cristae* morphology, in particular, the formation or stabilization of *cristae* junctions.

Recently, the group of Capaldi demonstrated that mitofilin reside in a mitochondrial complex spanning from the IMM to the OMM that can have an implication in regulating protein import (Xie et al., 2007). Interestingly, mitofilin is found to be reduced significantly in fetal Down's syndrome brain (Myung et al., 2003) and to be a target antigen in melanoma-associated retinopathy (Pfohler et al., 2007).

3.4.4.3.4 Mitochondrial dynamin-like proteins: A Role of OPA1/Mgm1p in *cristae* remodeling?

As proposed by Mannella, three-dimensional images provided by electron tomography strongly suggest that the topology of the inner mitochondrial membrane represents a balance between membrane fusion and fission processes. It should be noted that despite ATP synthase may regulate positive curvature of IMM it is still unclear how the negative curvature nearby *cristae* junction can be achieved and modulate in time. Dynamin related proteins can be natural

candidate for this role and, in fact, many studies are ongoing in which proteins involved in mitochondrial dynamics are genetically manipulated.

OPA1 (see 3.2.1.1.2 for more details), is the only member of the dynamin family of GTP-binding proteins, known so far to be resident in the IMM. EM analysis of OPA1-depleted cells suggested that this protein may have a role in *cristae* maintenance (Griparic et al., 2004; Olichon et al., 2003; Sesaki et al., 2003) since disorganized *cristae* with irregular shape, some of which showed large *cristae* junctions were observed. A possible role of OPA1/Mgm1 in structuring *cristae* is consistent with its mitochondrial localization which is basically in the *cristae*, as confirmed by biochemical (Griparic et al., 2004; Olichon et al., 2003; Pelloquin et al., 1999; Wong et al., 2000) and immunogold staining (Vogel et al., 2006), even if it not clear whether it concentrates at the *cristae* junction.

OPA1 is crucially involved in mitochondrial dynamics and levels of OPA1 directly correlate with extension of fusion event. However, since some defects of OPA1-depletion resemble *cristae* derangement characteristic of apoptosis it was tempting to speculate that OPA1 may have a dual role both in controlling mitochondrial dynamics and regulating *cristae* remodeling

The major aim of my PhD work has therefore been to determine the role of OPA1 in apoptotic *cristae* remodeling.

.

4 Experimental procedures

Frezza C, Cipolat S, Scorrano L.
Organelle isolation: functional mitochondria from mouse liver, muscle and cultured fibroblasts.
Nat Protoc. 2007;2(2):287-95.

Frezza C, Cipolat S, Scorrano L Frezza C, Cipolat S, Scorrano L
Measuring mitochondrial shape changes and their consequences on mitochondrial involvement during apoptosis.
Methods in Molecular Biology 2007, 372

PROTOCOL

Organelle isolation: functional mitochondria from mouse liver, muscle and cultured filroblasts

Christian Frezza, Sara Cipolat & Luca Scorrano

Dulbecco-Telethon Institute, Venetian Institute of Molecular Medicine, Via Orus 2, 35129 Padova, Italy. Correspondence should be addressed to L.S. (luca.scorrano@unipd.it).

Published online 22 February 2007; doi:10.1038/nprot.2006.478

Mitochondria participate in key metabolic reactions of the cell and regulate crucial signaling pathways including apoptosis. Although several approaches are available to study mitochondrial function *in situ* are available, investigating functional mitochondria that have been isolated from different tissues and from cultured cells offers still more unmatched advantages. This protocol illustrates a step-by-step procedure to obtain functional mitochondria with high yield from cells grown in culture, liver and muscle. The isolation procedures described here require 1–2 hours, depending on the source of the organelles. The polarographic analysis can be completed in 1 hour.

INTRODUCTION

Mitochondria are central organelles controlling the life and death of the cell. They participate in key metabolic reactions, synthesize most of the ATP and regulate a number of signaling cascades, including apoptosis[1].

Since the early years of "hard-core" bioenergetics when mechanisms behind energy conservation were avidly investigated, mitochondrial research has benefited from the availability of preparations of organelles isolated from tissues. We owe this to the pioneering work of George Palade and coworkers, who in the late 1940s developed a protocol to isolate mitochondria, based on differential centrifugation[2]. They built on the earlier work of Bensley and Hoerr[3], who isolated a mixed membranous fraction by centrifugation from freeze-thawed guinea-pig liver that was probably enriched in mitochondria. The intuition of Palade was to apply differential centrifugation to allow for separation of the constituents of the cell based on their different sedimentation properties following mechanical homogenization of the tissue. This approach was a real Copernican revolution for mitochondrial research, allowing the isolation of pure organelles with high yields. As a practical consequence, in the subsequent 20 years, we saw such amazing discoveries: the mechanism of energy conservation[4]; the identification of mitochondrial DNA[5,6] and of import of mitochondrial precursor proteins[7]; the definition of mitochondrial ultrastructure, with the development of the so-called "Palade's model"[8]; and last but not least, the discovery of inner mitochondrial membrane channels[9].

After almost 15 years during which mitochondria left the center stage of biomedical research, they made their grand *reentrée* in the 1990s, following the discovery that they amplify apoptosis by releasing cytochrome *c* and other intermembrane space proteins required to activate fully effector caspases[10,11]. Although it appears clear that mitochondria play a crucial role in apoptosis, the precise mechanism by which cytochrome *c* is released remains a matter of intense debate and research[12]. Moreover, evidence is mounting on the role of this organelle in several pathophysiological processes, including neurodegeneration[13], neuronal morphogenesis and plasticity[14] and infertility[15]. These findings, added to the results of old and new areas of research, aimed at unraveling the basic biological mechanisms of mitochondrial function. From the transport of metabolites and ions, to the elucidation of the mechanisms and proteins involved in protein import, and to the dynamic behavior of mitochondria, all of these fields benefit greatly from the availability of isolated, pure organelles.

This protocol describes how to obtain functional, purified, intact mitochondria from three different sources: liver[16], skeletal muscle[17] and cultured cells[18]. These variants intend to be exemplificative and not exhaustive, as they do not cover the different sources from which mitochondria can be isolated. For example, isolation of mitochondria from yeast cells is tailored on the mechanical and osmotic characteristics of these lower eucaryotes[19]. Since our intention is to give a general framework for different organs and for cultured cells that can be in any case modified by the individual researcher, following exactly these protocols is best suited only for isolation of organelles from the described tissues and cells. However, our experience indicates that the protocol used with fibroblasts can be adopted without modification to isolate mitochondria from other cell lines such as HeLa and the prostate cancer cell line LnCaP. On the other hand, the protocols to isolate mitochondria from organs other than muscle and liver differ from the ones described here. We therefore strongly advise the reader to refer to published protocols specific for brain[20], brown adipose tissue[21], and heart[22].

It should be stressed that protocols available to isolate mitochondria are somewhat differ from ours, especially in the speeds of the differential centrifugation steps and in the sugar used as osmolyte in the isolation buffer. While in our experience small changes in the sedimentation speeds (600 vs. 800*g*, 7,000 vs. 8,000*g*) do not affect quality and yield of the mitochondrial preparation, it has been reported that the use of monosaccharides such as mannitol results in better coupled isolated mitochondria[23,24]. In our experience the use of mannitol did not improve the quality of our mitochondrial preparations. Should the reader find that quality or yield of mitochondria isolated using our protocol is unsatisfactory, it is advisable to try to substitute sucrose with a monosaccharide like mannitol. The ultimate goal of a mitochondrial isolation is to obtain organelles as pure and as functional as possible. We strongly advise, especially if mitochondria are used in functional assays (e.g., release of cytochrome *c*, mitochondrial fusion, protein import and

PROTOCOL

production of reactive oxygen species), to always measure the coupling of the preparation using an oxygen electrode. These protocols therefore end with a description of how to measure mitochondrial respiration to ascertain the quality of the preparation. Well-coupled mitochondria are the first step to achieving reliable, reproducible results in assays aimed at investigating the mechanisms of mitochondrial involvement in complex biological phenomena.

In conclusion, these protocols represent a valuable starting point to obtain pure mitochondria from tissues and cells. Isolated mitochondria can then be used to study the function of the organelle, response to apoptotic stimuli, characteristics of cytochrome *c* release, protein import and many other aspects of mitochondrial biology and pathophysiology that require a source of pure and functional organelles.

MATERIALS

REAGENTS

- Cell line of interest or liver or muscle isolated from mice
- Mice of the desired genetic background (Charles River or Jackson Laboratories)
- Dulbecco's phosphate-buffered saline without Ca^{2+} and Mg^{2+} (PBS, Invitrogen, cat. no. 14200-067)
- Sucrose (Sigma, cat. no. 84100)
- Potassium phosphate monobasic (Pi, Sigma, cat. no. P5379)
- Sigma7-9 (Tris, Sigma, cat. no. T1378)
- 4-Morpholinepropanesulfonic acid (MOPS; Sigma, cat. no. M1254)
- Disodium ethylenediaminetetraacetate dihydrate (EDTA; Sigma, cat. no. ED2SS)
- Ethylene-bis(oxyethylenenitrilo)tetraacetic acid (EGTA; Sigma, cat. no. E4378)
- Potassium chloride (Baker, cat. no. 0208)
- Magnesium chloride hexahydrate (Sigma, cat. no. M9272)
- Bovine serum albumin (BSA; Sigma, cat. no. A6003)
- Dulbecco's modified Eagle's medium (Invitrogen, cat. no. 11971025)
- 200 mM L-glutamine (Invitrogen, cat. no. 25030024),
- Fetal bovine serum (Invitrogen, cat. no. 10270106)
- 5,000 U ml^{-1} penicillin/5,000 µg ml^{-1} streptomycin (Invitrogen, cat. no. 15070063)
- 10 mM minimal essential medium nonessential amino-acid solution (Invitrogen, cat. no. 11140)
- 0.25% (w/v) trypsin–EDTA solution (Invitrogen, cat. no. 25200072)
- Adenosine 5′-diphosphate sodium salt (ADP; Sigma, cat. no. A2754)
- Carbonyl cyanide 4-(trifluoromethoxy)phenylhydrazone (FCCP; Sigma, cat. no. C2920)
- Glutamic acid (Sigma, cat. no. 27647)
- Malic acid (Sigma, cat. no. M1000)
- Succinic acid (Sigma, cat. no. S3674)
- Rotenone (Sigma, cat. no. R8875)
- L-Ascorbic acid (Sigma, cat. no. 255564)
- *N,N,N,N*-Tetramethyl-*p*-phenylenediamine dihydrochloride (TMPD; Sigma, cat. no. T3134)
- Antimycin A (Sigma, cat. no. A8674)

EQUIPMENT

- 500 cm^2 dishes for cell culture (Nunclon, cat. no. 16 6508)
- 18-cm cell scrapers (Falcon, cat. no. 353085)
- Motor-driven tightly fitting glass/Teflon Potter Elvehjem homogenizer (**Fig. 1**)
- Clark-type oxygen electrode (Hansatech Oxygraph; **Fig. 2**)
- 50 ml polypropylene Falcon tubes
- 14 ml polypropylene Falcon tubes
- 1.5 ml microfuge test tube
- 30 ml round-bottomed glass centrifuge tube (Kimble, cat. no. 45500-30)
- Rubber adapter sleeve for centrifuge tube (Kimble, cat. no. 45500-15)
- Refrigerated centrifuge for 50 ml Falcon tubes and glass centrifuge tube
- Hamilton syringe: 10 µl (Hamilton, cat. no. 701 N) and 50 µl (Hamilton cat. no. 705 N)

REAGENT SETUP

Cell culture medium Use the medium recommended for your favorite cell line. For the cell lines mentioned in this protocol, use Dulbecco's modified Eagle's medium supplemented with 10% (v/v) fetal bovine serum, 0.1 mM minimal essential medium nonessential amino acids, 2 mM L-glutamine, penicillin–streptomycin 50 U ml^{-1} and 50 µg ml^{-1}, respectively.

Cells Two or three days before performing the experiments, plate cells in 500 cm^2 tissue-culture dishes. Use 70 ml of cell culture medium for each plate.

▲ CRITICAL Ensure that the cells are spread thoroughly wide on the plates: for high yield of isolated mitochondria, it is crucial to reach almost 100% confluence on the day of the experiment.

1 M sucrose Dissolve 342.3 g of sucrose in 1 liter of distilled water; mix well and prepare 20 ml aliquots; store them at −20 °C.

0.1 M Tris/MOPS Dissolve 12.1 g of Tris in 500 ml of distilled water, adjust pH to 7.4 using MOPS powder, bring the solution to 1 liter and store at 4 °C.

1 M Tris/HCl Dissolve 121.14 g of Tris in 500 ml of distilled water, adjust pH to 7.4 using HCl; bring the solution to 1 liter and store at room temperature.

0.1 M EGTA/Tris Dissolve 38.1 g of EGTA in 500 ml of distilled water, adjust pH to 7.4 using Tris powder, bring the solution to 1 liter and store at 4 °C.

0.5 M $MgCl_2$ Dissolve 101.7 g of $MgCl_2$ in 1 liter of distilled water and store at 4 °C.

1 M KCl Dissolve 74.6 g of KCl in 1 liter of distilled water and store at 4 °C.

1 M EDTA Dissolve 372.2 g of EDTA in 500 ml of distilled water, adjust pH to 7.4 using Tris powder, bring the solution to 1 liter and store at 4 °C.

10% BSA Dissolve 10 g of BSA in 100 ml of distilled water and store at −20 °C.

1 M Pi Dissolve 136.1 g of KH_2PO_4 in 500 ml of distilled water, adjust pH to 7.4 using Tris powder, bring the solution to 1 liter and store at 4 °C.

10 mM ADP Dissolve 4.7 mg of ADP in 1 ml of distilled water. Adjust pH to 7.4, prepare 100 µl aliquots and store in the dark at −20 °C for up to 6 months.

20 mM FCCP Dissolve 5.1 mg of FCCP in 1 ml of absolute ethanol. The color of the solution is faint yellow. Store at −20 °C. Dilute the stock solution to 100 µM by adding 10µl of 20 mM FCCP in 2 ml of absolute ethanol, just prior to use.

Figure 1 | Glass/Teflon Potter Elvehjem homogenizers. The homogenizer on the left (5 ml) is most suitable for isolation of mitochondria from cells, whereas the one on the right (30 ml) is more appropriate for isolation from tissues.

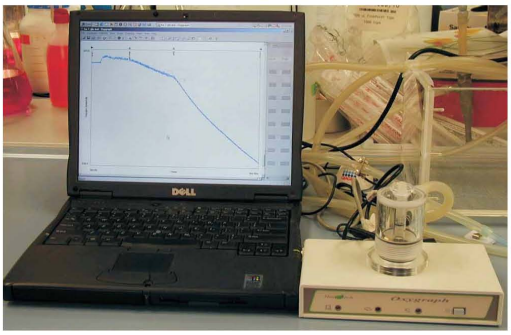

Figure 2 | A Clarke-type oxygen electrode connected to a laptop and a water bath. The trace on the screen corresponds to the recording of the experiment running when the photograph was taken.

0.25 M glutamate/0.125 M malate Dissolve 9.2 g of glutamic acid and 4.2 g of malic acid in 100 ml of distilled water. Adjust pH to 7.4 with Tris base to achieve complete dissolution of the salts. Add water to bring the volume to 250 ml, prepare 10 ml aliquots and store at −20 °C for up to 6 months.
0.5 M succinate stock solution (100×) Dissolve 3.0 g of succinic acid in 30 ml of distilled water. Adjust pH with Tris base to achieve complete solubilization of the salts. Add water to make up the volume to 50 ml, prepare 10 ml aliquots and store at −20 °C for up to 6 months.
2 mM rotenone stock solution Dissolve 4.7 mg of rotenone in 6 ml of absolute ethanol. Mix well for complete dissolution. ▲ CRITICAL Rotenone in organic solvents decomposes and is oxidized upon exposure to light and air. The solution, previously transparent, becomes brownish. It is imperative to protect the stock solution from direct light using an aluminum foil. ! CAUTION Rotenone is highly toxic: avoid skin contact and inhalation.

PROCEDURE

1| Mitochondria can be isolated from a variety of cells or tissues. Option A describes isolation of mitochondria from mouse embryonic fibroblasts (MEFs) (see **Fig. 3** for a timeline); option B describes isolation of mitochondria from mouse liver (see **Fig. 4** for a timeline); and option C describes isolation of mitochondria from mouse skeletal muscle (see **Fig. 5** for a timeline).

(A) Isolation of mitochondria from MEFs ● TIMING approximately 2 h

(i) Remove the medium from the cells and wash the cells once with PBS.
(ii) Remove PBS and detach the cells using a cell scraper.
(iii) Transfer the cell suspension to a 50 ml polypropylene Falcon tube.
(iv) Wash the plate once with PBS and scrape the dish to detach the remaining cells.
(v) Transfer the cells to the same polypropylene Falcon tube defined in Step 3. In our experience, seeding 120 × 10^6 MEFs per dish 2 days before the experiment results in a good yield of mitochondria (approximately 3 mg of mitochondrial protein).
(vi) Centrifuge cells at 600*g* at 4 °C for 10 min.
(vii) Discard the supernatant and resuspend cells in 3 ml of ice-cold IB_c.

600 mM ascorbate stock solution Dissolve 5.2 g of ascorbic acid in 50 ml of distilled water, adjust pH to 7.4 and store at −20 °C for up to 6 months.
30 mM TMPD stock solution Dissolve 0.36 g of TMPD in 50 ml of distilled water; adjust pH to 7.4; store at −20 °C for up to 6 months. The color of the solution is deep blue owing to the oxidation of the compound by oxygen.
25 mg ml^{-1} antimycin A stock solution Dissolve 50 mg of antimycin A in 2 ml of absolute ethanol. Dilute the stock solution to 25 μg ml^{-1}, by adding 2 μl of 25 mg ml^{-1} Antimycin A in 2 ml of absolute ethonal, just prior to use. ! CAUTION Antimycin A is highly toxic: avoid skin contact and inhalation.
Buffer for cell and mouse liver mitochondria isolation (IB_c) Prepare 100 ml of IB by adding 10 ml of 0.1 M Tris–MOPS and 1 ml of EGTA/Tris to 20 ml of 1 M sucrose. Bring the volume to 100 ml with distilled water. Adjust pH to 7.4.
Buffer 1 for muscle mitochondria isolation (IB_m1) Prepare 100 ml of IB_m1 by mixing 6.7 ml of 1 M sucrose, 5 ml of 1 M Tris/HCl, 5 ml of 1 M KCl, 1 ml of 1 M EDTA and 2 ml of 10% BSA. Adjust pH to 7.4. Bring the volume to 100 ml with distilled water.
Buffer 2 for muscle mitochondria isolation (IB_m2) Prepare 100 ml of IB_m12 by mixing 25 ml of 1 M sucrose, 3 ml of 0.1 M EGTA/Tris and 1 ml of 1 M Tris/HCl. Adjust pH to 7.4. Bring the volume to 100 ml with distilled water.
Experimental buffer for cell and mouse-liver mitochondria (EB_c) To prepare 100 ml of EB_c, mix 12.5 ml of 1 M KCl, 1 ml of 1 M Tris/MOPS, 10 ml of 100 μl 0.1 M EGTA/Tris and 100 μl of Pi. Adjust pH to 7.4. Bring the volume to 100 ml with distilled water.
Experimental buffer for muscle mitochondria (EB_m) To prepare 100 ml of EB_m, add 1 ml of 1 M Tris/HCl, 1 ml of 0.5 M $MgCl_2$, 200 μl of 1 M Pi and 20 μl of 0.1 M EGTA/Tris to 25 ml of 1 M sucrose. Adjust pH to 7.4. Bring the volume to 100 ml with distilled water. ▲ CRITICAL Wash all glassware three times with bidistilled water to avoid Ca^{2+} contamination. Ca^{2+} overload is the most common cause for the dysfunction of isolated mitochondria. ▲ CRITICAL Prepare all the buffers the same day of the experiment, to avoid bacterial/yeast growth in stored buffers. ▲ CRITICAL Since pH depends on temperature, measure the pH of all solutions at 25 °C.

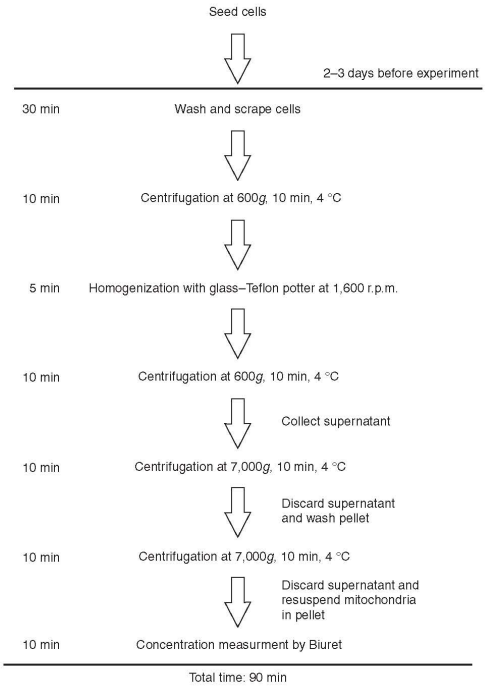

Figure 3 | Timing of isolation of mitochondria from MEFs.

PROTOCOL

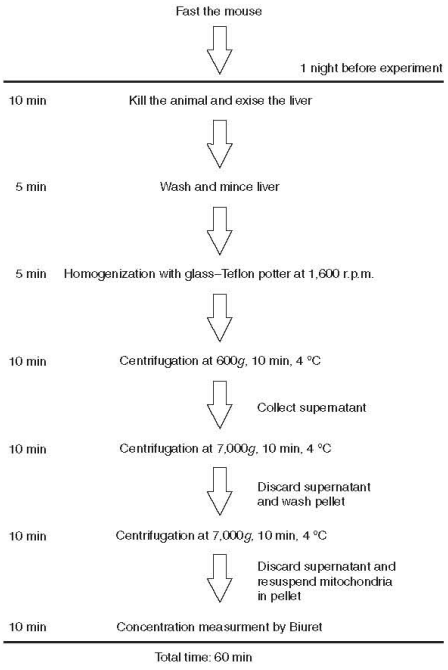

Figure 4 | Timing of isolation of mitochondria from mouse liver.

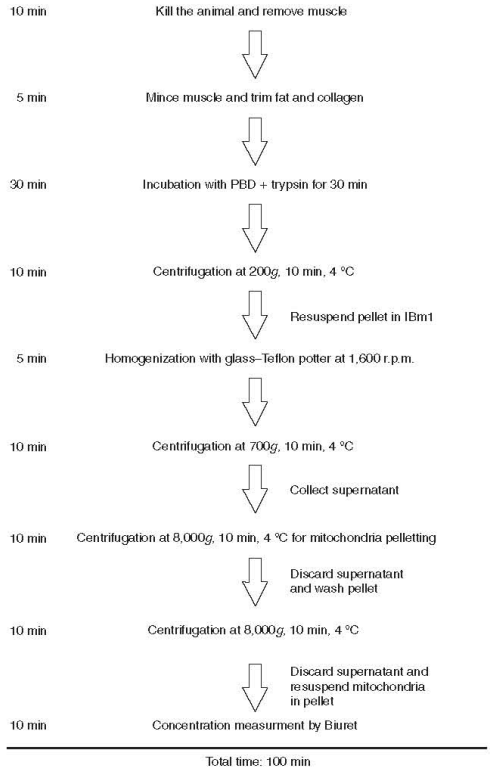

Figure 5 | Timing of isolation of mitochondria from mouse skeletal muscle.

(viii) Homogenize the cells using a Teflon pestle operated at 1,600 r.p.m.; stroke the cell suspension placed in a glass potter 30–40 times the cell suspension placed in a glass potter.
▲ **CRITICAL STEP** The Teflon–glass coupling represents the best compromise between homogenization of the cells and the preservation of mitochondrial integrity. Harsher techniques, including glass pestle in a glass potter, can easily damage mitochondria.
▲ **CRITICAL STEP** Precool the glassware in an ice-bath 5 min before starting the procedure. Homogenization as well as the following steps must be performed at 4 °C to minimize the activation of damaging phospholipases and proteases.
! **CAUTION** Wear protecting gloves while you are using the homogenizer to avoid possible injuries in the unlikely event that the potter breaks down.
? **TROUBLESHOOTING**

(ix) Transfer the homogenate to a 50 ml polypropylene Falcon tube and centrifuge at 600*g* for 10 min at 4 °C.

(x) Collect the supernatant, transfer it to a glass centrifuge tube and centrifuge it at 7,000*g* for 10 min at 4 °C.
? **TROUBLESHOOTING**

(xi) Discard the supernatant and wash the pellet with 200 µl of ice-cold IB_c. Resuspend the pellet in 200 µl of ice-cold IB_c and transfer the suspension to a 1.5 ml microfuge tube.

(xii) Centrifuge the homogenate at 7,000*g* for 10 min at 4 °C.

(xiii) Discard the supernatant and resuspend the pellet containing mitochondria. You can use a glass rod to loosen the pellet paste. Avoid adding IB and try to resuspend the mitochondria in the small amount of buffer that remains after discarding the supernatant. Use a 200 µl pipettor and avoid the formation of bubbles during the resuspension.

(xiv) Transfer the mitochondrial suspension to a microfuge and store it on ice.
▲ **CRITICAL STEP** Avoid diluting mitochondria with buffer. Mitochondria retain their functionality for a longer time, probably as a consequence of lower exposure to oxygen, when they are stored in a concentrated form.

(xv) Measure mitochondria concentration using the Biuret methods.
■ **PAUSE POINT** Mitochondria are now ready to be used in experiments: use the preparation within 1–3 h for better functional responses.
▲ **CRITICAL STEP** The typical yield of this preparation is ~50 mg ml^{-1} in a total volume of approximately 0.1 ml.

▲ CRITICAL STEP The Biuret method for measurement of mitochondrial concentration is accurate in the range of protein concentrations obtained from this protocol; other methods like the Bradford method can be used, but the mitochondrial lysate must be diluted in order to avoid saturation of the probe.

(B) Isolation of mitochondria from mouse liver ● TIMING approximately 1 h

(i) Starve the mouse overnight before the isolation experiment.

(ii) Kill an adult mouse (about 30 g) by cervical dislocation and rapidly explant the liver from the peritoneal cavity. Find the gallbladder and remove it using a scalpel. Immerse the liver in 50 ml of ice-cold IB_c in a small beaker.
▲ CRITICAL STEP Local and national regulations on animal care and handling vary. Check that you hold the appropriate authorization to perform animal experiments.

(iii) Rinse the liver free of blood by using ice-cold IB_c. Usually, four or five washes are sufficient to completely clarify the IB_c.

(iv) Mince the liver into small pieces using scissors. This should be performed while keeping the beaker in an ice bath.

(v) Discard the IB_c used during the mincing and replace it with 5 ml of ice-cold fresh IB_c. Transfer the suspension to the glass potter.
▲ CRITICAL STEP Homogenization, as well as the following steps, must be performed at 4 °C to minimize activation of damaging phospholipases and proteases.

(vi) Homogenize the liver using a Teflon pestle operated at 1,600 r.p.m., stroke the minced liver 3–4 times.
▲ CRITICAL STEP The optimal ratio between tissue and isolation buffer ranges between 1:5 to 1:10 (w:v).
▲ CRITICAL STEP Precool the glassware in an ice-bath 5 min before starting the procedure. Homogenization and the following steps must be performed at 4 °C to minimize activation of damaging phospholipases and proteases.
! CAUTION Wear protecting gloves while you are using the homogenizer to avoid possible injuries in the unlikely event that the potter breaks down.
? TROUBLESHOOTING

(vii) Transfer the homogenate to a 50 ml polypropylene Falcon tube and centrifuge at 600*g* for 10 min at 4 °C.

(viii) Transfer the supernatant to glass centrifuge tubes and centrifuge at 7,000*g* for 10 min at 4 °C.
? TROUBLESHOOTING

(ix) Discard the supernatant and wash the pellet with 5 ml of ice-cold IB_c.

(x) Centrifuge at 7,000*g* for 10 min at 4 °C.

(xi) Discard the supernatant and resuspend the pellet, containing mitochondria. You can use a glass rod to loosen the pellet paste. Avoid adding IB and try to resuspend the mitochondria in the small amount of buffer that remains after discarding the supernatant. Use a 1 ml pipettor and avoid the formation of bubbles during the resuspension process.

(xii) Transfer mitochondrial suspension into a 14 ml Falcon tube and store on ice.
▲ CRITICAL STEP Avoid diluting mitochondria with buffer as mitochondria retain their functionality for a longer time when kept concentrated, minimizing exposure to oxygen.
■ PAUSE POINT Mitochondria are now ready to be used in experiments; use the preparation within 1–3 h for better functional responses.

(xiii) Measure mitochondrial concentration using the Biuret methods.
▲ CRITICAL STEP The usual concentration of mitochondria in this kind of preparation is about 80 mg ml^{-1} and the total volume is about 1 ml.
▲ CRITICAL STEP The Biuret method for measurement of mitochondrial concentration is accurate in the range of protein concentrations obtained from this protocol; other methods like the Bradford method can be used, but the mitochondrial lysate must be diluted in order to avoid saturation of the probe.

(C) Isolation of mitochondria from mouse skeletal muscle ● TIMING approximately 1.5 h

(i) Kill the mouse by cervical dislocation. Using a scalpel, rapidly remove the skeletal muscles of interest and immerse them in a small beaker containing 5 ml of ice-cold PBS supplemented with 10 mM EDTA. A timeline of this protocol is outlined in **Figure 6**.
▲ CRITICAL STEP Local and national regulations on animal care and handling vary. Check that you hold the appropriate authorizations to perform animal experiments.
▲ CRITICAL STEP The use of EDTA instead of EGTA chelates also Mg^{2+}, which is extremely abundant in muscle tissue (given the high content in ATP). Mg^{2+} can influence mitochondrial function as well as the kinetics of cytochrome *c* release[25].

(ii) Mince the muscles into small pieces using scissors and trim visible fat, ligaments and connective tissue.

(iii) Wash the minced muscles twice or thrice with ice-cold PBS supplemented with 10 mM EDTA.

(iv) Resuspend the minced muscles in 5 ml of ice-cold PBS supplemented with 10 mM EDTA and 0.05% trypsin for 30 min.

(v) Centrifuge at 200*g* for 5 min and discard the supernatant.

(vi) Resuspend the pellet in IB_m1.

PROTOCOL

(vii) Homogenize the muscles using a Teflon pestle operated at 1,600 r.p.m.; stroke the minced muscle ten times.
▲ CRITICAL STEP The optimal ratio between tissue and isolation buffer ranges between 1:5 and 1:10 (w:v).
▲ CRITICAL STEP Precool the glassware in an ice-bath 5 min before starting the procedure. Homogenization, and the following steps, must be performed at 4 °C to minimize the activation of damaging phospholipases and proteases.
! CAUTION Wear protecting gloves while you are using the homogenizer to avoid possible injuries in the unlikely event that the potter breaks down.
Precool the glassware in an ice-bath for 5 min before starting the following steps.
? TROUBLESHOOTING
(viii) Transfer the homogenate to a 50 ml polypropylene Falcon tube and centrifuge at 700*g* for 10 min at 4 °C.
(ix) Transfer the supernatant to glass centrifuge tubes and centrifuge at 8,000*g* for 10 min at 4 °C.
? TROUBLESHOOTING
(x) Discard the supernatant and resuspend the pellet in 5 ml of ice-cold IB_m2.
(xi) Centrifuge at 8,000*g* for 10 min at 4 °C.
(xii) Discard the supernatant and resuspend the pellet containing mitochondria. You can use a glass rod to loosen the pellet paste. Avoid adding IB and try to resuspend the mitochondria in the small amount of buffer that remains after discarding the supernatant. Use a 200 µl pipettor and avoid the formation of bubbles during the resuspension process.
(xiii) Transfer mitochondrial suspension into a 14 ml Falcon tube and keep it on ice.
(xiv) Measure mitochondrial concentration using the Biuret methods.
▲ CRITICAL STEP This preparation normally yields 0.8 ml of 50 mg ml^{-1} mitochondria.
▲ CRITICAL STEP The Biuret method for measurement of mitochondrial concentration is accurate in the range of protein concentrations obtained from this protocol; other methods like the Bradford method can be used, but the mitochondrial lysate must be diluted in order to avoid saturation of the probe.

Measuring mitochondrial respiration ● TIMING approximately 1 h

2| Calibrate the Clarke-type oxygen electrode. Procedures vary from instrument to instrument. You should follow the manufacturer's instructions for the instrument you are using.

3| Equilibrate temperature and oxygen tension of EBc or EBm by placing open beakers containing the buffers in the water bath connected to the oxygraph. After 20–30 min, the temperature of the buffers is likely to be in equilibrium with that of the water bath.

4| Add an appropriate volume of EB to the oxygraph chamber. Use 0.5 ml for the mitochondria isolated from cells and 1 or 2 ml for the liver and muscle mitochondria. Close the oxygraph chamber.

5| Start the recording of the oxygen consumption.
▲ CRITICAL STEP Verify that the recording is stable and that no drifts are apparent. Drifts can mask the oxygen consumption by the mitochondrial preparation and thereby complicate the interpretation of the results.
? TROUBLESHOOTING

6| Wait for 2 min to obtain a stable baseline.

7| Using an appropriate Hamilton microsyringe, add mitochondria to obtain a final concentration of 1 mg ml^{-1}. A fast, transitory decrease in the oxygen content of the chamber will be observed, caused by anaerobiosis of the isolated mitochondria; this will be followed by a slower decrease caused by the respiration of the mitochondria. This is supported by endogenous substrates and is commonly referred to as "state 1" respiration[26].

8| Record oxygen consumption till it stops.
! CAUTION In liver mitochondria state 1 respiration commonly does not stop.

TABLE 1 | Substrates and inhibitors of the respiratory chain.

	Substrate (final concentration)	Inhibitor (final concentration)
Complexes I, III, IV	Glutamate (5 mM)/malate (2.5 mM)	///
Complexes II, III, IV	Succinate (5 mM)	Rotenone (2 µM)
Complex IV	Ascorbate (6 mM)/TMPD (300 µM)	Antimycin A (0.25 µg ml^{-1})

The span of the respiratory chain examined by each combination of substrate/inhibitor is indicated along with the final concentration to use in the oxygraphy experiments.

9| Using Hamilton microsyringes, add the appropriate concentrations of respiratory substrates and inhibitors for the complexes of the respiratory chain you wish to study (refer to **Table 1**). The mitochondrial suspension will now start consuming oxygen as a consequence of the basal activity of the respiratory chain in counteracting the inner mitochondrial membrane proton leak. This represents the so-called "state 2" respiration[26].
▲ CRITICAL STEP The rate of oxygen consumption should now be faster than the rate observed with buffer alone. This indicates that you have obtained functional, respiring mitochondria.
? TROUBLESHOOTING

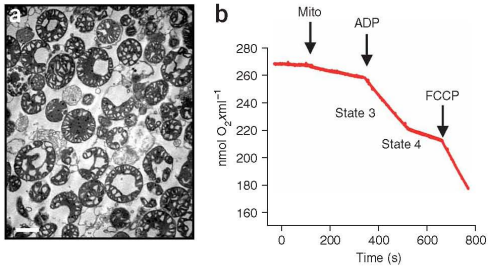

Figure 6 | Ultrastructure and oxygen consumption of mouse liver mitochondria isolated according to the protocol presented. (**a**) Mitochondrial ultrastructure. Mouse liver mitochondria (0.5 mg ml^{-1}) incubated in EB supplemented with 5 mM glutamate and 2.5 mM malate for 5 min were fixed by adding glutaraldehyde (final concentration 2.5% (v/v)). Transmission electron micrographs were acquired from randomly selected fields, as described[18]. (**b**) Oxygen consumption of 1 ml EB supplemented with 5 mM glutamate and 2.5 mM malate. Where indicated (arrows), mouse liver mitochondria (MLM, final concentration 1 mg ml^{-1}), ADP (100 μM) and FCCP (60 nM) were added. Respiration after ADP stimulation is indicated as "state 3", whereas respiration after consumption of added ADP is indicated as "state 4."

10| Record for 5 min.

11| Add ADP to obtain a final concentration of 100–150 μM. Faster consumption of oxygen will be observed. This has been caused by proton back-diffusion through the stalk portion of the ATPase, which has been compensated by faster electron flow through the respiratory chain to the terminal electron acceptor, O_2. This is classically referred to as "state 3" respiration[26].
▲ CRITICAL STEP The rate of oxygen consumption should now be faster than the rate observed with substrates alone, indicating that we have obtained well coupled mitochondria. The increase in respiration, observed with ADP, varies from tissue to tissue and from substrate to substrate. As a general rule, and for the sole purpose of quality control of the preparation, the minimum requirements to proceed with the experiment are as follows: using glutamate malate as a substrate, maintaining a ratio of 2 in mitochondria isolated from cell lines and a ratio of 4 in mitochondria isolated from tissues.
? TROUBLESHOOTING

12| Wait until the respiration slows down and returns to a rate comparable to that before the addition of ADP. This is caused by the consumption of the added ADP. The respiration, which follows ADP exhaustion, is classically referred to as "state 4" respiration[26].

13| Wait for 3 min.

14| Add the uncoupler FCCP to obtain a final concentration of 60–100 nM.

15| The respiration will speed up and reach values slightly higher than those observed during the recording of state-3 respiration.
? TROUBLESHOOTING

16| Record for a further 5 min and then stop recording.

● TIMING
Step 1A: approximately 2 h, depending on the amount of cells to be used; however, cells will need to be seeded 2 or 3 d in advance to let them grow
Step 1B: approximately 1 h; however the mouse will need to be fasted from the night before
Step 1C: 1.5 h, depending on the amount of muscle to be minced

? TROUBLESHOOTING
Troubleshooting advice can be found in **Table 2**.

TABLE 2 | Troubleshooting table.

Step	Problem	Possible causes	Solution
1Aviii, 1Bvi, 1Cvii	Low yield of isolated mitochondria	Low cell density during homogenization	Low cell density may result in better homogenization. However, mitochondria are usually of lower quality, probably as a consequence of mechanical damage during preparation

PROTOCOL

TABLE 2 | Troubleshooting table (continued).

Step	Problem	Possible causes	Solution
1Ax, 1Bviii, 1Cix	Low quality of isolated mitochondria	Pellet after centrifugation is lost	When the supernatant is poured off, the loose upper part of the mitochondrial pellet may be detached as well. Intact mitochondria tend to sediment more quickly than damaged mitochondria. The loose part of the pellet probably contains a high proportion of damaged (uncoupled) mitochondria and can be lost without affecting the overall quality of the mitochondrial preparation
1Ax, 1Bvii	Low quality of isolated mitochondria	Lipid contamination	The white foamy material near the top of the tube consists of lipids. Mixing of lipids with the mitochondria suspension will cause some degree of uncoupling. Therefore avoid contact with mitochondria: remove the foamy material by wiping the inside of the tube with a Kimwipe
5	Oxygen consumption baseline is not stable	Bacterial or yeast contamination of your buffer	Verify if your buffers are contaminated, by repeating the recording with bidistilled water in the oxygraph chamber
		Inadequate calibration of the instrument	Re-calibrate the instrument
		Tears in the polyethylene membrane of the electrode	Check response of the oxygraph by transiently stopping stirring: due to the immediate drop in the local oxygen concentration the recording should immediately fall and return to the original baseline only when the stirrer is restarted. If this *manoeuvre* does not give the expected results, inspect and if necessary substitute the membrane of the electrode
9	Mitochondrial preparation is not consuming oxygen	Overestimation of final protein concentration (therefore added too little protein in the oxygraph chamber)	Try to double mitochondrial concentration in the chamber
		Mechanical and osmotical damage to mitochondria during isolation	Substitute 0.2 M sucrose with 0.3 M mannitol in the isolation buffer
		Contamination by other intracellular membranes, such as endoplasmic reticulum or nuclei	In steps 1Axi, 1Bix or 1Cx, wash the mitochondrial pellet with twice the amount of isolation buffer
11	ADP-stimulated respiration rate is too low	The most trivial explanation is that you omitted Pi from your buffer	Add Pi and check the respiration
		High percentage of mitochondria with ruptured outer membranes that leaked cytochrome *c*	Add exogenous cytochrome *c* and check the respiration; if respiration starts, the outer membrane is leaky. See troubleshooting for step 9 (mechanical and osmotic damage)
		Unusually high basal respiration, as a consequence of uncoupling by Ca^{2+} overload	Follow carefully all the indicated critical steps to avoid the indicated contaminations; try washing glassware with isolation buffer, supplemented with EGTA
		Unusually high basal respiration, as a consequence of uncoupling by fatty acids	Include 0.1% fatty acid free albumin in the EB; if this procedure works increase FCCP concentration since albumin binds reversibly to FCCP
15	Uncoupled respiration rate is lower than ADP-stimulated respiration	Too much FCCP used	Since at high doses FCCP is also an inhibitor of the respiratory chain, you can overcome this problem by titrating down the concentration of FCCP used

ANTICIPATED RESULTS

The goal of a mitochondrial preparation is to obtain a good amount of relatively pure, well coupled mitochondria. The quality of the obtained organelles can be checked by using oxygraphy to measure their oxygen consumption. For example, mitochondria isolated from mouse liver and energized with glutamate/malate respond to stimulation of ATPase by added ADP with a sixfold

increase in the rate of oxygen consumption (**Fig. 6b**). This usually reflects mitochondria that are highly pure and intact. A closer look by conventional electron microscopy at the morphology and at the purity of the organelles isolated from other intracellular membranes revealed that most of the organelles displayed an intact inner and outer membrane and that the level of contamination by other membranes was kept to a minimum (**Fig. 6a**).

ACKNOWLEDGMENTS We thank Giuliano Dodoni and members of the Scorrano lab for helpful discussions. LS is an Assistant Telethon Scientist of the Dulbecco-Telethon Institute. Research in his laboratory is supported by Telethon Italy; AIRC Italy; Compagnia di San Paolo; Human Frontier Science Program Organization; United Mitochondrial Disease Fund USA, Muscular Dystrophy Association USA.

COMPETING INTERESTS STATEMENT The authors declare that they have no competing financial interests.

Published online at http://www.natureprotocols.com
Reprints and permissions information is available online at http://npg.nature.com/reprintsandpermissions

1. Dimmer, K.S. & Scorrano, L. (De)constructing mitochondria: what for? *Physiology (Bethesda)* **21**, 233–241 (2006).
2. Hogeboom, G.H., Schneider, W.C. & Pallade, G.E. Cytochemical studies of mammalian tissues. I. Isolation of intact mitochondria from rat liver; some biochemical properties of mitochondria and submicroscopic particulate material. *J. Biol. Chem.* **172**, 619–635 (1948).
3. Bensley, R.R. & Hoerr, N. Studies on cell structure by the freezing-drying method VI. The preparation and properties of mitochondria. *Anat. Rec.* **60**, 449–455 (1934).
4. Mitchell, P. & Moyle, J. Chemiosmotic hypothesis of oxidative phosphorylation. *Nature* **213**, 137–139 (1967).
5. Schatz, G., Haslbrunner, E. & Tuppy, H. Deoxyribonucleic acid associated with yeast mitochondria. *Biochem. Biophys. Res. Commun.* **15**, 127–132 (1964).
6. Nass, M.M. & Nass, S. Intramitochondrial fibers with DNA characteristics. I. Fixation and electron staining reactions. *J. Cell Biol.* **19**, 593–611 (1963).
7. Hallermayer, G., Zimmermann, R. & Neupert, W. Kinetic studies on the transport of cytoplasmically synthesized proteins into the mitochondria in intact cells of *Neurospora crassa*. *Eur. J. Biochem.* **81**, 523–532 (1977).
8. Palade, G.E. The fine structure of mitochondria. *Anat. Rec.* **114**, 427–451 (1952).
9. Sorgato, M.C., Keller, B.U. & Stuhmer, W. Patch-clamping of the inner mitochondrial membrane reveals a voltage-dependent ion channel. *Nature* **330**, 498–500 (1987).
10. Liu, X., Kim, C.N., Yang, J., Jemmerson, R. & Wang, X. Induction of apoptotic program in cell-free extracts: requirement for dATP and cytochrome *c*. *Cell* **86**, 147–157 (1996).
11. Yang, J. *et al.* Prevention of apoptosis by Bcl-2: release of cytochrome *c* from mitochondria blocked. *Science* **275**, 1129–1132 (1997).
12. Scorrano, L. & Korsmeyer, S.J. Mechanisms of cytochrome *c* release by proapoptotic BCL-2 family members. *Biochem. Biophys. Res. Commun.* **304**, 437–444 (2003).
13. Bossy-Wetzel, E., Barsoum, M.J., Godzik, A., Schwarzenbacher, R. & Lipton, S.A. Mitochondrial fission in apoptosis, neurodegeneration and aging. *Curr. Opin. Cell Biol.* **15**, 706–716 (2003).
14. Li, Z., Okamoto, K., Hayashi, Y. & Sheng, M. The importance of dendritic mitochondria in the morphogenesis and plasticity of spines and synapses. *Cell* **119**, 873–887 (2004).
15. St. John, J.C., Jokhi, R.P. & Barratt, C.L. The impact of mitochondrial genetics on male infertility. *Int. J. Androl.* **28**, 65–73 (2005).
16. Cipolat, S. *et al.* Mitochondrial rhomboid parl regulates cytochrome *c* release during apoptosis via opa1-dependent cristae remodeling. *Cell* **126**, 163–175 (2006).
17. Fontaine, E., Eriksson, O., Ichas, F. & Bernardi, P. Regulation of the permeability transition pore in skeletal muscle mitochondria. Modulation by electron flow through the respiratory chain complex I. *J. Biol. Chem.* **273**, 12662–12668 (1998).
18. Frezza, C. *et al.* OPA1 controls apoptotic cristae remodeling independently from mitochondrial fusion. *Cell* **126**, 177–189 (2006).
19. Meeusen, S., McCaffery, J.M. & Nunnari, J. Mitochondrial fusion intermediates revealed *in vitro*. *Science* **305**, 1747–1752 (2004).
20. Stahl, W.L., Smith, J.C., Napolitano, L.M. & Basford, R.E. BRAIN MITOCHONDRIA: I. Isolation of Bovine Brain Mitochondria. *J. Cell Biol.* **19**, 293–307 (1963).
21. Cannon, B. & Lindberg, O. Mitochondria from brown adipose tissue: isolation and properties. *Methods Enzymol.* **55**, 65–78 (1979).
22. Mela, L. & Seitz, S. Isolation of mitochondria with emphasis on heart mitochondria from small amounts of tissue. *Methods Enzymol.* **55**, 39–46 (1979).
23. Siess, E.A. Different actions of mono- and disaccharides on rat liver mitochondria. *Hoppe Seylers. Z. Physiol Chem.* **364**, 835–838 (1983).
24. Siess, E.A. Influence of isolation media on the preservation of mitochondrial functions. *Hoppe Seylers. Z. Physiol Chem.* **364**, 279–289 (1983).
25. Eskes, R. *et al.* Bax-induced cytochrome c release from mitochondria is independent of the permeability transition pore but highly dependent on Mg^{2+} ions. *J. Cell Biol.* **143**, 217–224 (1998).
26. Nicholls, D.G. & Ferguson, S.J. *Bioenergetics*. Academic Press, London (2002).

29

Measuring Mitochondrial Shape Changes and Their Consequences on Mitochondrial Involvement During Apoptosis

Christian Frezza, Sara Cipolat, and Luca Scorrano

Summary

Mitochondria are key players in cell death following intrinsic and, in some cell types, extrinsic stimuli. The recruitment of the mitochondrial pathway results in mitochondrial dysfunction and release of intermembrane space proteins like cytochrome-c that are required in the cytosol for complete activation of effector caspases. Apoptotic shape changes of this organelle and the role of "mitochondria-shaping" proteins in cell death has attracted considerable attention. We present protocols to investigate how morphological changes of the mitochondrial reticulum regulate release of cytochrome-c, as evaluated quantitatively by an in situ approach, and changes in mitochondrial membrane potential measured in real time.

Key Words: Apoptosis; cytochrome-*c* release; fission; fusion; imaging; membrane potential; OPA1.

1. Introduction

Besides providing most cellular ATP, mitochondria participate in the early stages of programmed cell death or apoptosis. Apoptosis is essential for successful development and tissue homeostasis of all multicellular organisms, and it is accomplished by evolutionarily conserved pathways that result in an orderly process of cell demise with distinct morphological and biochemical parameters *(1)*. Dysregulation of apoptosis contributes to a variety of human diseases, including cancer *(2)*. In mammalian cells, there are two main pathways downstream of death signals that appear to be linked in certain cell types: the death receptor pathway and the mitochondrial pathway *(3)*. Both culminate in the activation of caspases, cysteine proteases that cleave a number of substrates

From: *Methods in Molecular Biology, vol. 372: Mitochondria: Practical Protocols*
Edited by: D. Leister and J. M. Herrmann © Humana Press Inc., Totowa, NJ

involved in maintenance of cytoskeletal and nuclear integrity, cell cycle progression, and deoxyribonucleic acid (DNA) repair, resulting in the orderly demise of the cell.

Mitochondria participate in the competent activation of caspases by releasing cytochrome-*c* and additional apoptogenic factors from the intermembrane space into the cytosol ***(3)***. Cytochrome-*c* in complex with Apaf-1 activates caspase-9 and other downstream caspases ***(4)***. The release of cytochrome-*c* is preceded by changes in the structure of the mitochondrial network and of mitochondrial cristae ***(5,6)***.

Besides mitochondrial shape changes during cell death, a vast variety of physiological and pathological conditions, ranging from elevated intracellular Ca^{2+} levels ***(7,8)*** to mitochondrial uncoupling ***(9)*** and inhibition of autophagocytosis ***(10)***, have been reported to affect morphology of the organelle. Mitochondrial shape is regulated by the balance between fusi on and fission processes ***(11)***. Several mitochondria-shaping proteins have been identified through genetic screens in yeast; their mammalian counterparts are less characterized ***(11)***.

Mitochondrial fission in mammalian cells is regulated by dynamin-related protein (DRP-1), a cytosolic dynamin that translocates to fission sites, where it interacts with its molecular adapter homolog fission (hFis1) ***(12)***, an integral protein of the outer mitochondrial membrane ***(13)***. Fusion is regulated by optic atrophy 1 (OPA1) and mitofusin (MFN) 1 and 2. MFNs are outer membrane proteins required for mitochondrial fusion ***(9,14–16)***. Interestingly, MFN1 seems to cooperate with the inner mitochondrial membrane protein OPA1 to fuse mitochondria ***(17)***.

DRP-1 has been shown to mediate mitochondrial fragmentation during developmental cell death of *Caenorhabditis elegans* ***(18)***. Moreover, an interesting crosstalk between "BH3-only" members (BCL-2 homology domain 3) of the B-cell lymphoma 2 (BCL-2) family, DRP-1, and remodeling of the cristae has been described ***(19)***.

Thus, considerable interest has developed in the relationship between mitochondrial shape and mitochondrial and cellular function, in particular, but not only in the course of apoptosis. Researchers exploiting these avenues face the major challenge of having to combine quantitative analysis of mitochondrial morphology and pathophysiology during apoptosis. How to reliably follow components of the latter process, such as depolarization and cytochrome-*c* release, is still a matter of debate (for a review, *see* **ref. *20***). A safe way that is less artifact prone is to use in situ methods accompanied by quantitative analyses. Here, we present protocols to address morphological changes of mitochondria and to verify if these changes play any role in controlling release of cytochrome-*c* and in mitochondrial depolarization in response to intrinsic apoptotic stimuli.

2. Materials

2.1. Mitochondrial Morphology

2.1.1. Seeding of Cells for Morphological Analysis

1. Sterile 75-cm^2 tissue culture flasks and six-well sterile tissue culture plates.
2. Sterile Dulbecco's modified Eagle's medium (DMEM) supplemented under sterile conditions with sterile 10% (v/v) fetal bovine serum (FBS), 50 U/mL penicillin, 50 µg/mL streptomycin, 100 µ*M* minimum essential medium (MEM) nonessential amino acids, and 2 m*M* glutamine. Filter sterilize through a 22-µm filter and store at 4°C.
3. Sterile phosphate-buffered saline (PBS): 2.7 m*M* KCl, 1.5 m*M* KH_2PO_4, 140 m*M* NaCl, 8 m*M* Na_2HPO_4. Alternatively, prepare working solution by dilution of one part of sterile 10X PBS (Gibco) with nine parts of sterile deionized water. Filter sterilize through a 22-µm filter and store at 4°C.
4. Sterile trypsin/ethylenediaminetetraacetic acid (EDTA) solution: sterile 0.25% (w/v) trypsin, 1 m*M* EDTA, pH 7.4. Divide under sterile conditions into 2-mL aliquots and store at 4°C.
5. Sterile Hanks' balanced salt solution (HBSS): prepare working solution by diluting one part sterile 10X HBSS (Gibco) with nine parts sterile deionized water; add 0.1 part sterile 100X HEPES (Gibco) and adjust to pH 7.4 with NaOH if necessary. Filter sterilize through a 0.22-µm filter and store at 4°C.
6. 24-mm Round glass grade 0 or 1 coverslips: coverslips must be ultraviolet (UV) sterilized by placing them under sterile conditions vertically inside the wells of a six-well plate (without the cover). Plates must be exposed to the UV source of a laminar flux hood for 45 min, with coverslips oriented toward the lamp (*see* **Note 1**).

2.1.2. Transfection of Cells for Morphological Analysis

1. Cationic lipid and colipid vehicle TransFectin lipid reagent (Bio-Rad) (*see* **Note 2**).
2. Plasmids for the expression of mitochondrially targeted DsRED. Always cotransfect it with the negative control plasmid (e.g., empty plasmid of the one containing the complementary deoxyribonucleic acid [cDNA] of your protein of interest) or with the one containing the cDNA of your protein of interest. In our experiments, we use pMSCV (BD-Clontech) and pMSCV containing murine *OPA1* cDNA (corresponding to human transcript variant 1) ***(17)*** (*see* **Note 3**).
3. Sterile DMEM (*see* **Subheading 2.1.1.**).

2.1.3. Confocal Imaging of Mitochondrial Morphology

1. HBSS: prepare as described in **Subheading 2.1.1.**, **item 5** (*see* **Note 4**).
2. Coverslip holder: 25-mm round Attofluor stainless steel coverslip holders (Molecular Probes).

3. An inverted confocal microscope with HeNe laser light line and appropriate emission filters and photomultipliers, with a motorized *z*-axis connected to a computer for image storage and analysis.
4. Image analysis software: the freeware ImageJ (National Institutes of Health [NIH]) is suitable for all postacquisition image editing and analysis and three-dimensional (3D) reconstruction.

2.2. Cytochrome-c Release Immunofluorescence Assay

2.2.1. Seeding of Cells for Cytochrome-c Release Immunofluorescence Assay

1. Sterile 75-cm^2 tissue culture flasks and 6- and 24-well sterile tissue culture plates.
2. Sterile DMEM supplemented under sterile conditions with sterile 10% (v/v) FBS, 50 U/mL penicillin, 50 µg/mL streptomycin, 100 µ*M* MEM nonessential amino acids and 2 m*M* glutamine. Filter sterilize through a 22-µm filter and store at 4°C.
3. Sterile trypsin/EDTA solution: sterile 0.25% (w/v) trypsin, 1 m*M* EDTA, pH 7.4. Divide under sterile conditions into 2-mL aliquots and store at 4°C.
4. Sterile HBSS: prepare working solution by diluting one part sterile 10X HBSS (Gibco) with nine parts of sterile deionized water; add 0.1 part sterile 100X HEPES (Gibco) and adjust to pH 7.4 with NaOH if necessary. Filter sterilize through a 0.22-µm filter and store at 4°C.
5. 13-mm Round glass grade 0 or 1 coverslips: coverslips must be UV sterilized by placing them under sterile conditions vertically inside the wells of a 24-well plate (without the cover). Plates must be exposed to the UV source of a laminar flux hood for 45 min, with coverslips oriented toward the lamp (*see* **Note 1**).

2.2.2. Transfection of Cells for Cytochrome-c Release Immunofluorescence Assay

1. Cationic lipid and colipid vehicle TransFectin lipid reagent (Bio-Rad) (*see* **Note 2**).
2. Plasmids for the expression of mitochondrially targeted DsRED. Always cotransfect it with the negative control plasmid (e.g., empty plasmid of the one containing the cDNA of your protein of interest) or with the one containing the cDNA of your protein of interest. In our experiments, we use pMSCV (BD-Clontech) and pMSCV containing murine *OPA1* cDNA (corresponding to human transcript variant 1) ***(17)*** (*see* **Note 3**).
3. Sterile DMEM (*see* **Subheading 2.1.1.**).

2.2.3. Treatment of Cells With an Apoptosis Inducer and Immunostaining and Confocal Immunofluorescence of Cytochrome-c

1. Freshly prepared hydrogen peroxide (Sigma) dissolved in sterile HBSS at a final concentration of 1 m*M* (*see* **Note 5**).
2. PBS: 2.7 m*M* KCl, 1.5 m*M* KH_2PO_4, 140 m*M* NaCl, 8 m*M* Na_2HPO_4. Alternatively, prepare working solution by dilution of one part 10X PBS (Gibco) with nine parts of deionized water.

3. Fixing solution: prepare working solution by diluting one part 37% (v/v) formaldehyde solution (Sigma) in nine parts PBS; adjust to pH 7.4 using NaOH. Store at 4°C and prepare fresh every 4 wk (*see* **Note 6**).
4. Permeabilization solution: 0.01% (v/v) Nonidet P-40 (Sigma) in PBS; adjust to pH 7.4 using HCl or NaOH as required.
5. Blocking solution: 0.5% (w/v) bovine serum albumin (BSA) in PBS; divide into 10-mL aliquots and store at −20°C.
6. Primary antibody: purified anti-cytochrome-*c* mouse monoclonal antibody (BD-Pharmingen clone 6H2.B4), 1:200 in PBS.
7. Secondary antibody: antimouse immunoglobulin G, fluorescein isothiocyanate conjugated (Calbiochem), 1:200 in PBS.
8. Mounting medium: Prolong Antifade Gold (Molecular Probes).
9. 76 × 26 mm rectangular microscope slides.
10. An upright confocal microscope with HeNe and Xe laser light lines and appropriate emission filters and photomultipliers and connected to a computer for image storage and analysis.
11. Image analysis software: the freeware ImageJ (NIH) is suitable for all postacquisition image processing and analysis.

2.3. Imaging of Mitochondrial Membrane Potential

2.3.1. Seeding of Cells for Analysis of Mitochondrial Membrane Potential

1. Sterile 75-cm^2 tissue culture flasks and 6- and 24-well sterile tissue culture plates.
2. Sterile DMEM supplemented under sterile conditions with sterile 10% (v/v) FBS, 50 U/mL penicillin, 50 µg/mL streptomycin, 100 µ*M* MEM nonessential amino acids, and 2 m*M* glutamine. Filter sterilize through a 22-µm filter and store at 4°C.
3. Sterile trypsin/EDTA solution: sterile 0.25% (w/v) trypsin, 1 m*M* EDTA, pH 7.4. Divide under sterile conditions into 2-mL aliquots and store at 4°C.
4. Sterile HBSS: prepare working solution by diluting one part of sterile 10X HBSS (Gibco) with nine parts of sterile deionized water; add 0.1 part of sterile 100X HEPES (Gibco) and adjust to pH 7.4 with NaOH if necessary. Filter sterilize through a 0.22-µm filter and store at 4°C.
5. 24-mm round glass grade 0 or 1 coverslips: coverslips must be UV sterilized by placing them under sterile conditions vertically inside the wells of a 6- or 24-well plate (without the cover), respectively. Plates must be exposed to the UV source of a laminar flux hood for 45 min, with coverslips oriented toward the lamp (*see* **Note 1**).

2.3.2. Transfection of Cells for Analysis of Mitochondrial Membrane Potential

1. Cationic lipid and colipid vehicle TransFectin lipid reagent (Bio-Rad) (*see* **Note 2**).
2. Plasmids for the expression of cytosolic green fluorescent protein (GFP) (like pEGFP, BD-Clontech). Always cotransfect it with the negative control plasmid (e.g., empty plasmid of the one containing the cDNA of your protein of interest) or with the one containing the cDNA of your protein of interest. In our experiments,

we use pMSCV (BD-Clontech) and pMSCV containing murine *OPA1* cDNA (corresponding to human transcript variant 1) ***(17)*** (*see* **Note 3**).

2.3.3. Imaging of Mitochondrial Membrane Potential

1. HBSS: 1.3 m*M* $CaCl_2$, 0.5 m*M* $MgCl_2$, 0.4 m*M* $MgSO_4$, 5.3 m*M* KCl, 4.4 m*M* KH_2PO_4, 138 m*M* NaCl, 0.3 m*M* Na_2HPO_4, 1000 mg/L D-glucose; add 0.1 part 100X HEPES (Gibco) and adjust to pH 7.4 with NaOH if necessary. Alternatively, prepare working solution by dilution of one part 10X HBSS (Gibco) with nine parts deionized water; add 0.1 part 100X HEPES (Gibco) and adjust to pH 7.4 with NaOH if necessary.
2. 0.1 m*M* Tetramethylrodhamine methyl ester (TMRM) (Molecular Probes) in dimethyl sulfoxide. Store at –20°C in the dark.
3. 10 mg/mL Cyclosporine H (CsH) (Sigma) in dimethyl sulfoxide. Store at –20°C (*see* **Note 7**).
4. 2 m*M* carbonyl cyanide(*p*-trifluoromethoxy)-phenylhydrazone (FCCP) (Sigma) in absolute ethanol. Store at –20°C (*see* **Note 8**).
5. 1 m*M* H_2O_2 prepared freshly as described in **Subheading 2.2**.
6. An imaging workstation including an inverted microscope equipped with a fluorescent light source, proper excitation and emission filters, a shutter to avoid photobleaching of the samples, and a 12-bit charge coupled device camera for image acquisition. All must be connected to a computer with imaging software (usually provided with the imaging workstation) to set up the acquisition routine and to store the imaging sequence.
7. Image analysis software to analyze gray levels in the selected regions of interest (ROIs). The freeware ImageJ (NIH) with the MultiMeasure plugin is suitable.

3. Methods

3.1. Mitochondrial Morphology

Our method of choice to analyze the effect of a putative mitochondria-shaping protein on mitochondrial morphology is to cotransfect it with a mitochondrially targeted fluorescent protein and to compare the shape of the mitochondrial reticulum with that of cells transfected with the mitochondrially targeted fluorescent protein alone (*see* **Note 9**). We prefer to image the mitochondria in living cells confocally to avoid possible fixation artifacts. It must be kept in mind that when performing confocal imaging, tubular structures that move in and out of the focal plane can be easily mistaken for individual rod or spherical organelles. We therefore strongly advise acquiring stacks of mitochondrial images along the *z*-axis of the entire cell, followed by 3D image reconstruction to confirm the single-plane confocal images.

3.1.1. Seeding of Cells for Morphological Analysis

1. Check a 75-cm^2 flask containing mouse embryonic fibroblasts (MEFs) by using a standard inverted, transmitted light microscope. If cells are approaching confluence,

then open the flask in a laminar flux hood, sterile aspirate the medium, and wash the cells three times with sterile PBS.
2. Detach cells from flasks using a 0.25% (v/v) sterile trypsin/EDTA solution. For a 75-cm^2 flask, evenly distribute 1 mL sterile solution on top of the cells, gently swirl the flasks, and incubate for 3 min at 37°C.
3. Check cells for detachment using a standard inverted microscope. Gently tap the bottom of the flask if cells are still attached. After complete detachment, inactivate trypsin by adding 10 mL complete DMEM.
4. Count the cells using a hemocytometer (Burker chamber).
5. Seed 10^5 cells in each well of a six-well plate containing the sterile 22-mm round coverslips (*see* **Note 10**).
6. Place the plate in the tissue culture incubator and leave for 24 h.
7. Check confluence after 24 h. A 50–60% confluence will yield optimal transfection efficiency. Proceed with transfection if confluence is optimal.

3.1.2. Transfection of Cells for Morphological Analysis

1. For each well, 3 μg plasmid DNA in 250 μL serum-free medium are required: 1.5 μg of the fluorescent protein plasmid DNA and 1.5 μg of plasmid DNA of the protein of interest or empty vector for the control transfection.
2. For each well, add 3 μL TransFectin transfection reagent to 250 μL serum-free medium.
3. Mix the DNA and TransFectin solutions together. Gently mix by tapping or pipeting.
4. Incubate for 20 min at room temperature.
5. Take the plate containing cells grown on coverslips from the incubator.
6. Add 500 μL DNA–TransFectin complexes directly to cells in serum-containing medium. Swirl gently.
7. Place the plate in the tissue culture incubator and leave for 4 h.
8. Change the medium with complete DMEM 4 h after the addition of the DNA–TransFectin complexes.
9. Place the plate in the tissue culture incubator and leave for 20 h.

3.1.3. Confocal Imaging for Morphological Analysis

1. At 24 h after transfection, place coverslips with transfected cells in the coverslip holder.
2. Wash the cells free of medium, add HBSS, and place cells on the stage of a confocal microscope (*see* **Note 11**).
3. Choose the appropriate objective. Good images with a great degree of definition can be acquired using a 60×, 1.4-numerical aperture (NA) Plan Apo objective (*see* **Note 12**).
4. Using the binocular and epifluorescence illumination, rapidly find a field with transfected cells.
5. Regulate the power of the laser beam to obtain contrasted images and at the same time to minimize photobleaching and phototoxicity. It is advisable not to exceed 10% of the maximum power of the laser.

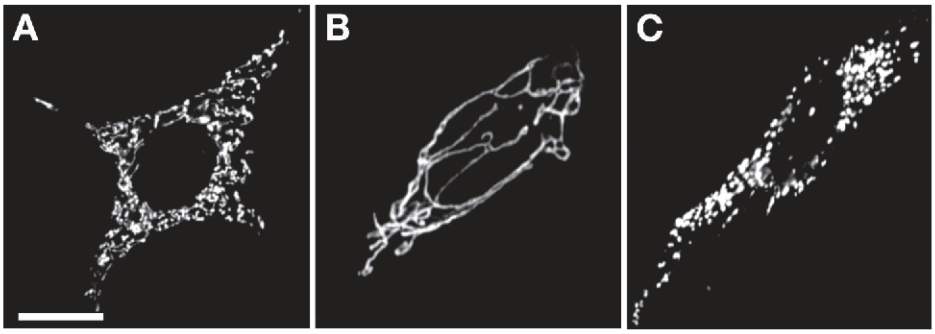

Fig. 1. Overexpression of OPA1 promotes mitochondrial elongation. Mouse embryonic fibroblasts (MEFs) grown on coverslips were cotransfected with mtRFP and empty vector (**A**), WT OPA1 (**B**), K301A OPA1 (**C**). After 24 h, confocal images of mtRFP fluorescence from randomly selected cells were acquired and stored. Bar: 10 μm.

6. Acquire and store images of transfected cells. If cells are expressing mitochondrially targeted red fluorescent protein (mtRFP), then excite using the 543-nm line of the HeNe laser and acquire emitted light through a 600-nm long-pass filter. Examples of images of MEFs expressing mtRFP and wild type (WT) or K301A *OPA1* are shown in **Fig. 1**.
7. Acquire and save stacks of images separated by 0.5 μm along the *z*-axis by using the appropriate function of your confocal microscope.
8. Open the acquired stacks with ImageJ and use the 3D reconstruction function of the program to reconstruct them.

3.2. Immunofluorescence Analysis of Cytochrome-c Release

Several methods are available to estimate the release of cytochrome-*c* from mitochondria during apoptosis. Most rely on the preparation by differential centrifugation of cytosolic and mitochondrial fractions, followed by semiquantitative determination of cytochrome-*c* content in each fraction, performed by enzyme-linked immunosorbent assay or immunoblotting. Separation of subcellular fractions by differential centrifugation requires the mechanical rupture of the plasma membrane, which can cause unspecific mitochondrial disruption with cytochrome-*c* release *(21)*. Moreover, it is always difficult to assess the effect of a transiently transfected protein at a bulk population level. On the other hand, these approaches are far more quantitative than the analysis of cytochrome-*c* subcellular localization by immunofluorescence. We therefore modified a double-immunofluorescence protocol coupled to a quantitative analysis of cytochrome-*c* distribution devised by Petronilli et al. *(22)* to evaluate quantitatively the effects of a transfected mitochondria-shaping protein on the release of cytochrome-*c*.

3.2.1. Seeding of Cells for Analysis of Cytochrome-c Release

1. Check a 75-cm^2 flask containing MEFs using a standard inverted, transmitted light microscope. If cells are approaching confluence, then open the flask in the hood, aspirate the medium, and wash the cells three times with sterile PBS.
2. Detach cells from flasks using the sterile trypsin/EDTA solution. For a 75-cm^2 flask, evenly distribute 1 mL sterile solution on top of the cells, gently swirl the flasks, and incubate for 3 min at 37°C.
3. Check cells for detachment. Gently tap the bottom of the flask if cells are still attached. After complete detachment, inactivate trypsin by adding 10 mL complete DMEM.
4. Count the cells using a hemocytometer (Burker chamber).
5. Seed 10^4 cells in each well of a 24-well plate containing the sterile 13-mm round coverslips (*see* **Note 10**).
6. Place the plate in the tissue culture incubator and leave for 24 h.
7. Check confluence after 24 h. A 50–60% confluence will yield optimal transfection efficiency. Proceed with transfection if confluence is optimal.

3.2.2. Transfection of Cells for Analysis of Cytochrome-c Release

1. For each well, 0.5 μg plasmid DNA in 50 μL serum-free medium is required: 0.25 μg of the fluorescent protein plasmid DNA and 0.25 μg of plasmid DNA of the protein of interest or empty vector for the control transfection.
2. For each well, add 1 μL TransFectin transfection reagent to 50 μL serum-free medium.
3. Mix the DNA and TransFectin solutions together. Gently mix by tapping or pipeting.
4. Incubate 20 min at room temperature.
5. Take the plate containing cells grown on coverslips from the incubator.
6. Add 100 μL DNA–TransFectin complexes directly to cells in serum-containing medium. Swirl gently.
7. Change the medium with complete DMEM 4 h after the addition of the DNA–TransFectin complexes.
8. Place the plate in the tissue culture incubator and leave for 20 h.

3.2.3. Treatment of Cells With an Apoptosis Inducer and Immunostaining and Confocal Immunofluorescence of Cytochrome-c

1. Seeded, transfected cells are now ready to be treated with the apoptotic stimulus of choice. We use H_2O_2, which at 1 m*M* is an intrinsic, mitochondria-utilizing apoptotic stimulus ***(23)***.
2. Aspirate medium and wash twice with PBS.
3. Add the solution of 1 m*M* H_2O_2 (freshly prepared; *see* **Note 5**) in HBSS.
4. Treat cells for 30, 60, and 90 min by placing the plate back in the tissue culture incubator (*see* **Note 13**).
5. Discard medium.
6. Add 0.3 mL 3.7% (v/v) ice-cold formaldehyde to each well.
7. Fix cells by leaving for 30 min at room temperature (*see* **Note 14**).
8. Discard formaldehyde by following your local hazardous waste regulations.

9. Wash samples twice with PBS.
10. Permeabilize cells by incubating with 0.3 mL 0.01% (v/v) ice-cold Nonidet NP40 for 20 min at room temperature.
11. Wash samples twice with PBS.
12. Block by adding 0.3 mL 0.5% (w/v) BSA for 15 min at room temperature.
13. Discard the blocking solution.
14. Add anti-cytochrome-*c* antibody (1:200) in PBS at room temperature for 30 min or at 4°C overnight.
15. Recover the primary antibody.
16. Wash samples twice with PBS.
17. Block by adding 0.3 mL 0.5% (w/v) BSA for 15 min at room temperature.
18. Add secondary antibody (1:200) in PBS at room temperature for 30 min at room temperature (*see* **Note 15**).
19. Wash samples twice with PBS and then with deionized water.
20. Add a drop (~5 µL) of mounting medium Prolong Antifade Gold to the microscopy slides.
21. Mount the coverslip on the slide with cells facing the mounting medium.
22. Remove any remaining water by blotting the coverslip against clean kimwipes.
23. When samples are completely dry, seal the coverslips with nail polish.
24. The sample can be viewed immediately after the nail polish dries or be stored in the dark at 4°C for up to a month.
25. Place slides on the stage of a confocal microscope.
26. For detection of mtRFP and of cytochrome-*c* immunodecorated with fluorescein isothiocyanate-conjugated antibodies, red and green channel images can be acquired simultaneously using two separate color channels on the detector assemblies of most confocal microscopes. Check that your microscope is equipped with 605-nm long-pass and 522- (± 25) nm band-pass filters, respectively.
27. Acquire and store RGB (red-green-blue) images of transfected, treated, and untreated cells for subsequent analysis.
28. Open the images using ImageJ.
29. Draw a line across the cell (**Fig. 2** illustrates such lines).
30. Using the Analyze >Plot Profile function of ImageJ, measure the fluorescence intensity of each pixel along the line in both the green and the red channels (**Fig. 2A′, B′** illustrates fluorescence intensity profiles along the lines drawn in **Fig. 2A,B**).
31. Export data to a spreadsheet program such as Excel™.
32. Calculate the localization index, defined as the ratio between the normalized standard deviations (SDs) of the fluorescence intensities of each channel: $(SD_{cyt\text{-}c}/\Sigma_{cyt\text{-}c})/(SD_{mtRFP}/\Sigma_{mtRFP})$. A punctuate distribution results in a higher SD; normalization allows correction for different fluorescence intensities in the two channels. A localization index of 1 indicates that cytochrome-*c* follows a mitochondrial distribution; an index lower than 1 means that cytochrome-*c* is randomly distributed (i.e., released cytochrome-*c*). In the example of **Fig. 2**, the localization index is 1 for the cell in panel A and 0.6 for the cell in panel B.
33. A macro can be conveniently recorded to repeat this calculation on several lines from different cells in separate experiments

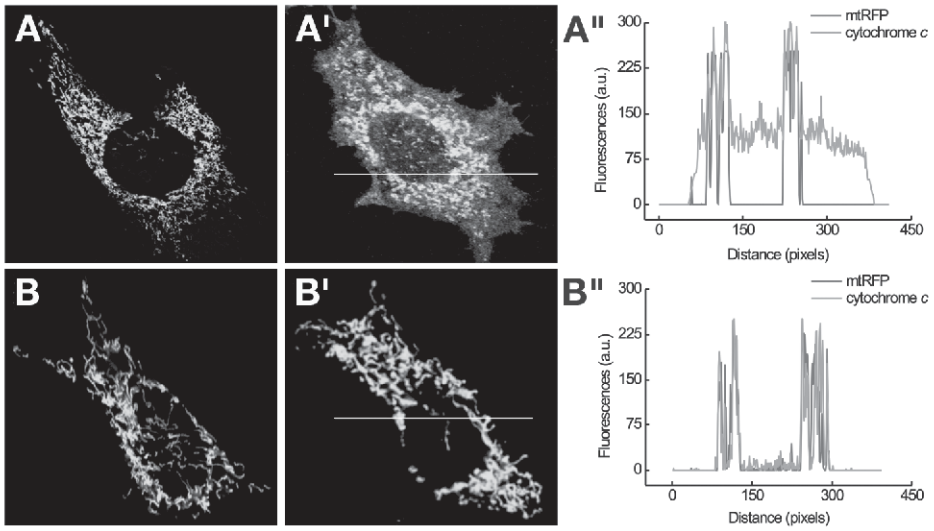

Fig. 2. Effect of the mitochondria-shaping protein OPA1 on cytochrome-*c* release evaluated by a quantitative *in situ* approach. MEFs were cotransfected with mtRFP and empty vector (**A**) or OPA1 (**B**). After 24 h, the cells were treated for 60 min with H_2O_2 (1 m*M*). Cells were then fixed, immunostained with an anti-cytochrome-*c* antibody (green), and imaged using a confocal microscope. Images of randomly selected cells before (**A**), (**B**) and after (**A′**), (**B′**) H_2O_2 treatment are shown. Sample lines are shown for the calculation of the localization index. Their fluorescence intensity profiles in the red and green channels of the lines drawn in panels **A′** and **B′** are reported in **A′** and **B′**, respectively. Bar: 10 μm.

3.3. Real-Time Imaging of Mitochondrial Membrane Potential During Apoptosis

Mitochondrial dysfunction accompanies cytochrome-*c* release during apoptosis. One of its aspects is the decrease in the mitochondrial membrane potential, which can be imaged using cationic lipophilic fluorescent dyes. To assess if overexpression of a protein of interest interferes with the apoptotic loss of mitochondrial membrane potential, transient cotransfection with a fluorescent protein such as GFP is needed to identify cells expressing the protein of interest.

3.3.1. Seeding and Transfection of Cells for Analysis of Mitochondrial Membrane Potential

Proceed exactly as indicated in the **Subheadings 3.1.1.** and **3.1.2.**

3.3.2. Imaging of Mitochondrial Membrane Potential

1. At 24 h after transfection, place coverslips with transfected cells in the coverslip holder.

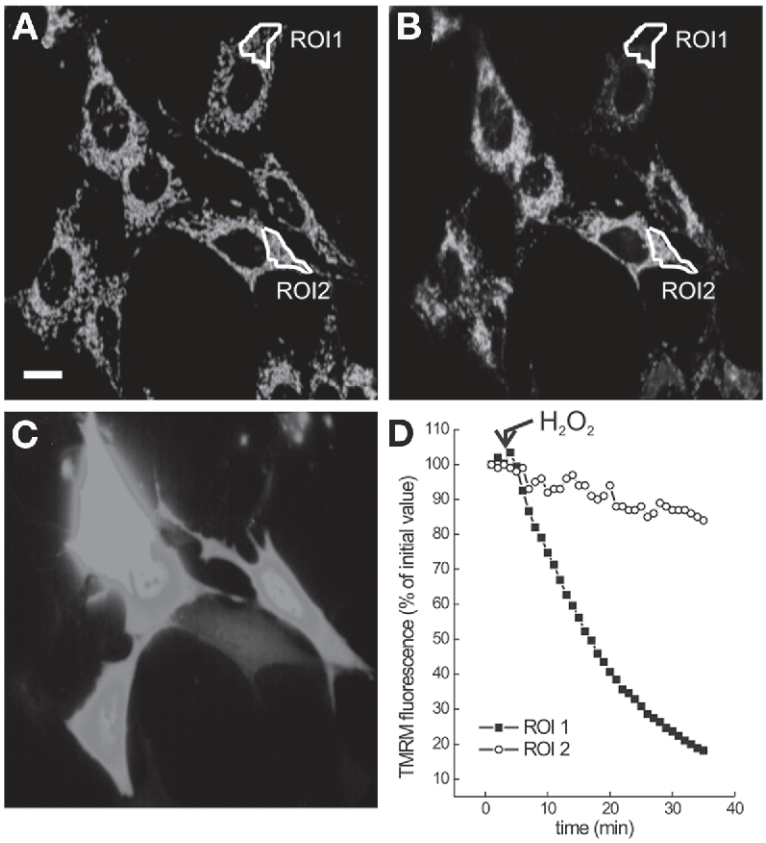

Fig. 3. Effect of the mitochondria-shaping protein OPA1 on apoptotic mitochondrial depolarization evaluated by a real-time approach. MEFs were cotransfected with GFP and OPA1. After 24 h, cells were loaded with TMRM and placed on the stage of an Olympus CellR Imaging system, and images of GFP fluorescence (**C**) were acquired and stored to identify cotransfected cells. Images of TMRM fluorescence were then acquired every 60 s for 40 min; after 3 min, cells were treated with 1 m*M* H_2O_2. Representative ROIs are drawn in images taken before (**A**) and 35 min after (**B**) addition of H_2O_2 in untransfected (ROI1) and transfected (ROI2) cells. The fluorescence intensity in the depicted ROIs was calculated, background subtracted, and normalized and is reported in (**D**). Where indicated, 1 m*M* H_2O_2 was added. Bar: 15 μm.

2. Add 1 mL 20 n*M* TMRM in HBSS supplemented with 2 μg/mL CsH.
3. Incubate for 30 min at 37°C in the dark.
4. Place coverslips on the stage of an inverted microscope (*see* **Note 11**).
5. Using the binocular and epifluorescence illumination, rapidly find a field with multiple GFP-positive cells. Check that TMRM fluorescence is stable before starting the experiment.

6. Regulate exposure times to obtain contrasted images and at the same time minimize photobleaching and phototoxicity. It is advisable not to exceed 50-ms exposure times.
7. Acquire and store the image of GFP fluorescence. This will be needed to identify the transfected cells. **Figure 3** shows GFP fluorescence in a field of transfected, TMRM-loaded MEFs.
8. Set up your imaging workstation to acquire sequential frames of TMRM fluorescence, one each 30 s to 1 min, for a total of 1–2 h.
9. After 5 min, add the apoptotic inducer.
10. Save the time series stack of images. **Figure 3** shows TMRM fluorescence before (panel B) and 35 min after (panel C) the addition of 1 m*M* H_2O_2.
11. Import the time series stack in ImageJ and proceed to analyze quantitatively the changes in mitochondrial TMRM fluorescence.
12. Open the MultiMeasure Plugin and freehand draw regions of interest on cytosolic areas comprising 10–20 mitochondria in both transfected and untransfected cells. **Figure 3** shows such ROIs. Draw a ROI on an area without cells, which will be identified as the background fluorescence.
13. Measure average fluorescence intensity values of the selected ROIs in the whole time series stack using the MultiMeasure function of ImageJ.
14. Copy the results in a spreadsheet, subtract the background, and normalize the values for the initial fluorescence. **Figure 3D** shows the quantitative analysis of changes of TMRM fluorescence in the depicted ROIs in response to 1 m*M* H_2O_2.

4. Notes

1. UV sterilization is essential for larger, 22-mm round coverslips. 13-mm round coverslips can also be sterilized by submerging them in a 1:3 isopropanol:ethanol mixture, followed by fast passage on a Bunsen flame. This protocol, however, is less safe, and free flames will disrupt the laminar flux of your sterile hood, increasing the risk of bacterial contamination.
2. Our personal experience is that this is the optimal transfection reagent for MEFs Other reagents, as well as alternative methods, such as Ca^{2+}-phosphate-mediated transfection, adenoviral infection, or electroporation, can be used successfully with this and other cell types.
3. Fluorescent proteins are essential for the morphological and functional analysis of the transfected cells. One should obtain mitochondrially targeted DsRED (mtRFP, BD-Clontech) and pEGFP (BD-Clontech) for the identification of mitochondria and the analysis of the mitochondrial morphology and for the visualization of the cotransfected cells, respectively; these fluorescent markers should be cotransfected with plasmids encoding the protein of interest. In our experiments, we use empty pMSCV and pMSCV containing murine *OPA1* cDNA. These fluorescent proteins are selected to minimize spectral interaction with other fluorescent molecules and probes exploited in the protocols presented here. Users can choose other spectral variants of GFP (like cyan and yellow fluorescent protein, for example), but it should be always kept in mind that their spectra should not overlap with those of

the other fluorescent probes used, and that the imaging workstation available to the user should have appropriate filters.

4. HBSS is used in imaging experiments to avoid spectral interference of emitting components of tissue culture media, such as phenol red. It can be replaced with phenol red-free complete media. FBS can also interfere with probes and fluorescent proteins with emission maxima around 560 nm, like TMRM and mtRFP.
5. H_2O_2 must be prepared fresh the day of the experiment as it tends to dismute spontaneously. Failure to do this will alter the formal concentration of the solution, having an impact on the reproducibility of the experiment.
6. 37% (w/v) Formaldehyde is highly toxic and a potential carcinogen, so always handle it very carefully and in a chemical hood. The use of free amines (like Tris-HCl) in the buffer will decrease the efficiency of formaldehyde, which reacts with amino groups. Efficiency will fade with time, dictating preparation of fresh solutions every month. The pH of the 3.7% (v/v) formaldehyde solution is crucial for the success of the cytochrome-*c* immunolocalization. The pH should be checked the day of the experiment.
7. CsH is an inhibitor of the P-glycoprotein multidrug resistance pump, of which all rhodamine derivatives are substrates ***(20)***. Failure to inhibit these pumps will introduce additional variables in the equilibrium distribution of TMRM, complicating the interpretation of any recorded changes. Alternatively, other multidrug resistance inhibitors, like verapamil, can be used ***(24)***.
8. FCCP is dissolved in absolute ethanol: always keep the 2 m*M* stock solution at 4°C (in an ice bath) during the whole experiment to avoid ethanol evaporation and consequent concentration of FCCP.
9. All the protocols presented in this chapter have been thoroughly tested with adherent mammalian cell lines, such as MEFs, HeLa, PC3, DU145 and several other cell lines. With minimal adjustments, they can be adapted to cells grown in suspension, such as Jurkat cells, which can adhere to coverslips in the absence of serum or once plated on polylysine-coated coverslips. We are unaware of the suitability of these protocols in cell lines derived from different organisms (i.e., insects or plants).
10. When passaging cell cultures, accurately resuspend MEFs by pipeting the suspension a few times. This will ensure an even distribution of the plated cells on the coverslips.
11. This is a delicate procedure because the coverslip is fragile. Always check that the cleft where the coverslip is placed is free of debris and use extreme caution when sealing the Attofluor chamber. Once HBSS is added, check for sealing by wiping the bottom of the coverslip with a dry kimwipe.
12. A detailed description of the optical limitations of confocal microscopy is beyond our scope, but the user should always remember that the resolution (i.e., the ability to image two adjacent fluorescent emitters as separate objects) of a confocal microscope depends on several factors, including the excitation-emission wavelength, the numerical aperture of the objective, the refraction index of the medium used by the objective (air, oil, water). When using a 60×, 1.4-NA oil immersion objective and probes emitting in the red zone of the light spectrum, the resolution can be around 200–300 nm.

13. Treatment with hydrogen peroxide may be influenced by intrinsic susceptibility of the cell type used; to assess the proper concentration and timing for treatment, a titration curve is needed; moreover, treatment with hydrogen peroxide may be influenced by cell density.
14. Immunofluorescence can be paused at this step if needed; after fixation, wash coverslips with PBS and keep at 4°C for no longer than 24 h.
15. During incubation with secondary antibody, wrap the plate with aluminum foil to protect conjugated fluorophores from light.

References

1. Hengartner, M. O. (2000) The biochemistry of apoptosis. *Nature* **407,** 770–776.
2. Thompson, C. B. (1995) Apoptosis in the pathogenesis and treatment of disease. *Science* **267,** 1456–1462.
3. Gross, A., McDonnell, J. M., and Korsmeyer, S. J. (1999) BCL-2 family members and the mitochondria in apoptosis. *Genes Dev.* **13,** 1899–1911.
4. Zou, H., Henzel, W. J., Liu, X., Lutschg, A., and Wang, X. (1997) Apaf-1, a human protein homologous to *C. elegans* CED-4, participates in cytochrome c-dependent activation of caspase-3. *Cell* **90,** 405–413.
5. Frank, S., Gaume, B., Bergmann-Leitner, E. S., et al. (2001) The role of dynamin-related protein 1, a mediator of mitochondrial fission, in apoptosis. *Dev. Cell* **1,** 515–525.
6. Scorrano, L., Ashiya, M., Buttle, K., et al. (2002) A distinct pathway remodels mitochondrial cristae and mobilizes cytochrome *c* during apoptosis. *Dev. Cell* **2,** 55–67.
7. Breckenridge, D. G., Stojanovic, M., Marcellus, R. C., and Shore, G. C. (2003) Caspase cleavage product of BAP31 induces mitochondrial fission through endoplasmic reticulum calcium signals, enhancing cytochrome c release to the cytosol. *J. Cell Biol.* **160,** 1115–1127.
8. Scorrano, L. (2003) Divide et impera: Ca^{2+} signals, mitochondrial fission and sensitization to apoptosis. *Cell Death. Differ.* **10,** 1287–1289.
9. Legros, F., Lombes, A., Frachon, P., and Rojo, M. (2002) Mitochondrial fusion in human cells is efficient, requires the inner membrane potential, and is mediated by mitofusins. *Mol. Biol. Cell* **13,** 4343–4354.
10. Terman, A., Dalen, H., Eaton, J. W., Neuzil, J., and Brunk, U. T. (2003) Mitochondrial recycling and aging of cardiac myocytes: the role of autophagocytosis. *Exp. Gerontol.* **38,** 863–876.
11. Yaffe, M. P. (1999) The machinery of mitochondrial inheritance and behavior. *Science* **283,** 1493–1497.
12. Yoon, Y., Krueger, E. W., Oswald, B. J., and McNiven, M. A. (2003) The mitochondrial protein hFis1 regulates mitochondrial fission in mammalian cells through an interaction with the dynamin-like protein DLP1. *Mol. Cell Biol.* **23,** 5409–5420.
13. James, D. I., Parone, P. A., Mattenberger, Y., and Martinou, J. C. (2003) hFis1, a novel component of the mammalian mitochondrial fission machinery. *J. Biol. Chem.* **278,** 36,373–36,379.

14. Chen, H., Detmer, S. A., Ewald, A. J., Griffin, E. E., Fraser, S. E., and Chan, D. C. (2003) Mitofusins Mfn1 and Mfn2 coordinately regulate mitochondrial fusion and are essential for embryonic development. *J. Cell Biol.* **160,** 189–200.
15. Koshiba, T., Detmer, S. A., Kaiser, J. T., Chen, H., McCaffery, J. M., and Chan, D. C. (2004) Structural basis of mitochondrial tethering by mitofusin complexes. *Science* **305,** 858–862.
16. Ishihara, N., Eura, Y., and Mihara, K. (2004) Mitofusin 1 and 2 play distinct roles in mitochondrial fusion reactions via GTPase activity. *J. Cell Sci.* **117,** 6535–6546.
17. Cipolat, S., de Brito, O. M., Dal Zilio, B., and Scorrano, L. (2004) OPA1 requires mitofusin 1 to promote mitochondrial fusion. *Proc. Natl. Acad. Sci. U. S. A.* **101,** 15,927–15,932.
18. Jagasia, R., Grote, P., Westermann, B., and Conradt, B. (2005) DRP-1-mediated mitochondrial fragmentation during EGL-1-induced cell death in *C. elegans*. *Nature* **433,** 754–760.
19. Germain, M., Mathai, J. P., McBride, H. M., and Shore, G. C. (2005) Endoplasmic reticulum BIK initiates DRP1-regulated remodelling of mitochondrial cristae during apoptosis. *EMBO J.* **24,** 1546–1556.
20. Bernardi, P., Scorrano, L., Colonna, R., Petronilli, V., and Di Lisa F. (1999) Mitochondria and cell death. Mechanistic aspects and methodological issues. *Eur. J. Biochem.* **264,** 687–701.
21. Adachi, S., Gottlieb, R. A., and Babior, B. M. (1998) Lack of release of cytochrome *c* from mitochondria into cytosol early in the course of Fas-mediated apoptosis of Jurkat cells. *J. Biol. Chem.* **273,** 19,892–19,894.
22. Petronilli, V., Penzo, D., Scorrano, L., Bernardi, P., and Di Lisa, F. (2001) The mitochondrial permeability transition, release of cytochrome c and cell death. Correlation with the duration of pore openings in situ. *J. Biol. Chem.* **276,** 12,030–12,034.
23. Hockenbery, D. M., Oltvai, Z. N., Yin, X. M., Milliman, C. L., and Korsmeyer, S. J. (1993) Bcl-2 functions in an antioxidant pathway to prevent apoptosis. *Cell* **75,** 241–251.
24. Cornwell, M. M., Pastan, I., and Gottesman, M. M. (1987) Certain calcium channel blockers bind specifically to multidrug-resistant human KB carcinoma membrane vesicles and inhibit drug binding to P-glycoprotein. *J. Biol. Chem.* **262,** 2166–2170.

5 Results

Frezza C, Cipolat S, Martins de Brito O, Micaroni M, Beznoussenko GV, Rudka T,Bartoli D, Polishuck RS, Danial NN, De Strooper B, Scorrano L.
OPA1 controls apoptotic cristae remodeling independently from mitochondrial fusion.
Cell. 2006 Jul 14;126(1):177-89.

Cipolat S, Rudka T, Hartmann D, Costa V, Serneels L, Craessaerts K, Metzger K, Frezza C, Annaert W, D'Adamio L, Derks C, Dejaegere T, Pellegrini L, D'Hooge R, Scorrano L, De Strooper B.
Mitochondrial rhomboid PARL regulates cytochrome c release during apoptosis via OPA1-dependent cristae remodeling.
Cell. 2006 Jul 14;126(1):163-75.

Frezza C, Basso M, Bonetto V, Scorrano L.
Exploring the molecular composition of OPA1 complexes

Frezza C, Cogliati S, Bortolato A, Moro S, Scorrano L
Targeting OPA1 GTPase function enhances cytochrome c release from isolated mitochondria.

Cell

OPA1 Controls Apoptotic Cristae Remodeling Independently from Mitochondrial Fusion

Christian Frezza,[1] Sara Cipolat,[1] Olga Martins de Brito,[1] Massimo Micaroni,[2] Galina V. Beznoussenko,[2] Tomasz Rudka,[3] Davide Bartoli,[1] Roman S. Polishuck,[2] Nika N. Danial,[4] Bart De Strooper,[3] and Luca Scorrano[1,*]
[1]Dulbecco-Telethon Institute, Venetian Institute of Molecular Medicine, Padova, Italy
[2]Department of Cell Biology and Oncology, Consorzio "Mario Negri Sud," Santa Maria Imbaro, Italy
[3]Neuronal Cell Biology and Gene Transfer Laboratory, Center for Human Genetics, Flanders Interuniversity Institute for Biotechnology (VIB4) and K.U. Leuven, Belgium
[4]Department of Cancer Biology, Dana-Farber Cancer Institute, Harvard Medical School, Boston, MA 02115, USA
*Contact: luca.scorrano@unipd.it
DOI 10.1016/j.cell.2006.06.025

SUMMARY

Mitochondria amplify activation of caspases during apoptosis by releasing cytochrome c and other cofactors. This is accompanied by fragmentation of the organelle and remodeling of the cristae. Here we provide evidence that Optic Atrophy 1 (OPA1), a profusion dynamin-related protein of the inner mitochondrial membrane mutated in dominant optic atrophy, protects from apoptosis by preventing cytochrome c release independently from mitochondrial fusion. OPA1 does not interfere with activation of the mitochondrial "gatekeepers" BAX and BAK, but it controls the shape of mitochondrial cristae, keeping their junctions tight during apoptosis. Tightness of cristae junctions correlates with oligomerization of two forms of OPA1, a soluble, intermembrane space and an integral inner membrane one. The proapoptotic BCL-2 family member BID, which widens cristae junctions, also disrupts OPA1 oligomers. Thus, OPA1 has genetically and molecularly distinct functions in mitochondrial fusion and in cristae remodeling during apoptosis.

INTRODUCTION

Mitochondria amplify apoptosis induced by several stimuli (Green and Kroemer, 2004). They release cytochrome c and other proapoptotic proteins activating a postmitochondrial pathway that culminates in cell demise (Wang, 2001). Proteins of the BCL-2 family control the release of cytochrome c from mitochondria required for the activation of effector caspases (Adams and Cory, 2001). The "BH3-only" proapoptotic members of the family transmit the different apoptotic signals to the multidomain members BAX and BAK that are required for cytochrome c release and mitochondrial dysfunction (Scorrano and Korsmeyer, 2003). In a widely accepted model, these proteins can form a channel for the efflux of cytochrome c across the outer mitochondrial membrane (Green and Kroemer, 2004). Additional pathways downstream of the BH3-only proteins ensure complete release of cytochrome c and mitochondrial dysfunction. They include fragmentation of the mitochondrial network and remodeling of the cristae characterized by fusion of individual cristae and opening of the cristae junctions (Frank et al., 2001; Scorrano et al., 2002).

Mitochondrial morphology is controlled by a growing family of "mitochondria-shaping" proteins (Griparic and van der Bliek, 2001). Mitofusin (MFN) -1 and -2 are dynamin-related proteins of the outer membrane (OM) essential for mitochondrial tethering and fusion (Santel and Fuller, 2001; Legros et al., 2002; Santel et al., 2003; Chen et al., 2003). MFN2 is presumed to have mostly a regulatory role (Ishihara et al., 2004), while MFN1 tethers two juxtaposed organelles (Koshiba et al., 2004) and cooperates with Optic Atrophy 1 (OPA1) in the fusion process (Cipolat et al., 2004). OPA1 is also a dynamin-related protein that resides in the inner mitochondrial membrane (IM). Dynamin-related protein 1 (DRP-1) is located in the cytoplasm but during fission translocates to mitochondria where it binds to hFis1, its adaptor in the OM (Smirnova et al., 2001; Yoon et al., 2003; James et al., 2003). It is presumed that DRP-1 can sever both membranes either directly or by recruiting other IM proteins.

A growing body of evidence suggests that mitochondria-shaping proteins participate in cell death. Dnm1p, the yeast ortholog of DRP-1, mediates mitochondrial fragmentation and apoptosis-like death in *S. cerevisiae* (Fannjiang et al., 2004). Blocking Drp-1 in *C. elegans* inhibits apoptotic mitochondrial fragmentation and results in the accumulation of supernumerary cells during development (Jagasia et al., 2005). Expression of a dominant negative mutant of DRP-1 or downregulation of hFis1 in

mammalian cells delays cytochrome c release and apoptosis (Frank et al., 2001; Lee et al., 2004). MFN1 and MFN2, alone or in combination, prevent death by some intrinsic stimuli (Sugioka et al., 2004; Neuspiel et al., 2005), consistent with early inhibition of MFN1-dependent fusion during apoptosis (Karbowski et al., 2004). Following several death stimuli, including the BH3-only proteins BID and BIK, mitochondria remodel their internal structure: individual cristae fuse and cristae junctions widen, allowing complete cytochrome c release (Scorrano et al., 2002; Germain et al., 2005). While the molecular details of mitochondrial fragmentation during apoptosis have been partially unraveled, little is known about the mechanisms controlling cristae remodeling, and we wished to further elucidate this process. OPA1 protects from apoptosis and is so far the only mitochondria-shaping protein associated with the IM (Olichon et al., 2003), making it a potential candidate to control cristae remodeling. Downregulation of OPA1 not only causes mitochondrial fragmentation but also alters the shape of the cristae (Olichon et al., 2003). Since cristae contain the bulk of cytochrome c, the regulation of this process could explain the known antiapoptotic effect of OPA1. Alternatively, OPA1 could act by counteracting mitochondrial fission (Lee et al., 2004). Here we genetically dissect the role of OPA1 in apoptosis and find that this can be separated from its role in mitochondrial fusion.

RESULTS

OPA1 Protects from Apoptosis by Preventing Cytochrome c Release and Mitochondrial Dysfunction

Expression of wild-type (wt) OPA1 protected mouse embryonic fibroblasts (MEFs) from death induced by apoptotic stimuli that activate the mitochondrial pathway like H_2O_2, etoposide, staurosporine, and truncated, active BID (tBID) (Wei et al., 2001; Scorrano et al., 2003) (Figures 1A–1D). OPA1 did not affect the extrinsic pathway of apoptosis recruited by TNFα since MEFs used in these experiments behave like type I cells not safeguarded by expression of BCL-2 (not shown). In type I cells, death receptors directly activate effector caspases, bypassing the mitochondrial amplificatory loop (Scaffidi et al., 1998). Mutation of a conserved Lys of the GTPase domain to Ala ($OPA1^{K301A}$), or truncation of a part of the C-terminal coiled-coil domain ($OPA1^{R905*}$) impair OPA1 pro-fusion activity (Cipolat et al., 2004). When these mutants were expressed at similar levels to wt OPA1 (data not shown and Cipolat et al., 2004), they failed to protect from all the stimuli tested (Figure 1). Thus, the GTPase and the C-terminal coiled-coil domains of OPA1 are required for protection from apoptosis.

OPA1 delayed release of cytochrome c following H_2O_2 (Figure 2A; quantification in Figure 2B), staurosporine (Figure S1B), etoposide, and tBID (not shown). Release of cytochrome c is accompanied by mitochondrial dysfunction and loss of mitochondrial membrane potential.

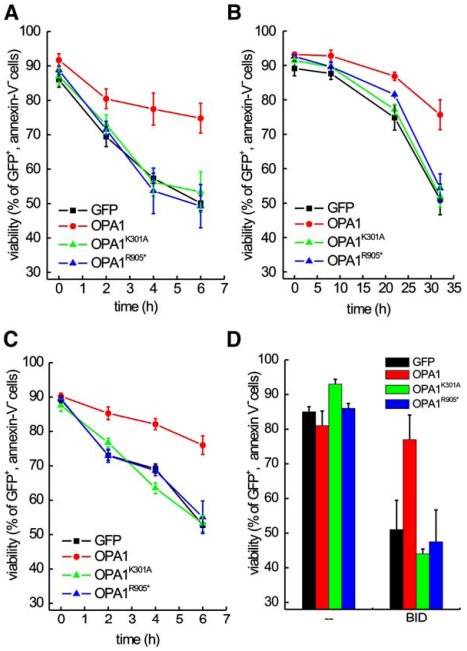

Figure 1. OPA1 Protects Against Apoptosis by Intrinsic Stimuli

wt MEFs were cotransfected with GFP and the indicated plasmids and after 24 hr treated with 1 mM H_2O_2 (A) (mean ± SEM of 12 independent experiments), 2 μM etoposide (B) (mean ± SEM of 12 independent experiments), or 2 μM staurosporine (C) (mean ± SEM of 12 independent experiments) for the indicated times. In (D) cells were cotransfected with GFP and pcDNA3.1 or with pcDNA3.1-tBID and after 24 hr viability was determined. Data represent average ± SEM of 7–12 independent experiments.

We followed in real time changes in the mitochondrial fluorescence of the potentiometric probe tetramethylrhodamine methylester (TMRM). OPA1 prevented depolarization induced by H_2O_2 (Figures 2C and 2D). Conversely, $OPA1^{K301A}$ had no such protective effects on cytochrome c release and mitochondria depolarization (Figures 2C and 2D). These results indicate that functional OPA1 decreases release of cytochrome c and loss of mitochondrial membrane potential during apoptosis.

OPA1 Does Not Require Mitofusins to Protect from Apoptosis

OPA1 requires *Mfn1* for its profusion activity (Cipolat et al., 2004). To check whether OPA1 protects against apoptosis by promoting fusion, we expressed OPA1 in MEFs lacking *Mfn1*. OPA1 protected *Mfn1*$^{-/-}$ cells from apoptosis induced by all the intrinsic stimuli tested to an extent similar to that observed in wt cells (Figures 3A–3C). Since residual mitochondrial fusion is still observed in *Mfn1*$^{-/-}$ MEFs, we

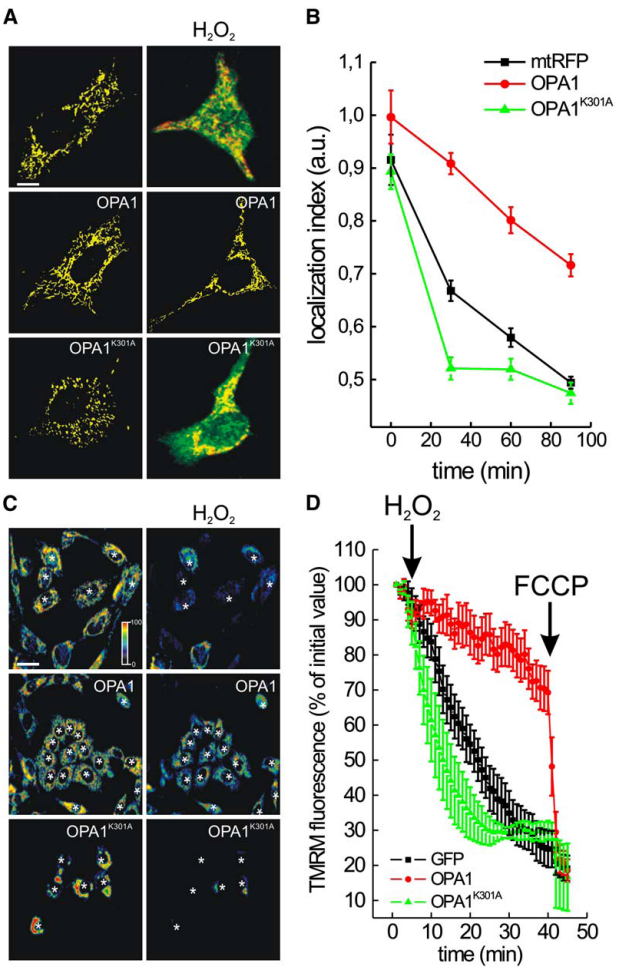

Figure 2. OPA1 Delays Release of Cytochrome c and Mitochondrial Dysfunction during Apoptosis

(A) Representative images of subcellular cytochrome c distribution. wt MEFs were cotransfected with mtRFP (red), and the indicated plasmids were left untreated or treated for 30 min with 1 mM H_2O_2, fixed and immunostained for cytochrome c (green). Bar, 15 μm.

(B) Localization index of cytochrome c. Experiments were performed as in (A), but cells were fixed at the indicated times. Data represent mean ± SEM of five independent experiments.

(C) Pseudocolor-coded images of TMRM fluorescence in wt MEFs cotransfected with GFP and the indicated plasmids. Left images represent the initial frame of the real-time sequence, while right ones were acquired at time = 40 min. Asterisks indicate GFP-positive cells. The pseudocolor scale is shown. Bar, 40 μm.

(D) Quantitative analysis of TMRM fluorescence changes over mitochondrial regions. When indicated (arrows), 1 mM H_2O_2, and 2 μM FCCP were added. Data represent average ± SEM of eight independent experiments performed as in (C).

turned to cells doubly deficient for *Mfn1* and *Mfn2* (DMF), where fusion is completely blocked (Chen et al., 2005). DMF cells appeared as sensitive to staurosporine and H_2O_2 as wt and single *Mfn1* $^{-/-}$ cells, and OPA1 was effective in protecting them from apoptosis (Figures 3D and 3E). We confirmed that OPA1 inhibited release of cytochrome c in *Mfn1* $^{-/-}$ and in DMF cells induced by H_2O_2 (Figures 3F and 3G) or by staurosporine (Figures S1C and S1D). Of note, *Mfn1* $^{-/-}$ and DMF mitochondria expressing OPA1 remained completely fragmented, yet they retained cytochrome c, further dissociating blockage of cytochrome c release from mitochondrial fusion. Thus, OPA1 protects from apoptosis in the absence of MFN1 and MFN2. The profusion activity of OPA1 is therefore not necessary for its antiapoptotic activity.

OPA1 Controls Cytochrome c Mobilization from Mitochondrial Cristae

We verified whether OPA1 influenced the release of cytochrome c in an in vitro quantitative assay using purified organelles and recombinant proteins. Cytochrome c release from mitochondria isolated from control MEF clones carrying an empty vector with a Puromycin resistance gene (wt::*Puro* and *Mfn1* $^{-/-}$::*Puro*) in response to recombinant, caspase-8-cleaved p7/p15 BID (cBID) was almost complete after 15 min. We generated clones expressing high levels of OPA1 (wt::*Opa1* and *Mfn1* $^{-/-}$::*Opa1*) as confirmed by immunoblotting (Figure S2). Mitochondria isolated from these cells conversely retained a significant fraction of cytochrome c even after 15 min (Figures 4A–4D). Release was extremely fast in mitochondria isolated

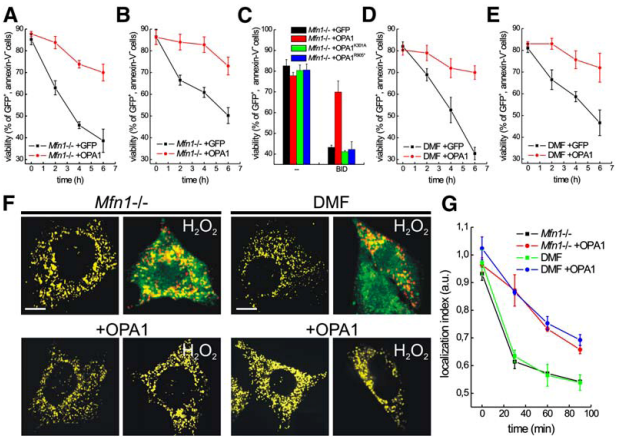

Figure 3. Mitofusins Are Not Required for the Antiapoptotic Effect of OPA1

(A–E) Cells of the indicated genotype were cotransfected with GFP and the indicated plasmids and treated with 1 mM H_2O_2 (A and D) or 2 μM staurosporine (B and E). At the indicated times, cells were harvested and viability was determined. In (C), *Mfn1*$^{-/-}$ MEFs were cotransfected with GFP and pcDNA3.1 or pcDNA3.1-tBID and after 24 hr viability was determined. Data represent average ± SEM of ten independent experiments.

(F) Representative images of subcellular cytochrome c distribution. Cells of the indicated genotype cotransfected with mtRFP (red) and the indicated plasmid were left untreated or treated for 30 min with 1 mM H_2O_2, fixed, and immunostained for cytochrome c (green). Bar, 10 μm.

(G) Localization index of cytochrome c. Experiments were performed as in (F), except that cells were fixed at the indicated times. Data represent average ± SEM of five independent experiments.

from MEFs expressing high levels of OPA1^{K301A} (wt::*Opa1*^{K301A}) or a short hairpin RNA interference targeting OPA1 (wt::*shOpa1*) (Figure S2), reaching ~85% of the total pool of cytochrome c after only 5 min (Figures 4B and 4C). Thus, levels of active OPA1 regulate the release of cytochrome c from mitochondria. The final step of cytochrome c release from mitochondria requires activation and oligomerization of the multidomain proapoptotic BCL-2 family members BAX and BAK. We found that OPA1 did not delay activation and translocation of BAX to mitochondria in response to staurosporine (Figure S1A). Furthermore, BAK activation, measured by its oligomerization in purified mitochondria upon BID stimulation, was also unaltered (Figures 4F and 4G). Thus, OPA1 does not interfere with activation of proapoptotic members of the BCL-2 family, crucial for the permeabilization of the OM.

A small fraction of cytochrome c, corresponding to ~15%–20% of the total, is found free in the IMS, while most is located in the cristae (Scorrano et al., 2002). The OM of mitochondria can be selectively permeabilized

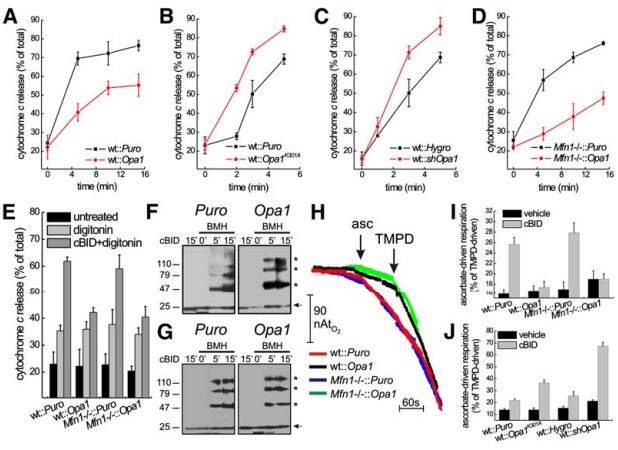

Figure 4. OPA1 Controls Mobilization of Cytochrome c from Mitochondrial Cristae in Response to BID

(A–D) Mitochondria isolated from MEFs of the indicated genotype were treated for the indicated times with cBID. After centrifugation the amount of cytochrome c in supernatant and pellet was determined by a specific ELISA. Data represent average ± SEM of four independent experiments.

(E) Mitochondria isolated from MEFs of the indicated genotype were incubated with cBID for 3 min. The OM was then permeabilized with 40 pmol digitonin × mg^{-1} mitochondria for 5 min. After centrifugation, cytochrome c content in supernatant and pellet was measured as in (A).

(F and G) wt (F) and *Mfn1*$^{-/-}$ (G) mitochondria of the indicated genotype were treated with cBID for the indicated times. DMSO or 10 mM BMH was then added and after 30 min the crosslinking reaction was quenched (Wei et al., 2000). Equal amounts (40 μg) of mitochondrial proteins were analyzed by SDS-PAGE/immunoblotting using anti-BAK antibody. Asterisks: BAK multimers.

(H) Representative traces of ascorbate-driven respiration following BID treatment. Mitochondria of the indicated genotype were treated for 5 min with cBID and then transferred into an oxygen electrode chamber. Where indicated (arrows), 6 mM ascorbate-Tris and 300 μM TMPD were added.

(I and J) Quantitative analysis of the effect of OPA1 levels and function on BID-induced cytochrome c mobilization. Mitochondria of the indicated genotype were treated with cBID for 5 (I) or 3 min (J), and cytochrome c in the supernatant was assayed as in (D). Data represent average ± SEM of five independent experiments.

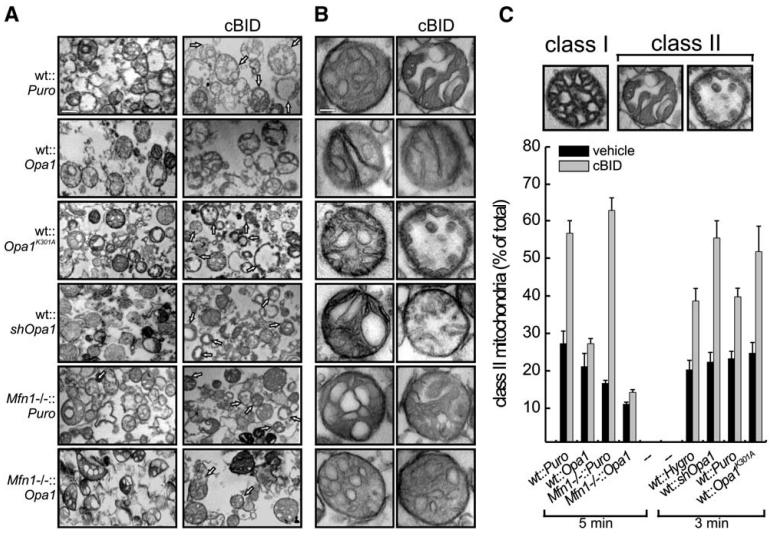

Figure 5. Mitochondrial Morphological Changes in Response to BID: Regulation by OPA1

(A) Representative EM fields of mitochondria of the indicated genotype. Where indicated, mitochondria were treated for 5 min with cBID, except for wt::*shOpa1* and wt::$Opa1^{K301A}$ mitochondria, which were treated for 3 min. Arrows indicate class II mitochondria. Bar, 600 nm.

(B) Magnifications of representative transmission EM of mitochondria. Experiments were performed as in (A). Bar, 200 nm.

(C) Blind morphometric analysis of randomly selected EM fields of mitochondria of the indicated genotype. The experiments were performed as in (A). Inset shows representative class I and class II (remodeled) morphologies (Scorrano et al., 2002). Data represent average ± SEM of three independent experiments.

using titrated amounts of digitonin to selectively release the IMS pool of cytochrome c (Scorrano et al., 2002). Approximately 15% of total cytochrome c was released upon permeabilization of the outer membrane in wt and *Mfn1* $^{-/-}$ mitochondria, irrespective of OPA1. When wt and *Mfn1* $^{-/-}$ mitochondria were pretreated with cBID for 3 min, ~60% of total cytochrome c was recovered in the supernatant, confirming that at this early timepoint cBID promotes mobilization of cytochrome c from cristae to the IMS (Scorrano et al., 2002). This increase in digitonin-releasable cytochrome c upon cBID treatment was not observed in mitochondria from cells expressing OPA1 (Figure 4E). Thus, OPA1 appears to selectively stabilize the pool of cytochrome c that cBID mobilizes towards the IMS.

We therefore measured cytochrome c mobilization from cristae using a specific assay. Given the different redox potential and accessibility of membrane bound and free cytochrome c, these two pools can be specifically reduced by ascorbate and N,N,N′,N′-tetramethyl-p-phenylenediamine (TMPD) (Scorrano et al., 2002; Nicholls et al., 1980). The ratio of ascorbate over TMPD-driven O_2 consumption (asc/TMPD) therefore provides an estimate of the pool of free cytochrome c in the IMS relative to the total mitochondrial cytochrome c. An increase in asc/TMPD ratio reflects the mobilization of cytochrome c from the cristae stores towards the IMS (Scorrano et al., 2002). cBID almost doubled this ratio in wt and *Mfn1* $^{-/-}$ mitochondria (Figures 4H and 4I). OPA1 did not affect basal asc/TMPD ratio, but it blocked the increase in the ratio observed upon cBID treatment in wt and *Mfn1* $^{-/-}$ mitochondria (Figures 4H and 4I). Conversely, $OPA1^{K301A}$ and downregulation of OPA1 levels augmented the effect of cBID on the asc/TMPD ratio (Figure 4J). Of note, lower OPA1 levels resulted in a small but significant increase in basal asc/TMPD ratio (Figure 4J, $p < 0.05$ compared to control wt::*Hygro* mitochondria). Thus, OPA1 regulates apoptotic redistribution of cytochrome c from the cristae.

OPA1 Controls Apoptotic Remodeling of Mitochondrial Cristae

The changes in mitochondrial ultrastructure defined as "cristae remodeling" correlate with redistribution of cytochrome c from the cristae (Scorrano et al., 2002). Using conventional transmission electron microscopy (TEM), it is possible to identify remodeled "class II" mitochondria and normal "class I" mitochondria based on the appearance of the electron transparent cristae (see Figure 5C for representative images). We therefore turned to TEM of mitochondria isolated from the generated cellular models to investigate whether OPA1 influenced remodeling of the cristae. OPA1 promoted juxtaposition of the cristae membranes, generating extremely narrow structures not seen in control mitochondria (Figures 5A and 5B).

In contrast, cristae appeared wider and in wt::*Opa1*^{K301A} and wt::*shOpa1* mitochondria (Figures 5A and 5B). *Mfn1* $^{-/-}$::*Puro* and *Mfn1* $^{-/-}$::*Opa1* mitochondria displayed hyperconvex, balloon-like cristae, connected by narrow, tubular, elongated junctions to the intermembrane space (Figures 5A and 5B). cBID induced the appearance of several class II organelles in control populations (arrows in Figure 5A; magnification in Figure 5B). These remodeled mitochondria were predominant in wt::*Opa1*^{K301A} or wt::*shOpa1* as soon as 3 min after cBID (arrows in Figure 5A; magnification in Figure 5B). On the other hand, cristae of wt::*Opa1* and *Mfn1* $^{-/-}$::*Opa1* mitochondria remained narrow, and mainly class I mitochondria were retrieved following cBID (Figure 5A; magnification in Figure 5B). These observations were further corroborated by a morphometric analysis (Figure 5C).

The effect of OPA1 on mitochondrial morphology and remodeling warranted a more detailed structural investigation by electron tomography. Cristae of wt::*Puro* mitochondria appeared as pleomorphic individual structures connected to the IMS by a narrow tubular junction of 16.2 ± 2.1 nm (n = 9 in two different tomograms). wt OPA1 promoted close juxtaposition of the cristae membranes, and some cristae spanned the diameter of the reconstructed mitochondrion. The cristae junction was extremely narrow, measuring 15.2 ± 2.3 nm (n = 9 in two different tomograms) (Figure 6A). Conversely, wt::*Opa1*^{K301A} and wt::*shOpa1* cristae protruded in the matrix for less than the radius of the organelle. The narrow tubular junction was unaltered in wt::*Opa1*^{K301A} (17.1 ± 2.1 nm, n = 9 in two different tomograms) and in wt::*shOpa1* mitochondria (20.2 ± 1.6 nm, n = 9 in two different tomograms) (Figure 6A).

In wt::*Puro* mitochondria cBID promoted fusion of cristae in few intercommunicating compartments and widened the cristae junctions (45.4 ± 3.2 nm, n = 9 in two different tomograms). In wt::*Opa1* mitochondria, in contrast, cristae fused following cBID, but they retained an extremely narrow aspect, and the diameter of the tubular junction remained small (20.2 ± 3.1 nm, n = 9 in two different tomograms). Cristae junction diameter increased extremely in wt::*Opa1*^{K301A} mitochondria (65.3 ± 4.2 nm, n = 9 in two different tomograms) and in wt::*shOpa1* (73.3 ± 2.1 nm, n = 9 in two different tomograms) (Figure 6A). Rotation of a volume-rendered 3D reconstruction where the outer membrane had been peeled out allowed clear visualization of the cristae junctions (Figure 6B). In untreated mitochondria, these narrow structures were unaffected by expression of OPA1. Following cBID they became greatly enlarged, and this enlargement was entirely prevented by OPA1 expression (Figure 6B). To investigate whether OPA1 required *Mfn1* to control shape and remodeling of the cristae, we turned to *Mfn1* $^{-/-}$ mitochondria. *Mfn1* $^{-/-}$::*Puro* mitochondria showed balloon-like, hyperconvex, individual cristae coexisting with more conventional pleomorphic ones. Independently from their shape, cristae had narrow junctions of 19.0 ± 2.1 nm (n = 9 in two different tomograms). *Mfn1* $^{-/-}$::*Opa1* mitochondria showed balloon cristae with some aspects of close juxtaposition of cristae membranes similar to those observed in wt::*Opa1* organelles. The narrow tubular junction of these cristae measured 18.3 ± 2.2 nm (n = 9 in two different tomograms). cBID caused fusion of *Mfn1* $^{-/-}$::*Puro* cristae and widening of their tubular junctions (41.4 ± 2.2 nm, n = 9 in two different tomograms). Conversely, junctions remained tight in *Mfn1* $^{-/-}$::*Opa1* cristae, their diameter measuring 18.5 ± 2.0 nm (n = 9 in two different tomograms) (Figure 6A). Thus, OPA1 counteracts the widening of the tubular junctions induced by cBID independently of MFN1.

Oligomers of Soluble and Membrane Bound OPA1 Are Disrupted by BID Early during Apoptosis

We turned to a biochemical approach to determine how OPA1 could control cristae shape. OPA1 is synthesized as an integral IM protein from one single gene. Alternative splicing generates eight different transcripts, all of them containing the transmembrane domain (Delettre et al., 2001), but a minor fraction of OPA1 is released in the IMS in a process that is regulated by the IM rhomboid protease PARL (Cipolat et al, 2006). The IMS form is crucial for OPA1 antiapoptotic activity (Cipolat et al., 2006). We verified whether expression of OPA1 in wt and *Mfn1* $^{-/-}$ cells resulted in an increase in IMS OPA1. Immunoblotting of membrane (pellet) and IMS (supernatant) fractions generated by hypotonic swelling and salt washes of mitochondria revealed that following expression, levels of IMS OPA1 were increased (Figure 7A). OPA1 in the membrane-enriched fraction was resistant to carbonate extraction, further indicating that this OPA1 form is integrally inserted in the IM (not shown). Consistent with this, only a minor fraction of OPA1 was released from mitochondria treated with cBID, even when cytochrome c release was complete (Figure S3). Thus, complete release of OPA1 does not occur in isolated mitochondria upon cBID treatment and can therefore not explain cristae remodeling, as previously suggested (Arnoult et al., 2005).

We therefore analyzed in greater detail OPA1 in normal and apoptotic mitochondria. Percoll-purified normal and cBID-treated, CHAPS-solubilized mouse liver mitochondria displayed very similar elution patterns from Superose 6 columns (not shown) (Danial et al., 2003). Fractions were pooled according to their size exclusion properties, designated B to E4 in descending order of molecular weight, and analyzed by SDS-PAGE and immunoblot. OPA1 was revealed in the high-molecular-weight fractions B to E2, indicating that OPA1 was part of a multimolecular complex. The matrix protein cyclophilin D used as a control was found only in fractions E3 and E4. Another OPA1 immunoreactive band with a MW corresponding to that of the soluble IMS form (Figure 7A) was found in fractions E2 (~180–230 kDa), E1 (~230–440 kDa), and D (~440–670 kDa), indicating that IMS OPA1 is also part of a multiprotein complex (Figure 7B). Following cBID, OPA1 was retrieved in fractions D, E2, and E3. p15 fragment of BID was specifically enriched in this last fraction and to a lower extent in

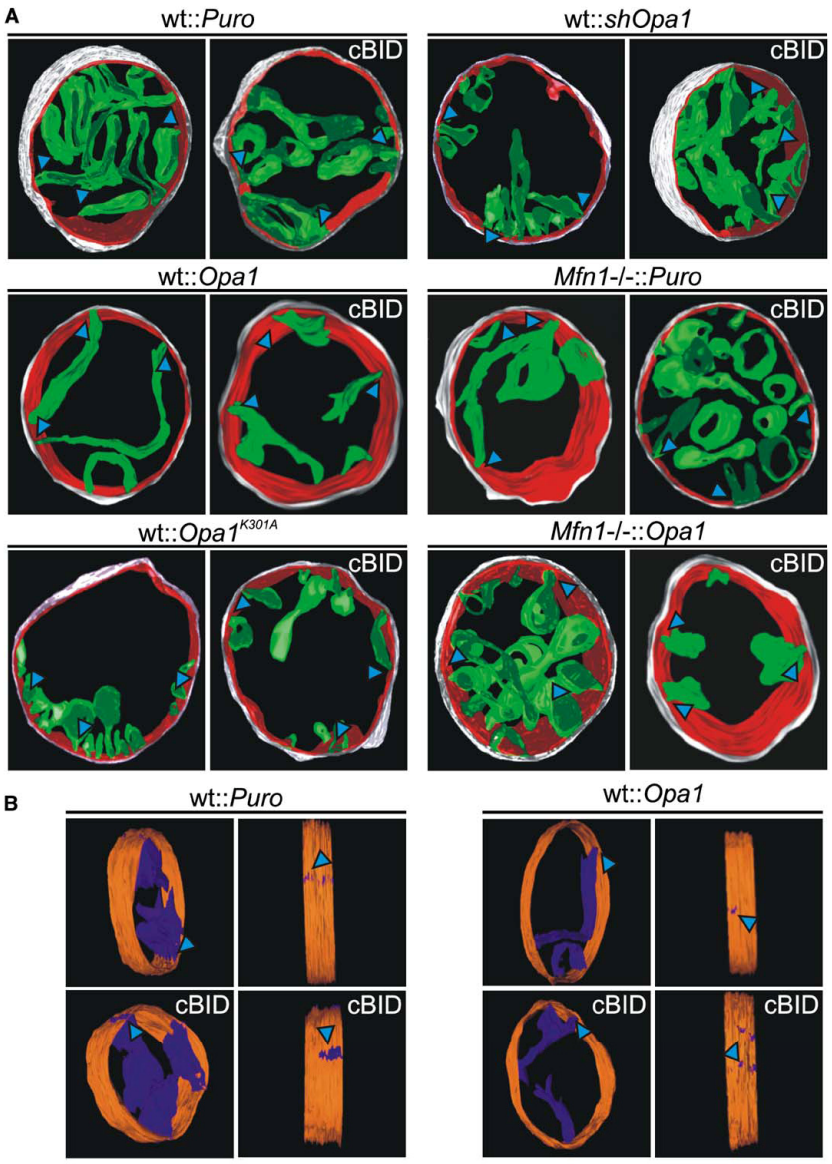

Figure 6. Electron Tomography of Mitochondrial Morphological Changes in Response to BID: Regulation by OPA1

(A) Surface-rendered views of tomographic reconstructions of mitochondria of the indicated genotype. Where indicated, mitochondria were treated with cBID for 5 min before fixation. wt::*shOpa1* and wt::*Opa1*^{K301A} mitochondria were treated for 3 min. Outer membrane is depicted in light gray, inner boundary membrane in red, and cristae in green. Cyan arrowheads point to cristae junctions. Note that selected, representative cristae were traced when their degree of interconnectivity allowed it.

(B) Rotations of representative surface rendered views of tomographic reconstructions of mitochondria. Experiment was as in (A). Cristae are depicted in purple and inner boundary membrane in orange. Outer membrane has been peeled out to highlight individual openings of the cristae junctions (arrowheads).

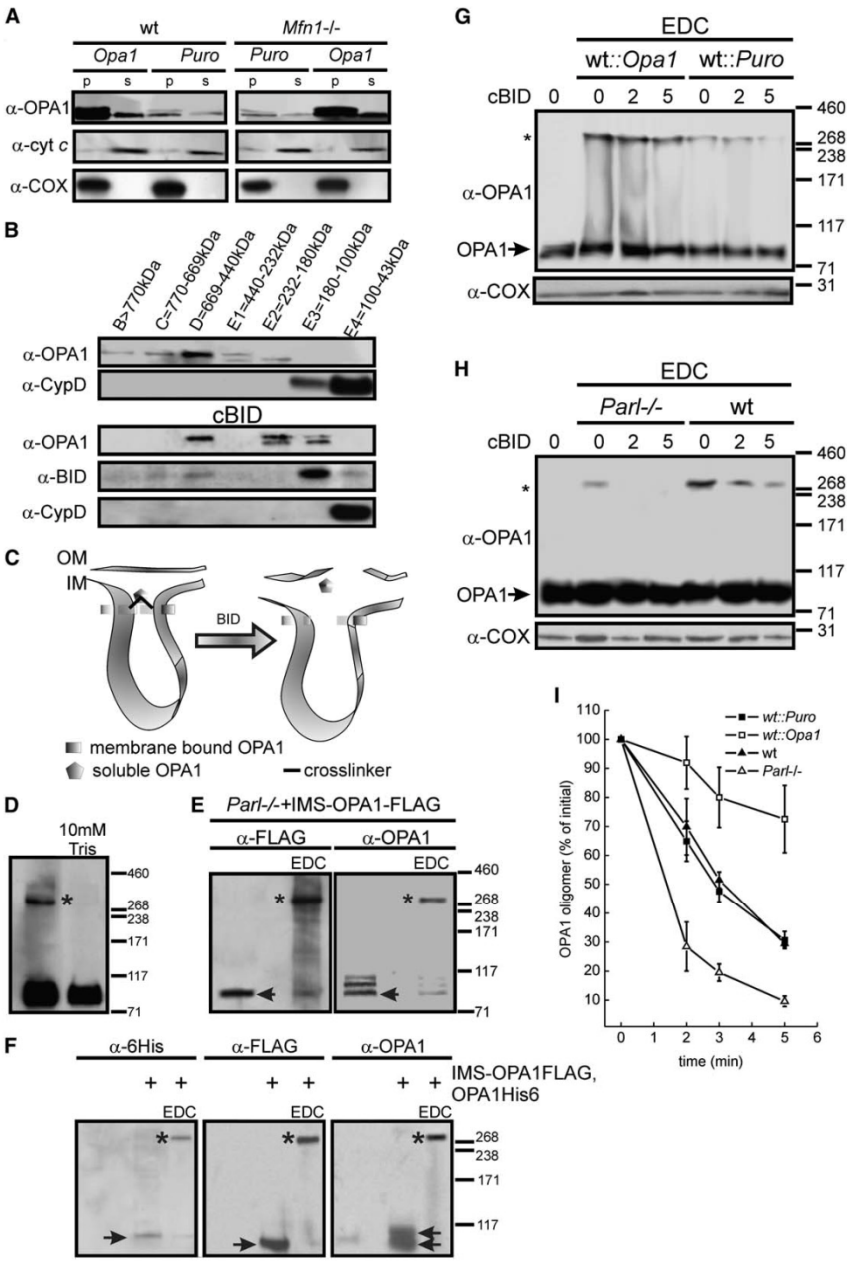

Figure 7. Oligomers Comprising IMS and Transmembrane OPA1 Are Early Targets of BID

(A) Mitochondria of the indicated genotype were hypotonically swollen and membrane (p) and soluble (intermembrane space, s) fractions were recovered. Proteins were separated by SDS-PAGE and immunoblotted with the indicated antibodies. COX indicates cytochrome c oxidase III.

fractions D, C, and E4. The matrix protein cyclophilin D was selectively enriched in low MW fraction E4 (Figure 7B). Thus, OPA1 is mainly found in high MW complexes; the lower MW form of OPA1, corresponding to IMS OPA1, is specifically enriched in fractions D to E2; and OPA1 is mainly found in lower MW fractions in apoptotic mitochondria, corresponding to smaller protein complexes.

Dynamin-related proteins are known to homo-hetero oligomerize (Danino and Hinshaw, 2001). We asked whether OPA1 could also form oligomers containing IMS and/or transmembrane forms. Such a structure could represent a molecular staple that juxtaposes the cristae membranes and could participate in the formation of the narrow tubular junction (Figure 7C). We tested whether chemical crosslinking revealed higher-order complexes immunoreactive for OPA1. A complex of OPA1 of ~290 kDa was indeed identified in mitochondria treated with the zero-length crosslinker 1-ethyl-3-(3-dimethylaminopropyl)carbodiimide (EDC) (Figure 7D). Identical results were observed with the 16 Å crosslinker bismaleimidohexane (not shown). This complex was absent in mitochondria whose cristae had been mechanically distended by osmotic swelling (asterisk in Figure 7D). Thus, OPA1 can be crosslinked into a high-order complex only when cristae are intact. In order to understand the composition of this complex, we turned to *Parl*$^{-/-}$ mitochondria where IMS OPA1 is greatly reduced (Cipolat et al., 2006). Levels of OPA1 complex were also reduced, suggesting a role for IMS OPA1 in its formation (Figure 7H). A FLAG-tagged version of OPA1 selectively targeted to the IMS (IMS-OPA1-FLAG) (Otera et al., 2005; Cipolat et al., 2006) expressed in *Parl*$^{-/-}$ mitochondria was retrieved in the EDC-crosslinked complex by specific anti-FLAG immunoblotting (asterisk in Figure 7E). Reprobing of the membrane with an anti-OPA1 antibody revealed that IMS-OPA1-FLAG displayed an apparent MW of ~88 kDa (arrowhead in Figure 7E), while endogenous OPA1 run at ~100 kDa. Following crosslinking, levels of 100 kDa endogenous and of 88 kDa IMS-OPA1-FLAG were decreased, while the levels of the larger complex increased, suggesting that both IMS and transmembrane forms of OPA1 constitute an oligomer. We further tested this by coexpressing a His-tagged version of OPA1 (OPA1-6His) with IMS-OPA1-FLAG in *Parl*$^{-/-}$ MEFs. As expected, ~98% of OPA1-6His remained transmembrane in mitochondria lacking PARL, as judged by immunoblotting of membrane and IMS fractions (not shown). Transmembrane OPA1-6His and IMS OPA1-FLAG were both found in the oligomer by specific immunoblotting (Figure 7F). Thus, the oligomer contains both transmembrane and IMS OPA1.

We next assessed the fate of this OPA1 oligomer during apoptosis. The oligomer rapidly disappeared following cBID, becoming almost undetectable after 5 min (Figures 7G and 7H). Expression of OPA1 augmented levels of this oligomer and, more importantly, stabilized it in cBID-treated mitochondria (Figure 7G). In *Parl*$^{-/-}$ mitochondria with greatly reduced IMS-OPA1 (Cipolat et al., 2006), OPA1 oligomer was weakly represented and early disrupted by cBID (Figure 7H). A quantitative, densitometric analysis confirmed faster disappearance of the oligomer in *Parl*$^{-/-}$ mitochondria and its stabilization following expression of OPA1 in wt organelles (Figure 7I). Of note, destabilization of OPA1 oligomer is an initial event following cBID, occurring before the complete release of cytochrome c. In as early as 5 min, levels in the oligomer are reduced by ~70%. This almost complete destabilization correlates with the release of approximately 80% of the cytochrome c observed at the same timepoint (Figure 4A). OPA1 oligomer is therefore an early target during cytochrome c release induced by BID. Expression of IMS-OPA1-FLAG protected *Parl*$^{-/-}$ MEFs from apoptosis (Cipolat et al., 2006) and prevented the enhanced cristae remodeling observed in response to cBID (Figure S4), substantiating the role of OPA1 oligomerization in this pathway.

DISCUSSION

The initial assumption that mitochondrial structure is not affected during apoptosis has been challenged during the last years. Mitochondrial fragmentation (Frank et al., 2001; Jagasia et al., 2005) and cristae remodeling (Scorrano et al., 2002; Germain et al., 2005) augment

(B) Mouse liver mitochondria were treated when indicated with cBID for 10 min, solubilized in 6 mM CHAPS, and subjected to gel filtration on Superose 6, and fractions were collected according to the indicated size exclusion properties, pooled, and concentrated. Fifty micrograms of proteins from the indicated fractions were separated by SDS-PAGE and immunoblotted with the indicated antibodies. CypD indicates cyclophilin D.
(C) Cartoon depicting the effect of BID-induced cristae remodeling on putative OPA1 oligomers; OM and IM indicate outer and inner mitochondrial membrane.
(D) Mitochondria left untreated or osmotically swollen for 10 min were incubated with 10 mM EDC for 30 min followed by centrifugation. Proteins in the pellets were separated by SDS-PAGE and immunoblotted using anti-OPA1 antibodies; the asterisk indicates OPA1 oligomer.
(E) Mitochondria were isolated from *Parl*$^{-/-}$ MEFs transfected with IMS-OPA1-FLAG and treated with the crosslinker EDC as in (D). Proteins were separated by SDS-PAGE and immunoblotted using the indicated antibodies; arrows indicate IMS-OPA1-FLAG, while asterisks denote OPA1 oligomer.
(F) *Parl*$^{-/-}$ MEFs were cotransfected with GFP and where indicated with IMS-OPA1-FLAG and OPA1-6His, sorted, and mitochondria were isolated. Where indicated, mitochondria were treated with EDC as in (D). Equal amounts of protein were separated by SDS-PAGE and immunoblotted using the indicated antibodies. Arrows indicate IMS-OPA1-FLAG and OPA1-6His, while asterisks denote OPA1 oligomer.
(G and H) Mitochondria of the indicated genotype were treated with cBID for the indicated times and then crosslinked with EDC as in (D). Proteins were separated by SDS–PAGE and immunoblotted using the indicated antibodies. Asterisk denotes OPA1 oligomer. Arrow indicates nonoligomerized OPA1. COX is cytochrome c oxidase III.
(I) Kinetics of OPA1 oligomer destabilization by cBID. OPA1 oligomer was analyzed by densitometry on Immunoblots following normalization for loading based on levels of COX. Data were normalized to levels of OPA1 oligomer in untreated mitochondria and represent average ± SEM of five independent experiments.

cytochrome c release and complete the program of mitochondrial dysfunction (Green and Kroemer, 2004). Little is known about the molecular mechanisms behind this remodeling process, but a likely candidate protein is OPA1, a dynamin-related protein of the IM, which mediates fusion of the organelle. We demonstrate here that mitochondrial remodeling and cytochrome c mobilization are regulated by levels of functional OPA1 and that this occurs independently from mitochondrial fusion. We also show that IMS and transmembrane OPA1 form oligomers that are early targets of BID during cristae remodeling.

OPA1 reduces cytochrome c release, mitochondrial dysfunction, and cell death induced by intrinsic stimuli without interfering with activation of the mitochondrial gatekeepers, the multidomain proapoptotics BAX and BAK (Scorrano and Korsmeyer, 2003). Given its function in mitochondrial fusion, one could predict that OPA1 protects by counteracting apoptotic fragmentation of mitochondria, a process observed in several paradigms of cell death (Youle and Karbowski, 2005). This appeared not to be the case since OPA1 efficiently protects cells lacking *Mfn1*, essential for OPA1-mediated mitochondrial fusion (Cipolat et al., 2004), and doubly *Mfn* null MEFs where fusion is completely abolished (Chen et al., 2005). Active OPA1 on the other hand blocks intramitochondrial cytochrome c redistribution that follows cristae remodeling (Scorrano et al., 2002; Germain et al., 2005). Previous approaches using conventional EM of mitochondria in cells with downregulated OPA1 or mgm1p (its yeast homolog) showed a gross disruption of the overall cristae morphology (Olichon et al., 2003; Amutha et al., 2004; Griparic et al., 2004). Loss of mitochondrial DNA and therefore of components of the respiratory chain contributed to this phenotype in yeast (Amutha et al., 2004). In mammalian cells, the remodeling of the cristae observed in situ can follow the activation of apoptosis caused by ablation of *Opa1* (Olichon et al., 2003). We therefore reinvestigated the role of OPA1 in biogenesis and remodeling of the cristae using tomography of mitochondria isolated from cellular models with defined levels of this protein. Electron tomography showed that OPA1 regulates shape and length of mitochondrial cristae and more importantly cristae remodeling during apoptosis. OPA1 keeps tight the cristae junction, which is likely to regulate mobilization of cytochrome c to the IMS following BID treatment. *Mfn1*$^{-/-}$ cristae appeared hyperconvex. Nevertheless, they were still connected by a narrow tubular junction to the IMS, and this junction widened following BID treatment. OPA1 did not change curvature of *Mfn1*$^{-/-}$ cristae but, significantly, blocked enlargement of the cristae junction. Thus, curvature of the cristae is not the determining factor in cytochrome c release.

How does OPA1 regulate remodeling of the cristae? One possibility is that OPA1 is released completely during apoptosis, as it has been previously reported (Arnoult et al., 2005). On the other hand, OPA1 has been found to be mainly an integral IM protein (Griparic et al., 2004; Satoh et al., 2003). We indeed observed the release of only a small pool of OPA1 corresponding to a fraction of the protein that is present in the IMS of untreated mitochondria. OPA1 exists in multiple splicing variants. Nevertheless, a transmembrane domain is present in all eight different variants and ensures integral insertion in the IM. So, how is this IMS pool of OPA1 produced? In yeast, pcp1p/rbd1p, a rhomboid protease of the IM, cleaves the transmembrane domain of mgm1p, the yeast homolog of OPA1, to generate a short form soluble in the IMS (McQuibban et al., 2003; Herlan et al., 2003). In an accompanying manuscript, evidence is provided that formation of IMS OPA1 in mammalian mitochondria appears to depend on PARL, the ortholog of rbd1p. *Parl* is also a prerequisite for the antiapoptotic function of OPA1 (Cipolat et al., 2006). This correlates with decreased levels of soluble IMS OPA1 and can be rescued by IMS OPA1 expression (Cipolat et al., 2006). We therefore investigated the potential role of IMS OPA1 at the molecular level. An indication came from studies on dynamin I, which tubulates membranes and assembles in oligomers that are crucial to sever membranes (Sweitzer and Hinshaw, 1998). OPA1 is, however, located inside the bilayer on which it should act. It therefore was unlikely that OPA1 could operate in a similar way as dynamin I. We therefore tested an alternative hypothesis in which transmembrane OPA1 uses the soluble, IMS form to oligomerize. These oligomers could "staple" the membranes of the cristae. We found support for this hypothesis in a series of experiments. First, gel filtration chromatography showed that OPA1 was found in fractions containing high MW complexes (also in HeLa mitochondria [Satoh et al., 2003]). Second, cBID destabilized these oligomers, correlating with increased cytochrome c release and apoptosis. Third, chemical crosslinking identified an ~290 kDa OPA1 immunoreactive band that disappeared when membranes of cristae were separated by osmotic swelling. This oligomer contained the soluble IMS form and the transmembrane IM form of OPA1, as demonstrated using tagged versions of IMS and IM OPA1. Fourth, the presence and disappearance of this oligomer correlates with protection against and induction of apoptosis and cytochrome c release, respectively. Fifth, levels of IMS OPA1 are crucial for the formation of the oligomer to protect from apoptosis (Cipolat et al., 2006) and to prevent cristae remodeling. Taken together, these results suggest that OPA1 oligomers participate in formation and maintenance of the cristae junction.

The size of the OPA1 oligomer as determined by crosslinking and the retrieval of tagged versions of IMS and IM OPA1 in this oligomer suggest the hypothesis of at least a trimer comprising two IM and one IMS OPA1. However, OPA1 is also found in fractions of higher MW in both normal and apoptotic mitochondria. Thus, we cannot exclude the possibility that other proteins participate in this complex. The fact that we found OPA1 in a ~230 to ~180 kDa fraction following treatment with cBID would indeed suggest that OPA1 can associate with other proteins during apoptosis. This is a next challenge requiring copurification experiments and proteomic approaches in normal and apoptotic mitochondria.

Our work shows that OPA1 is a bifunctional protein. On one hand it in promotes mitochondrial fusion, depending on MFN1. On the other, it regulates apoptosis by controlling cristae remodeling and cytochrome c redistribution. This correlates with OPA1 oligomerization and is dependent on its cleavage by PARL. In conclusion, oligomerization of OPA1 appears to be a mechanism that regulates apoptosis by maintaining the tightness of cristae junctions. This unexpected role of OPA1 needs to be further explored. This mechanism could, for example, contribute to the pathogenesis of dominant optic atrophy since mutations causing this disease cluster in the GTPase and coiled-coil domains of OPA1, possibly impairing assembly and/or function of the OPA1 oligomer.

EXPERIMENTAL PROCEDURES

Cell Culture, Transfection, Sorting, and Generation of Stable Clones

SV40 transformed wt and *Mfn1* $^{-/-}$ MEFs were cultured as described in Cipolat et al. (2004); DMF MEFs were cultured as described in Chen et al. (2005). Cells were transfected using Transfectin (Biorad) following manufacturer's instructions.

For sorting, 1×10^8 cotransfected MEFs were analyzed by light forward and side scatter and for GFP fluorescence through a 530 nm band pass filter as they traversed the beam of an argon ion laser (488 nm, 100 mW) of an FACSAria (BD). Nontransfected MEFs were used to set the background fluorescence. Sorted cells were checked for viability by Trypan Blue exclusion.

The single clones were generated by limited dilution following transfection and antibiotic selection of expressing cells.

Analysis of Cell Death

1×10^5 MEFs of the indicated genotype grown in 12-well plates were cotransfected with pEGFP and the indicated vector. After 24 hr cells were treated as described and stained with Annexin-V-Alexa568 (Roche) according to manufacturer's protocol. Apoptosis was measured by flow cytometry (FACSCalibur) as the percentage of annexin-V-positive events in the GFP-positive population.

Transmission Electron Microscopy, Tomographic Reconstruction, and Mitochondrial Morphometry

Mitochondria were fixed for 1 hr at 25°C using glutaraldehyde at a final concentration of 2.5% (V/V). Thin sections were imaged on a Tecnai-12 electron microscope (Philips-FEI) at the Telethon EM Core Facility (TeEMCoF, Istituto Mario Negri Sud). For tomography, colloidal gold particles were applied to one side of 200 nm-thick sections as alignment markers. Tilt series of 122 images were recorded around one tilt axis, over an angular range of 120° with a 1° tilt interval. Images were aligned and reconstructed as previously described (Scorrano et al., 2002). The reconstructed volumes had dimensions of 512 × 512 × 80–100 pixels depending on section thickness, with a pixel size range of 2.5–4.1 nm. Surface-rendered models were produced using IMOD (Mironov et al., 2001) or Reconstruct (Fiala, 2005). Measurements were made directly on 1 pixel-thick tomogram slices.

Molecular Biology

p3 × FLAG-CMV14-AIF-Opa1 (IMS-OPA1-FLAG) and pCDNA3-OPA1-HA-HisTag (OPA1-6His) were kind gifts from K. Mihara (Kyushu University, Fukuoka, Japan) and P. Belenguer (U. of Toulouse, France), respectively. shRNAi were constructed to target the nucleotide region 1813–1831 of murine OPA1. All other plasmids are described in Cipolat et al. (2004).

Imaging

For cytochrome c immunolocalization, cells grown on coverslips were transfected with mtRFP and after 24 hr incubated as detailed. Immunostaining for cytochrome c was performed as described in Scorrano et al. (2003). For cytochrome c and mtRFP detection, green and red channel images were acquired simultaneously using two separate color channels on the detector assembly of a Nikon Eclipse E600 microscope equipped with a Biorad MRC-1024 laser scanning confocal imaging system. The localization index was calculated as described in Petronilli et al. (2001).

For imaging of mitochondrial membrane potential, MEFs grown on coverslips were cotransfected as indicated and after 24 hr loaded with 10 nM TMRM (Molecular Probes) in the presence of 2 μg/ml cyclosporine H, a P-glycoprotein inhibitor (30 min at 37°C). Clusters of GFP-positive cells were identified and sequential images of TMRM fluorescence were acquired every 30 s using an Olympus IMT-2 inverted microscope equipped with a CellR Imaging system.

Recombinant Proteins

p7/p15 recombinant BID was produced, purified, and cleaved with caspase-8 as described in Scorrano et al. (2002). Unless noted, it was used at a final concentration of 32 pmol × mg $^{-1}$.

In Vitro Mitochondrial Assays

Mitochondria were isolated by standard differential centrifugation in isolation buffer (IB). Oxygen consumption of mitochondria incubated in experimental buffer (EB) was measured using a Clarke-type oxygen electrode (Hansatech Instruments) (Scorrano et al., 2002). Cytochrome c redistribution and release in response to recombinant cBID was determined as described in Scorrano et al. (2002).

Biochemistry

For protein crosslinking, mitochondria were treated with 10 mM BMH (Pierce) or with 10 mM EDC (Pierce) for 30 min at 37°C. Samples were centrifuged for 10 min at 12000 × g at 4°C, and the mitochondrial pellets were resuspended in SDS-PAGE sample loading buffer. DTT in the sample buffer quenched the crosslinking reaction. Proteins were separated by 3%–8% Tris-Acetate or 4%–12% Tris-MES SDS-PAGE (NuPage, Invitrogen), transferred onto PVDF membranes (Millipore), and probed using the indicated primary antibodies and isotype matched secondary antibodies conjugated to horseradish peroxidase. Signals were detected using ECL (Amersham). Details on the antibodies used can be found in Supplemental Data. Densitometry was performed using a GS170 Calibrated Imaging densitometer, and data were analyzed using Quantity One software (Biorad).

For Superose 6 filtration, purified mouse liver mitochondria (50 mg) were solubilized in the presence of 6 mM CHAPS passed onto a Superose 6 column, and fractions were collected, pooled, and concentrated as described (Danial et al., 2003).

Additional details on the experimental procedures can be found in Supplemental Data available with this article online.

Supplemental Data

Supplemental Data include four figures and can be found with this article online at http://www.cell.com/cgi/content/full/126/1/■■■/DC1/.

ACKNOWLEDGMENTS

L.S. is an Assistant Telethon Scientist of the Dulbecco-Telethon Institute. This research is supported by Telethon; AIRC; Compagnia di San Paolo; and the Human Frontier Science Program Organization. The TeEMCoF is supported by Telethon Italy (GTF03006). We thank Drs. K. Mihara and P. Belenguer for the gift of plasmids and D. Chan for *Mfn1* $^{-/-}$ and DMF cells. Research in BDS laboratory is supported by a Freedom to Discover grant from Bristol Myers Squib, a Pioneer award from the Alzheimer's Association, the Fund for Scientific

Research, Flanders; K.U.Leuven (GOA); European Union (APOPIS: LSHM-CT-2003-503330); and Federal Office for Scientific Affairs, Belgium.

Received: July 11, 2005
Revised: March 8, 2006
Accepted: June 8, 2006
Published: July 13, 2006

REFERENCES

Adams, J.M., and Cory, S. (2001). Life-or-death decisions by the Bcl-2 protein family. Trends Biochem. Sci. *26*, 61–66.

Amutha, B., Gordon, D.M., Gu, Y., and Pain, D. (2004). A novel role of Mgm1p, a dynamin-related GTPase, in ATP synthase assembly and cristae formation/maintenance. Biochem. J. *381*, 19–23.

Arnoult, D., Grodet, A., Lee, Y.J., Estaquier, J., and Blackstone, C. (2005). Release of OPA1 during apoptosis participates in the rapid and complete release of cytochrome c and subsequent mitochondrial fragmentation. J. Biol. Chem. *280*, 35742–35750.

Chen, H., Detmer, S.A., Ewald, A.J., Griffin, E.E., Fraser, S.E., and Chan, D.C. (2003). Mitofusins Mfn1 and Mfn2 coordinately regulate mitochondrial fusion and are essential for embryonic development. J. Cell Biol. *160*, 189–200.

Chen, H., Chomyn, A., and Chan, D.C. (2005). Disruption of fusion results in mitochondrial heterogeneity and dysfunction. J. Biol. Chem. *280*, 26185–26192.

Cipolat, S., de Brito, O.M., Dal Zilio, B., and Scorrano, L. (2004). OPA1 requires mitofusin 1 to promote mitochondrial fusion. Proc. Natl. Acad. Sci. USA *101*, 15927–15932.

Cipolat, S., Rudka, T., Hartmann, D., Costa, V., Serneels, L., Craessaerts, K., Metzger, K., Frezza, C., Annaert, W., D'Adamio, L., Derks, C., Dejaegere, T., Pellegrini, L., D'Hooge, R., Scorrano, L., and De Strooper, B. (2006). Mitochondrial rhomboid PARL regulates cytochrome c release during apoptosis via OPA1-dependent cristae remodelling. Cell *126*, this issue, ■■■–■■■.

Danial, N.N., Gramm, C.F., Scorrano, L., Zhang, C.Y., Krauss, S., Ranger, A.M., Datta, S.R., Greenberg, M.E., Licklider, L.J., Lowell, B.B., et al. (2003). BAD and glucokinase reside in a mitochondrial complex that integrates glycolysis and apoptosis. Nature *424*, 952–956.

Danino, D., and Hinshaw, J.E. (2001). Dynamin family of mechanoenzymes. Curr. Opin. Cell Biol. *13*, 454–460.

Delettre, C., Griffoin, J.M., Kaplan, J., Dollfus, H., Lorenz, B., Faivre, L., Lenaers, G., Belenguer, P., and Hamel, C.P. (2001). Mutation spectrum and splicing variants in the OPA1 gene. Hum. Genet. *109*, 584–591.

Fannjiang, Y., Cheng, W.C., Lee, S.J., Qi, B., Pevsner, J., McCaffery, J.M., Hill, R.B., Basanez, G., and Hardwick, J.M. (2004). Mitochondrial fission proteins regulate programmed cell death in yeast. Genes Dev. *18*, 2785–2797.

Fiala, J.C. (2005). Reconstruct: a free editor for serial section microscopy. J. Microsc. *218*, 52–61.

Frank, S., Gaume, B., Bergmann-Leitner, E.S., Leitner, W.W., Robert, E.G., Catez, F., Smith, C.L., and Youle, R.J. (2001). The role of dynamin-related protein 1, a mediator of mitochondrial fission, in apoptosis. Dev. Cell *1*, 515–525.

Germain, M., Mathai, J.P., McBride, H.M., and Shore, G.C. (2005). Endoplasmic reticulum BIK initiates DRP1-regulated remodelling of mitochondrial cristae during apoptosis. EMBO J. *24*, 1546–1556.

Green, D.R., and Kroemer, G. (2004). The pathophysiology of mitochondrial cell death. Science *305*, 626–629.

Griparic, L., and van der Bliek, A.M. (2001). The many shapes of mitochondrial membranes. Traffic *2*, 235–244.

Griparic, L., van der Wel, N.N., Orozco, I.J., Peters, P.J., and van der Bliek, A.M. (2004). Loss of the intermembrane space protein Mgm1/OPA1 induces swelling and localized constrictions along the lengths of mitochondria. J. Biol. Chem. *279*, 18792–18798.

Herlan, M., Vogel, F., Bornhovd, C., Neupert, W., and Reichert, A.S. (2003). Processing of Mgm1 by the rhomboid-type protease Pcp1 is required for maintenance of mitochondrial morphology and of mitochondrial DNA. J. Biol. Chem. *278*, 27781–27788.

Ishihara, N., Eura, Y., and Mihara, K. (2004). Mitofusin 1 and 2 play distinct roles in mitochondrial fusion reactions via GTPase activity. J. Cell Sci. *117*, 6535–6546.

Jagasia, R., Grote, P., Westermann, B., and Conradt, B. (2005). DRP-1-mediated mitochondrial fragmentation during EGL-1-induced cell death in C. elegans. Nature *433*, 754–760.

James, D.I., Parone, P.A., Mattenberger, Y., and Martinou, J.C. (2003). hFis1, a novel component of the mammalian mitochondrial fission machinery. J. Biol. Chem. *278*, 36373–36379.

Karbowski, M., Arnoult, D., Chen, H., Chan, D.C., Smith, C.L., and Youle, R.J. (2004). Quantitation of mitochondrial dynamics by photolabeling of individual organelles shows that mitochondrial fusion is blocked during the Bax activation phase of apoptosis. J. Cell Biol. *164*, 493–499.

Koshiba, T., Detmer, S.A., Kaiser, J.T., Chen, H., McCaffery, J.M., and Chan, D.C. (2004). Structural basis of mitochondrial tethering by mitofusin complexes. Science *305*, 858–862.

Lee, Y.J., Jeong, S.Y., Karbowski, M., Smith, C.L., and Youle, R.J. (2004). Roles of the mammalian mitochondrial fission and fusion mediators Fis1, Drp1, and Opa1 in apoptosis. Mol. Biol. Cell *15*, 5001–5011.

Legros, F., Lombes, A., Frachon, P., and Rojo, M. (2002). Mitochondrial fusion in human cells is efficient, requires the inner membrane potential, and is mediated by mitofusins. Mol. Biol. Cell *13*, 4343–4354.

McQuibban, G.A., Saurya, S., and Freeman, M. (2003). Mitochondrial membrane remodelling regulated by a conserved rhomboid protease. Nature *423*, 537–541.

Mironov, A.A., Beznoussenko, G.V., Nicoziani, P., Martella, O., Trucco, A., Kweon, H.S., Di Giandomenico, D., Polishchuk, R.S., Fusella, A., Lupetti, P., et al. (2001). Small cargo proteins and large aggregates can traverse the Golgi by a common mechanism without leaving the lumen of cisternae. J. Cell Biol. *155*, 1225–1238.

Neuspiel, M., Zunino, R., Gangaraju, S., Rippstein, P., and McBride, H.M. (2005). Activated Mfn2 signals mitochondrial fusion, interferes with Bax activation and reduces susceptibility to radical induced depolarization. J. Biol. Chem. *26*, 25060–25070.

Nicholls, P., Hildebrandt, V., Hill, B.C., Nicholls, F., and Wrigglesworth, J.M. (1980). Pathways of cytochrome c oxidation by soluble and membrane-bound cytochrome aa3. Can. J. Biochem. *58*, 969–977.

Olichon, A., Baricault, L., Gas, N., Guillou, E., Valette, A., Belenguer, P., and Lenaers, G. (2003). Loss of OPA1 perturbates the mitochondrial inner membrane structure and integrity, leading to cytochrome c release and apoptosis. J. Biol. Chem. *278*, 7743–7746.

Otera, H., Ohsakaya, S., Nagaura, Z., Ishihara, N., and Mihara, K. (2005). Export of mitochondrial AIF in response to proapoptotic stimuli depends on processing at the intermembrane space. EMBO J. *24*, 1375–1386.

Petronilli, V., Penzo, D., Scorrano, L., Bernardi, P., and Di Lisa, F. (2001). The mitochondrial permeability transition, release of cytochrome c and cell death. Correlation with the duration of pore openings in situ. J. Biol. Chem. *276*, 12030–12034.

Santel, A., and Fuller, M.T. (2001). Control of mitochondrial morphology by a human mitofusin. J. Cell Sci. *114*, 867–874.

Santel, A., Frank, S., Gaume, B., Herrler, M., Youle, R.J., and Fuller, M.T. (2003). Mitofusin-1 protein is a generally expressed mediator of mitochondrial fusion in mammalian cells. J. Cell Sci. *116*, 2763–2774.

Satoh, M., Hamamoto, T., Seo, N., Kagawa, Y., and Endo, H. (2003). Differential sublocalization of the dynamin-related protein OPA1 isoforms in mitochondria. Biochem. Biophys. Res. Commun. *300*, 482–493.

Scaffidi, C., Fulda, S., Srinivasan, A., Friesen, C., Li, F., Tomaselli, K.J., Debatin, K.M., Krammer, P.H., and Peter, M.E. (1998). Two CD95 (APO-1/Fas) signaling pathways. EMBO J. *17*, 1675–1687.

Scorrano, L., and Korsmeyer, S.J. (2003). Mechanisms of cytochrome c release by proapoptotic BCL-2 family members. Biochem. Biophys. Res. Commun. *304*, 437–444.

Scorrano, L., Ashiya, M., Buttle, K., Weiler, S., Oakes, S.A., Mannella, C.A., and Korsmeyer, S.J. (2002). A distinct pathway remodels mitochondrial cristae and mobilizes cytochrome c during apoptosis. Dev. Cell *2*, 55–67.

Scorrano, L., Oakes, S.A., Opferman, J.T., Cheng, E.H., Sorcinelli, M.D., Pozzan, T., and Korsmeyer, S.J. (2003). BAX and BAK regulation of endoplasmic reticulum Ca^{2+}: a control point for apoptosis. Science *300*, 135–139.

Smirnova, E., Griparic, L., Shurland, D.L., and van der Bliek, A.M. (2001). Dynamin-related protein Drp1 is required for mitochondrial division in mammalian cells. Mol. Biol. Cell *12*, 2245–2256.

Sugioka, R., Shimizu, S., and Tsujimoto, Y. (2004). Fzo1, a protein involved in mitochondrial fusion, inhibits apoptosis. J. Biol. Chem. *279*, 52726–52734.

Sweitzer, S.M., and Hinshaw, J.E. (1998). Dynamin undergoes a GTP-dependent conformational change causing vesiculation. Cell *93*, 1021–1029.

Wang, X. (2001). The expanding role of mitochondria in apoptosis. Genes Dev. *15*, 2922–2933.

Wei, M.C., Lindsten, T., Mootha, V.K., Weiler, S., Gross, A., Ashiya, M., Thompson, C.B., and Korsmeyer, S.J. (2000). tBID, a membrane-targeted death ligand, oligomerizes BAK to release cytochrome c. Genes Dev. *14*, 2060–2071.

Wei, M.C., Zong, W.X., Cheng, E.H., Lindsten, T., Panoutsakopoulou, V., Ross, A.J., Roth, K.A., MacGregor, G.R., Thompson, C.B., and Korsmeyer, S.J. (2001). Proapoptotic BAX and BAK: a requisite gateway to mitochondrial dysfunction and death. Science *292*, 727–730.

Yoon, Y., Krueger, E.W., Oswald, B.J., and McNiven, M.A. (2003). The mitochondrial protein hFis1 regulates mitochondrial fission in mammalian cells through an interaction with the dynamin-like protein DLP1. Mol. Cell. Biol. *23*, 5409–5420.

Youle, R.J., and Karbowski, M. (2005). Mitochondrial fission in apoptosis. Nat. Rev. Mol. Cell Biol. *6*, 657–663.

Cell

Mitochondrial Rhomboid PARL Regulates Cytochrome c Release during Apoptosis via OPA1-Dependent Cristae Remodeling

Sara Cipolat,[1,7] Tomasz Rudka,[2,7] Dieter Hartmann,[2,7] Veronica Costa,[1] Lutgarde Serneels,[2] Katleen Craessaerts,[2] Kristine Metzger,[2] Christian Frezza,[1] Wim Annaert,[3] Luciano D'Adamio,[5] Carmen Derks,[2] Tim Dejaegere,[2] Luca Pellegrini,[6] Rudi D'Hooge,[4] Luca Scorrano,[1,*] and Bart De Strooper[2,*]

[1]Dulbecco-Telethon Institute, Venetian Institute of Molecular Medicine, Padova, Italy
[2]Neuronal Cell Biology and Gene Transfer Laboratory
[3]Membrane Trafficking Laboratory
Center for Human Genetics, Flanders Interuniversity Institute for Biotechnology (VIB4) and K.U.Leuven, Leuven, Belgium
[4]Laboratory of Biological Psychology, K.U.Leuven, Leuven, Belgium
[5]Albert Einstein College of Medicine, Bronx, NY 10461, USA
[6]Centre de Recherche Robert Giffard, Universitè Laval, G1J 2G3 Quebec, Canada
[7]These authors contribute equally to this work.
*Contact: luca.scorrano@unipd.it (L.S.); bart.destrooper@med.kuleuven.be (B.D.S.)
DOI 10.1016/j.cell.2006.06.021

SUMMARY

Rhomboids, evolutionarily conserved integral membrane proteases, participate in crucial signaling pathways. Presenilin-associated rhomboid-like (PARL) is an inner mitochondrial membrane rhomboid of unknown function, whose yeast ortholog is involved in mitochondrial fusion. *Parl*$^{-/-}$ mice display normal intrauterine development but from the fourth postnatal week undergo progressive multisystemic atrophy leading to cachectic death. Atrophy is sustained by increased apoptosis, both in and ex vivo. *Parl*$^{-/-}$ cells display normal mitochondrial morphology and function but are no longer protected against intrinsic apoptotic death stimuli by the dynamin-related mitochondrial protein OPA1. *Parl*$^{-/-}$ mitochondria display reduced levels of a soluble, intermembrane space (IMS) form of OPA1, and OPA1 specifically targeted to IMS complements *Parl*$^{-/-}$ cells, substantiating the importance of PARL in OPA1 processing. *Parl*$^{-/-}$ mitochondria undergo faster apoptotic cristae remodeling and cytochrome c release. These findings implicate regulated intramembrane proteolysis in controlling apoptosis.

INTRODUCTION

Rhomboid proteases constitute probably the most widely conserved polytopic-membrane-protein family identified until now (Koonin et al., 2003). Seven rhomboids have been identified in *D. melanogaster* (Freeman, 2004), where they function as essential activators of the epidermal growth factor (EGF) signaling pathway, proteolytically cleaving the EGF receptor ligands Spitz, Gurken, and Keren. Since all Rhomboids share a conserved serine protease catalytic dyad (Lemberg et al., 2005), it has been suggested that they are able to cleave proteins in the transmembrane domain. Therefore, together with the presenilin aspartyl proteases and the Site 2 metalloproteases, they have been functionally assigned to a previously unidentified class of highly hydrophobic proteases involved in "regulated intramembranous proteolytic cleavage," a novel cell-signaling mechanism (Brown et al., 2000). Our knowledge of the mammalian rhomboids is extremely scarce. For example, they are unlikely to be involved in EGF signaling, since TGFα, the major mammalian ligand of the EGFR pathway, is released by metalloproteases of the ADAM family (Freeman, 2004).

Recently, a mitochondrial rhomboid, *rbd1/pcp1*, was identified in *Saccharomyces cerevisiae* (Esser et al., 2002; Herlan et al., 2003; McQuibban et al., 2003; Sesaki et al., 2003). Δ*rbd1* cells display fragmented mitochondria and impaired growth on nonfermentable carbon sources, similar to the phenotype caused by deletion of the dynamin-related protein Mgm1p, which turned out to be a substrate for Rbd1p. The short isoform of Mgm1p produced by Rbd1p is required to maintain mitochondrial morphology and fusion (Herlan et al., 2003; McQuibban et al., 2003). Thus, rhomboids and intramembrane proteolysis appear to control mitochondrial dynamics and function in yeast.

Mitochondria are crucial organelles in intermediate metabolism and energy production (Danial et al., 2003), Ca^{2+} signaling (Rizzuto et al., 2000), and integration and amplification of apoptotic signals (Green and Kroemer, 2004). Such functional versatility is mirrored by their

complex and dynamic morphology, controlled by a growing family of "mitochondria-shaping" proteins that regulate fusion and fission events. In mammals, fission is controlled by the dynamin-related protein DRP-1 (Smirnova et al., 2001) and its outer membrane (OM) adaptor hFis1 (James et al., 2003; Yoon et al., 2003). Fusion is mediated by two OM proteins, mitofusin (MFN) -1 and -2. Optic atrophia 1 (OPA1), the homolog of *S. cerevisiae* Mgm1p, is the only dynamin-related protein identified in the inner membrane (IM) so far (Olichon et al., 2002). OPA1 promotes mitochondrial fusion by cooperating with MFN1 (Cipolat et al., 2004) and is mutated in dominant optic atrophy, the most common cause of inherited optic neuropathy (Alexander et al., 2000; Delettre et al., 2000). The homolog of yeast Rbd1p in mammals is the so-called "presenilin-associated rhomboid-like" (PARL). PARL is a rhomboid protease originally identified in a two-hybrid screen to interact with presenilin, the enzymatically active core protein of γ-secretase (Pellegrini et al., 2001), and later found to be mitochondrial (Sik et al., 2004). We used a genetic approach to investigate the function of PARL and its potential role in OPA1 processing.

RESULTS

Targeted Inactivation of the Mouse *Parl* Gene

Mice with loxP sites inserted in the *Parl* gene ($Parl^{flx/flx}$) were generated by homologous recombination (Figure 1A). They were crossed with a mouse strain expressing Cre from the PGK promoter, resulting in Cre-mediated excision of the region between the loxP sites in all tissues. The resulting *Parl* null allele ($Parl^{-/-}$) (Figure 1A) still generated a small amount of aberrantly migrating RNA (Figure 1C). RT-PCR and sequencing showed the absence of exon 2. Since this resulted in a frame shift and premature stop codon, the remaining RNA is no longer functional (Figures 1D and 1F). Immunoblotting confirmed the loss of PARL in fibroblasts derived from $Parl^{-/-}$ mice (Figure 1E).

Parl$^{-/-}$ Mice Prematurely Die of Progressive Cachexia

$Parl^{-/-}$ mice were born in a normal Mendelian frequency and developed normally up to 4 weeks. From then on, mice displayed severe growth retardation (Figures 2A and 2B). $Parl^{-/-}$ mice lost muscle mass (erector spinae, abdominal muscles, and diaphragm), leading to postural defects with hunchback deformity (Figure 2A). All animals died between 8 and 12 weeks (Figure 2C), most likely as a consequence of moving and breathing problems and general cachexia.

Microscopically, the diameter of individual muscle fibers was reduced (Figure 2O). Spinal motoneurons were normal, and AChE histochemistry failed to reveal signs of neurogenic atrophy (data not shown). At 8 weeks, thymus and spleen were massively atrophic, weighing 10% or less compared to controls (Figures 2D and 2I), with severe lymphocyte loss (Figures 2E and 2J). Uteri remained prepuberal, while ovaries were histologically

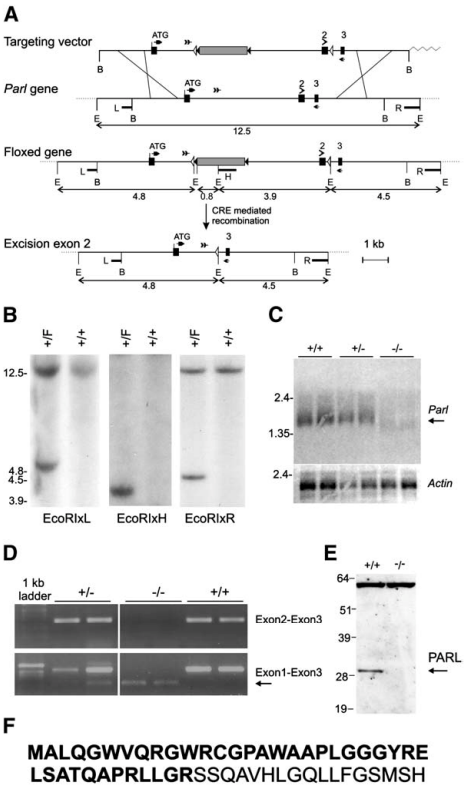

Figure 1. Generation of *Parl* Knockout Mice

(A) Maps of the targeting vector, the wild-type *Parl* allele, the conditional targeted allele (floxed allele), and the disrupted *Parl* allele. Exons (black boxes), LoxP and FRT recombination sites (white and black arrowheads, respectively), and locations of PCR primers are indicated. The expected sizes for restriction fragments detected by 5′ (L), 3′ (R) flanking or internal probes (H) (PCR fragments, black bars) from targeted and wild-type alleles are indicated with line diagrams. Positive selection marker is indicated as a gray box. Relevant restriction sites are shown (BglII, indicated as B and EcoRI as E).

(B) Examples of Southern blot of DNA isolated from ES cells, digested with EcoRI, and hybridized with the different probes (L, R, and internal [H]).

(C) Northern blot: the *Parl* transcript is detected in wt and heterozygous embryos. In $Parl^{-/-}$, a weak signal corresponding to an aberrant transcript is detected. The *β-actin* transcript is detected as control.

(D) RT-PCR analysis of *Parl* transcripts in wt and $Parl^{-/-}$ MEF cells. A shorter transcript of *Parl* is detected in the $Parl^{-/-}$ cells. Sequencing of the aberrant transcript confirmed a reading shift in remaining transcript.

(E) 100 μg of wt and $Parl^{-/-}$ MEFs lysate was resolved by SDS-PAGE and probed with anti-PARL antibody (specific band around 30 kDa). The unspecific upper band was used as loading control.

(F) Prediction of the maximal possible aberrant PARL protein. Bold amino acids are identical to wt PARL.

normal. Males showed cryptorchidism with size reduction of testes, epididymis, and accessory glands (data not shown). Fluoro-Jade (Figure 2N) staining and activated caspase-3 immunoreactivity (data not shown) indicated (mild) neurodegenerative changes and apoptotic cell death in thalamus and striatum. Latency of the acoustic startle response was increased in *Parl*$^{-/-}$ mice ($p < 0.001$), which could relate to defects in neural conduction, striatal dysfunction, and/or increased reaction time (data not shown).

Parl$^{-/-}$ mice have thus greatly reduced life span due to progressive cachexia and are characterized by severe atrophy of muscular tissue, spleen, and thymus and indications of increased apoptosis. We investigated the extent to which mitochondrial dysfunction and/or apoptotic dysregulation contributed to this multisystemic atrophy.

Parl Is Not Required for Mitochondrial Respiratory Function

Total ATP content in limb muscles isolated from *Parl*$^{-/-}$ and wild-type (wt) animals was comparable (67.5 ± 11.3 nmol ATP/μg protein in *wt* versus 62.6 ± 16.4 nmol ATP/μg protein in *Parl*$^{-/-}$ muscle). Basal (state 4), ADP-stimulated (state 3), and maximal (uncoupled) respiratory rates (J_{O2}) of wt and *Parl*$^{-/-}$ mitochondria isolated from liver (data not shown), fibroblasts (data not shown), or muscle (Figure 2P) were similar, irrespective of the substrates used to feed the respiratory chain. Moreover, uptake of the potentiometric dye tetramethyl rhodamine methyl ester (TMRM) was unaltered in *Parl*$^{-/-}$ mouse embryonic fibroblasts (MEFs) (see Figure S1A in the Supplemental Data available with this article online) and in primary myoblasts and myotubes isolated from *Parl*$^{-/-}$ diaphragms (Figure 6E). Mitochondrial depolarization in response to the F_1F_0ATPase inhibitor oligomycin is a sensitive test of latent mitochondrial dysfunction in intact cells (Irwin et al., 2003). Real-time imaging of mitochondrial TMRM fluorescence in response to oligomycin showed no depolarization in *Parl*$^{-/-}$ MEFs, myoblasts, or myotubes (Figures S1B–S1D). Thus, *Parl*$^{-/-}$ mitochondria do not display primary respiratory defects or latent mitochondrial dysfunction in hepatocytes, MEFs, myocytes, or myotubes. Mitochondrial dysfunction therefore does not explain *Parl*$^{-/-}$ muscular atrophy and multisystemic failure.

Absence of *Parl* Results in Massive Apoptosis of T and B Lymphocytes

Muscle atrophy can be caused by apoptosis, but apoptotic segments of muscle fibers are rapidly cleared, making them difficult to detect (Sandri and Carraro, 1999). We turned therefore to thymus and spleen, where apoptosis determines cellular content and fate. Severe cell depletion and marked TUNEL staining was evident in both organs of *Parl*$^{-/-}$ animals (Figures 2E and 2J). In the thymus, the great majority of T cells follow the normal developmental sequence CD4 CD8 (double negative, DN)→$CD4^+$ $CD8^+$(double positive, DP)→$CD4^+CD8^-$ or CD4 $CD8^+$ (single positive). Numerically, DN thymocytes were unchanged, while DP cells were reduced over 100-fold in *Parl*$^{-/-}$ mice (Figures 2F and 2G) as a result of massive apoptosis revealed by their counterstaining with annexin-V (Figure 2H, gray bars). Similarly, apoptosis depleted the $B220^+$ B cell population in *Parl*$^{-/-}$ spleens (Figures 2K–2M). *Parl*$^{-/-}$ thymocytes isolated from 7-week-old mice and cultured in complete media also displayed increased death (Figure 2H, hatched bars), suggesting a cell-autonomous effect (Hao et al., 2005). Overall our results show that in adult *Parl*$^{-/-}$ mouse, $B220^+$ B cells as well as DP T cells undergo increased apoptosis in and ex vivo. Together with the caspase-3 positivity of brain sections (data not shown) and the muscular atrophy, these results suggest that increased susceptibility to apoptosis could contribute to the multisystemic failure of *Parl*$^{-/-}$ mice.

Parl Regulates Cytochrome c Release from Mitochondria

To analyze the effects of PARL deficiency on apoptosis at the molecular level, we turned to MEFs. SV40-transformed *Parl*$^{-/-}$ MEFs proved very susceptible to a panoply of intrinsic apoptotic stimuli acting via mitochondria, including the "BH3-only" member of the BCL-2 family BID. Conversely, death by the extrinsic stimulus TNF-α was comparable in wt and *Parl*$^{-/-}$ MEFs (Figure 3A). Thus, PARL does not influence the extrinsic pathway of apoptosis induced by TNF-α in MEFs. Expression of BCL-2 did not protect (data not shown), demonstrating that MEFs behave like type I cells, bypassing mitochondria in this form of apoptosis (Scaffidi et al., 1998). This was confirmed in primary MEFs from a different clone (data not shown). Finally, primary myoblasts from *Parl*$^{-/-}$ mice also showed increased TUNEL-positive nuclei in response to H_2O_2 (Figure 3A). Reintroduction of active PARL in *Parl*$^{-/-}$ MEFs decreased death to wt levels, irrespective of the stimulus employed (Figures 3B–3D). Conversely, a catalytically inactive mutant of PARL, 335His→Gly ($PARL^{H335G}$), corrected PARL expression (Figure 3E) but was unable to rescue apoptosis of *Parl*$^{-/-}$ MEFs (Figure 3H).

Following treatment with H_2O_2, *Parl*$^{-/-}$ MEFs and primary myoblasts released cytochrome *c* more rapidly than their wt counterparts (Figures 4A–4D). Mitochondrial dysfunction, which accompanies cytochrome c release, also occurred faster in *Parl*$^{-/-}$ MEFs (Figures 4E and 4F), while multidomain proapoptotics BAK and BAX, required for release of cytochrome c through the outer membrane (Wei et al., 2001), were equally activated (data not shown). Isolated *Parl*$^{-/-}$ liver mitochondria also released cytochrome c faster than their wt counterparts upon treatment with recombinant caspase-8-cleaved BID (cBID) (Figure 4G). This was again not due to enhanced BAK activation, as higher-order BAK oligomers appeared with the same kinetics in wt and *Parl*$^{-/-}$ mitochondria (Figure 4H).

The major store of cytochrome c released during apoptosis is located in the mitochondrial cristae. We therefore measured cytochrome c redistribution following treatment of isolated wt and *Parl*$^{-/-}$ mitochondria with cBID using

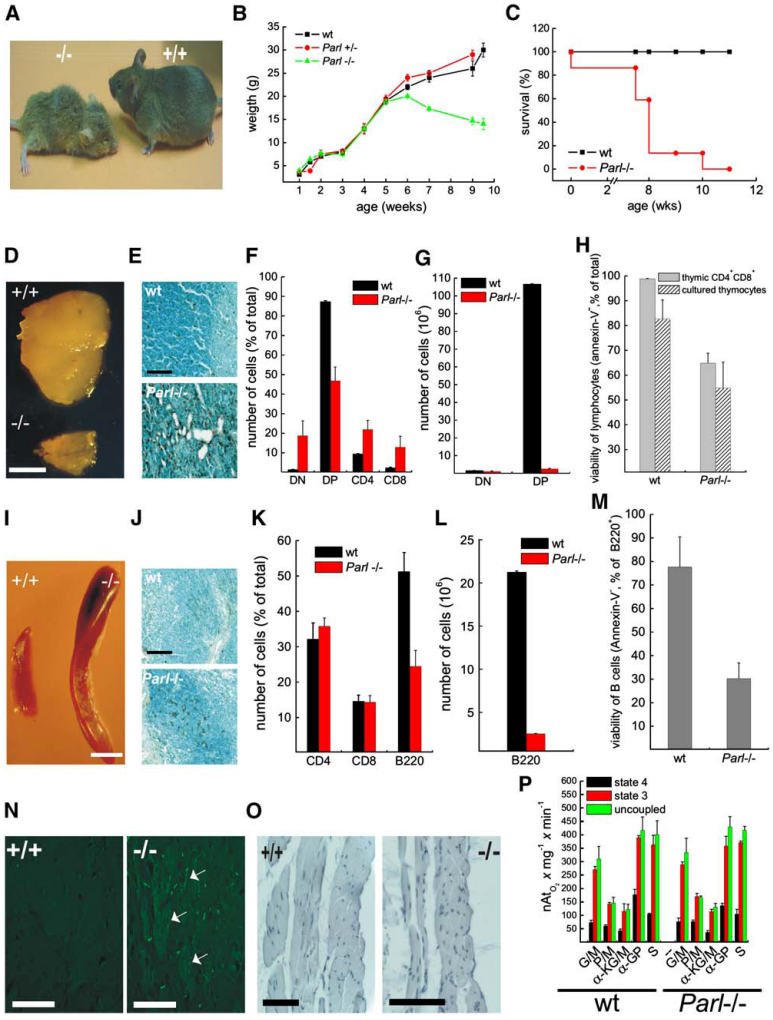

Figure 2. Wasting Phenotype of the *Parl*$^{-/-}$ Mice Is Characterized by Increased Apoptosis

(A) Representative photograph of wt (+/+) and *Parl* $^{-/-}$ (−/−) 8-week-old littermates.

(B) Growth curve of wt, *Parl*$^{+/-}$, and *Parl* $^{-/-}$ female littermates (mean ± SEM).

(C) Kaplan-Meier survival curve of wt and *Parl* $^{-/-}$ littermates.

(D) Images of thymuses dissected from 8-week-old wt (+/+) and *Parl* $^{-/-}$ (−/−) mice. Scale bar, 1 mm.

(E) TUNEL staining of wt and *Parl* $^{-/-}$ 7-week-old thymuses. Scale bar, 75 μm.

(F) Cumulative analysis of subset distribution of thymic lymphocytes of the indicated genotype, stained with anti-CD4-FITC and anti-CD8-PECy5 antibodies. Data represent mean ± SE of eight 7- to 9-week-old littermates.

(G) Numbers of DN and DP thymic lymphocytes (±SE) from eight different wt and *Parl* $^{-/-}$ littermates.

(H) Decreased viability of DP (gray bars) and cultured (hatched bars) *Parl* $^{-/-}$ thymic lymphocytes. Viability of DP was calculated as the percentage of annexin-V-Alexa 568-negative events in gated CD4-FITC, CD8-PECy5-positive thymic lymphocytes of the indicated genotype. Data represent mean ± SE of five wt and *Parl* $^{-/-}$ littermates.

(I) Images of spleens dissected from 8-week-old wt and *Parl* $^{-/-}$ littermates. Scale bar, 1 mm.

(J) TUNEL staining of wt and *Parl* $^{-/-}$ 7-week-old spleens. Scale bar, 75 μm.

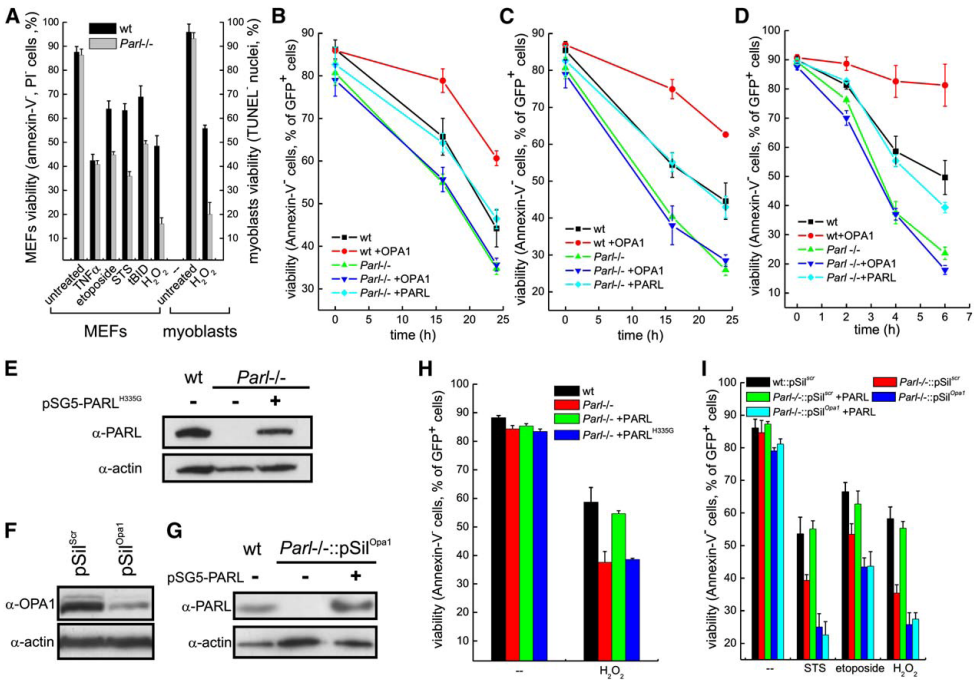

Figure 3. PARL Controls Apoptosis Induced by Intrinsic Stimuli and Is Required for Antiapoptotic Activity of OPA1

(A) MEFs (bars on the left) or primary myoblasts (bars on the right) of the indicated genotype were treated with TNF-α, etoposide, staurosporine, H_2O_2, or transfected with tBID-GFP. Viability was determined as the percentage of annexin-V-Fluos, PI-negative cells by flow cytometry, as the percentage of GFP-positive, annexin-V-Alexa 568-negative cells in the case of tBID, or as the number of TUNEL-negative nuclei by imaging in the case of myoblasts. Data represent mean ± SE of five independent experiments.

(B–D) MEFs of the indicated genotype transfected as indicated were treated with etoposide (B), staurosporine (C), or H_2O_2 (D). At the indicated times, viability was determined cytofluorimetrically as the percentage of GFP-positive, annexin-V-Alexa568-negative cells.

(E) MEFs were transfected as indicated and lysed after 24 hr. Protein (50 μg) was analyzed by SDS-PAGE/immunoblotting.

(F) *Parl* $^{-/-}$ MEFs stably expressing the indicated shRNA-generating pSilencer (pSil) plasmids (scr: scrambled) were lysed, and 40 μg of protein were analyzed by SDS-PAGE/immunoblotting.

(G) MEFs were transfected as indicated and lysed after 24 hr. Protein (40 μg) was analyzed by SDS-PAGE/immunoblotting.

(H) MEFs cotransfected with GFP and the indicated plasmids were treated after 24 hr with 1 mM H_2O_2, and viability was measured after further 4 hr as the percentage of GFP-positive, annexin-V-Alexa 568-negative cells. Data represent mean ± SE of five independent experiments.

(I) Cells of the indicated genotype were treated with H_2O_2, etoposide, or staurosporine, and viability was determined as the percentage of GFP-positive, annexin-V-Alexa 568-negative cells. Data represent mean ± SE of five independent experiments.

the differential ability of ascorbate and N,N,N′,N′-tetramethyl-p-phenylenediamine (TMPD) to reduce free (intramembrane space located) and membrane-bound (cristae located) cytochrome c, respectively. The ratio of ascorbate-driven over TMPD-driven respiration increases when cytochrome c is mobilized from its binding sites on

(K) Cumulative analysis of subset distribution of splenic lymphocytes stained with CD4-FITC, CD8-PECy5, and B220-PE antibodies. Data represent mean ± SE of eight 7-week-old littermates.

(L) Absolute values of $B220^+$ splenic lymphocytes ±SE from eight different wt and *Parl* $^{-/-}$ littermates.

(M) Decreased viability of B lymphocytes in *Parl* $^{-/-}$ spleens. Viability was calculated as the percentage of annexin-V-Fluos-negative cells in gated $B220^+$ splenic lymphocytes. Data represent mean ± SE of five wt and *Parl* $^{-/-}$ littermates.

(N) Fluoro-Jade staining of *Capsula interna* from wt (+/+) and *Parl* $^{-/-}$ (−/−) 8-week-old littermates. Arrows indicate degenerating neurons. Scale bars, 100 μm.

(O) Hematoxylin staining of abdominal wall muscles of 8-week-old wt (+/+) and *Parl* $^{-/-}$ (−/−) littermates. Scale bars, 120 μm.

(P) Quantitative analysis of oxygen consumption in mitochondria isolated from limb muscles of 8-week-old littermates of the indicated genotype. Mitochondria were incubated with glutamate/malate (G/M), pyruvate/malate (P/M), α-ketoglutarate/malate (α-KG/M), α-glycerophosphate (α-GP), or succinate (S) into an oxygen electrode chamber. Data represent average ± SE of five independent experiments.

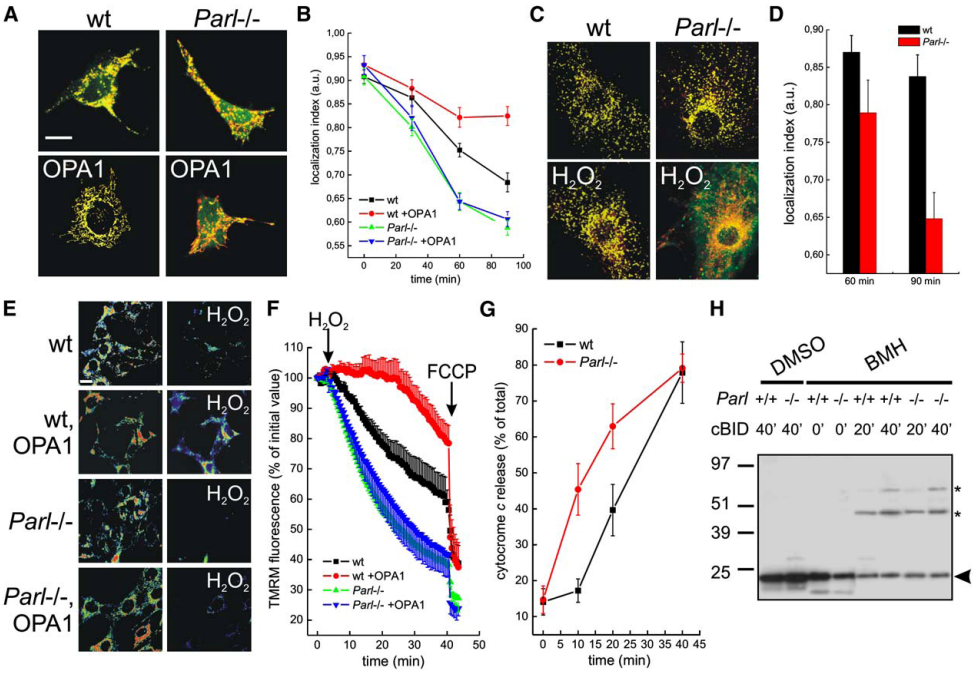

Figure 4. PARL Regulates the Mitochondrial Pathway of Apoptosis by Controlling OPA1-Dependent Mobilization of Cytochrome c

(A) Representative confocal images of wt and *Parl* $^{/}$ MEFs cotransfected with mtRFP (red) and empty vector or OPA1. Cells were treated for 90 min with 1 mM H_2O_2, fixed, and immunostained with a FITC-conjugated anti-cytochrome c antibody (green).

(B) Experiments as in (A), except that cells were fixed at the indicated times. Localization index was calculated from 30 randomly selected images. Data represent mean ± SE of five independent experiments.

(C) Representative confocal images of wt and *Parl* $^{/}$ primary myoblasts immunostained with anti-cytochrome c (green) and anti-TOM20 (red) antibodies. When indicated, cells were treated for 90 min with 1 mM H_2O_2.

(D) Localization index for cytochrome c in myoblasts. Experiments were performed as in (B). Data represent mean ± SE of three independent experiments.

(E) Representative pseudocolor-coded images of TMRM fluorescence in wt and *Parl* $^{/}$ MEFs transfected with GFP and empty vector or OPA1. Cells were loaded with 20 nM TMRM and real-time imaging sequences were acquired. Initial (left) and t = 35 min (right) frames are shown. Scale bar, 20 μm.

(F) Quantitative analysis of TMRM fluorescence changes over mitochondrial regions in transfected cells identified from their GFP fluorescence. Data represent mean ± SE of six independent experiments performed as in (E). Where indicated (arrows), 1 mM H_2O_2 and 2 μM FCCP were added.

(G) Liver mitochondria were treated with cBID and the amount of cytochrome c in the supernatant and in the pellet was determined by ELISA. Data represent the average ± SE of three independent experiments.

(H) Liver mitochondria were treated with cBID. DMSO or 10 mM BMH was added at the indicated time (Wei et al., 2000). Mitochondrial proteins (40 μg) were analyzed by SDS-PAGE/immunoblotting using anti-BAK antibody. Arrowhead, BAK; asterisks, BAK multimers.

cristae membranes (Scorrano et al., 2002). We also measured cytochrome b_5-mediated NADH oxidation, which is rate limited by free cytochrome c in the intermembrane space (IMS) (Bernardi and Azzone, 1981; Scorrano et al., 2002). Both assays showed that cytochrome c redistributed faster into the IMS in *Parl* $^{/}$ compared to wt mitochondria in response to cBID (Figures 5A–5C). Electron microscopy and morphometric analysis showed that remodeled class II morphology, which accounts for mobilized cytochrome c (Scorrano et al., 2002), appeared earlier in *Parl* $^{/}$ mitochondria following cBID (Figure 5D,E). Thus, PARL participates in the mechanism keeping in check cristae and cytochrome c redistribution during apoptosis.

Parl Is Dispensable for Mitochondrial Fusion

The yeast ortholog of *Parl*, *RBD1*, is required for maintenance of mitochondrial morphology, which in turn influences mitochondrial participation to apoptosis (Youle and Karbowski, 2005). Rbd1p cleaves Mgm1p, and expression of an Rbd1p-cleaved Mgm1p isoform in Δ*rbd1* cells partially complements mitochondrial shape defects (McQuibban et al., 2003). The mammalian ortholog of

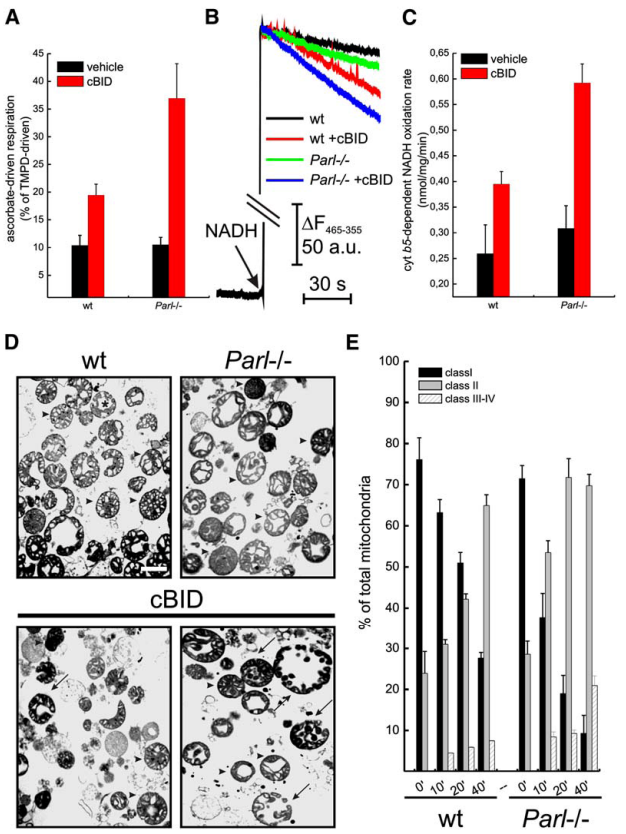

Figure 5. Kinetics of Cytochrome c Mobilization and Cristae Remodeling in Mitochondria Lacking PARL

(A) Liver mitochondria were treated with cBID or with vehicle, transferred into an oxygen electrode chamber, and ascorbate/TMPD respiratory ratio was determined. Data represent average ± SE of five independent experiments.

(B) Representative traces of NADH fluorescence changes caused by cytochrome b_5-dependent NADH oxidation. Liver mitochondria were incubated with cBID or with vehicle. Where indicated (arrow), 20 nmol NADH × mg protein $^{-1}$ were added.

(C) Experiment was performed as in (B). Data represent average ± SE of five independent experiments.

(D) Representative electron micrographs of wt and *Parl* $^{-/-}$ mitochondria. Mitochondria from livers were treated for the indicated time with cBID, fixed, and TEM images of randomly selected fields were acquired. Arrowheads denote class I (normal) mitochondria, arrows class II (remodelled) mitochondria. Scale bar, 500 nm.

(E) Morphometric analysis of wt and *Parl* $^{-/-}$ mitochondria treated with cBID for the indicated times. Experiments were performed as in (A). Data represent average ± SE of three independent experiments.

Mgm1p is OPA1, which requires MFN1 to promote fusion of mitochondria (Cipolat et al., 2004).

We decided therefore to investigate whether PARL, like its yeast homolog Rbd1p, controlled OPA1-dependent mitochondrial dynamics. Mitochondria of *Parl* $^{-/-}$ MEFs transfected with a mitochondrially targeted yellow fluorescent protein (mtYFP) appeared globular or rod-shaped, their elongation being visually (Figure 6A) and quantitatively (Figure 6B) undistinguishable from that of wt cells. Fusion rates of mitochondria were identical in wt and *Parl* $^{-/-}$ MEFs (Figures 6C and 6D). Mitochondrial morphology was similar in wt and *Parl* $^{-/-}$ primary myoblasts as well (Figure 6E). Levels of OPA1 were not changed in *Parl* $^{-/-}$ MEFs (Figure S2A), and its expression (Figure S2A) caused mitochondrial elongation (Figures 6A and 6B) comparable to that observed in wt cells (Cipolat et al., 2004). Thus, *Parl* is not required for the pro-fusion effect of OPA1. MFN1 and MFN2 also promoted equal mitochondrial elongation in wt and *Parl* $^{-/-}$ cells (Figures 6A and 6B), and expression of PARL had no effect on mitochondrial shape (Figures 6A and 6B) or fusion (data not shown) in wt MEFs. In total, these data indicate that *Parl* is not required for maintenance of mitochondrial shape and/or fusion, even in tissues severely affected by *Parl* ablation, like muscle, and that *Parl* is dispensable for regulation of mitochondrial dynamics by OPA1.

Parl and OPA1 Act in the Same Antiapoptotic Pathway

OPA1 regulates mitochondrial shape, but is also an antiapoptotic protein (Lee et al., 2004). We considered the possibility that both functions could be (partially) independent from each other and investigated whether *Parl* was required for the antiapoptotic function of OPA1. OPA1 protected wt but not *Parl* $^{-/-}$ MEFs from death by etoposide, staurosporine, and H_2O_2 (Figures 3B–3D). Furthermore, expression of OPA1 in *Parl* $^{-/-}$ MEFs did not reduce cytochrome c release (Figures 4A and 4B) or mitochondrial depolarization (Figures 4E and 4F) following intrinsic stimuli. Thus, in the absence of *Parl*, OPA1 is unable to

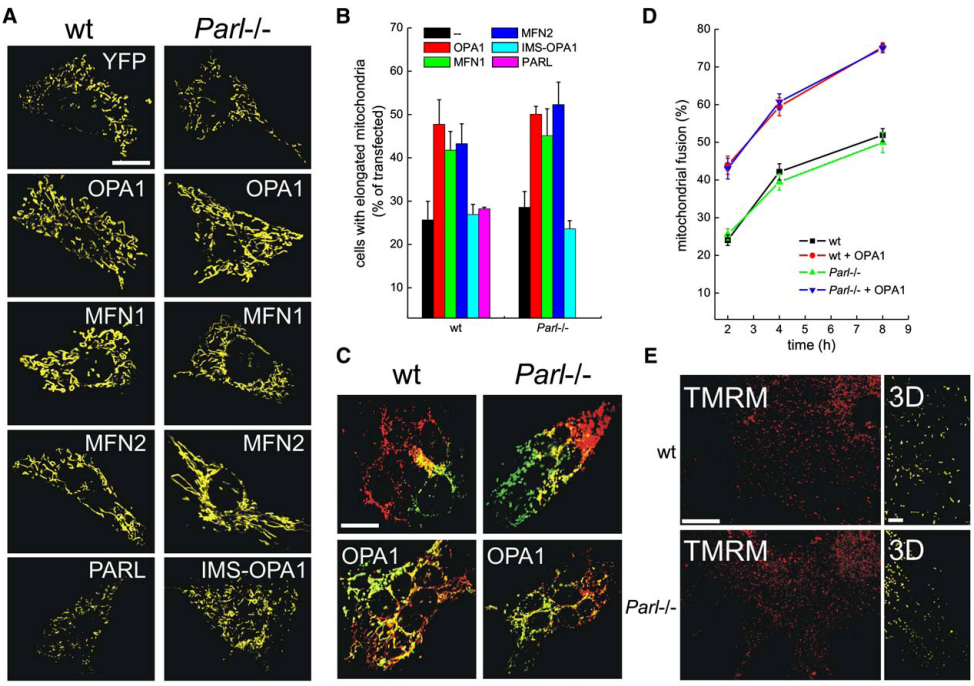

Figure 6. PARL Is Not Required for Mitochondrial Fusion

(A) MEFs were cotransfected with mtYFP and empty vector or the indicated plasmid. Confocal images of mtYFP fluorescence from randomly selected cells. Scale bar, 10 μm.

(B) Morphometric analysis of mitochondrial shape. Experiments were as in (A). Fifty randomly selected images of mtYFP fluorescence were acquired, stored, and classified as described. Data represent mean ± SE of five independent experiments.

(C) MEFs transfected with mtRFP and mtGFP or cotransfected with OPA1 were fused with PEG1500 and fixed after 4 hr. Scale bar, 20 μm.

(D) Time course of mitochondrial fusion in wt and *Parl* $^{-/-}$ MEFs. Experiments were performed as in (C), except that cells were fixed at the indicated times. Mitochondrial fusion was measured from 30 randomly selected polykaryons. Data represent mean ± SE of three independent experiments.

(E) Mitochondrial morphology in myoblasts isolated from diaphragm of wt and *Parl* $^{-/-}$ 7-week-old littermates. Myoblasts were loaded with 10 nM TMRM. Randomly selected confocal, 20 μm deep z axis stacks of TMRM fluorescence were acquired, stored, reconstructed, and volume rendered. Images on the left side are middle sections of the z-stacks, on the right, magnified (3×) volume-rendered 3D reconstructions of the stacks. Scale bars, 10 μm on the left, 3 μm on the right.

block apoptosis, placing PARL and OPA1 in the same genetic pathway. We next ablated OPA1 using short hairpin RNA interference (shRNAi) in wt and *Parl* $^{-/-}$ MEFs (Figure 3F). This rendered both cell types more susceptible to apoptosis (Figure 3I and Lee et al., 2004). Reintroduction of PARL in *Parl* $^{-/-}$ MEFs in which OPA1 was silenced (Figure 3G) did not rescue from enhanced apoptosis (Figure 3I). Thus, PARL is genetically positioned upstream of OPA1 in this pathway of death.

PARL Is Involved in the Production of Soluble, Antiapoptotic OPA1

PARL is apparently upstream of OPA1 in a pathway regulating cytochrome c release during apoptosis. Further experiments suggested that PARL and OPA1 interacted at the protein level as well. Subfractionation of mitochondria showed that both PARL and OPA1 were localized in the inner mitochondrial membrane (Figure 7A) and anti-PARL antibody specifically coimmunoprecipitated OPA1 in wt but not *Parl* $^{-/-}$ MEFs (Figure 7B). Finally, OPA1 interacted with PARL in a yeast two-hybrid interaction experiment (Table S1). As the proteins interact and the catalytic site of PARL is required to regulate cytochrome c release (Figure 3H), we investigated whether OPA1 could be a substrate of PARL. OPA1 is synthesized as an integral IM protein from one single gene. Alternative splicing generates at least eight different transcripts, all of them containing the transmembrane domain (Delettre et al., 2001). This complicated considerably the identification of potential processed OPA1 forms in immunoblots of mitochondrial

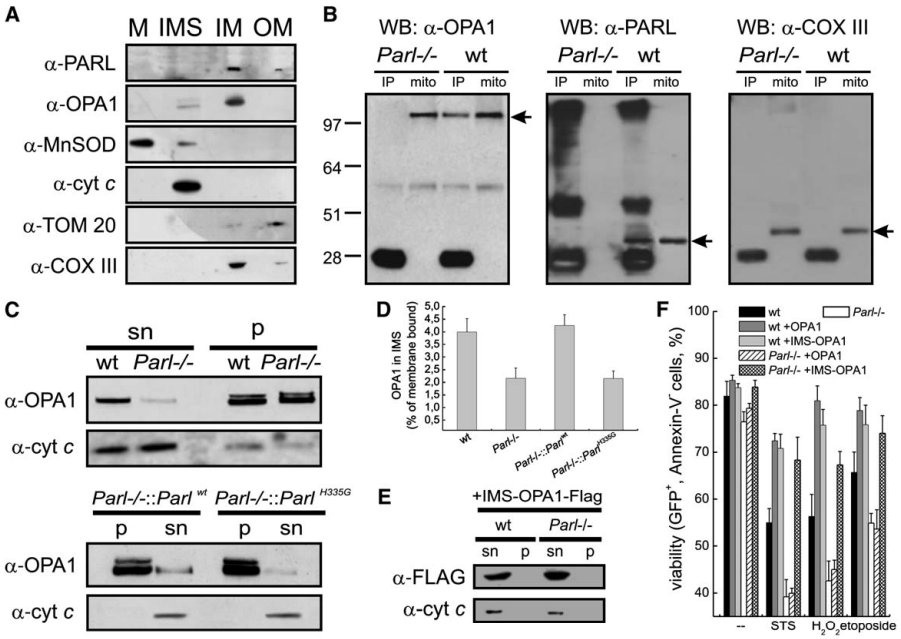

Figure 7. PARL Interacts with OPA1 and Participates in the Production of an Intermembrane Space Form Required to Protect from Apoptosis

(A) Mouse liver mitochondria were subfractionated, and 50 μg of matrix (M), intermembrane space (IMS), inner membrane (IM) and outer membrane (OM) proteins were separated by SDS-PAGE and immunoblotted with the indicated antibodies.

(B) Western blots (WB) using OPA1, PARL, and COXIII antibodies as indicated of mitochondrial proteins immunoprecipitated with PARL antibodies (IP) or present in total mitochondrial lysate (mito). Arrows indicate OPA1, PARL, and COX III, respectively.

(C) Pellet (p, 10 μg) and supernatant (sn, 100 μg) of hypotonically swollen, KCl-washed mitochondria isolated from MEFs of the indicated genotypes to release IMS proteins were analyzed by SDS-PAGE/immunoblotting using anti-OPA1 and anti-cytochrome c (cyt c) antibodies.

(D) Densitometric analysis of IMS OPA1. Experiments were as in (C). Data represent average ± SE of eight independent experiments.

(E) Cells were transfected with IMS-OPA1-FLAG, and the IMS and membrane fractions from isolated mitochondria were separated as in (D) and analyzed by SDS-PAGE/immunoblotting.

(F) MEFs cotransfected with GFP and empty vectors or with the indicated plasmids were treated with staurosporine, H_2O_2, and etoposide. Viability was determined cytofluorimetrically as the percentage of GFP-positive, annexin-V-Alexa 568-negative cells. Data represent mean ± SE of five independent experiments.

fractions isolated from different tissues (data not shown). In order to enrich for potential cleaved, soluble OPA1 forms, we generated membrane (pellet) and IMS (supernatant) fractions from mitochondria by hypotonic swelling and salt washes, a treatment that dissociates weakly bound proteins from the IM (Jacobs and Sanadi, 1960). An OPA1 form characterized by lower MW was found in the IMS (Figures 7A and 7C), and levels of this IMS OPA1 were reduced in *Parl* $^{-/-}$ mitochondria (Figure 7C and densitometry in 7D). Accordingly, stable reintroduction in *Parl* $^{-/-}$ MEFs of wt but not the catalytic dyad mutant H335G PARL restored levels of IMS OPA1 (Figure 7C and densitometry in 7D). This was not due to differences in expression of these reintroduced PARLs (Figure S2B), suggesting that the catalytic activity of PARL is involved in the generation of this soluble IMS form, although we cannot exclude at this point that the action of PARL on OPA1 could be indirect. Some OPA1 remained detectable in the IMS of *Parl* $^{-/-}$ mitochondria, suggesting the existence of at least one additional protease that cleaves OPA1.

The reduced levels of IMS OPA1 could explain increased susceptibility of *Parl* $^{-/-}$ cells to apoptosis. A FLAG-tagged OPA1 in which residues 1–229 were replaced with the IMS targeting signal of AIF (IMS-OPA1) (Otera et al., 2005) was targeted to the IMS (Figure 7E). IMS-OPA1 protected wt but notably also *Parl* $^{-/-}$ MEFs from apoptosis induced by all intrinsic stimuli tested (Figure 7F), substantiating a pivotal role for IMS-OPA1 in the regulation of cell death. IMS-OPA1 did not induce mitochondrial elongation (Figures 6A and 6B), dissociating even further the profusion effect from the antiapoptotic function of OPA1.

DISCUSSION

We demonstrate here that PARL is an antiapoptotic protein. Ablation of this gene causes faster release of the cytochrome c pool from the mitochondrial cristae. This function critically depends on a genetic interaction with OPA1 and involves the generation of a soluble, IMS-located form of OPA1. As demonstrated in the accompanying manuscript (Frezza et al., 2006), membrane bound and soluble IMS OPA1 participate in the formation of oligomers, and their disruption correlates with the tightness of the cristae junctions and cytochrome c release. The reduced levels of IMS-OPA1 in the *Parl* $^{-/-}$ cells could therefore represent a mechanistic explanation for the increased apoptosis observed in the *Parl* $^{-/-}$ mice.

Parl Deficiency Causes Increased Apoptosis, Resulting in Generalized Wasting and Premature Death

PARL was initially identified in a two-hybrid screen using the carboxy-terminal part of presenilin as bait (Pellegrini et al., 2001). We anticipated therefore that *Parl* ablation would cause embryonic phenotypes overlapping with those observed in presenilin-deficient animals (Marjaux et al., 2004). However, the phenotype of *Parl* $^{-/-}$ mice is completely different, being characterized by progressive cachexia from the fourth week on, eventually leading to death. In addition, APP is normally processed in *Parl* $^{-/-}$ mice (data not shown). It is reasonable to conclude that presenilin binds PARL only in vitro.

We next turned to rbd1p, the PARL ortholog in *S. cerevisiae*. Rbd1p deficiency causes mitochondrial fission, respiratory dysfunction, and growth arrest (Esser et al., 2002; Herlan et al., 2003; McQuibban et al., 2003; Sesaki et al., 2003). However, *Parl* $^{-/-}$ mitochondria from multiple tissues did not display overt or latent respiratory dysfunction in vitro or in situ or changes in mitochondrial morphology. Thus, the function of Rbdp1p in yeast seems not to be conserved in PARL in mice, an evolutionary divergence seen also with other rhomboids (Freeman, 2004).

Parl $^{-/-}$ mice shared several phenotypical characteristics with *Bcl-2* $^{-/-}$ mice, including early postnatal mortality with muscular atrophy and massive apoptotic involution of thymus and spleen (Veis et al., 1993). Muscle wasting is also compatible with increased apoptosis (Kujoth et al., 2005). *Parl* $^{-/-}$ primary myoblasts indeed displayed higher sensitivity to intrinsic stimuli of apoptosis, which together with analysis of other tissues and cells, further substantiates a role for PARL in the control of cell death.

PARL Is Epistatic to OPA1 in Controlling Cytochrome c Mobilization from Cristae during Apoptosis

Rbd1p interacts with Mgm1p in yeast to regulate mitochondrial fusion. We therefore evaluated whether PARL interacts with OPA1, the mammalian ortholog of Mgm1p. OPA1 has pro-fusion ability, which depends on MFN1 (Cipolat et al., 2004), and antiapoptotic activity, which could be dependent or separated from its fusion ability (Lee et al., 2004). PARL deficiency did not affect fusion by OPA1 or MFN1, but was clearly involved in the antiapoptotic function of OPA1. Furthermore, when *Opa1* was silenced by siRNA in *Parl* $^{-/-}$ cells, they were no longer rescued by reexpression of PARL, demonstrating that PARL is genetically positioned upstream of OPA1. Yeast two-hybrid and coimmunoprecipitation assays indicated a direct protein-protein interaction between PARL and OPA1. In the accompanying paper, we demonstrate that disruption of OPA1-containing oligomers correlates with mitochondrial cristae remodeling and completion of cytochrome c release (Frezza et al., 2006). Accordingly, we observed in *Parl* $^{-/-}$ fibroblasts and myoblasts, as well as in purified *Parl* $^{-/-}$ liver mitochondria, enhanced mitochondrial remodeling and mobilization of cristae stores of cytochrome c, corroborating the conclusion that PARL and OPA1 are part of the same molecular pathway of death.

PARL Participates in the Generation of Soluble IMS OPA1

Rbd1p regulates mitochondrial shape by proteolytic processing of Mgm1p, and PARL can rescue Rbd1p proteolytic processing of Mgm1p in yeast (McQuibban et al., 2003), indicating that PARL proteolytic activity, as opposed to its function in mitochondrial morphology, is maintained in evolution. However, multiple splice variants of OPA1 complicate the comparison of its electrophoretic migration pattern in mammalian wt and *Parl* $^{-/-}$ tissues. We therefore focused on the hypothesis that PARL could be involved in the generation of an IMS, soluble form of OPA1. We found indeed a small (~4%) fraction of IMS-OPA1 that decreased strongly in *Parl* $^{-/-}$ mitochondria. Expression of a version of OPA1 targeted to the IMS (Otera et al., 2005) protected *Parl* $^{-/-}$ fibroblasts from apoptosis like wt OPA1 did in wt cells. Finally, PARL^{H335G}, mutated in its catalytic dyad (Lemberg et al., 2005), did not rescue production of IMS OPA1 in *Parl* $^{-/-}$ mitochondria and also failed to rescue the apoptotic phenotype of *Parl* $^{-/-}$ cells, suggesting that OPA1 could indeed be a substrate for PARL. Obviously, we cannot exclude that PARL could act indirectly via activation of another, unknown protease (Arnoult et al., 2005) or that OPA1 is processed independently by multiple proteases. These possibilities are supported by the retrieval of traces of IMS-OPA1 in *Parl* $^{-/-}$ MEFs. Our overall analysis strongly supports, however, our conclusion that PARL has a crucial role in proteolytic processing of OPA1.

IMS and integral IM OPA1 both participate in oligomers that are disrupted during cristae remodeling and release of cytochrome c. These oligomers are greatly reduced in *Parl* $^{-/-}$ mitochondria (Frezza et al., 2006). We therefore suggest that the reduced OPA1 processing in *Parl* $^{-/-}$ tissues can account for the faster cristae remodeling and cytochrome c mobilization and ultimately for the increased apoptosis observed in the *Parl*-deficient mice.

It remains unclear why only a small fraction of OPA1 becomes cleaved by PARL (or by a yet unknown protease).

In other examples of intramembrane proteolysis, like Notch signaling (Mumm et al., 2000), the substrate is cleaved after a conformational switch induced by binding to a ligand and/or cleavage by a second protease. Alternatively, cleavage of OPA1 could be regulated by compartmentalization, a case exemplified by the couple Spitz/Rhomboid-1. Before cleavage, Spitz is kept at the endoplasmic reticulum, while Rhomboid-1 resides in Golgi. Since PARL and OPA1 are both located in the inner membrane, one has to speculate that the two proteins are sequestered in different domains and that only a small fraction of total OPA1 becomes available for cleavage, a possibility supported by the high level of compartmentalization of the IM (Perotti et al., 1983).

Intramembrane Proteolysis Involved in the Regulation of Apoptosis

In the last few years, several intramembrane cleaving proteases have been identified, overturning the dogma that proteolysis (a hydrolyzing reaction) occurs only in aqueous environments (Annaert and De Strooper, 2002; Brown et al., 2000; Freeman, 2004; Kopan and Ilagan, 2004). Intramembrane proteolysis often generates an active soluble protein fragment that translocates to the nucleus to activate gene transcription or acts as a soluble ligand in a paracrine way. In *Drosophila*, rhomboids are important regulators of the EGFR pathway (Freeman, 2004). In bacteria and parasites, rhomboids are involved in quorum sensing (Gallio et al., 2002) and in invasion of host cells (Brossier et al., 2005). In all eukaryotes, a mitochondrial rhomboid is present, which in yeast is involved in the regulation of mitochondrial fusion and respiration. Little is known about the function of rhomboids in mammals, but the analysis of the *Parl*-deficient mouse now implicates the mitochondrial rhomboid in the regulation of apoptosis. The fact that *Parl* deficiency affects mice only in their early adult life suggests that this rhomboid protease could become an important drug target to modulate apoptosis in diseases of adult life, like cancer and neurodegenerative disorders.

EXPERIMENTAL PROCEDURES

Generation of *Parl*-Deficient Mice

The hygromycin B resistance gene flanked with two FRT sequences and one loxP sequence was inserted into intron 2 of a 9.5 kb BglII DNA restriction fragment of *Parl* covering the ATG start codon, exons 2 and 3, and a part of intron 4. A second loxP sequence was inserted into the SmaI site in intron 3 (Figure 1A). Hygromycin B-resistant E14 ES colonies were screened by Southern blot analysis (Figure 1B). Two mutated ES cell lines were microinjected into blastocysts of C57Bl/6J mice. Animals carrying a null allele were obtained after breeding with transgenic females expressing a PGK-driven Cre-recombinase.

Antibodies

A Parl carboxy-terminal antibody was generated by immunizing rabbits with a synthetic peptide (HEIRTNGPKKGGGSK) coupled to keyhole limpet haemocyanin (KLH). Other antibodies used are described in the Supplemental Data.

Analysis of Cell Death

Thymic lymphocytes were stained with CD4-FITC, CD8-PECy5, and annexin-V-Alexa 568. Splenic lymphocytes were stained with B220-PE and annexin-V-Fluos (Roche). Viability was determined by the percentage of annexin-V-negative events in the gated CD4, CD8-positive or B220-positive population. 1×10^5 MEFs were treated with TNF-α (100 IU and 0.5 μg/mL actinomycin, 6 hr), etoposide (5 μM, 16 hr), staurosporine (1 μM, 16 hr), H_2O_2 (1 mM, 4 hr), or transfected with tBID-GFP (48 hr) and stained with propidium iodide (PI) and annexin-V-FLUOS. Viability was measured by flow cytometry as the percentage annexin-V, PI-negative cells or as the percentage of annexin-V-negative events in the GFP cotransfected positive population. TUNEL staining of myoblasts was performed using the Apop-Tag kit (Roche).

Mitochondrial Assays

MEFs, liver, and muscle mitochondria were isolated by differential centrifugation. Details can be found in the Supplemental Data.

Mitochondrial oxygen consumption in the presence of 5 mM glutamate/2.5 mM malate or 2.5 mM pyruvate/1 mM malate or α-ketoglutarate 15 mM/1 mM malate for the analysis of complex I-driven respiration; 5 mM succinate or 5 mM α-glycerophosphate in the presence of 2 μM rotenone for complex II-driven respiration; or 3 mM ascorbate plus 150 μM TMPD in the presence of 0.5 μg/ml antimycin A for complex IV-driven respiration was measured with a Clarke-type oxygen electrode (Hansatech).

Cytochrome c redistribution and release in response to recombinant cBID was determined as described (Scorrano et al., 2002). Unless specified, cBID was used at a concentration of 32 pmol × mg^{-1} of mitochondria.

PEG fusion assays were performed as described in Cipolat et al. (2004).

For protein cross-linking, mitochondria were treated with 10 mM BMH (Pierce) for 30 min, dissolved in gel loading buffer, and proteins were analyzed by SDS-PAGE.

Imaging

Transfected cells were analyzed with a Nikon Eclipse TE300 inverted microscope equipped with a Perkin Elmer Ultraview LCI, a piezoelectric z axis motorized stage (Pifoc), and an Orca ER 12-bit CCD camera (Hamamatsu). Morphometric analysis was performed as described in Cipolat et al. (2004). Stacks of 20 images separated by 1 μm along the z axis were acquired. 3D reconstruction and volume rendering were performed using a plug-in of ImageJ (NIH). For imaging of polykarions and of cytochrome c release, a Nikon Eclipse E600FN upright microscope equipped with a Biorad Radiance 2100 CLS was used. Colocalization index was calculated as described (Frezza et al., 2006). Details on objectives and excitation/emission wavelengths can be found in the Supplemental Data.

Electron Microscopy

Fixation, embedding, TEM, and morphometric analysis of isolated mitochondria was performed by the Telethon EM Core Facility (TEEMCoF) as described (Scorrano et al., 2002).

Submitochondrial Fractionation and Immunoblotting

For detection of IMS proteins, freeze-thawn mitochondria were hypotonically swollen in 10 mM Tris-Cl (pH 7.4), spun at 10,000 × g, and the pellet was further washed in 150 mM KCl, 10 mM Tris-Cl (pH 7.4). The supernatants were pooled, concentrated 10-fold using a Centricon-10 filter unit (Millipore), and constituted the IMS fraction. Proteins were dissolved in gel-loading buffer (NuPAGE, Invitrogen) and electrophoresed.

Submitochondrial fractionation was performed according to Sottocasa et al. (1967). Briefly, mitochondria (50 mg) were incubated in 10 mM KH_2PO_4. After centrifugation, the pellet was resuspended in 125 mM KCl, 10 mM Tris-MOPS (pH 7.4), and centrifuged again. The combined supernatants constituted the IMS fraction. The pellet was

then resuspended in 10 mM KH_2PO_4, 1.8 M sucrose, 2 mM ATP, 2 mM $MgSO_4$, and centifuged over a 1.18 M sucrose cushion at 90,000 × g. The upper clear layer corresponded to the matrix (M) fraction, the yellow interphase to the OM, and the pellet to the IM.

For immunoprecipitation, 200 μg of mitochondria isolated from MEFs were dissolved in RIPA buffer. Anti-PARL immunocomplexes were adsorbed on 50 μl agarose beads conjugated with protein-G and boiled in loading buffer.

Supplemental Data

The Supplemental Data for this article can be found online at http://www.cell.com/cgi/content/full/126/1/163/DC1/.

ACKNOWLEDGMENTS

Research in BDS laboratory is supported by a Freedom to Discover grant from Bristol-Myers-Squibb; a Pioneer award from the Alzheimer's Association; the Fund for Scientific Research, Flanders; K.U. Leuven (GOA); European Union (APOPIS: LSHM-CT-2003-503330); and Federal Office for Scientific Affairs, Belgium (IUAP P5/19). L.S. is an Assistant Telethon Scientist of the Dulbecco-Telethon Institute. This research was supported by Telethon Italy; AIRC Italy; Compagnia di San Paolo; Human Frontier Science Program Organization. We thank Dr. Katsuyoshi Mihara (Kyushu University, Fukuoka, Japan) for the kind gift of the p3xFLAG-CMV14-AIF-Opa1 (IMS-OPA1-FLAG) plasmid.

Received: June 30, 2005
Revised: March 8, 2006
Accepted: June 8, 2006
Published: July 13, 2006

REFERENCES

Alexander, C., Votruba, M., Pesch, U.E., Thiselton, D.L., Mayer, S., Moore, A., Rodriguez, M., Kellner, U., Leo-Kottler, B., Auburger, G., et al. (2000). OPA1, encoding a dynamin-related GTPase, is mutated in autosomal dominant optic atrophy linked to chromosome 3q28. Nat. Genet. *26*, 211–215.

Annaert, W., and De Strooper, B. (2002). A cell biological perspective on Alzheimer's disease. Annu. Rev. Cell Dev. Biol. *18*, 25–51.

Arnoult, D., Grodet, A., Lee, Y.J., Estaquier, J., and Blackstone, C. (2005). Release of OPA1 during apoptosis participates in the rapid and complete release of cytochrome c and subsequent mitochondrial fragmentation. J. Biol. Chem. *280*, 35742–35750.

Bernardi, P., and Azzone, G.F. (1981). Cytochrome c as an electron shuttle between the outer and inner mitochondrial membranes. J. Biol. Chem. *256*, 7187–7192.

Brossier, F., Jewett, T.J., Sibley, L.D., and Urban, S. (2005). A spatially localized rhomboid protease cleaves cell surface adhesins essential for invasion by Toxoplasma. Proc. Natl. Acad. Sci. USA *102*, 4146–4151.

Brown, M.S., Ye, J., Rawson, R.B., and Goldstein, J.L. (2000). Regulated intramembrane proteolysis: a control mechanism conserved from bacteria to humans. Cell *100*, 391–398.

Cipolat, S., Martins de Brito, O., Dal Zilio, B., and Scorrano, L. (2004). OPA1 requires mitofusin 1 to promote mitochondrial fusion. Proc. Natl. Acad. Sci. USA *101*, 15927–15932.

Danial, N.N., Gramm, C.F., Scorrano, L., Zhang, C.Y., Krauss, S., Ranger, A.M., Datta, S.R., Greenberg, M.E., Licklider, L.J., Lowell, B.B., et al. (2003). BAD and glucokinase reside in a mitochondrial complex that integrates glycolysis and apoptosis. Nature *424*, 952–956.

Delettre, C., Lenaers, G., Griffoin, J.M., Gigarel, N., Lorenzo, C., Belenguer, P., Pelloquin, L., Grosgeorge, J., Turc-Carel, C., Perret, E., et al. (2000). Nuclear gene OPA1, encoding a mitochondrial dynamin-related protein, is mutated in dominant optic atrophy. Nat. Genet. *26*, 207–210.

Delettre, C., Griffoin, J.M., Kaplan, J., Dollfus, H., Lorenz, B., Faivre, L., Lenaers, G., Belenguer, P., and Hamel, C.P. (2001). Mutation spectrum and splicing variants in the OPA1 gene. Hum. Genet. *109*, 584–591.

Esser, K., Tursun, B., Ingenhoven, M., Michaelis, G., and Pratje, E. (2002). A novel two-step mechanism for removal of a mitochondrial signal sequence involves the mAAA complex and the putative rhomboid protease Pcp1. J. Mol. Biol. *323*, 835–843.

Freeman, M. (2004). Proteolysis within the membrane: rhomboids revealed. Nat. Rev. Mol. Cell Biol. *5*, 188–197.

Frezza, C., Cipolat, S., de Brito, O.M., Micaroni, M., Beznoussenko, G.V., Rudka, T., Bartoli, D., Polishchuk, R.S., Danial, N.N., De Strooper, B., and Scorrano, L. (2006). OPA1 controls apoptotic cristae remodeling independently from mitochondrial fusion. Cell *126*, this issue, 177–189.

Gallio, M., Sturgill, G., Rather, P., and Kylsten, P. (2002). A conserved mechanism for extracellular signaling in eukaryotes and prokaryotes. Proc. Natl. Acad. Sci. USA *99*, 12208–12213.

Green, D.R., and Kroemer, G. (2004). The pathophysiology of mitochondrial cell death. Science *305*, 626–629.

Hao, Z., Duncan, G.S., Chang, C.C., Elia, A., Fang, M., Wakeham, A., Okada, H., Calzascia, T., Jang, Y., You-Ten, A., et al. (2005). Specific ablation of the apoptotic functions of cytochrome C reveals a differential requirement for cytochrome C and Apaf-1 in apoptosis. Cell *121*, 579–591.

Herlan, M., Vogel, F., Bornhovd, C., Neupert, W., and Reichert, A.S. (2003). Processing of Mgm1 by the rhomboid-type protease Pcp1 is required for maintenance of mitochondrial morphology and of mitochondrial DNA. J. Biol. Chem. *278*, 27781–27788.

Irwin, W.A., Bergamin, N., Sabatelli, P., Reggiani, C., Megighian, A., Merlini, L., Braghetta, P., Columbaro, M., Volpin, D., Bressan, G.M., et al. (2003). Mitochondrial dysfunction and apoptosis in myopathic mice with collagen VI deficiency. Nat. Genet. *35*, 367–371.

Jacobs, E.E., and Sanadi, D.R. (1960). The reversible removal of cytochrome c from mitochondria. J. Biol. Chem. *235*, 531–534.

James, D.I., Parone, P.A., Mattenberger, Y., and Martinou, J.C. (2003). hFis1, a novel component of the mammalian mitochondrial fission machinery. J. Biol. Chem. *278*, 36373–36379.

Koonin, E.V., Makarova, K.S., Rogozin, I.B., Davidovic, L., Letellier, M.C., and Pellegrini, L. (2003). The rhomboids: a nearly ubiquitous family of intramembrane serine proteases that probably evolved by multiple ancient horizontal gene transfers. Genome Biol. *4*, R19.

Kopan, R., and Ilagan, M.X. (2004). Gamma-secretase: proteasome of the membrane? Nat. Rev. Mol. Cell Biol. *5*, 499–504.

Kujoth, G.C., Hiona, A., Pugh, T.D., Someya, S., Panzer, K., Wohlgemuth, S.E., Hofer, T., Seo, A.Y., Sullivan, R., Jobling, W.A., et al. (2005). Mitochondrial DNA mutations, oxidative stress, and apoptosis in mammalian aging. Science *309*, 481–484.

Lee, Y.J., Jeong, S.Y., Karbowski, M., Smith, C.L., and Youle, R.J. (2004). Roles of the mammalian mitochondrial fission and fusion mediators Fis1, Drp1, and Opa1 in apoptosis. Mol. Biol. Cell *15*, 5001–5011.

Lemberg, M.K., Menendez, J., Misik, A., Garcia, M., Koth, C.M., and Freeman, M. (2005). Mechanism of intramembrane proteolysis investigated with purified rhomboid proteases. Embo J. *24*, 464–472.

Marjaux, E., Hartmann, D., and De Strooper, B. (2004). Presenilins in memory, Alzheimer's disease, and therapy. Neuron *42*, 189–192.

McQuibban, G.A., Saurya, S., and Freeman, M. (2003). Mitochondrial membrane remodelling regulated by a conserved rhomboid protease. Nature *423*, 537–541.

Mumm, J.S., Schroeter, E.H., Saxena, M.T., Griesemer, A., Tian, X., Pan, D.J., Ray, W.J., and Kopan, R. (2000). A ligand-induced

extracellular cleavage regulates gamma-secretase-like proteolytic activation of Notch1. Mol. Cell *5*, 197–206.

Olichon, A., Emorine, L.J., Descoins, E., Pelloquin, L., Brichese, L., Gas, N., Guillou, E., Delettre, C., Valette, A., Hamel, C.P., et al. (2002). The human dynamin-related protein OPA1 is anchored to the mitochondrial inner membrane facing the inter-membrane space. FEBS Lett. *523*, 171–176.

Otera, H., Ohsakaya, S., Nagaura, Z., Ishihara, N., and Mihara, K. (2005). Export of mitochondrial AIF in response to proapoptotic stimuli depends on processing at the intermembrane space. Embo J. *24*, 1375–1386.

Pellegrini, L., Passer, B.J., Canelles, M., Lefterov, I., Ganjei, J.K., Fowlkes, B.J., Koonin, E.V., and D'Adamio, L. (2001). PAMP and PARL, two novel putative metalloproteases interacting with the COOH-terminus of Presenilin-1 and -2. J. Alzheimers Dis. *3*, 181–190.

Perotti, M.E., Anderson, W.A., and Swift, H. (1983). Quantitative cytochemistry of the diaminobenzidine cytochrome oxidase reaction product in mitochondria of cardiac muscle and pancreas. J. Histochem. Cytochem. *31*, 351–365.

Rizzuto, R., Bernardi, P., and Pozzan, T. (2000). Mitochondria as all-round players of the calcium game. J. Physiol. *529*, 37–47.

Sandri, M., and Carraro, U. (1999). Apoptosis of skeletal muscles during development and disease. Int. J. Biochem. Cell Biol. *31*, 1373–1390.

Scaffidi, C., Fulda, S., Srinivasan, A., Friesen, C., Li, F., Tomaselli, K.J., Debatin, K.M., Krammer, P.H., and Peter, M.E. (1998). Two CD95 (APO-1/Fas) signaling pathways. EMBO J. *17*, 1675–1687.

Scorrano, L., Ashiya, M., Buttle, K., Weiler, S., Oakes, S.A., Mannella, C.A., and Korsmeyer, S.J. (2002). A distinct pathway remodels mitochondrial cristae and mobilizes cytochrome c during apoptosis. Dev. Cell *2*, 55–67.

Sik, A., Passer, B.J., Koonin, E.V., and Pellegrini, L. (2004). Self-regulated cleavage of the mitochondrial intramembrane-cleaving protease PARL yields Pbeta, a nuclear-targeted peptide. J. Biol. Chem. *279*, 15323–15329.

Sesaki, H., Southard, S.M., Hobbs, A.E., and Jensen, R.E. (2003). Cells lacking Pcp1p/Ugo2p, a rhomboid-like protease required for Mgm1p processing, lose mtDNA and mitochondrial structure in a Dnm1p-dependent manner, but remain competent for mitochondrial fusion. Biochem. Biophys. Res. Commun. *308*, 276–283.

Smirnova, E., Griparic, L., Shurland, D.L., and van der Bliek, A.M. (2001). Dynamin-related protein Drp1 is required for mitochondrial division in mammalian cells. Mol. Biol. Cell *12*, 2245–2256.

Sottocasa, G.L., Kuylenstierna, B., Ernster, L., and Bergstrand, A. (1967). An electron-transport system associated with the outer membrane of liver mitochondria. A biochemical and morphological study. J. Cell Biol. *32*, 415–438.

Veis, D.J., Sorenson, C.M., Shutter, J.R., and Korsmeyer, S.J. (1993). Bcl-2-deficient mice demonstrate fulminant lymphoid apoptosis, polycystic kidneys, and hypopigmented hair. Cell *75*, 229–240.

Wei, M.C., Lindsten, T., Mootha, V.K., Weiler, S., Gross, A., Ashiya, M., Thompson, C.B., and Korsmeyer, S.J. (2000). tBID, a membrane-targeted death ligand, oligomerizes BAK to release cytochrome c. Genes Dev. *14*, 2060–2071.

Wei, M.C., Zong, W.X., Cheng, E.H., Lindsten, T., Panoutsakopoulou, V., Ross, A.J., Roth, K.A., MacGregor, G.R., Thompson, C.B., and Korsmeyer, S.J. (2001). Proapoptotic BAX and BAK: a requisite gateway to mitochondrial dysfunction and death. Science *292*, 727–730.

Yoon, Y., Krueger, E.W., Oswald, B.J., and McNiven, M.A. (2003). The mitochondrial protein hFis1 regulates mitochondrial fission in mammalian cells through an interaction with the dynamin-like protein DLP1. Mol. Cell. Biol. *23*, 5409–5420.

Youle, R.J., and Karbowski, M. (2005). Mitochondrial fission in apoptosis. Nat. Rev. Mol. Cell Biol. *6*, 657–663.

Exploring the molecular composition of OPA1 complexes

Christian Frezza[1], Manuela Basso[2], Valentina Bonetto[2] and Luca Scorrano[1]

1 Dulbecco-Telethon Institute, Venetian Institute of Molecular Medicine, Padova, Italy

2 Dulbecco-Telethon Institute, Ricerche Farmacologiche Mario Negri, Milano, Italy

Summary

Optic Atrophy 1 (OPA1) is a pro-fusion dynamin-related protein of the inner mitochondrial membrane mutated in dominant optic atrophy. It protects from apoptosis by preventing cytochrome *c* release independently from mitochondrial fusion. This function correlates with the oligomerization of two forms of OPA1, a soluble, intermembrane space and an inner membrane integral one. During apoptosis, the pro-apoptotic BCL-2 family member BID disrupts OPA1 oligomers, while high levels of OPA1 stabilize them and prevent mobilization of cytochrome *c*. We are investigating the composition of OPA1-containing complexes taking advantage of blue native (BN) electrophoresis. OPA1 displays supramolecular assemblies spanning from ≈300 KDa up to ≈1000 KDa. BID results in a decrease of OPA1 oligomers and in the parallel increase of monomeric OPA1. Complexes of OPA1 retained in the native dimension were dissociated using an orthogonal denaturing SDS electrophoresis (2D BN/SDS electrophoresis). We studied the interaction partners of OPA1 and their stoichiometry using mass spectroscopy analysis. These data indicate that 2D BN/SDS electrophoresis can be a useful approach to analyze in details composition and function of OPA1 complexes in normal and apoptotic mitochondria.

Introduction

Mitochondria are central organelles in metabolism, signal transduction, and programmed cell death. Their shape is extremely complex, with the organelle bound by two distinct membranes. An higher degree of complexity is found in the ultrastructure of mitochondria where the inner membrane (IMM) is organized in distinct compartments, the peripheral inner membrane and the cristae (Frey and Mannella, 2000), defined by several lines of evidence the active site of oxidative phosphorilation (Vogel et al., 2006; Perotti et al., 1983; D'Herde et al., 2001) , separated from the peripheral inner membrane by narrow tubular junctions.

In order to grant complete cytochrome *c* mobilization from the cristae compartment to the cytosol, individual cristae fuse and the narrow tubular cristae junctions widen. Membrane dynamics, caveolae internalization and trafficking events all require dynamin for vesiculation. These proteins self-assemble into spirals into areas of fission and by tightening this protein collar, following GTP hydrolysis by, they constrict the membrane inducing negative curvature (Zhang and Hinshaw, 2001).

Cristae remodeling is a fast and highly dynamic process , whose biochemical regulators are still unknown. We have recently demonstrated that OPA1, the only dynamin-related protein of the IMM known so far, regulates cristae shape and prevents the apoptotic cristae remodeling independently from its role in mitochondrial fusion.

In a model similar to membrane constriction regulated by dynamins, we reasoned that OPA1 could keep in check cristae junctions by forming oligomers. These contain two forms of OPA1, one soluble in the intermembrane space and another one integral to the inner membrane . During apoptosis, the pro-apoptotic BCL-2 family member BID disrupts OPA1 oligomers, while high levels of OPA1 stabilize them and prevent mobilization of cytochrome *c* (Frezza et al., 2006).

Interestingly, OPA1-containing oligomers are retrieved at multiple sizes, suggesting that other proteins participate in their formation. Given the multiple role of OPA1 in mitochondrial fusion and biogenesis and stability of the cristae, it is conceivable that the partners of this mitochondria-shaping protein participate in the regulation of its biological functions. Furthermore, the analysis of the complexes in normal and apoptotic mitochondria is expected to clarify which proteins are required for the pro-fusion vs. the antiapoptotic effect of OPA1.

In order to analyze the exact composition of these complexes we took advantage of blue-native electrophoresis (BN-PAGE), a technique that was developed by Schagger in 1995 (Schagger, 1995) to study organization of respiratory chain complexes and that allows to the isolation of native protein complexes that retains their structure and enzymatic activity, trough the use of specific detergents.

Results

OPA1 complexes analyzed by blue native electrophoresis

Using different type of detergents, we were able to detect supramolecular assemblies of OPA1 spanning from ≈300 KDa up to ≈1000 KDa. This is compatible with the hypothesis that different micelle generated by different detergents can solubilize protein complexes that can differ both from size and, likely, partners. (Figure 1 A)

In order to confirm that the immunoreactive bands were specifically generated by OPA1 complexes, we performed the BN experiments in mitochondria isolated Opa1-/- : of note in OPA1-/- any signal was detected and rescuing OPA1 levels re-establish the OPA1 containing complexes (Figure 1 B).

It has been demonstrated that Mgm1p, the orthologue of OPA1 in yeast, interacts with component of the fusion machinery of the OMM (Wong et al., 2003), namely Fzo1p and Ugo1p; moreover recent involvement of OPA1 in controlling apoptosis suggest that it can cooperate with upstream component of the apoptotic machinery like Bid or Bax/Bak to signal the trigger from OMM to IMM (for a scheme see Fig 2 B). In order to indirectly undertand whether OPA1 complexes could contain the indicated proteins, we performed a BN electrophoresis analysis from isolated mitochondria of Mfn1-/- and Bax-/-;Bak-/-; the lack of these proteins doesn't change OPA1 complexes pattern, suggesting that these proteins are dispensable for correct organization of the complexes.

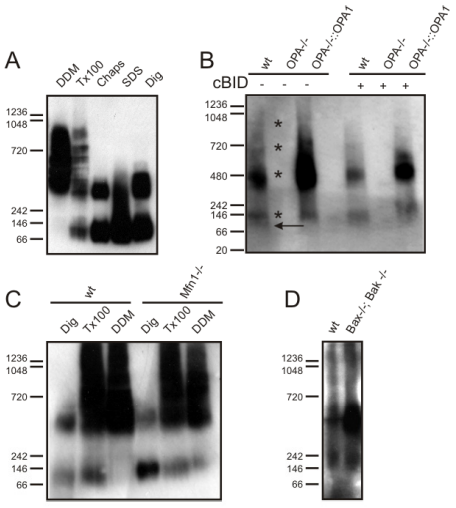

Figure 1 **Blue native electrophoresis analysis of OPA1 complexes**
(A) BN electrophoresis on mouse liver isolated mitochondria using the indicated detergent to solubilize native protein complexes; proteins separated were blotted and immunodecorated with anti OPA1 monoclonal antibody
(B) Same as (A) using but performed on isolated mitochondria from the indicated genotype; proteins separated were blotted and immunodecorated with anti OPA1 monoclonal antibody. Arrow indicate OPA1 monomer while asterisks indicate OPA1 containing complexes. When indicated isolated mitochondria were incubated with 40 pmol*mg^{-1} of cBID for 30 minutes at RT

OPA1 complexes change upon cBID incubation

Supramolecular assemblies that are retained during 1D BN-PAGE can be dissociated into the individual complexes by applying an orthogonal modified BN-PAGE for the second native dimension, thereby identifying the interaction partners and their stoichiometric ratio (Wittig et al., 2006). This second dimension of BN-PAGE is less mild because low detergent amounts are added to the cathode buffer. The mixture of nonionic detergent and anionic Coomassie dye has some resemblance to an anionic detergent: it can dissociate detergentlabile associations but keeps individual complexes intact. With this technique we could also improve the resolution power of BN in order to clearly identify changes in OPA1 complexes upon cBID incubation. A 2D BN/BN analysis showed higher resolution the typical pattern of OPA1 complexes separated in 1D-BN; of note, in the absence of Mfn1 this pattern is equal to wt background confirming the previous result (compare figure 1 C and figure 2 A)

We previously demonstrated that cBID incubation of isolated mitochondria results in disruption of high-molecular weight complexes of OPA1 (Frezza et al., 2006). Our 2D-BN/BN electrophoresis confirmed this phenomenon and demonstrated that cBID induced a decrease of OPA1 oligomers paralleled by an increase of monomeric OPA1 (figure 2 A).

Analysis of OPA1 complexes

Complexes retained in the 1D-BN can be denatured and incubated with SDS to completely dissociate the components of the former native complex in individual protein. With the 2D BN/SDS electrophoresis we aim to study both the interaction partners of OPA1 and their stoichiometry using mass spectroscopy analysis. Our preliminary data indicate that the stress induced protein HSP70 seems to associate with OPA1 in normal and apoptotic mitochondria. Moreover, this analysis confirmed that in response to BID the amount of high molecular weight complexes are quantitatively reduced.

Discussion

These preliminary data indicate that BN electrophoresis can be a useful approach to analyze in details composition and function of OPA1 complexes in normal and apoptotic mitochondria. We demonstrated that OPA1 complexes span up to 1000 KDa and their composition is independent of Mfn1 and Bax/Bak; we confirmed that these complexes change their molecular weight upon cBID incubation and this is likely due to a change in complexes aggregation and composition.

Experimental procedures

Recombinant proteins and Antibodies

p7/p15 recombinant BID was produced, purified and cleaved with caspase-8 exacity as described in (Scorrano et al., 2002). Unless noted, it was used at a final concentration of 32 pmol x mg-1. For immunoblotting experiments, the following antibodies were employed: monoclonal anti-OPA1 (1:500, BD pharmingen), monoclonal anti complex IV (COX) subunit II (1:1000, Molecular Probes). Isotype matched, horseradish peroxidase conjugated secondary antibodies (Sigma) were used followed by detection by chemiluminescence (Amersham).

Isolation of mitochondria

Mitochondria were isolated from CD1 mouse liver by standard differential centrifugation in isolation buffer (0.2 M sucrose, 10mM Tris-Mops pH 7.4, 0.1mM EGTA-tris). Protein concentration was determinated by Biuret assay (Bio-Rad).

BN-PAGE 1D

Mitochondria (400 µg) were resuspended in 800 in µL of isolation buffer and spun at 12000g at 4°C for 10 minutes; pellet was resuspended in 40 µL of Native Loading Buffer (Invitrogen) with 1X protease inhibitor cocktail (Sigma). The suspension was then incubated with 10 µL of digitonin 10% (Invitrogen) for 20 minutes at 4 °C and then spun at 20000g at 4°C for 20 minutes

Supernatant was incubated with 2.5 µL of Native Additive G250 5% (Invitrogen) and then 10 µL were loaded onto a 3-12% Native Gels (Invitrogen).

Protein were separated in Catode Buffer Dark Blue for 30 minutes at 150 V at 4°C and then Catode Buffer was changed with Light Blue Catode Buffer for about 90 minutes at 250 at 4°C.

The BN gel can be then transferred onto PVDF membranes (Millipore) and probed using the indicated antibodies.

Alternatively, using non-fixed BN gels, blue bands can be excised and processed as described the following section

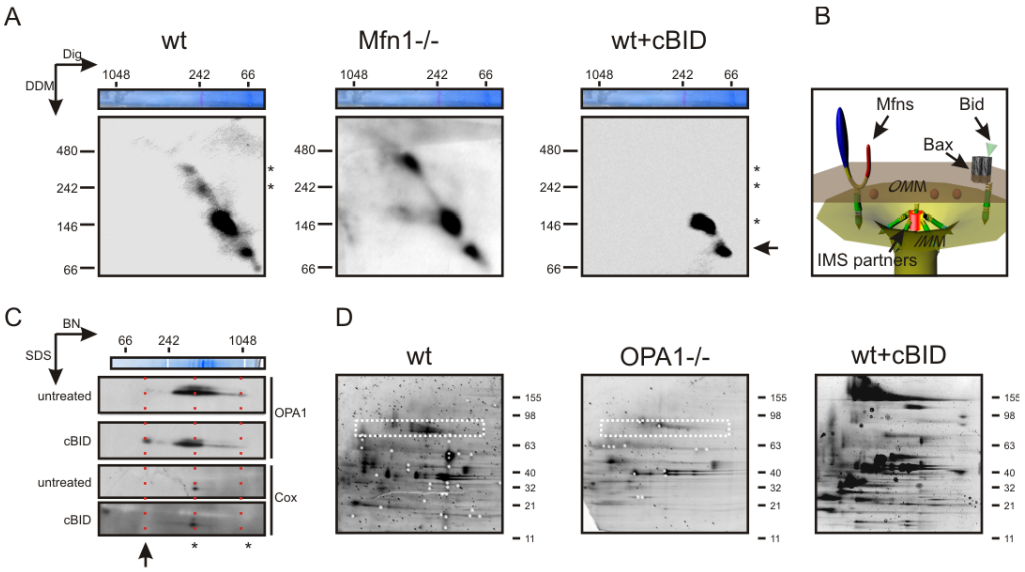

Figure 2 **Exploring OPA1 containing complexes**
(A) **Two dimensional BN/BN electrophoresis**: isolated mitochondria of the indicated genotype were solubilized with 1,25% digitonin and separated on 3-14% native gels; lanes of the gel were excised in and subsequently separated using orthogonal Native electrophoresis, adding 0,01% DDM in cathode buffer. When indicated, isolated mitochondria were treated with 40 pmol°mg^{-1} of cBID for 30 minutes at 25°C before digitonin solubilization; proteins separated were blotted and immunodecorated with anti OPA1 monoclonal antibody
(B) Scheme of putative interactors of OPA1 from OMM and IMS
(C) **Two dimensional BN/SDS electrophoresis**: isolated mitochondria of the indicated genotype were solubilized with 1,25% and separated on 3-14% native gels; lanes of the gel were excised in and denatured with 1% b-mercaptoethanol and then separated using orthogonal SDS electrophoresis. When indicated, isolated mitochondria were treated with 40 pmol°mg^{-1} of cBID for 30 minutes at 25°C before digitonin solubilization. proteins separated were blotted and immunodecorated with the indicated antibodies
(D) **Sypro staining of 2D BN/SDS gels**: proteins were separated as in (c) and then stained with Sypro Ruby Staining; the dashed rectangle indicates OPA1 immunoreactive area after superimposition of western-blot of the same gel. White spots indicate picked proteins for ongoing MS analysis.

BN/BN-2D PAGE

Two-dimensional blue native PAGE (2D BN/BN-PAGE; native in two dimensions)

Strip of the gel excised from 1D BN electrophoresis are inserted in the slab of a 4-12% Zoom Gel (Invitrogen) and an orthogonal electrophoresis was performed. Add 0.02% dodecylmaltoside to cathode buffer. Anode and gel buffers are the same as used for 1D. 2D BN-PAGE run under the running conditions of 1D-BN-PAGE. In contrast to 1D BN gels, the 2D BN/BN gels should be stopped late in order to focus streaking protein bands finally into sharp protein spots.

BN/SDS-2D PAGE

Strips of the gel excised from 1D-BN-PAGE are rinsed for several seconds with water; soak strips for 15 minutes with reducing solution (suggested volume for each strip is 5 mL composed of 5 mL of LDS 1X Loading buffer (NuPage, Invitrogen) and 1% β-mercaptoethanol); waste reducing solution and incubate the strip in alchilating solution for 15 minutes (volume 5 mL composed of 5 mL of LDS LB 1X and 50 mM dimethyl-acrilamide (DMA)); waste this solution and add quenching solution for 15 minutes (5 mL solution composed of 4 mL LDS LB 1X, 1 mL absolute ethanol and 0.1% β-mercaptoethanol). Gently push the native gel strip down to the 4-12% Zoom gel; remove water and fill the gaps to the left and right of the native gel strip using a 1% agarose. Start electrophoresis at room temperature with a maximal voltage of 200 V. The 2D BN/SDS gel can be then transferred onto PVDF membranes (Millipore) and probed using the indicated antibodies.

Alternatively, the gel can be fixed with 25% methanol and 10% acetic acid and then processed for Sypro staining using the manufacturer's instruction.

Reference list

D'Herde,K., De Prest,B., Mussche,S., Schotte,P., Beyaert,R., Coster,R.V., and Roels,F. (2001). Ultrastructural localization of cytochrome c in apoptosis demonstrates mitochondrial heterogeneity. Cell Death. Differ. *7*, 331-337.

Frey,T.G. and Mannella,C.A. (2000). The internal structure of mitochondria. Trends. Biochem. Sci. *25*, 319-324.

Frezza,C., Cipolat,S., Martins,d.B., Micaroni,M., Beznoussenko,G.V., Rudka,T., Bartoli,D., Polishuck,R.S., Danial,N.N., De Strooper,B., and Scorrano,L. (2006). OPA1 Controls Apoptotic Cristae Remodeling Independently from Mitochondrial Fusion. Cell *126*, 177-189.

Perotti,M.E., Anderson,W.A., and Swift,H. (1983). Quantitative cytochemistry of the diaminobenzidine cytochrome oxidase reaction product in mitochondria of cardiac muscle and pancreas. J. Histochem. Cytochem. *31*, 351-365.

Schagger,H. (1995). Native electrophoresis for isolation of mitochondrial oxidative phosphorylation protein complexes. Methods Enzymol. *260*, 190-202.

Scorrano,L., Ashiya,M., Buttle,K., Weiler,S., Oakes,S.A., Mannella,C.A., and Korsmeyer,S.J. (2002). A Distinct Pathway Remodels Mitochondrial Cristae and Mobilizes Cytochrome c during Apoptosis. Dev. Cell *2*, 55-67.

Vogel,F., Bornhovd,C., Neupert,W., and Reichert,A.S. (2006). Dynamic subcompartmentalization of the mitochondrial inner membrane. J. Cell Biol. *175*, 237-247.

Wittig,I., Braun,H.P., and Schagger,H. (2006). Blue native PAGE. Nat. Protoc. *1*, 418-428.

Wong,E.D., Wagner,J.A., Scott,S.V., Okreglak,V., Holewinske,T.J., Cassidy-Stone,A., and Nunnari,J. (2003). The intramitochondrial dynamin-related GTPase, Mgm1p, is a component of a protein complex that mediates mitochondrial fusion. J. Cell Biol. *160*, 303-311.

Zhang,P. and Hinshaw,J.E. (2001). Three-dimensional reconstruction of dynamin in the constricted state. Nat Cell Biol *3*, 922-926.

Targeting OPA1 GTPase activity enhances cytochrome *c* release from isolated mitochondria

Christian Frezza[1], Sara Cogliati[1], Andrea Bortolato[2], Stefano Moro[2] and Luca Scorrano[1]

1 Dulbecco-Telethon Institute, Venetian Institute of Molecular Mecicine, Padova

2 Department of Medicinal Chemistry, Molecular Modeling Section, University of Padova

Summary

OPA1 is an inner mitochondrial membrane dynamin-related protein that has genetically distinguishable functions in mitochondrial fusion and apoptosis. OPA1 forms oligomers whose disruption is associated with remodelling of the mitochondrial cristae and complete release of cytochrome c, required in the cytosol to fully activate effector caspases during cell death. Inactivating mutations in the GTPase domain of OPA1 impair this antiapoptotic activity, enhancing susceptibility to mitochondrial-dependent apoptosis. Thus, the inhibition of the GTPase domain of OPA1 could represent a novel target to enhance death of cancer cells. Suramin is a known commercially available GTPase inhibitor. *In silico* modelling showed that suramin can bind to the GTPase cleft of the protein. Since suramin is known for its inhibitory effect on mitochondrial respiratory chain, we sought a micromolar window of concentration that does not affect basal and ADP-stimulated respiration. These same safe concentrations enhanced cytochrome *c* release induced by the BID, a proapoptotic BH3-only member of the Bcl-2 family, without interfering with the activation of BAX and BAK, the mitochondrial receptors of BID. Interestingly, OPA1 oligomers were apparently targeted by suramin. Suramin seems therefore a good candidate to test whether OPA1 can be targeted to enhance apoptosis of cancer cell. We are now addressing the specificity of suramin using *Opa1-/-* mitochondria and we are extending our analysis to novel compounds derived from suramin that display better in silico binding to the GTPase domain of OPA1.

Introduction

Besides producing most cellular ATP, mitochondria integrate several cellular processes such as Ca^{2+} signaling, volume regulation, redox balance and programmed cell death. Defects in any of these processes regulated by mitochondria can have severe consequence for the cell: a large amount of diseases are indeed consequence of, or aggravated by mitochondrial dysfunction [for a review see (Schapira, 2006)]. Moreover, it is now established that mitochondria play a crucial role in the amplification of apoptosis, whose dysregulation is crucial in tumorigenic transformation,

In mammalian cells, the death receptor pathway and the mitochondrial pathway of apoptosis occur downstream of death signals and appear to be linked in certain cell types (Hengartner, 2000). Both culminate in the activation of caspases, cysteine proteases that cleave a number of substrates, eventually resulting in the orderly demise of the cell. Mitochondria participate in the activation of caspases, by releasing cytochrome *c* and additional apoptogenic factors from the intermembrane space into the cytosol. Cytochrome *c* in complex with Apaf-1 activates caspase-9 and other downstream caspases (Li et al., 1997).

Recently, changes in the structure of the mitochondrial network and in the internal organization of the mitochondria have been described during apoptosis. This modification of the mitochondrial reticulum appears to be crucial to ensure the progression of the apoptotic cascade. Several stimuli, including the proapoptotic multidomain BCL-2 family member BAX, induce mitochondrial fragmentation dependent on the dynamin related protein DRP-1 and inhibition of MFN1-dependent mitochondrial fusion (Frank et al., 2001; Karbowski et al., 2004). Our laboratory has identified that during apoptosis mitochondria remodel their internal structure, with fusion of the individual cristae and opening of the tight, tubular cristae junctions. This accounts for the ability of mitochondria to release the bulk of cytochrome *c* that is normally stored in the cristae compartment (Scorrano et al., 2002).

The shape of the mitochondrial network and of the individual mitochondria results from a net balance of fusion-fission processes regulated by a family of "mitochondria-shaping proteins" including specific mitochondrial dynamin-related proteins (Griparic and van der Bliek, 2001). Dynamins are large, ubiquitous mechanoenzymatic GTPases that control the dynamics of membrane fusion, tubulation, budding and of vesicles formation (McNiven et al., 2000). The role of dynamins in controlling mitochondrial shape was first identified in yeast, where deletion of specific genes resulted in gross alterations of the mitochondrial network, and ultimately in functional abnormalities including loss of mitochondrial DNA, growth defects and petite strains (Yaffe, 1999). In mammalian, known proteins regulating mitochondrial fission include DRP-1 (Smirnova et al., 2001), a cytosolic dynamin that translocate to fission sites where it interacts with its molecular adapter hFis1, an integral protein of the outer mitochondrial membrane (James et al., 2003). Mitofusin (MFN) 1 and -2 also reside in the OM and regulate mitochondrial fusion (Chen et al., 2003). The inner mitochondrial membrane protein OPA1, mutated in dominant optic atrophy (DOA) (Alexander et al., 2000; Delettre et al., 2000), also appears to be crucial for the maintenance of the mitochondrial reticulum and ultrastructure (Olichon et al., 2003).

We have recently shown that OPA1 controls the cristae remodelling pathway of apoptosis, independently of mitochondrial fusion. OPA1 does not interfere with the activation of the core mitochondrial apoptotic pathway of BAX, BAK activation, yet it inhibits the release of cytochrome *c* by preventing the remodelling of the cristae and the intramitochondrial redistribution of cytochrome c. This correlates with the formation of OPA1 oligomers that are disrupted early in the course of apoptosis. Inactivating mutations in the GTPase domain of OPA1 impair its anti-apoptotic activity, enhancing susceptibility to apoptosis induced by stimuli that recruit the mitochondrial pathway (Frezza et al., 2006).

Thus, inhibition of oligomerization of OPA1 could represent a novel target to induce death of cancer cells.

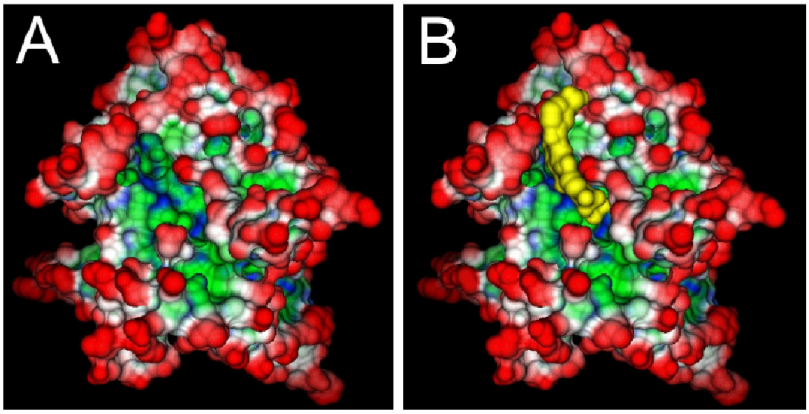

Figure 1 **Fitting of suramin in the GTPase domain of OPA1.** Structure of GTPase domain of OPA1 based on homology modeling using dynamin A of Dyctiostelium Discoideum as template (A). In B, we fitted one half of suramin (yellow) in the GTPase binding site and we found high affinity for binding in this cleft

Results

Suramin: a candidate inhibitor of GTPase activity of OPA1

We reasoned that a chemical inhibitor of the GTPase domain of OPA1 could mimic the inactivating mutations in the GTPase domain.
Suramin is a known commercially available GTPase inhibitor that is currently used in the therapy of androgen-resistant (AR) prostate cancer. AR prostate cancer is characterized by the up-regulation of Bcl-2 and the inhibition of the mitochondrial pathway of apoptosis. Suramin is a symmetric polysulphonated naphtylamine-benzene-derivative, used for more than 70 years in the treatment of sleeping disease. It inhibits different mammalian targets like purinergic P2 receptors, and α-subunit of G-proteins, where suramin impairs release of GDP (Voogd et al., 1993; Freissmuth et al., 1996). We established that suramin could be a candidate inhibitor of GTPase activity of OPA1 using an *in silico* approach: thanks to the high similarity of the OPA1 GTPase domain with that of *Dyctostelium Discoideum* dynamin A, in collaboration with the group of S. Moro (Department of Pharmaceutical Sciences, Molecular Modelling Section, University of Padova) we fitted suramin in this site and found good binding properties to the GTPase domain of OPA1 (Figure 1).

Titration of mitochondrio toxic effects of suramin shows a safe windows

It was reported that suramin could impair mitochondrial function and respiration (Rago et al., 1992; Bernardes et al., 2001); to test toxicity of suramin in our model we performed polarographic analysis using Clark type oxygen electrode and titrated suramin effects on CD1 mouse liver isolated mitochondria respiration. Mitochondrial respiration was induced by addition of ADP using either glutamate/malate, succinate as substrates or of FCCP as uncoupler.

Suramin inhibited ADP-stimulated respiration at concentrations higher than 50 μM, while it had no effects on uncoupled respiration (Figure 2). This suggests that its effects are not related to inhibition of respiratory chain complexes but, rather, are dependent either on ADP/ATP exchange or on inhibition of ATP-synthase. A detailed analysis on ATP synthase function, excluded any effects of suramin on ATP synthase (Figure 3). We concluded that suramin mitochondrio-toxic effects, displayed at concentration higher than 50 μM, are related to impairment of ADP/ATP exchange. Of note, we found a concentration of suramin that can be used without any detectable impact on mitochondrial bioenergetic.

Suramin enhances cytochrome c release induced by cBID

We verified whether non mitochondrio-toxic doses of suramin could to counteract the inhibitory effect of OPA1 on cytochrome *c* release. We started our approach testing the effects of suramin on cytochrome *c* release induced by recombinant caspase 8 cleaved BID (cBID). Mitochondria isolated from CD1 mouse liver were incubated in respiratory buffer added with micromolar concentrations of suramin that do not affect function of the organelle and treated with cBID. The amount of cytochrome *c* released has been determined using a specific ELISA as previously described (Frezza et al., 2006).
We found that 2 μM suramin did not induced cytochrome *c* release *per se* but, at the same time, it enhanced cytochrome *c* release in response to cBID (Figure 4).

Suramin aggravates cristae remodeling induced by cBID

We fixed and embedded cBID and suramin treated isolated mitochondria and performed classical electron microscopy and evidences of cristae remodeling has been evaluated as previously described (Frezza et al., 2006) (Figure 5).
Moreover, we will perform 3D tomographic reconstruction to allow specific measurement of cristae junction opening, an indicator of cristae remodelling, controlled by OPA1.

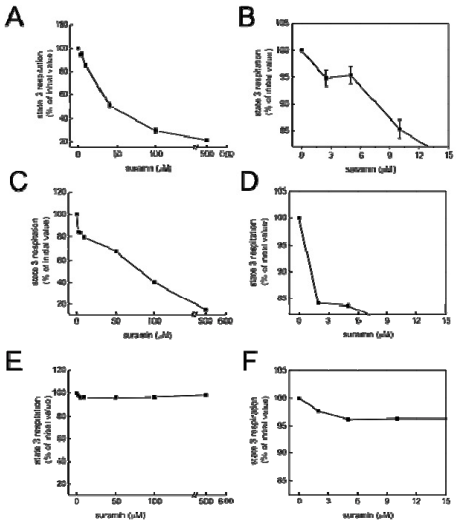

Figure 2 **Micromolar doses of suramin do not inhibit respiratory chain activity.** O_2 consumption were measured in ADP stimulated mitochondria using glutamate/malate (A) or succinate (C) as substrates or uncoupled (E) mitochondria in presence of increasing doses of suramin. B,D and F are enlargement of the non mitochondrio-toxic window of suramin.

Suramin increases OPA1 oligomers disruption by cBID

To test specificity of suramin on the antiapoptotic mode of action of OPA1, we wanted to analyzed whether suramin was influencing BAK oligomerization and OPA1 oligomerization. Importantly, we found that in response to cBID, suramin did not increase BAK oligomerization kinetic (Figure 6A) but, indeed, increased OPA1 oligomer disruption (Figure 6B), suggesting that the enhancing effect on cytochrome *c* release is not depenent on upstream signalling that would increase outer mitochondrial membrane permeability but rather, correlates with OPA1 oligomers disruption.

Discussion

Our preliminary data suggest that non mitochondrio-toxic, micromolar doses of suramin sensitizes cytochrome *c* release in isolated mitochondria incubated with recombinant cBID in time dependent manner; these effects are independent of BAK oligomerization, and hence, on upstream apoptotic signalling but correlates with an increased OPA1 oligomers disruption.
In addition, classical EM analysis confirmed that suramin can increase the kinetic of cristae remodelling induced by cBID.

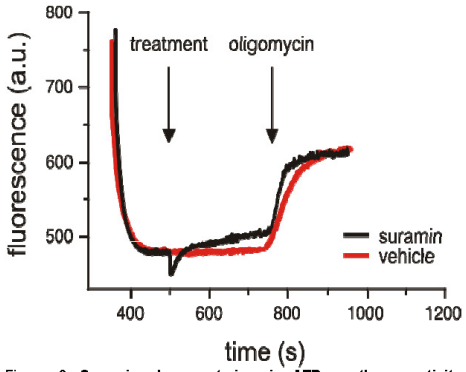

Figure 3 **Suramin does not impair ATP synthase activity.** Mitochondria were loaded with Rhodamine 123, energized with glutamate/malate and respiratory chain were then inhibited with 1 mM KCN. 10 mM ATP reversed ATP synthase to sustain mitochondrial potential. Fluorescence were measured spectrophotometrically; high fluorescence indicates low $\Delta\Psi_m$. 500 μM suramin was added where indicated; oligomycin, an ATP synthase inhibitor was used as positive control.

To address whether the mechanism of action of suramin is specific and directly acting on OPA1 oligomerization we are taking advantage of OPA1 -/- mouse embryonic fibroblast and of previously generated OPA1 overexpressing stable clones.
Mitochondria will be isolated from, wt::Puro, wt::Opa1, wt::Opa1^{K301A}, wt::Hygro, wt::shRNAi^{Opa1} MEFs, treated with suramin and the ability of the drug to increase the redistribution and release of cytochrome *c* will be measured as described above.
Finally, in order to find more specific inhibitors of OPA1, we are performing a virtual screening on a library of GTPase inhibitors generated by the group of S. Moro. They. already scored 4 drugs with a high affinity for the GTPase cleft of OPA1 and with acceptable pharmacokinetic properties. We have just started a toxicological profile analysis on one of these drugs.
In conclusion, these preliminary data suggest that inhibiting OPA1 GTPase function can be a promising strategy to sensitize cells with aberrant apoptotic machinery to death: this approach could be therapeutic for tumors that overexpress OPA1 like non-small cell lung cancer.

Experimental procedures

Recombinant proteins and Antibodies

p7/p15 recombinant BID was produced, purified and cleaved with caspase-8 exactly as described in (Scorrano et al., 2002). Unless noted, it was used at a final concentration of 32 pmol x mg^{-1}. For immunoblotting experiments, the following antibodies were employed: monoclonal anti-OPA1 (1:500, BD pharmingen), rabbit polyclonal anti-BAKNT (1:1000, Upstate). Isotype matched, horseradish peroxidase conjugated secondary antibodies (Sigma) were used followed by detection by chemiluminescence (Amersham).

In vitro mitochondrial assays.

Isolation of mitochondria

Mitochondria were isolated from CD1 mouse liver by standard differential centrifugation in isolation buffer (0.2 M sucrose, 10mM Tris-Mops pH 7.4, 0.1mM EGTA-tris). Protein concentration was determinated by Biuret assay (Bio-Rad).

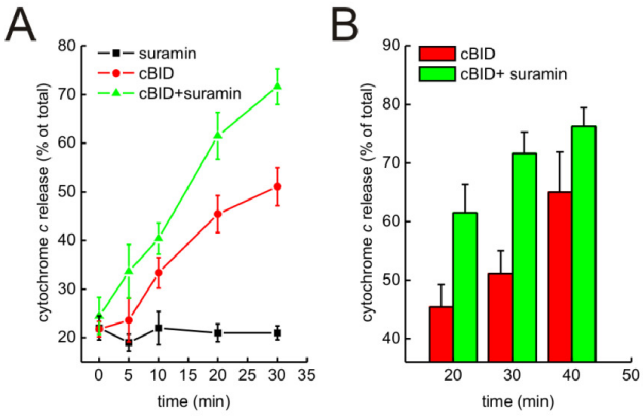

Figure 4 **Suramin enhances cytochrome *c* release in response to cBID.** Isolated mitochondria were preincubated with 2 μM suramin in presence or absence of 40 pmol*mg^{-1} of cBID for the indicated time (A). Histograms in B show that enhancing effect of suramin is also time dependent.

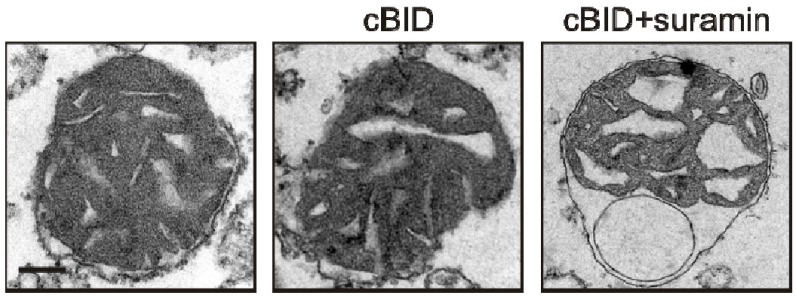

Figure 5 **Suramin increase the cristae remodelling effect induced by cBID.** Isolated mitochondria treated as in Figure 4 were fixed and stained as described in Experimental Procedures. High magnification of a representative mitochondria clearly show that suramin could enhance cristae remodeling in response to cBID. Bar: 100 nm

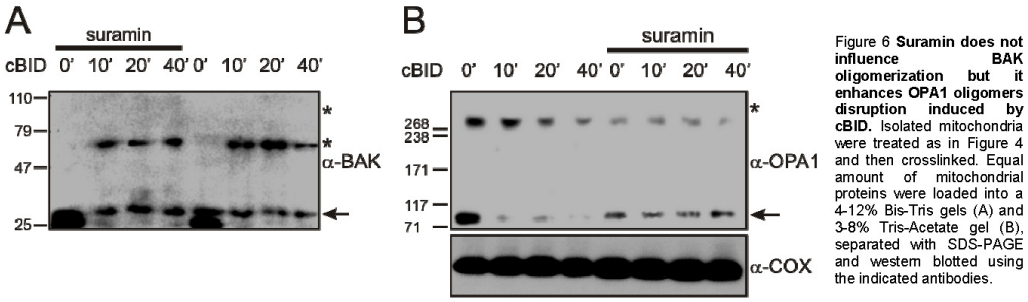

Figure 6 **Suramin does not influence BAK oligomerization but it enhances OPA1 oligomers disruption induced by cBID.** Isolated mitochondria were treated as in Figure 4 and then crosslinked. Equal amount of mitochondrial proteins were loaded into a 4-12% Bis-Tris gels (A) and 3-8% Tris-Acetate gel (B), separated with SDS-PAGE and western blotted using the indicated antibodies.

Mitochondrial oxygen consumption was measured by using a Clarke-type oxygen electrode (Hansatech Instruments). Mitochondria were incubated in experimental buffer (EB, 125 mM KCl, 10 mM Tris-MOPS, 1 mM KPi, 10 µM EGTATris, pH 7.4, 25°C) supplemented with the substrates detailed in the figure legend and treated as indicated.

Cytochrome c release

Cytochrome *c* release in response to recombinant p7/p15 BID was determined as described in (Scorrano et al., 2002; Frezza et al., 2006). Briefly, mitochondria (0.5 mg/ml) were incubated in experimental buffer (EB) supplemented with 5 mM glutamate and 2.5 mM malate and treated as described at 25°C. At the indicated time, mitochondria were pelleted by centrifugation at 12000 x g at 4°C for 3 min, and resuspended in the same volume of EB. Cytochrome *c* release was determined by using a mouse specific cytochrome *c* ELISA performed on mitochondrial pellet and supernatant diluted 1:20 in PBS containing 0.5% Triton X- 100 (R&D systems, MN). Cytochrome *c* release is reported as the percentage of the supernatant over the total (pellet plus supernatant) measured cytochrome *c*

ATPase activity

Mitochondria (0.5 mg/mL) were incubated in EB supplemented with glutamate/malate as substrates and 0,1 µM rhodamin 123 at pH 7,4, 25°C. Rhodamine fluorescence was measured using a Shimadzu RF 5301PC spectrofluorimeter using λ_{ecc}=505, λ_{em}=535 nm and 2.5 nm slit. After stabilization of the baseline, 10 mM KCN and 10mM ATP were added to maintain $\Delta\Psi_m$ by using the reversal of the ATPase

Protein crosslinking and immunoblotting

For protein crosslinking, mitochondria were treated with 10 mM BMH (Pierce) in DMSO for 30 min at 25° *c* for BAK oligomerization or with 10 mM EDC (pierce) in IB for 30 minutes at 25°C for OPA1 oligomerization. Reactions were spun for 10 mins at 12000 x g at 4°C, and the mitochondrial pellets resuspended in SDS-PAGE sample loading buffer. DTT in the sample buffer quenched the crosslinking reaction. Proteins dissolved in reduced gel loading buffer (NuPAGE, Invitrogen) were separated by 4-12% SDS-PAGE (NuPAGE, Invitrogen) for BAK and 3-8% SDS-PAGE for OPA1 transferred onto PVDF membranes (Millipore) and probed using the indicated antibodies.

Transmission Electron Microscopy

Mitochondria were fixed for 1 h at 25°C using glutaraldehyde dissolved in EB at a final concentration of 1.25%, embedded in plastic, sectioned, and stained with uranyl acetate and lead citrate. Thin sections were imaged on a Tecnai-12 electron microscope (Philips-FEI) at the EM Facility (University of Padova).

Reference list

Alexander,C., Votruba,M., Pesch,U.E., Thiselton,D.L., Mayer,S., Moore,A., Rodriguez,M., Kellner,U., Leo-Kottler,B., Auburger,G., Bhattacharya,S.S., and Wissinger,B. (2000). CPA1, encoding a dynamin-related GTPase, is mutated in autosomal dominant optic atrophy linked to chromosome 3q28. Nat. Genet. *26*, 211-215.

Bernardes,C.F., Fagian,M.M., Meyer-Fernandes,J.R., Castilho,R.F., and Vercesi,A.E. (2001). Suramin inhibits respiration and induces membrane permeability transition in isolated rat liver mitochondria. Toxicology. *169*, 17-23.

Chen,H., Detmer,S.A., Ewald,A.J., Griffin,E.E., Fraser,S.E., and Chan,D.C. (2003). Mitofusins Mfn1 and Mfn2 coordinately regulate mitochondrial fusion and are essential for embryonic development. J. Cell Biol. *160*, 189-200.

Delettre,C., Lenaers,G., Griffoin,J.M., Gigarel,N., Lorenzo,C., Belenguer,P., Pelloquin,L., Grosgeorge,J., Turc-Carel,C., Perret,E., Astarie-Dequeker,C., Lasquellec,L., Arnaud,B., Ducommun,B., Kaplan,J., and Hamel,C.P. (2000). Nuclear gene OPA1, encoding a mitochondrial dynamin-related protein, is mutated in dominant optic atrophy. Nat. Genet. *26*, 207-210.

Frank,S., Gaume,B., Bergmann-Leitner,E.S., Leitner,W.W., Robert,E.G., Catez,F., Smith,C.L., and Youle,R.J. (2001). The role of dynamin-related protein 1, a mediator of mitochondrial fission, in apoptosis. Dev. Cell *1*, 515-525.

Freissmuth,M., Boehm,S., Beindl,W., Nickel,P., Ijzerman,A.P., Hohenegger,M., and Nanoff,C. (1996). Suramin analogues as subtype-selective G protein inhibitors. Mol. Pharmacol. *49*, 602-611.

Frezza,C., Cipolat,S., Martins,d.B., Micaroni,M., Beznoussenko,G.V., Rudka,T., Bartoli,D., Polishuck,R.S., Danial,N.N., De Strooper,B., and Scorrano,L. (2006). OPA1 Controls Apoptotic Cristae Remodeling Independently from Mitochondrial Fusion. Cell *126*, 177-189.

Griparic,L. and van der Bliek,A.M. (2001). The many shapes of mitochondrial membranes. Traffic *2*, 235-244.

Hengartner,M.O. (2000). The biochemistry of apoptosis. Nature *407*, 770-776.

James,D.I., Parone,P.A., Mattenberger,Y., and Martinou,J.C. (2003). hFis1, a novel component of the mammalian mitochondrial fission machinery. J. Biol. Chem. *278*, 36373-36379.

Karbowski,M., Arnoult,D., Chen,H., Chan,D.C., Smith,C.L., and Youle,R.J. (2004). Quantitation of mitochondrial dynamics by photolabeling of individual organelles shows that mitochondrial fusion is blocked during the Bax activation phase of apoptosis. J. Cell Biol. *164*, 493-499.

Li,P., Nijhawan,D., Budihardjo,I., Srinivasula,S.M., Ahmad,M., Alnemri,E.S., and Wang,X. (1997). Cytochrome c and dATP-dependent formation of Apaf-1/caspase-9 complex initiates an apoptotic protease cascade. Cell *91*, 479-489.

McNiven,M.A., Cao,H., Pitts,K.R., and Yoon,Y. (2000). The dynamin family of mechanoenzymes: pinching in new places. Trends Biochem. Sci. *25*, 115-120.

Olichon,A., Baricault,L., Gas,N., Guillou,E., Valette,A., Belenguer,P., and Lenaers,G. (2003). Loss of OPA1 perturbates the mitochondrial inner membrane structure and integrity, leading to cytochrome c release and apoptosis. J. Biol. Chem. *278*, 7743-7746.

Rago,R.P., Brazy,P.C., and Wilding,G. (1992). Disruption of mitochondrial function by suramin measured by rhodamine 123 retention and oxygen consumption in intact DU145 prostate carcinoma cells. Cancer. Res. *52*, 6953-6955.

Schapira,A.H. (2006). Mitochondrial disease. Lancet *368*, 70-82.

Scorrano,L., Ashiya,M., Buttle,K., Weiler,S., Oakes,S.A., Mannella,C.A., and Korsmeyer,S.J. (2002). A Distinct Pathway Remodels Mitochondrial Cristae and Mobilizes Cytochrome c during Apoptosis. Dev. Cell *2*, 55-67.

Smirnova,E., Griparic,L., Shurland,D.L., and van der Bliek,A.M. (2001). Dynamin-related protein Drp1 is required for mitochondrial division in mammalian cells. Mol. Biol. Cell *12*, 2245-2256.

Voogd,T.E., Vansterkenburg,E.L., Wilting,J., and Janssen,L.H. (1993). Recent research on the biological activity of suramin. Pharmacol. Rev. *45*, 177-203.

Yaffe,M.P. (1999). The machinery of mitochondrial inheritance and behavior. Science *283*, 1493-1497.

6 Conclusion and Perspectives

In this Thesis we performed a genetic analysis of the role of OPA1, a mitochondrial pro-fusion protein, on apoptosis.

In 2000 it was demonstrated that *OPA1* mutations are associated with dominant optic atrophy, a neurodegenerative disorder of the optic nerve. The link between mutations in a dynamin related protein and apoptosis remained elusive until an increasing body of evidences demonstrated that during apoptosis mitochondrial network undergoes massive fragmentation. Mutation in OPA1 appear to increase cell death of retinal ganglion cells and we demonstrated that OPA1 overexpression protected from mitochondria-apoptosis. It was then hypothesized that the possible role of OPA1 in apoptosis could be related to its pro-fusion activity, demonstrated in our laboratory. We embarked in a biochemical and genetic study to understand at which level OPA1 exerted its regulatory function on apoptosis, by counteracting mitochondrial fragmentation or by regulating the *cristae* remodeling that occurs during apoptosis. Interestingly, we found that biological functions of OPA1in mammalian cells could be genetically differentiated: we established that OPA1 can regulate cytochrome *c* mobilization and apoptotic *cristae* remodeling independently of its pro-fusion activity. The former occurs via assembly of OPA1 into high molecular weight complexes that are disrupted early during apoptosis. We demonstrated that time dependent disruption of these OPA1 containing complexes correlates with remodeling of *cristae* (Frezza et al., 2006).

Interestingly, the group of Nunnari proposed a similar model in yeast where the OPA1 orthologue Mgm1 was found to be required to tether and fuse mitochondrial inner membranes. Using specific fusion assay, they observed an additional role of Mgm1 in inner-membrane dynamics, specifically in the maintenance of *cristae* structures trough Mgm1 interactions on opposing inner membranes and proposed a model for how this mitochondrial dynamin function to facilitate fusion (Meeusen et al., 2006). These data confirmed the role of OPA1 in regulating inner mitochondrial membrane morphology and likely the role in apoptotic *cristae* remodeling.

We are now trying to establish the composition of OPA1-containing complexes through a biochemical analysis of native protein complexes from isolated mitochondria in normal and apoptotic conditions. This will allow us to better understand the players of *cristae* remodeling pathway during apoptosis, which basic tenets remain still unclear.

Moreover, we are studying a possible approach to target OPA1 antiapoptotic functions to sensitize cell to apoptosis, by inhibiting OPA1 GTPase function: by these mean we propose to use OPA1 inhibitors as sensitizing agents to induce cell death in cancer cells that denote high levels of OPA1 expression like non small cell lung cancer.

In conclusion, the work presented in this Thesis elucidates that OPA1 has genetically dissectable roles in mitochondrial dynamics and apoptosis. Our data suggest that the inability of OPA1 to regulate mitochondrial ultrastructure could represent a pathogenic mechanism in ADOA. This appears to be confirmed by the fact that pathogenic mutations in OPA1 impair its ability to retain cytochrome *c* in *cristae* compartments.

7 Reference list

Adams,J.M. and Cory,S. (2007). Bcl-2-regulated apoptosis: mechanism and therapeutic potential. Curr. Opin. Immunol. *19*, 488-496.

Aijaz,S., Erskine,L., Jeffery,G., Bhattacharya,S.S., and Votruba,M. (2004). Developmental expression profile of the optic atrophy gene product: OPA1 is not localized exclusively in the mammalian retinal ganglion cell layer. Invest. Ophthalmol. Vis. Sci. *45*, 1667-1673.

Alavi,M.V., Bette,S., Schimpf,S., Schuettauf,F., Schraermeyer,U., Wehrl,H.F., Ruttiger,L., Beck,S.C., Tonagel,F., Pichler,B.J., Knipper,M., Peters,T., Laufs,J., and Wissinger,B. (2007). A splice site mutation in the murine Opa1 gene features pathology of autosomal dominant optic atrophy. Brain *130*, 1029-1042.

Alexander,C., Votruba,M., Pesch,U.E., Thiselton,D.L., Mayer,S., Moore,A., Rodriguez,M., Kellner,U., Leo-Kottler,B., Auburger,G., Bhattacharya,S.S., and Wissinger,B. (2000). OPA1, encoding a dynamin-related GTPase, is mutated in autosomal dominant optic atrophy linked to chromosome 3q28. Nat. Genet. *26*, 211-215.

Alirol,E., James,D., Huber,D., Marchetto,A., Vergani,L., Martinou,J.C., and Scorrano,L. (2006). The mitochondrial fission protein hFis1 requires the endoplasmic reticulum gateway to induce apoptosis. Mol. Biol. Cell *17*, 4593-4605.

Allen,R.D., Schroeder,C.C., and Fok,A.K. (1989). An investigation of mitochondrial inner membranes by rapid-freeze deep-etch techniques. J. Cell. Biol. *108*, 2233-2240.

Amati-Bonneau,P., Guichet,A., Olichon,A., Chevrollier,A., Viala,F., Miot,S., Ayuso,C., Odent,S., Arrouet,C., Verny,C., Calmels,M.N., Simard,G., Belenguer,P., Wang,J., Puel,J.L., Hamel,C., Malthiery,Y., Bonneau,D., Lenaers,G., and Reynier,P. (2005). OPA1 R445H mutation in optic atrophy associated with sensorineural deafness. Ann. Neurol. *58*, 958-963.

Amati-Bonneau,P., Valentino,M.L., Reynier,P., Gallardo,M.E., Bornstein,B., Boissiere,A., Campos,Y., Rivera,H., de la Aleja,J.G., Carroccia,R., Iommarini,L., Labauge,P., Figarella-Branger,D., Marcorelles,P., Furby,A., Beauvais,K., Letournel,F., Liguori,R., La,M.C., Montagna,P., Liguori,M., Zanna,C., Rugolo,M., Cossarizza,A., Wissinger,B., Verny,C., Schwarzenbacher,R., Martin,M.A., Arenas,J.I., Ayuso,C., Garesse,R., Lenaers,G., Bonneau,D., and Carelli,V. (2007). OPA1 mutations induce mitochondrial DNA instability and optic atrophy 'plus' phenotypes. Brain.

Andrews,R.M., Griffiths,P.G., Johnson,M.A., and Turnbull,D.M. (1999). Histochemical localisation of mitochondrial enzyme activity in human optic nerve and retina. Br. J. Ophthalmol. *83*, 231-235.

Annis,M.G., Soucie,E.L., Dlugosz,P.J., Cruz-Aguado,J.A., Penn,L.Z., Leber,B., and Andrews,D.W. (2005). Bax forms multispanning monomers that oligomerize to permeabilize membranes during apoptosis. EMBO J. *24*, 2096-2103.

Antignani,A. and Youle,R.J. (2006). How do Bax and Bak lead to permeabilization of the outer mitochondrial membrane? Curr. Opin. Cell Biol. *18*, 685-689.

Arnoult,D., Grodet,A., Lee,Y.J., Estaquier,J., and Blackstone,C. (2005). Release of OPA1 during apoptosis participates in the rapid and complete release of cytochrome c and subsequent mitochondrial fragmentation. J. Biol. Chem. *280*, 35742-35750.

Bach,D., Naon,D., Pich,S., Soriano,F.X., Vega,N., Rieusset,J., Laville,M., Guillet,C., Boirie,Y., Wallberg-Henriksson,H., Manco,M., Calvani,M., Castagneto,M., Palacin,M., Mingrone,G., Zierath,J.R., Vidal,H., and Zorzano,A. (2005). Expression of Mfn2, the Charcot-Marie-Tooth neuropathy type 2A gene, in human skeletal muscle: effects of type 2 diabetes, obesity, weight loss, and the regulatory role of tumor necrosis factor alpha and interleukin-6. Diabetes *54*, 2685-2693.

Bach,D., Pich,S., Soriano,F.X., Vega,N., Baumgartner,B., Oriola,J., Daugaard,J.R., Lloberas,J., Camps,M., Zierath,J.R., Rabasa-Lhoret,R., Wallberg-Henriksson,H., Laville,M., Palacin,M., Vidal,H., Rivera,F., Brand,M., and Zorzano,A. (2003). Mitofusin-2 determines mitochondrial network architecture and mitochondrial metabolism. A novel regulatory mechanism altered in obesity. J. Biol. Chem. *278*, 17190-17197.

Bakeeva,L.E., Chentsov,Y., and Skulachev,V.P. (1978). Mitochondrial framework (reticulum mitochondriale) in rat diaphragm muscle. Biochim. Biophys. Acta *501*, 349-369.

Baricault,L., Segui,B., Guegand,L., Olichon,A., Valette,A., Larminat,F., and Lenaers,G. (2007). OPA1 cleavage depends on decreased mitochondrial ATP level and bivalent metals. Exp. Cell. Res. *313*, 3800-3808.

Bayir,H., Fadeel,B., Palladino,M.J., Witasp,E., Kurnikov,I.V., Tyurina,Y.Y., Tyurin,V.A., Amoscato,A.A., Jiang,J., Kochanek,P.M., DeKosky,S.T., Greenberger,J.S., Shvedova,A.A., and Kagan,V.E. (2006). Apoptotic interactions of cytochrome c: redox flirting with anionic phospholipids within and outside of mitochondria. Biochim. Biophys. Acta. *1757*, 648-659.

Bereiter-Hahn,J. and Voth,M. (1994). Dynamics of mitochondria in living cells: shape changes, dislocations, fusion, and fission of mitochondria. Microsc. Res. Tech. *27*, 198-219.

Bernardi,P. (1999). Mitochondrial transport of cations: Channels, exchangers and permeability transition. Physiol. Rev. *79*, 1127-1155.

Bernardi,P. and Azzone,G.F. (1981). Cytochrome c as an electron shuttle between the outer and inner mitochondrial membranes. J. Biol. Chem. *256*, 7187-7192.

Bernardi,P., Krauskopf,A., Basso,E., Petronilli,V., Blachly-Dyson,E., Di,L.F., and Forte,M.A. (2006). The mitochondrial permeability transition from in vitro artifact to disease target. FEBS J. *273*, 2077-2099.

Bristow,E.A., Griffiths,P.G., Andrews,R.M., Johnson,M.A., and Turnbull,D.M. (2002). The distribution of mitochondrial activity in relation to optic nerve structure. Arch. Ophthalmol. *120*, 791-796.

Buono,L.M., Foroozan,R., Sergott,R.C., and Savino,P.J. (2002). Is normal tension glaucoma actually an unrecognized hereditary optic neuropathy? New evidence from genetic analysis. Curr. Opin. Ophthalmol. *13*, 362-370.

Carelli,V., Ross-Cisneros,F.N., and Sadun,A.A. (2004). Mitochondrial dysfunction as a cause of optic neuropathies. Prog. Retin. Eye. Res. *23*, 53-89.

Celotto,A.M., Frank,A.C., Seigle,J.L., and Palladino,M.J. (2006). Drosophila model of human inherited triosephosphate isomerase deficiency glycolytic enzymopathy. Genetics. *174*, 1237-1246.

Cereghetti,G.M. and Scorrano,L. (2006). The many shapes of mitochondrial death. Oncogene *25*, 4717-4724.

Chang,C.R. and Blackstone,C. (2007). Drp1 phosphorylation and mitochondrial regulation. EMBO. Rep. *8*, 1088-1089.

Chen,H., Chomyn,A., and Chan,D.C. (2005). Disruption of fusion results in mitochondrial heterogeneity and dysfunction. J Biol Chem. *280*, 26185-26192.

Chen,H., Detmer,S.A., Ewald,A.J., Griffin,E.E., Fraser,S.E., and Chan,D.C. (2003). Mitofusins Mfn1 and Mfn2 coordinately regulate mitochondrial fusion and are essential for embryonic development. J. Cell Biol. *160*, 189-200.

Chen,K.H., Guo,X., Ma,D., Guo,Y., Li,Q., Yang,D., Li,P., Qiu,X., Wen,S., Xiao,R.P., and Tang,J. (2004). Dysregulation of HSG triggers vascular proliferative disorders. Nat. Cell Biol. *6*, 872-883.

Chipuk,J.E., Bouchier-Hayes,L., and Green,D.R. (2006). Mitochondrial outer membrane permeabilization during apoptosis: the innocent bystander scenario. Cell Death. Differ. *13*, 1396-1402.

Choi,S.Y., Gonzalvez,F., Jenkins,G.M., Slomianny,C., Chretien,D., Arnoult,D., Petit,P.X., and Frohman,M.A. (2007). Cardiolipin deficiency releases cytochrome c from the inner mitochondrial membrane and accelerates stimuli-elicited apoptosis. Cell. Death. Differ. *14*, 597-606.

Choi,S.Y., Huang,P., Jenkins,G.M., Chan,D.C., Schiller,J., and Frohman,M.A. (2006). A common lipid links Mfn-mediated mitochondrial fusion and SNARE-regulated exocytosis. Nat. Cell Biol. *8*, 1255-1262.

Cipolat,S., de Brito,O.M., Dal Zilio,B., and Scorrano,L. (2004). OPA1 requires mitofusin 1 to promote mitochondrial fusion. Proc. Natl. Acad. Sci. U. S. A *101*, 15927-15932.

Clipstone,N.A. and Crabtree,G.R. (1992). Identification of calcineurin as a key signalling enzyme in T-lymphocyte activation. Nature *357*, 695-697.

Cohn,A.C., Toomes,C., Potter,C., Towns,K.V., Hewitt,A.W., Inglehearn,C.F., Craig,J.E., and Mackey,D.A. (2007). Autosomal dominant optic atrophy: penetrance and expressivity in patients with OPA1 mutations. Am. J. Ophthalmol. *143*, 656-662.

Cortese,J.D., Voglino,A.L., and Hackenbrock,C.R. (1998). Multiple conformations of physiological membrane-bound cytochrome c. Biochemistry. *37*, 6402-6409.

Cortopassi,G.A. and Wong,A. (1999). Mitochondria in organismal aging and degeneration. Biochem. Biophys. Acta. *1410*.

Cribbs,J.T. and Strack,S. (2007). Reversible phosphorylation of Drp1 by cyclic AMP-dependent protein kinase and calcineurin regulates mitochondrial fission and cell death. EMBO. Rep. *8*, 939-944.

D'Herde,K., De Prest,B., Mussche,S., Schotte,P., Beyaert,R., Coster,R.V., and Roels,F. (2001). Ultrastructural localization of cytochrome c in apoptosis demonstrates mitochondrial heterogeneity. Cell Death. Differ. *7*, 331-337.

Danial,N.N. and Korsmeyer,S.J. (2004). Cell death: critical control points. Cell *116*, 205-219.

Davies,V.J., Hollins,A.J., Piechota,M.J., Yip,W., Davies,J.R., White,K.E., Nicols,P.P., Boulton,M.E., and Votruba,M. (2007). Opa1 deficiency in a mouse model of autosomal dominant optic atrophy impairs mitochondrial morphology, optic nerve structure and visual function. Hum Mol Genet *16*, 1307-1318.

Dejean,L.M., Martinez-Caballero,S., and Kinnally,K.W. (2006). Is MAC the knife that cuts cytochrome c from mitochondria during apoptosis? Cell Death. Differ. *13*, 1387-1395.

Delettre,C., Griffoin,J.M., Kaplan,J., Dollfus,H., Lorenz,B., Faivre,L., Lenaers,G., Belenguer,P., and Hamel,C.P. (2001). Mutation spectrum and splicing variants in the OPA1 gene. Hum. Genet. *109*, 584-591.

Delettre,C., Lenaers,G., Griffoin,J.M., Gigarel,N., Lorenzo,C., Belenguer,P., Pelloquin,L., Grosgeorge,J., Turc-Carel,C., Perret,E., Astarie-Dequeker,C., Lasquellec,L., Arnaud,B., Ducommun,B., Kaplan,J., and Hamel,C.P. (2000). Nuclear gene OPA1, encoding a mitochondrial dynamin-related protein, is mutated in dominant optic atrophy. Nat. Genet. *26*, 207-210.

Delettre,C., Lenaers,G., Pelloquin,L., Belenguer,P., and Hamel,C.P. (2002). OPA1 (Kjer type) dominant optic atrophy: a novel mitochondrial disease. Mol. Genet. Metab. *75*, 97-107.

Deveraux,Q.L., Roy,N., Stennicke,H.R., Van Arsdale,T., Zhou,Q., Srinivasula,S.M., Alnemri,E.S., Salvesen,G.S., and Reed,J.C. (1998). IAPs block apoptotic events induced by caspase-8 and cytochrome c by direct inhibition of distinct caspases. EMBO J. *17*, 2215-2223.

Di,B.A. and Gill,G. (2006). SUMO-specific proteases and the cell cycle. An essential role for SENP5 in cell proliferation. Cell. Cycle. *5*, 2310-2313.

Dimmer,K.S. and Scorrano,L. (2006). (De)constructing mitochondria: what for? Physiology. (Bethesda.) *21*, 233-241.

Du,C., Fang,M., Li,Y., Li,L., and Wang,X. (2000). Smac, a mitochondrial protein that promotes cytochrome c-dependent caspase activation by eliminating IAP inhibition. Cell *102*, 33-42.

Dudkina,N.V., Heinemeyer,J., Keegstra,W., Boekema,E.J., and Braun,H.P. (2005). Structure of dimeric ATP synthase from mitochondria: an angular association of monomers induces the strong curvature of the inner membrane. FEBS. Lett. *579*, 5769-5772.

Durr,M., Escobar-Henriques,M., Merz,S., Geimer,S., Langer,T., and Westermann,B. (2006). Nonredundant roles of mitochondria-associated F-box proteins Mfb1 and Mdm30 in maintenance of mitochondrial morphology in yeast. Mol. Biol. Cell. *17*, 3745-3755.

Duvezin-Caubet,S., Jagasia,R., Wagener,J., Hofmann,S., Trifunovic,A., Hansson,A., Chomyn,A., Bauer,M.F., Attardi,G., Larsson,N.G., Neupert,W., and Reichert,A.S. (2006). Proteolytic processing of OPA1 links mitochondrial dysfunction to alterations in mitochondrial morphology. J. Biol. Chem.

Duvezin-Caubet,S., Koppen,M., Wagener,J., Zick,M., Israel,L., Bernacchia,A., Jagasia,R., Rugarli,E.I., Imhof,A., Neupert,W., Langer,T., and Reichert,A.S. (2007). OPA1 processing reconstituted in yeast depends on the subunit composition of the m-AAA protease in mitochondria. Mol. Biol. Cell. *18*, 3582-3590.

Epand,R.F., Martinou,J.C., Fornallaz-Mulhauser,M., Hughes,D.W., and Epand,R.M. (2002). The apoptotic protein tBid promotes leakage by altering membrane curvature. J. Biol. Chem. *277*, 32632-32639.

Escobar-Henriques,M., Westermann,B., and Langer,T. (2006). Regulation of mitochondrial fusion by the F-box protein Mdm30 involves proteasome-independent turnover of Fzo1. J. Cell. Biol. *173*, 645-650.

Eskes,R., Antonsson,B., Osen-Sand A., Montessuit,S., Richter,C., Sadoul,R., Mazzei,G., Nichols,A., and Martinou,J.-C. (1998). Bax-induced cytochrome c release from mitochondria is

independent of the permeability transition pore but highly dependent on Mg^{2+} ions. J. Cell Biol. *143*, 217-224.

Esposti,M.D., Erler,J.T., Hickman,J.A., and Dive,C. (2001). Bid, a widely expressed proapoptotic protein of the Bcl-2 family, displays lipid transfer activity. Mol. Cell Biol. *21*, 7268-7276.

Estaquier,J. and Arnoult,D. (2007). Inhibiting Drp1-mediated mitochondrial fission selectively prevents the release of cytochrome c during apoptosis. Cell. Death. Differ. *14*, 1086-1094.

Eura,Y., Ishihara,N., Oka,T., and Mihara,K. (2006). Identification of a novel protein that regulates mitochondrial fusion by modulating mitofusin (Mfn) protein function. J. Cell. Sci. *119*, 4913-4925.

Eura,Y., Ishihara,N., Yokota,S., and Mihara,K. (2003). Two mitofusin proteins, mammalian homologues of FZO, with distinct functions are both required for mitochondrial fusion. J. Biochem. (Tokyo) *134*, 333-344.

Fannjiang,Y., Cheng,W.C., Lee,S.J., Qi,B., Pevsner,J., McCaffery,J.M., Hill,R.B., Basanez,G., and Hardwick,J.M. (2004). Mitochondrial fission proteins regulate programmed cell death in yeast. Genes Dev. *18*, 2785-2797.

Ferguson-Miller,S., Brautigan,D.L., and Margoliash,E. (1976). Correlation of the kinetics of electron transfer activity of various eukaryotic cytochromes c with binding to mitochondrial cytochrome c oxidase. J. Biol. Chem. *251*, 1104-1115.

Ferre,M., Amati-Bonneau,P., Tourmen,Y., Malthiery,Y., and Reynier,P. (2005). eOPA1: an online database for OPA1 mutations. Hum. Mutat. *25*, 423-428.

Frank,S., Gaume,B., Bergmann-Leitner,E.S., Leitner,W.W., Robert,E.G., Catez,F., Smith,C.L., and Youle,R.J. (2001). The role of dynamin-related protein 1, a mediator of mitochondrial fission, in apoptosis. Dev. Cell *1*, 515-525.

Frey,T.G. and Mannella,C.A. (2000). The internal structure of mitochondria. Trends. Biochem. Sci. *25*, 319-324.

Frezza,C., Cipolat,S., Martins,d.B., Micaroni,M., Beznoussenko,G.V., Rudka,T., Bartoli,D., Polishuck,R.S., Danial,N.N., De Strooper,B., and Scorrano,L. (2006). OPA1 Controls Apoptotic Cristae Remodeling Independently from Mitochondrial Fusion. Cell *126*, 177-189.

Fritz,S., Weinbach,N., and Westermann,B. (2003). Mdm30 is an F-box protein required for maintenance of fusion-competent mitochondria in yeast. Mol Biol Cell *14*.

Gallop,J.L., Butler,P.J., and McMahon,H.T. (2005). Endophilin and CtBP/BARS are not acyl transferases in endocytosis or Golgi fission. Nature. *438*, 675-678.

Gallop,J.L., Jao,C.C., Kent,H.M., Butler,P.J., Evans,P.R., Langen,R., and McMahon,H.T. (2006). Mechanism of endophilin N-BAR domain-mediated membrane curvature. EMBO. J. *25*, 2898-2910.

Gallop,J.L. and McMahon,H.T. (2005). BAR domains and membrane curvature: bringing your curves to the BAR. Biochem. Soc. Symp. 223-231.

Garcia-Saez,A.J., Mingarro,I., Perez-Paya,E., and Salgado,J. (2004). Membrane-insertion fragments of Bcl-xL, Bax, and Bid. Biochemistry *43*, 10930-10943.

Germain,M., Mathai,J.P., McBride,H.M., and Shore,G.C. (2005). Endoplasmic reticulum BIK initiates DRP1-regulated remodelling of mitochondrial cristae during apoptosis. EMBO J. *24*, 1546-1556.

Gieffers,C., Korioth,F., Heimann,P., Ungermann,C., and Frey,J. (1997). Mitofilin is a transmembrane protein of the inner mitochondrial membrane expressed as two isoforms. Exp. Cell Res. *232*, 395-399.

Goldstein,J.C., Waterhouse,N.J., Juin,P., Evan,G.I., and Green,D.R. (2000). The coordinate release of cytochrome c during apoptosis is rapid, complete and kinetically invariant. Nat. Cell Biol. *2*, 156-162.

Gonzalvez,F., Bessoule,J.J., Rocchiccioli,F., Manon,S., and Petit,P.X. (2005). Role of cardiolipin on tBid and tBid/Bax synergistic effects on yeast mitochondria. Cell. Death. Differ. *12*, 659-667.

Gottlieb,E., Armour,S.M., Harris,M.H., and Thompson,C.B. (2003). Mitochondrial membrane potential regulates matrix configuration and cytochrome c release during apoptosis. Cell. Death. Differ. *10*, 709-717.

Grijalba,M.T., Andrade,P.B., Meinicke,A.R., Castilho,R.F., Vercesi,A.E., and Schreier,S. (1998). Inhibition of membrane lipid peroxidation by a radical scavenging mechanism: a novel function for hydroxyl-containing ionophores. Free. Radic. Res. *28*, 301-318.

Griparic,L., Kanazawa,T., and van der Bliek,A.M. (2007). Regulation of the mitochondrial dynamin-like protein Opa1 by proteolytic cleavage. J. Cell Biol *178*, 757-764.

Griparic,L., van der Wel,N.N., Orozco,I.J., Peters,P.J., and van der Bliek,A.M. (2004). Loss of the intermembrane space protein Mgm1/OPA1 induces swelling and localized constrictions along the lengths of mitochondria. J. Biol. Chem. *279*, 18792-18798.

Gross,A., Yin,X.M., Wang,K., Wei,M.C., Jockel,J., Milliman,C., Erdjument,B.H., Tempst,P., and Korsmeyer,S.J. (1999). Caspase cleaved BID targets mitochondria and is required for cytochrome c release, while BCL-XL prevents this release but not tumor necrosis factor-R1/Fas death. J. Biol. Chem. *274*, 1156-1163.

Guillery,O., Malka,F., Landes,T., Guillou,E., Blackstone,C., Lombes,A., Belenguer,P., Arnoult,D., and Rojo,M. (2007). Metalloprotease-mediated OPA1 processing is modulated by the mitochondrial membrane potential. Biol. Cell.

Hackenbrock,C.R. (1966). Ultrastructural bases for metabolically linked mechanical activity in mitochondria. I. Reversible ultrastructural changes with change in metabolic steady state in isolated liver mitochondria. J. Cell Biol. *30*, 269-297.

Hajek,P., Chomyn,A., and Attardi,G. (2007). Identification of a novel mitochondrial complex containing mitofusin 2 and stomatin-like protein 2. J. Biol. Chem. *282*, 5670-5681.

Hajek,P., Villani,G., and Attardi,G. (2001). Rate-limiting step preceding cytochrome c release in cells primed for Fas-mediated apoptosis revealed by analysis of cellular mosaicism of respiratory changes. J. Biol. Chem. *276*, 606-615.

Hales,K.G. and Fuller,M.T. (1997). Developmentally regulated mitochondrial fusion mediated by a conserved, novel, predicted GTPase. Cell *90*, 121-129.

Harder,Z., Zunino,R., and McBride,H. (2004). Sumo1 conjugates mitochondrial substrates and participates in mitochondrial fission. Curr. Biol. *14*, 340-345.

Hengartner,M.O. (2000). The biochemistry of apoptosis. Nature *407*, 770-776.

Herlan,M., Vogel,F., Bornhovd,C., Neupert,W., and Reichert,A.S. (2003). Processing of Mgm1 by the rhomboid-type protease Pcp1 is required for maintenance of mitochondrial morphology and of mitochondrial DNA. J. Biol. Chem. *278*, 27781-27788.

Hermann,G.J., Thatcher,J.W., Mills,J.P., Hales,K.G., Fuller,M.T., Nunnari,J., and Shaw,J.M. (1998). Mitochondrial fusion in yeast requires the transmembrane GTPase Fzo1p. J. Cell Biol. *143*, 359-373.

Hinshaw,J.E. (1999). Dynamin spirals. Curr. Opin. Struct. Biol *9*, 260-267.

Hitchcock,A.L., Auld,K., Gygi,S.P., and Silver,P.A. (2003). A subset of membrane-associated proteins is ubiquitinated in response to mutations in the endoplasmic reticulum degradation machinery. Proc. Natl. Acad. Sci. U. S. A. *100*, 12735-12740.

Hockenbery,D., Nunez,G., Milliman,C., Schreiber,R.D., and Korsmeyer,S.J. (1990). Bcl-2 is an inner mitochondrial membrane protein that blocks programmed cell death. Nature *348*, 334-336.

Hoffmann,B., Stockl,A., Schlame,M., Beyer,K., and Klingenberg,M. (1994). The reconstituted ADP/ATP carrier activity has an absolute requirement for cardiolipin as shown in cysteine mutants. J. Biol. Chem. *269*, 1940-1944.

Hudson,G., mati-Bonneau,P., Blakely,E.L., Stewart,J.D., He,L., Schaefer,A.M., Griffiths,P.G., Ahlqvist,K., Suomalainen,A., Reynier,P., McFarland,R., Turnbull,D.M., Chinnery,P.F., and Taylor,R.W. (2007). Mutation of OPA1 causes dominant optic atrophy with external ophthalmoplegia, ataxia, deafness and multiple mitochondrial DNA deletions: a novel disorder of mtDNA maintenance. Brain.

Huser,J., Rechenmacher,C.E., and Blatter,L.A. (1998). Imaging the permeability pore transition in single mitochondria. Biophys. J. *74*, 2129-2137.

Ishihara,N., Eura,Y., and Mihara,K. (2004). Mitofusin 1 and 2 play distinct roles in mitochondrial fusion reactions via GTPase activity. J. Cell Sci. *117*, 6535-6546.

Ishihara,N., Fujita,Y., Oka,T., and Mihara,K. (2006). Regulation of mitochondrial morphology through proteolytic cleavage of OPA1. EMBO J. *25*, 2966-2977.

Jacobs,E.E. and Sanadi,D.R. (1960). Reversible Removal of Cytochrome *c* from Mitochondria. J. Biol. Chem. *235*, 531-534.

Jagasia,R., Grote,P., Westermann,B., and Conradt,B. (2005). DRP-1-mediated mitochondrial fragmentation during EGL-1-induced cell death in C. elegans. Nature *433*, 754-760.

James,D.I., Parone,P.A., Mattenberger,Y., and Martinou,J.C. (2003). hFis1, a novel component of the mammalian mitochondrial fission machinery. J. Biol. Chem. *278*, 36373-36379.

John,G.B., Shang,Y., Li,L., Renken,C., Mannella,C.A., Selker,J.M., Rangell,L., Bennett,M.J., and Zha,J. (2005). The mitochondrial inner membrane protein mitofilin controls cristae morphology. Mol. Biol. Cell *16*, 1543-1554.

Jones,B.A. and Fangman,W.L. (1992). Mitochondrial DNA maintenance in yeast requires a protein containing a region related to the GTP-binding domain of dynamin. Genes. Dev. *6*, 380-389.

Ju,W.K., Misaka,T., Kushnareva,Y., Nakagomi,S., Agarwal,N., Kubo,Y., Lipton,S.A., and Bossy-Wetzel,E. (2005). OPA1 expression in the normal rat retina and optic nerve. J. Comp. Neurol. *488*, 1-10.

Jurgensmeier,J.M., Xie,Z., Deveraux,Q., Ellerby,L., Bredesen,D., and Reed,J.C. (1998). Bax directly induces release of cytochrome c from isolated mitochondria. Proc. Natl. Acad. Sci. U. S. A *95*, 4997-5002.

Kamei,S., Chen-Kuo-Chang,M., Cazevieille,C., Lenaers,G., Olichon,A., Belenguer,P., Roussignol,G., Renard,N., Eybalin,M., Michelin,A., Delettre,C., Brabet,P., and Hamel,C.P. (2005). Expression of the Opa1 mitochondrial protein in retinal ganglion cells: its downregulation causes aggregation of the mitochondrial network. Invest. Ophthalmol. Vis. Sci. *46*, 4288-4294.

Karbowski,M., Arnoult,D., Chen,H., Chan,D.C., Smith,C.L., and Youle,R.J. (2004a). Quantitation of mitochondrial dynamics by photolabeling of individual organelles shows that mitochondrial fusion is blocked during the Bax activation phase of apoptosis. J. Cell Biol. *164*, 493-499.

Karbowski,M., Jeong,S.Y., and Youle,R.J. (2004b). Endophilin B1 is required for the maintenance of mitochondrial morphology. J. Cell Biol. *166*, 1027-1039.

Karbowski,M., Lee,Y.J., Gaume,B., Jeong,S.Y., Frank,S., Nechushtan,A., Santel,A., Fuller,M., Smith,C.L., and Youle,R.J. (2002). Spatial and temporal association of Bax with mitochondrial fission sites, Drp1, and Mfn2 during apoptosis. J. Cell Biol. *159*, 931-938.

Karbowski,M., Norris,K.L., Cleland,M.M., Jeong,S.Y., and Youle,R.J. (2006). Role of Bax and Bak in mitochondrial morphogenesis. Nature *443*, 658-662.

Kay,B.K., Kasanov,J., Knight,S., and Kurakin,A. (2000). Convergent evolution with combinatorial peptides. FEBS Lett *480*.

Kerr,J.F., Cooksley,W.G., Searle,J., Halliday,J.W., Halliday,W.J., Holder,L., Roberts,I., Burnett,W., and Powell,L.W. (1979). The nature of piecemeal necrosis in chronic active hepatitis. Lancet *2*, 827-828.

Kerr,J.F., Wyllie,A.H., and Currie,A.R. (1972). Apoptosis: a basic biological phenomenon with wide-ranging implications in tissue kinetics. Br. J. Cancer. *26*, 239-257.

Kim,M.R., Jeong,E.G., Lee,J.W., and Lee,S.H. (2006). Absence of the BH3 domain mutation of proapoptotic Bcl-2 family gene BAD in serous and mucinous tumors of ovary. Gynecol. Oncol. *102*, 412-413.

Kim,P.K., Annis,M.G., Dlugosz,P.J., Leber,B., and Andrews,D.W. (2004). During apoptosis bcl-2 changes membrane topology at both the endoplasmic reticulum and mitochondria. Mol. Cell *14*, 523-529.

Kinnunen,P.K., Koiv,A., Lehtonen,J.Y., Rytomaa,M., and Mustonen,P. (1994). Lipid dynamics and peripheral interactions of proteins with membrane surfaces. Chem. Phys. Lipids. *73*, 181-207.

Kjer,P. (1959). Infantile optic atrophy with dominant mode of inheritance: a clinical and genetic study of 19 Danish families. Acta. Ophthalmol. Suppl. *164*, 1-147.

Klingenberg,M. (1973). The adenine nucleotide carrier in the mitochondrial membrane. Boll. Soc. Ital. Biol. Sper. *49*, 2pp.

Klingenberg,M. (1976). The state of ADP or ATP fixed to the mitochondria by bongkrekate. Eur. J. Biochem. *65*, 601-605.

Klingenberg,M. (1992). Structure-function of the ADP/ATP carrier. Biochem Soc Trans *20*.

Kluck,R.M., Esposti,M.D., Perkins,G., Renken,C., Kuwana,T., Bossy-Wetzel,E., Goldberg,M., Allen,T., Barber,M.J., Green,D.R., and Newmeyer,D.D. (1999). The pro-apoptotic proteins, Bid and Bax, cause a limited permeabilization of the mitochondrial outer membrane that is enhanced by cytosol. J. Cell Biol. *147*, 809-822.

Koshiba,T., Detmer,S.A., Kaiser,J.T., Chen,H., McCaffery,J.M., and Chan,D.C. (2004). Structural basis of mitochondrial tethering by mitofusin complexes. Science *305*, 858-862.

Kuwana,T., Mackey,M.R., Perkins,G., Ellisman,M.H., Latterich,M., Schneiter,R., Green,D.R., and Newmeyer,D.D. (2002). Bid, Bax, and lipids cooperate to form supramolecular openings in the outer mitochondrial membrane. Cell *111*, 331-342.

Labrousse,A.M., Zappaterra,M.D., Rube,D.A., and van der Bliek,A.M. (1999). C. elegans dynamin-related protein DRP-1 controls severing of the mitochondrial outer membrane. Mol. Cell *4*, 815-826.

Lee,Y.J., Jeong,S.Y., Karbowski,M., Smith,C.L., and Youle,R.J. (2004). Roles of the mammalian mitochondrial fission and fusion mediators Fis1, Drp1, and Opa1 in apoptosis. Mol. Biol. Cell *15*, 5001-5011.

Legros,F., Lombes,A., Frachon,P., and Rojo,M. (2002). Mitochondrial fusion in human cells is efficient, requires the inner membrane potential, and is mediated by mitofusins. Mol Biol Cell *13*, 4343-4354.

Letai,A., Bassik,M.C., Walensky,L.D., Sorcinelli,M.D., Weiler,S., and Korsmeyer,S.J. (2002). Distinct BH3 domains either sensitize or activate mitochondrial apoptosis, serving as prototype cancer therapeutics. Cancer Cell *2*, 183-192.

Li,L.Y., Luo,X., and Wang,X. (2001). Endonuclease G is an apoptotic DNase when released from mitochondria. Nature *412*, 95-99.

Lindsten,T., Ross,A.J., King,A., Zong,W.X., Rathmell,J.C., Shiels,H.A., Ulrich,E., Waymire,K.G., Mahar,P., Frauwirth,K., Chen,Y., Wei,M., Eng,V.M., Adelman,D.M., Simon,M.C., Ma,A., Golden,J.A., Evan,G., Korsmeyer,S.J., MacGregor,G.R., and Thompson,C.B. (2000). The combined functions of proapoptotic Bcl-2 family members bak and bax are essential for normal development of multiple tissues. Mol. Cell *6*, 1389-1399.

Liu,X., Kim,C.N., Yang,J., Jemmerson,R., and Wang,X. (1996). Induction of apoptotic program in cell-free extracts: requirement for dATP and cytochrome c. Cell *86*, 147-157.

Lockshin,R.A. and Williams,C.M. (1965). Programmed cell death. V. Cytolytic enzymes in relation to the breakdown of the intersegmental muscles of silkmoths. J. Insect Physiol *11*, 831-844.

Lodi,R., Tonon,C., Valentino,M.L., Iotti,S., Clementi,V., Malucelli,E., Barboni,P., Longanesi,L., Schimpf,S., Wissinger,B., Baruzzi,A., Barbiroli,B., and Carelli,V. (2004). Deficit of in vivo mitochondrial ATP production in OPA1-related dominant optic atrophy. Ann. Neurol. *56*, 719-723.

Luo,X., Budihardjo,I., Zou,H., Slaughter,C., and Wang,X. (1998). Bid, a Bcl2 interacting protein, mediates cytochrome c release from mitochondria in response to activation of cell surface death receptors. Cell *94*, 481-490.

Mannella,C.A., Marko,M., Penczek,P., Barnard,D., and Frank,J. (1994). The internal compartmentation of rat-liver mitochondria: tomographic study using the high-voltage transmission electron microscope. Microsc. Res. Tech. *27*, 278-283.

Mannella,C.A., Pfeiffer,D.R., Bradshaw,P.C., Moraru,I.I., Slepchenko,B., Loew,L.M., Hsieh,C.E., Buttle,K., and Marko,M. (2001). Topology of the mitochondrial inner membrane: dynamics and bioenergetic implications. IUBMB. Life *52*, 93-100.

Marchbank,N.J., Craig,J.E., Leek,J.P., Toohey,M., Churchill,A.J., Markham,A.F., Mackey,D.A., Toomes,C., and Inglehearn,C.F. (2002). Deletion of the OPA1 gene in a dominant optic atrophy family: evidence that haploinsufficiency is the cause of disease. J. Med. Genet. *39*, e47.

Martins,L.M., Morrison,A., Klupsch,K., Fedele,V., Moisoi,N., Teismann,P., Abuin,A., Grau,E., Geppert,M., Livi,G.P., Creasy,C.L., Martin,A., Hargreaves,I., Heales,S.J., Okada,H., Brandner,S., Schulz,J.B., Mak,T., and Downward,J. (2004). Neuroprotective role of the Reaper-related serine protease HtrA2/Omi revealed by targeted deletion in mice. Mol. Cell Biol. *24*, 9848-9862.

Marzo,I., Brenner,C., Zamzami,N., Jurgensmeier,J.M., Susin,S.A., Vieira,H.L., Prevost,M.C., Xie,Z., Matsuyama,S., Reed,J.C., and Kroemer,G. (1998). Bax and adenine nucleotide translocator cooperate in the mitochondrial control of apoptosis. Science *281*, 2027-2031.

mati-Bonneau,P., Valentino,M.L., Reynier,P., Gallardo,M.E., Bornstein,B., Boissiere,A., Campos,Y., Rivera,H., de la Aleja,J.G., Carroccia,R., Iommarini,L., Labauge,P., Figarella-Branger,D., Marcorelles,P., Furby,A., Beauvais,K., Letournel,F., Liguori,R., La,M.C., Montagna,P., Liguori,M., Zanna,C., Rugolo,M., Cossarizza,A., Wissinger,B., Verny,C., Schwarzenbacher,R., Martin,M.A., Arenas,J.I., Ayuso,C., Garesse,R., Lenaers,G., Bonneau,D., and Carelli,V. (2007). OPA1 mutations induce mitochondrial DNA instability and optic atrophy 'plus' phenotypes. Brain.

Mattenberger,Y., James,D.I., and Martinou,J.C. (2003). Fusion of mitochondria in mammalian cells is dependent on the mitochondrial inner membrane potential and independent of microtubules or actin. FEBS Lett. *538*, 53-59.

McQuibban,G.A., Saurya,S., and Freeman,M. (2003). Mitochondrial membrane remodelling regulated by a conserved rhomboid protease. Nature *423*, 537-541.

Meeusen,S., DeVay,R., Block,J., Cassidy-Stone,A., Wayson,S., McCaffery,J.M., and Nunnari,J. (2006). Mitochondrial inner-membrane fusion and crista maintenance requires the dynamin-related GTPase Mgm1. Cell *127*.

Meeusen,S., McCaffery,J.M., and Nunnari,J. (2004). Mitochondrial fusion intermediates revealed in vitro. Science *305*, 1747-1752.

Minauro-Sanmiguel,F., Wilkens,S., and Garcia,J.J. (2005). Structure of dimeric mitochondrial ATP synthase: novel F0 bridging features and the structural basis of mitochondrial cristae biogenesis. Proc. Natl. Acad. Sci. U. S. A. *102*, 12356-12358.

Misaka,T., Miyashita,T., and Kubo,Y. (2002). Primary structure of a dynamin-related mouse mitochondrial GTPase and its distribution in brain, subcellular localization, and effect on mitochondrial morphology. J. Biol. Chem. *277*, 15834-15842.

Mitchell,P. and Moyle,J. (1965). Stoichiometry of proton translocation through the respiratory chain and adenosine triphosphatase systems of rat liver mitochondria. Nature *208*, 147-151.

Mootha,V.K., Wei,M.C., Buttle,K.F., Scorrano,L., Panoutsakopoulou,V., Mannella,C.A., and Korsmeyer,S.J. (2001). A reversible component of mitochondrial respiratory dysfunction in apoptosis can be rescued by exogenous cytochrome c. EMBO J. *20*, 661-671.

Moraru, I. I. Role of cristae morphology in regulating mitochondrial adenine nucleotide and H^+ dynamics. Biophys.J. [78], 194A. 2000.
Ref Type: Abstract

Muchmore,S.W., Sattler,M., Liang,H., Meadows,R.P., Harlan,J.E., Yoon,H.S., Nettesheim,D., Chang,B.S., Thompson,C.B., Wong,S.L., Ng,S.L., and Fesik,S.W. (1996). X-ray and NMR structure of human Bcl-xL, an inhibitor of programmed cell death. Nature *381*, 335-341.

Myung,J.K., Gulesserian,T., Fountoulakis,M., and Lubec,G. (2003). Deranged hypothetical proteins Rik protein, Nit protein 2 and mitochondrial inner membrane protein, Mitofilin, in fetal Down syndrome brain. Cell. Mol. Biol. (Noisy. -le. -grand.) *49*, 739-746.

Nakamura,N., Kimura,Y., Tokuda,M., Honda,S., and Hirose,S. (2006). MARCH-V is a novel mitofusin 2- and Drp1-binding protein able to change mitochondrial morphology. EMBO Rep. *7*, 1019-1022.

Narita,M., Shimizu,S., Ito,T., Chittenden,T., Lutz,R.J., Matsuda,H., and Tsujimoto,Y. (1998). Bax interacts with the permeability transition pore to induce permeability transition and cytochrome c release in isolated mitochondria. Proc. Natl. Acad. Sci. U. S. A *95*, 14681-14686.

Neuspiel,M., Zunino,R., Gangaraju,S., Rippstein,P., and McBride,H.M. (2005). Activated Mfn2 signals mitochondrial fusion, interferes with Bax activation and reduces susceptibility to radical induced depolarization. J. Biol. Chem. *280*, 25060-25070.

Neutzner,A. and Youle,R.J. (2005). Instability of the mitofusin Fzo1 regulates mitochondrial morphology during the mating response of the yeast Saccharomyces cerevisiae. J Biol Chem *280*.

Oakley,M.G. and Hollenbeck,J.J. (2001). The design of antiparallel coiled coils. Curr. Opin. Struct. Biol. *11*, 450-457.

Olichon,A., Baricault,L., Gas,N., Guillou,E., Valette,A., Belenguer,P., and Lenaers,G. (2003). Loss of OPA1 perturbates the mitochondrial inner membrane structure and integrity, leading to cytochrome c release and apoptosis. J. Biol. Chem. *278*, 7743-7746.

Olichon,A., Emorine,L.J., Descoins,E., Pelloquin,L., Brichese,L., Gas,N., Guillou,E., Delettre,C., Valette,A., Hamel,C.P., Ducommun,B., Lenaers,G., and Belenguer,P. (2002). The human dynamin-related protein OPA1 is anchored to the mitochondrial inner membrane facing the inter-membrane space. FEBS Lett. *523*, 171-176.

Ott,M., Robertson,J.D., Gogvadze,V., Zhivotovsky,B., and Orrenius,S. (2002). Cytochrome c release from mitochondria proceeds by a two-step process. Proc. Natl. Acad. Sci. U. S. A *99*, 1259-1263.

Pacher,P. and Hajnoczky,G. (2001). Propagation of the apoptotic signal by mitochondrial waves. EMBO J. *20*, 4107-4121.

Palade,G.E. (1952). The fine structure of mitochondria. Anat. Rec. *114*, 427-451.

Parone,P.A., James,D.I., Da,C.S., Mattenberger,Y., Donze,O., Barja,F., and Martinou,J.C. (2006). Inhibiting the mitochondrial fission machinery does not prevent Bax/Bak-dependent apoptosis. Mol. Cell. Biol. *26*, 7397-7408.

Pastorino,J.G., Chen,S.T., Tafani,M., Snyder,J.W., and Farber,J.L. (1998). The overexpression of Bax produces cell death upon induction of the mitochondrial permeability transition. J. Biol. Chem. *273*, 7770-7775.

Paumard,P., Vaillier,J., Coulary,B., Schaeffer,J., Soubannier,V., Mueller,D.M., Brethes,D., di Rago,J.P., and Velours,J. (2002). The ATP synthase is involved in generating mitochondrial cristae morphology. EMBO J. *21*, 221-230.

Pavlov,E.V., Priault,M., Pietkiewicz,D., Cheng,E.H., Antonsson,B., Manon,S., Korsmeyer,S.J., Mannella,C.A., and Kinnally,K.W. (2001). A novel, high conductance channel of mitochondria linked to apoptosis in mammalian cells and Bax expression in yeast. J. Cell Biol. *155*, 725-731.

Pelloquin,L., Belenguer,P., Menon,Y., Gas,N., and Ducommun,B. (1999). Fission yeast Msp1 is a mitochondrial dynamin-related protein. J. Cell Sci. *112*.

Perotti,M.E., Anderson,W.A., and Swift,H. (1983). Quantitative cytochemistry of the diaminobenzidine cytochrome oxidase reaction product in mitochondria of cardiac muscle and pancreas. J. Histochem. Cytochem. *31*, 351-365.

Pesch,U.E., Fries,J.E., Bette,S., Kalbacher,H., Wissinger,B., Alexander,C., and Kohler,K. (2004). OPA1, the disease gene for autosomal dominant optic atrophy, is specifically expressed in ganglion cells and intrinsic neurons of the retina. Invest. Ophthalmol. Vis. Sci. *45*, 4217-4225.

Pesch,U.E., Leo-Kottler,B., Mayer,S., Jurklies,B., Kellner,U., Apfelstedt-Sylla,E., Zrenner,E., Alexander,C., and Wissinger,B. (2001). OPA1 mutations in patients with autosomal dominant optic atrophy and evidence for semi-dominant inheritance. Hum. Mol Genet. *10*, 1359-1368.

Petronilli,V., Miotto,G., Canton,M., Colonna,R., Bernardi,P., and Di Lisa,F. (1999). Transient and long-lasting openings of the mitochondrial permeability transition pore can be monitored directly in intact cells by changes of mitochondrial calcein fluorescence. Biophys. J. *76*, 725-734.

Petrosillo,G., Ruggiero,F.M., and Paradies,G. (2003). Role of reactive oxygen species and cardiolipin in the release of cytochrome c from mitochondria. FASEB. J. *17*, 2202-2208.

Petrosillo,G., Ruggiero,F.M., Pistolese,M., and Paradies,G. (2004). Ca2+-induced reactive oxygen species production promotes cytochrome c release from rat liver mitochondria via mitochondrial permeability transition (MPT)-dependent and MPT-independent mechanisms: role of cardiolipin. J. Biol. Chem. *279*, 53103-53108.

Pfohler,C., Preuss,K.D., Tilgen,W., Stark,A., Regitz,E., Fadle,N., and Pfreundschuh,M. (2007). Mitofilin and titin as target antigens in melanoma-associated retinopathy. Int. J. Cancer. *120*, 788-795.

Praefcke,G.J. and McMahon,H.T. (2004). The dynamin superfamily: universal membrane tubulation and fission molecules? Nat Rev Mol Cell Biol *5*, 133-147.

Rak,M., Tetaud,E., Godard,F., Sagot,I., Salin,B., Duvezin-Caubet,S., Slonimski,P.P., Rytka,J., and di Rago,J.P. (2007). Yeast cells lacking the mitochondrial gene encoding the ATP synthase subunit 6 exhibit a selective loss of complex IV and unusual mitochondrial morphology. J. Biol. Chem. *282*, 10853-10864.

Rojo,M., Legros,F., Chateau,D., and Lombes,A. (2002). Membrane topology and mitochondrial targeting of mitofusins, ubiquitous mammalian homologs of the transmembrane GTPase Fzo. J. Cell Sci. *115*, 1663-1674.

Roucou,X., Montessuit,S., Antonsson,B., and Martinou,J.C. (2002). Bax oligomerization in mitochondrial membranes requires tBid (caspase-8-cleaved Bid) and a mitochondrial protein. Biochem. J. *368*, 915-921.

Rytomaa,M. and Kinnunen,P.K. (1995). Reversibility of the binding of cytochrome c to liposomes. Implications for lipid-protein interactions. J. Biol. Chem. *270*, 3197-3202.

Saito,M., Korsmeyer,S.J., and Schlesinger,P.H. (2000). BAX-dependent transport of cytochrome c reconstituted in pure liposomes. Nat. Cell Biol. *2*, 553-555.

Santel,A., Frank,S., Gaume,B., Herrler,M., Youle,R.J., and Fuller,M.T. (2003). Mitofusin-1 protein is a generally expressed mediator of mitochondrial fusion in mammalian cells. J. Cell Sci. *116*, 2763-2774.

Santel,A. and Fuller,M.T. (2001). Control of mitochondrial morphology by a human mitofusin. J. Cell Sci. *114*, 867-874.

Satoh,M., Hamamoto,T., Seo,N., Kagawa,Y., and Endo,H. (2003). Differential sublocalization of the dynamin-related protein OPA1 isoforms in mitochondria. Biochem. Biophys. Res. Commun. *300*, 482-493.

Schatz,G. (2007). The magic garden. Annu. Rev. Biochem. *76*, 673-678.

Schlame,M., Brody,S., and Hostetler,K.Y. (1993). Mitochondrial cardiolipin in diverse eukaryotes. Comparison of biosynthetic reactions and molecular acyl species. Eur. J. Biochem. *212*, 727-735.

Schmidt,A., Wolde,M., Thiele,C., Fest,W., Kratzin,H., Podtelejnikov,A.V., Witke,W., Huttner,W.B., and Soling,H.D. (1999). Endophilin I mediates synaptic vesicle formation by transfer of arachidonate to lysophosphatidic acid. Nature *401*, 133-141.

Scorrano,L., Ashiya,M., Buttle,K., Weiler,S., Oakes,S.A., Mannella,C.A., and Korsmeyer,S.J. (2002). A Distinct Pathway Remodels Mitochondrial Cristae and Mobilizes Cytochrome c during Apoptosis. Dev. Cell *2*, 55-67.

Scorrano,L. and Korsmeyer,S.J. (2003). Mechanisms of cytochrome c release by proapoptotic BCL-2 family members. Biochemical and Biophysical Research Communications *304*, 437-444.

Sesaki,H., Southard,S.M., Yaffe,M.P., and Jensen,R.E. (2003). Mgm1p, a dynamin-related GTPase, is essential for fusion of the mitochondrial outer membrane. Mol. Biol. Cell *14*, 2342-2356.

Shidoji,Y., Komura,S., Ohishi,N., and Yagi,K. (2002). Interaction between cytochrome c and oxidized mitochondrial lipids. Subcell. Biochem. *36*, 19-37.

Shimizu,S., Narita,M., and Tsujimoto,Y. (1999). Bcl-2 family proteins regulate the release of apoptogenic cytochrome c by the mitochondrial channel VDAC. Nature *399*, 483-487.

Smirnova,E., Griparic,L., Shurland,D.L., and van der Bliek,A.M. (2001). Dynamin-related protein Drp1 is required for mitochondrial division in mammalian cells. Mol. Biol. Cell *12*, 2245-2256.

Song,Z., Chen,H., Fiket,M., Alexander,C., and Chan,D.C. (2007). OPA1 processing controls mitochondrial fusion and is regulated by mRNA splicing, membrane potential, and Yme1L. J. Cell Biol *178*, 749-755.

Stojanovski,D., Koutsopoulos,O.S., Okamoto,K., and Ryan,M.T. (2004). Levels of human Fis1 at the mitochondrial outer membrane regulate mitochondrial morphology. J. Cell Sci. *117*, 1201-1210.

Sugioka,R., Shimizu,S., and Tsujimoto,Y. (2004). Fzo1, a protein involved in mitochondrial fusion, inhibits apoptosis. J. Biol. Chem. *279*, 52726-52734.

Sun,M.G., Williams,J., Munoz-Pinedo,C., Perkins,G.A., Brown,J.M., Ellisman,M.H., Green,D.R., and Frey,T.G. (2007). Correlated three-dimensional light and electron microscopy reveals transformation of mitochondria during apoptosis. Nat. Cell Biol. *9*, 1057-1065.

Susin,S.A., Lorenzo,H.K., Zamzami,N., Marzo,I., Snow,B.E., Brothers,G.M., Mangion,J., Jacotot,E., Costantini,P., Loeffler,M., Larochette,N., Goodlett,D.R., Aebersold,R.,

Siderovski,D.P., Penninger,J.M., and Kroemer,G. (1999). Molecular characterization of mitochondrial apoptosis-inducing factor. Nature *397*, 441-446.

Suzuki,M., Jeong,S.Y., Karbowski,M., Youle,R.J., and Tjandra,N. (2003). The solution structure of human mitochondria fission protein Fis1 reveals a novel TPR-like helix bundle. J. Mol. Biol. *334*, 445-458.

Suzuki,M., Youle,R.J., and Tjandra,N. (2000). Structure of Bax: coregulation of dimer formation and intracellular localization. Cell *103*, 645-654.

Szabadkai,G., Simoni,A.M., Chami,M., Wieckowski,M.R., Youle,R.J., and Rizzuto,R. (2004). Drp-1-dependent division of the mitochondrial network blocks intraorganellar Ca^{2+} waves and protects against Ca^{2+}-mediated apoptosis. Mol Cell *16*, 59-68.

Taguchi,N., Ishihara,N., Jofuku,A., Oka,T., and Mihara,K. (2007). Mitotic phosphorylation of dynamin-related GTPase Drp1 participates in mitochondrial fission. J. Biol. Chem. *282*, 11521-11529.

Thornberry,N.A. and Lazebnik,Y. (1998). Caspases: enemies within. Science *281*, 1312-1316.

Tondera,D., Czauderna,F., Paulick,K., Schwarzer,R., Kaufmann,J., and Santel,A. (2005). The mitochondrial protein MTP18 contributes to mitochondrial fission in mammalian cells. J Cell Sci *118*.

Tondera,D., Santel,A., Schwarzer,R., Dames,S., Giese,K., Klippel,A., and Kaufmann,J. (2004). Knockdown of MTP18, a novel phosphatidylinositol 3-kinase-dependent protein, affects mitochondrial morphology and induces apoptosis. J Biol Chem *279*.

Tuominen,E.K., Wallace,C.J., and Kinnunen,P.K. (2002). Phospholipid-cytochrome c interaction: evidence for the extended lipid anchorage. J. Biol. Chem. *277*, 8822-8826.

van,L.G., van,G.M., Depuydt,B., Srinivasula,S.M., Rodriguez,I., Alnemri,E.S., Gevaert,K., Vandekerckhove,J., Declercq,W., and Vandenabeele,P. (2002). The serine protease Omi/HtrA2 is released from mitochondria during apoptosis. Omi interacts with caspase-inhibitor XIAP and induces enhanced caspase activity. Cell. Death. Differ. *9*, 20-26.

Verhagen,A.M., Ekert,P.G., Pakusch,M., Silke,J., Connolly,L.M., Reid,G.E., Moritz,R.L., Simpson,R.J., and Vaux,D.L. (2000). Identification of DIABLO, a mammalian protein that promotes apoptosis by binding to and antagonizing IAP proteins. Cell. *102*, 43-53.

Vogel,F., Bornhovd,C., Neupert,W., and Reichert,A.S. (2006). Dynamic subcompartmentalization of the mitochondrial inner membrane. J. Cell Biol. *175*, 237-247.

Votruba,M., Aijaz,S., and Moore,A.T. (2003). A review of primary hereditary optic neuropathies. J. Inherit. Metab. Dis. *26*, 209-227.

Walensky,L.D., Pitter,K., Morash,J., Oh,K.J., Barbuto,S., Fisher,J., Smith,E., Verdine,G.L., and Korsmeyer,S.J. (2006). A stapled BID BH3 helix directly binds and activates BAX. Mol. Cell. *24*, 199-210.

Wang,J., Rosconi,M.P., and London,E. (2006a). Topography of the hydrophilic helices of membrane-inserted diphtheria toxin T domain: TH1-TH3 as a hydrophilic tether. Biochemistry *45*, 8124-8134.

Wang,J., Rosconi,M.P., and London,E. (2006b). Topography of the hydrophilic helices of membrane-inserted diphtheria toxin T domain: TH1-TH3 as a hydrophilic tether. Biochemistry *45*, 8124-8134.

Wang,L., Dong,J., Cull,G., Fortune,B., and Cioffi,G.A. (2003). Varicosities of intraretinal ganglion cell axons in human and nonhuman primates. Invest. Ophthalmol. Vis. Sci. *44*, 2-9.

Wei,M.C., Lindsten,T., Mootha,V.K., Weiler,S., Gross,A., Ashiya,M., Thompson,C.B., and Korsmeyer,S.J. (2000). tBID, a membrane-targeted death ligand, oligomerizes BAK to release cytochrome c. Genes Dev. *14*, 2060-2071.

Wei,M.C., Zong,W.X., Cheng,E.H., Lindsten,T., Panoutsakopoulou,V., Ross,A.J., Roth,K.A., MacGregor,G.R., Thompson,C.B., and Korsmeyer,S.J. (2001). Proapoptotic BAX and BAK: a requisite gateway to mitochondrial dysfunction and death. Science *292*, 727-730.

Wells,R.C., Picton,L.K., Williams,S.C., Tan,F.J., and Hill,R.B. (2007). Direct binding of the dynamin-like GTPase, Dnm1, to mitochondrial dynamics protein Fis1 is negatively regulated by the Fis1 N-terminal arm. J. Biol. Chem. *282*, 33769-33775.

Wojtczak,L., Zaluska,H., Wroniszewska,A., and Wojtczak,A.B. (1972). Assay for the intactness of the outer membrane in isolated mitochondria. Acta. Biochim. Pol. *19*, 227-234.

Wong,E.D., Wagner,J.A., Gorsich,S.W., McCaffery,J.M., Shaw,J.M., and Nunnari,J. (2000). The dynamin-related GTPase, Mgm1p, is an intermembrane space protein required for maintenance of fusion competent mitochondria. J. Cell Biol. *151*, 341-352.

Wong,E.D., Wagner,J.A., Scott,S.V., Okreglak,V., Holewinske,T.J., Cassidy-Stone,A., and Nunnari,J. (2003). The intramitochondrial dynamin-related GTPase, Mgm1p, is a component of a protein complex that mediates mitochondrial fusion. J. Cell Biol. *160*, 303-311.

Xie,J., Marusich,M.F., Souda,P., Whitelegge,J., and Capaldi,R.A. (2007). The mitochondrial inner membrane protein mitofilin exists as a complex with SAM50, metaxins 1 and 2, coiled-coil-helix coiled-coil-helix domain-containing protein 3 and 6 and DnaJC11. FEBS. Lett. *581*, 3545-3549.

Yoon,Y., Krueger,E.W., Oswald,B.J., and McNiven,M.A. (2003). The mitochondrial protein hFis1 regulates mitochondrial fission in mammalian cells through an interaction with the dynamin-like protein DLP1. Mol. Cell Biol. *23*, 5409-5420.

Youle,R.J. and Karbowski,M. (2005). Mitochondrial fission in apoptosis. Nat Rev Mol Cell Biol *6*, 657-663.

Zha,J., Weiler,S., Oh,K.J., Wei,M.C., and Korsmeyer,S.J. (2000). Posttranslational N-myristoylation of BID as a molecular switch for targeting mitochondria and apoptosis. Science *290*, 1761-1765.

Zhang,M., Mileykovskaya,E., and Dowhan,W. (2002). Gluing the respiratory chain together. Cardiolipin is required for supercomplex formation in the inner mitochondrial membrane. J. Biol. Chem. *277*, 43553-43556.

Zhang,Y. and Chan,D.C. (2007). Structural basis for recruitment of mitochondrial fission complexes by Fis1. Proc. Natl. Acad. Sci. U. S. A. *104*, 18526-18530.

Zhivotovsky,B., Orrenius,S., Brustugun,O.T., and Doskeland,S.O. (1998). Injected cytochrome c induces apoptosis. Nature *391*, 449-450.

Zhu,P.P., Patterson,A., Stadler,J., Seeburg,D.P., Sheng,M., and Blackstone,C. (2004). Intra- and intermolecular domain interactions of the C-terminal GTPase effector domain of the multimeric dynamin-like GTPase Drp1. J. Biol. Chem. *279*, 35967-35974.

Zoratti,M. and Szabo,I. (1995). The mitochondrial permeability transition. Biochim. Biophys. Acta *1241*, 139-176.

Zou,H., Henzel,W.J., Liu,X., Lutschg,A., and Wang,X. (1997). Apaf-1, a human protein homologous to C. elegans CED-4, participates in cytochrome c-dependent activation of caspase-3. Cell *90*, 405-413.

Zunino,R., Schauss,A., Rippstein,P., ndrade-Navarro,M., and McBride,H.M. (2007). The SUMO protease SENP5 is required to maintain mitochondrial morphology and function. J. Cell. Sci. *120*, 1178-1188.

Adams,J.M. and Cory,S. (2007). Bcl-2-regulated apoptosis: mechanism and therapeutic potential. Curr. Opin. Immunol. *19*, 488-496.
Aijaz,S., Erskine,L., Jeffery,G., Bhattacharya,S.S., and Votruba,M. (2004). Developmental expression profile of the optic atrophy gene product: OPA1 is not localized exclusively in the mammalian retinal ganglion cell layer. Invest. Ophthalmol. Vis. Sci. *45*, 1667-1673.

Alavi,M.V., Bette,S., Schimpf,S., Schuettauf,F., Schraermeyer,U., Wehrl,H.F., Ruttiger,L., Beck,S.C., Tonagel,F., Pichler,B.J., Knipper,M., Peters,T., Laufs,J., and Wissinger,B. (2007). A splice site mutation in the murine Opa1 gene features pathology of autosomal dominant optic atrophy. Brain *130*, 1029-1042.

Alexander,C., Votruba,M., Pesch,U.E., Thiselton,D.L., Mayer,S., Moore,A., Rodriguez,M., Kellner,U., Leo-Kottler,B., Auburger,G., Bhattacharya,S.S., and Wissinger,B. (2000). OPA1, encoding a dynamin-related GTPase, is mutated in autosomal dominant optic atrophy linked to chromosome 3q28. Nat. Genet. *26*, 211-215.

Alirol,E., James,D., Huber,D., Marchetto,A., Vergani,L., Martinou,J.C., and Scorrano,L. (2006). The mitochondrial fission protein hFis1 requires the endoplasmic reticulum gateway to induce apoptosis. Mol. Biol. Cell *17*, 4593-4605.

Allen,R.D., Schroeder,C.C., and Fok,A.K. (1989). An investigation of mitochondrial inner membranes by rapid-freeze deep-etch techniques. J. Cell. Biol. *108*, 2233-2240.

Amati-Bonneau,P., Guichet,A., Olichon,A., Chevrollier,A., Viala,F., Miot,S., Ayuso,C., Odent,S., Arrouet,C., Verny,C., Calmels,M.N., Simard,G., Belenguer,P., Wang,J., Puel,J.L., Hamel,C., Malthiery,Y., Bonneau,D., Lenaers,G., and Reynier,P. (2005). OPA1 R445H mutation in optic atrophy associated with sensorineural deafness. Ann. Neurol. *58*, 958-963.

Amati-Bonneau,P., Valentino,M.L., Reynier,P., Gallardo,M.E., Bornstein,B., Boissiere,A., Campos,Y., Rivera,H., de la Aleja,J.G., Carroccia,R., Iommarini,L., Labauge,P., Figarella-Branger,D., Marcorelles,P., Furby,A., Beauvais,K., Letournel,F., Liguori,R., La,M.C., Montagna,P., Liguori,M., Zanna,C., Rugolo,M., Cossarizza,A., Wissinger,B., Verny,C., Schwarzenbacher,R., Martin,M.A., Arenas,J.I., Ayuso,C., Garesse,R., Lenaers,G., Bonneau,D., and Carelli,V. (2007). OPA1 mutations induce mitochondrial DNA instability and optic atrophy 'plus' phenotypes. Brain.

Andrews,R.M., Griffiths,P.G., Johnson,M.A., and Turnbull,D.M. (1999). Histochemical localisation of mitochondrial enzyme activity in human optic nerve and retina. Br. J. Ophthalmol. *83*, 231-235.

Annis,M.G., Soucie,E.L., Dlugosz,P.J., Cruz-Aguado,J.A., Penn,L.Z., Leber,B., and Andrews,D.W. (2005). Bax forms multispanning monomers that oligomerize to permeabilize membranes during apoptosis. EMBO J. *24*, 2096-2103.

Antignani,A. and Youle,R.J. (2006). How do Bax and Bak lead to permeabilization of the outer mitochondrial membrane? Curr. Opin. Cell Biol. *18*, 685-689.

Arnoult,D., Grodet,A., Lee,Y.J., Estaquier,J., and Blackstone,C. (2005). Release of OPA1 during apoptosis participates in the rapid and complete release of cytochrome c and subsequent mitochondrial fragmentation. J. Biol. Chem. *280*, 35742-35750.

Bach,D., Naon,D., Pich,S., Soriano,F.X., Vega,N., Rieusset,J., Laville,M., Guillet,C., Boirie,Y., Wallberg-Henriksson,H., Manco,M., Calvani,M., Castagneto,M., Palacin,M., Mingrone,G., Zierath,J.R., Vidal,H., and Zorzano,A. (2005). Expression of Mfn2, the Charcot-Marie-Tooth neuropathy type 2A gene, in human skeletal muscle: effects of type 2 diabetes, obesity, weight loss, and the regulatory role of tumor necrosis factor alpha and interleukin-6. Diabetes *54*, 2685-2693.

Bach,D., Pich,S., Soriano,F.X., Vega,N., Baumgartner,B., Oriola,J., Daugaard,J.R., Lloberas,J., Camps,M., Zierath,J.R., Rabasa-Lhoret,R., Wallberg-Henriksson,H., Laville,M., Palacin,M., Vidal,H., Rivera,F., Brand,M., and Zorzano,A. (2003). Mitofusin-2 determines mitochondrial network architecture and mitochondrial metabolism. A novel regulatory mechanism altered in obesity. J. Biol. Chem. *278*, 17190-17197.

Bakeeva,L.E., Chentsov,Y., and Skulachev,V.P. (1978). Mitochondrial framework (reticulum mitochondriale) in rat diaphragm muscle. Biochim. Biophys. Acta *501*, 349-369.

Baricault,L., Segui,B., Guegand,L., Olichon,A., Valette,A., Larminat,F., and Lenaers,G. (2007). OPA1 cleavage depends on decreased mitochondrial ATP level and bivalent metals. Exp. Cell. Res. *313*, 3800-3808.

Bayir,H., Fadeel,B., Palladino,M.J., Witasp,E., Kurnikov,I.V., Tyurina,Y.Y., Tyurin,V.A., Amoscato,A.A., Jiang,J., Kochanek,P.M., DeKosky,S.T., Greenberger,J.S., Shvedova,A.A., and Kagan,V.E. (2006). Apoptotic interactions of cytochrome c: redox flirting with anionic phospholipids within and outside of mitochondria. Biochim. Biophys. Acta. *1757*, 648-659.

Bereiter-Hahn,J. and Voth,M. (1994). Dynamics of mitochondria in living cells: shape changes, dislocations, fusion, and fission of mitochondria. Microsc. Res. Tech. *27*, 198-219.

Bernardi,P. (1999). Mitochondrial transport of cations: Channels, exchangers and permeability transition. Physiol. Rev. *79*, 1127-1155.

Bernardi,P. and Azzone,G.F. (1981). Cytochrome c as an electron shuttle between the outer and inner mitochondrial membranes. J. Biol. Chem. *256*, 7187-7192.

Bernardi,P., Krauskopf,A., Basso,E., Petronilli,V., Blachly-Dyson,E., Di,L.F., and Forte,M.A. (2006). The mitochondrial permeability transition from in vitro artifact to disease target. FEBS J. *273*, 2077-2099.

Bristow,E.A., Griffiths,P.G., Andrews,R.M., Johnson,M.A., and Turnbull,D.M. (2002). The distribution of mitochondrial activity in relation to optic nerve structure. Arch. Ophthalmol. *120*, 791-796.

Buono,L.M., Foroozan,R., Sergott,R.C., and Savino,P.J. (2002). Is normal tension glaucoma actually an unrecognized hereditary optic neuropathy? New evidence from genetic analysis. Curr. Opin. Ophthalmol. *13*, 362-370.

Carelli,V., Ross-Cisneros,F.N., and Sadun,A.A. (2004). Mitochondrial dysfunction as a cause of optic neuropathies. Prog. Retin. Eye. Res. *23*, 53-89.

Celotto,A.M., Frank,A.C., Seigle,J.L., and Palladino,M.J. (2006). Drosophila model of human inherited triosephosphate isomerase deficiency glycolytic enzymopathy. Genetics. *174*, 1237-1246.

Cereghetti,G.M. and Scorrano,L. (2006). The many shapes of mitochondrial death. Oncogene *25*, 4717-4724.

Chang,C.R. and Blackstone,C. (2007). Drp1 phosphorylation and mitochondrial regulation. EMBO. Rep. *8*, 1088-1089.

Chen,H., Chomyn,A., and Chan,D.C. (2005). Disruption of fusion results in mitochondrial heterogeneity and dysfunction. J Biol Chem. *280*, 26185-26192.

Chen,H., Detmer,S.A., Ewald,A.J., Griffin,E.E., Fraser,S.E., and Chan,D.C. (2003). Mitofusins Mfn1 and Mfn2 coordinately regulate mitochondrial fusion and are essential for embryonic development. J. Cell Biol. *160*, 189-200.

Chen,K.H., Guo,X., Ma,D., Guo,Y., Li,Q., Yang,D., Li,P., Qiu,X., Wen,S., Xiao,R.P., and Tang,J. (2004). Dysregulation of HSG triggers vascular proliferative disorders. Nat. Cell Biol. *6*, 872-883.

Chipuk,J.E., Bouchier-Hayes,L., and Green,D.R. (2006). Mitochondrial outer membrane permeabilization during apoptosis: the innocent bystander scenario. Cell Death. Differ. *13*, 1396-1402.

Choi,S.Y., Gonzalvez,F., Jenkins,G.M., Slomianny,C., Chretien,D., Arnoult,D., Petit,P.X., and Frohman,M.A. (2007). Cardiolipin deficiency releases cytochrome c from the inner mitochondrial membrane and accelerates stimuli-elicited apoptosis. Cell. Death. Differ. *14*, 597-606.

Choi,S.Y., Huang,P., Jenkins,G.M., Chan,D.C., Schiller,J., and Frohman,M.A. (2006). A common lipid links Mfn-mediated mitochondrial fusion and SNARE-regulated exocytosis. Nat. Cell Biol. *8*, 1255-1262.

Cipolat,S., de Brito,O.M., Dal Zilio,B., and Scorrano,L. (2004). OPA1 requires mitofusin 1 to promote mitochondrial fusion. Proc. Natl. Acad. Sci. U. S. A *101*, 15927-15932.

Clipstone,N.A. and Crabtree,G.R. (1992). Identification of calcineurin as a key signalling enzyme in T-lymphocyte activation. Nature *357*, 695-697.

Cohn,A.C., Toomes,C., Potter,C., Towns,K.V., Hewitt,A.W., Inglehearn,C.F., Craig,J.E., and Mackey,D.A. (2007). Autosomal dominant optic atrophy: penetrance and expressivity in patients with OPA1 mutations. Am. J. Ophthalmol. *143*, 656-662.

Cortese,J.D., Voglino,A.L., and Hackenbrock,C.R. (1998). Multiple conformations of physiological membrane-bound cytochrome c. Biochemistry. *37*, 6402-6409.

Cortopassi,G.A. and Wong,A. (1999). Mitochondria in organismal aging and degeneration. Biochem. Biophys. Acta. *1410*.

Cribbs,J.T. and Strack,S. (2007). Reversible phosphorylation of Drp1 by cyclic AMP-dependent protein kinase and calcineurin regulates mitochondrial fission and cell death. EMBO. Rep. *8*, 939-944.

D'Herde,K., De Prest,B., Mussche,S., Schotte,P., Beyaert,R., Coster,R.V., and Roels,F. (2001). Ultrastructural localization of cytochrome c in apoptosis demonstrates mitochondrial heterogeneity. Cell Death. Differ. *7*, 331-337.

Danial,N.N. and Korsmeyer,S.J. (2004). Cell death: critical control points. Cell *116*, 205-219.

Davies,V.J., Hollins,A.J., Piechota,M.J., Yip,W., Davies,J.R., White,K.E., Nicols,P.P., Boulton,M.E., and Votruba,M. (2007). Opa1 deficiency in a mouse model of autosomal

dominant optic atrophy impairs mitochondrial morphology, optic nerve structure and visual function. Hum Mol Genet *16*, 1307-1318.

Dejean,L.M., Martinez-Caballero,S., and Kinnally,K.W. (2006). Is MAC the knife that cuts cytochrome c from mitochondria during apoptosis? Cell Death. Differ. *13*, 1387-1395.

Delettre,C., Griffoin,J.M., Kaplan,J., Dollfus,H., Lorenz,B., Faivre,L., Lenaers,G., Belenguer,P., and Hamel,C.P. (2001). Mutation spectrum and splicing variants in the OPA1 gene. Hum. Genet. *109*, 584-591.

Delettre,C., Lenaers,G., Griffoin,J.M., Gigarel,N., Lorenzo,C., Belenguer,P., Pelloquin,L., Grosgeorge,J., Turc-Carel,C., Perret,E., Astarie-Dequeker,C., Lasquellec,L., Arnaud,B., Ducommun,B., Kaplan,J., and Hamel,C.P. (2000). Nuclear gene OPA1, encoding a mitochondrial dynamin-related protein, is mutated in dominant optic atrophy. Nat. Genet. *26*, 207-210.

Delettre,C., Lenaers,G., Pelloquin,L., Belenguer,P., and Hamel,C.P. (2002). OPA1 (Kjer type) dominant optic atrophy: a novel mitochondrial disease. Mol. Genet. Metab. *75*, 97-107.

Deveraux,Q.L., Roy,N., Stennicke,H.R., Van Arsdale,T., Zhou,Q., Srinivasula,S.M., Alnemri,E.S., Salvesen,G.S., and Reed,J.C. (1998). IAPs block apoptotic events induced by caspase-8 and cytochrome c by direct inhibition of distinct caspases. EMBO J. *17*, 2215-2223.

Di,B.A. and Gill,G. (2006). SUMO-specific proteases and the cell cycle. An essential role for SENP5 in cell proliferation. Cell. Cycle. *5*, 2310-2313.

Dimmer,K.S. and Scorrano,L. (2006). (De)constructing mitochondria: what for? Physiology. (Bethesda.) *21*, 233-241.

Du,C., Fang,M., Li,Y., Li,L., and Wang,X. (2000). Smac, a mitochondrial protein that promotes cytochrome c-dependent caspase activation by eliminating IAP inhibition. Cell *102*, 33-42.

Dudkina,N.V., Heinemeyer,J., Keegstra,W., Boekema,E.J., and Braun,H.P. (2005). Structure of dimeric ATP synthase from mitochondria: an angular association of monomers induces the strong curvature of the inner membrane. FEBS. Lett. *579*, 5769-5772.

Durr,M., Escobar-Henriques,M., Merz,S., Geimer,S., Langer,T., and Westermann,B. (2006). Nonredundant roles of mitochondria-associated F-box proteins Mfb1 and Mdm30 in maintenance of mitochondrial morphology in yeast. Mol. Biol. Cell. *17*, 3745-3755.

Duvezin-Caubet,S., Jagasia,R., Wagener,J., Hofmann,S., Trifunovic,A., Hansson,A., Chomyn,A., Bauer,M.F., Attardi,G., Larsson,N.G., Neupert,W., and Reichert,A.S. (2006). Proteolytic processing of OPA1 links mitochondrial dysfunction to alterations in mitochondrial morphology. J. Biol. Chem.

Duvezin-Caubet,S., Koppen,M., Wagener,J., Zick,M., Israel,L., Bernacchia,A., Jagasia,R., Rugarli,E.I., Imhof,A., Neupert,W., Langer,T., and Reichert,A.S. (2007). OPA1 processing reconstituted in yeast depends on the subunit composition of the m-AAA protease in mitochondria. Mol. Biol. Cell. *18*, 3582-3590.

Epand,R.F., Martinou,J.C., Fornallaz-Mulhauser,M., Hughes,D.W., and Epand,R.M. (2002). The apoptotic protein tBid promotes leakage by altering membrane curvature. J. Biol. Chem. *277*, 32632-32639.

Escobar-Henriques,M., Westermann,B., and Langer,T. (2006). Regulation of mitochondrial fusion by the F-box protein Mdm30 involves proteasome-independent turnover of Fzo1. J. Cell. Biol. *173*, 645-650.

Eskes,R., Antonsson,B., Osen-Sand A., Montessuit,S., Richter,C., Sadoul,R., Mazzei,G., Nichols,A., and Martinou,J.-C. (1998). Bax-induced cytochrome c release from mitochondria is independent of the permeability transition pore but highly dependent on Mg^{2+} ions. J. Cell Biol. *143*, 217-224.

Esposti,M.D., Erler,J.T., Hickman,J.A., and Dive,C. (2001). Bid, a widely expressed proapoptotic protein of the Bcl-2 family, displays lipid transfer activity. Mol. Cell Biol. *21*, 7268-7276.

Estaquier,J. and Arnoult,D. (2007). Inhibiting Drp1-mediated mitochondrial fission selectively prevents the release of cytochrome c during apoptosis. Cell. Death. Differ. *14*, 1086-1094.

Eura,Y., Ishihara,N., Oka,T., and Mihara,K. (2006). Identification of a novel protein that regulates mitochondrial fusion by modulating mitofusin (Mfn) protein function. J. Cell. Sci. *119*, 4913-4925.

Eura,Y., Ishihara,N., Yokota,S., and Mihara,K. (2003). Two mitofusin proteins, mammalian homologues of FZO, with distinct functions are both required for mitochondrial fusion. J. Biochem. (Tokyo) *134*, 333-344.

Fannjiang,Y., Cheng,W.C., Lee,S.J., Qi,B., Pevsner,J., McCaffery,J.M., Hill,R.B., Basanez,G., and Hardwick,J.M. (2004). Mitochondrial fission proteins regulate programmed cell death in yeast. Genes Dev. *18*, 2785-2797.

Ferguson-Miller,S., Brautigan,D.L., and Margoliash,E. (1976). Correlation of the kinetics of electron transfer activity of various eukaryotic cytochromes c with binding to mitochondrial cytochrome c oxidase. J. Biol. Chem. *251*, 1104-1115.

Ferre,M., Amati-Bonneau,P., Tourmen,Y., Malthiery,Y., and Reynier,P. (2005). eOPA1: an online database for OPA1 mutations. Hum. Mutat. *25*, 423-428.

Frank,S., Gaume,B., Bergmann-Leitner,E.S., Leitner,W.W., Robert,E.G., Catez,F., Smith,C.L., and Youle,R.J. (2001). The role of dynamin-related protein 1, a mediator of mitochondrial fission, in apoptosis. Dev. Cell *1*, 515-525.

Frey,T.G. and Mannella,C.A. (2000). The internal structure of mitochondria. Trends. Biochem. Sci. *25*, 319-324.

Frezza,C., Cipolat,S., Martins,d.B., Micaroni,M., Beznoussenko,G.V., Rudka,T., Bartoli,D., Polishuck,R.S., Danial,N.N., De Strooper,B., and Scorrano,L. (2006). OPA1 Controls Apoptotic Cristae Remodeling Independently from Mitochondrial Fusion. Cell *126*, 177-189.

Fritz,S., Weinbach,N., and Westermann,B. (2003). Mdm30 is an F-box protein required for maintenance of fusion-competent mitochondria in yeast. Mol Biol Cell *14*.

Gallop,J.L., Butler,P.J., and McMahon,H.T. (2005). Endophilin and CtBP/BARS are not acyl transferases in endocytosis or Golgi fission. Nature. *438*, 675-678.

Gallop,J.L., Jao,C.C., Kent,H.M., Butler,P.J., Evans,P.R., Langen,R., and McMahon,H.T. (2006). Mechanism of endophilin N-BAR domain-mediated membrane curvature. EMBO. J. *25*, 2898-2910.

Gallop,J.L. and McMahon,H.T. (2005). BAR domains and membrane curvature: bringing your curves to the BAR. Biochem. Soc. Symp. 223-231.

Garcia-Saez,A.J., Mingarro,I., Perez-Paya,E., and Salgado,J. (2004). Membrane-insertion fragments of Bcl-xL, Bax, and Bid. Biochemistry *43*, 10930-10943.

Germain,M., Mathai,J.P., McBride,H.M., and Shore,G.C. (2005). Endoplasmic reticulum BIK initiates DRP1-regulated remodelling of mitochondrial cristae during apoptosis. EMBO J. *24*, 1546-1556.

Gieffers,C., Korioth,F., Heimann,P., Ungermann,C., and Frey,J. (1997). Mitofilin is a transmembrane protein of the inner mitochondrial membrane expressed as two isoforms. Exp. Cell Res. *232*, 395-399.

Goldstein,J.C., Waterhouse,N.J., Juin,P., Evan,G.I., and Green,D.R. (2000). The coordinate release of cytochrome c during apoptosis is rapid, complete and kinetically invariant. Nat. Cell Biol. *2*, 156-162.

Gonzalvez,F., Bessoule,J.J., Rocchiccioli,F., Manon,S., and Petit,P.X. (2005). Role of cardiolipin on tBid and tBid/Bax synergistic effects on yeast mitochondria. Cell. Death. Differ. *12*, 659-667.

Gottlieb,E., Armour,S.M., Harris,M.H., and Thompson,C.B. (2003). Mitochondrial membrane potential regulates matrix configuration and cytochrome c release during apoptosis. Cell. Death. Differ. *10*, 709-717.

Grijalba,M.T., Andrade,P.B., Meinicke,A.R., Castilho,R.F., Vercesi,A.E., and Schreier,S. (1998). Inhibition of membrane lipid peroxidation by a radical scavenging mechanism: a novel function for hydroxyl-containing ionophores. Free. Radic. Res. *28*, 301-318.

Griparic,L., Kanazawa,T., and van der Bliek,A.M. (2007). Regulation of the mitochondrial dynamin-like protein Opa1 by proteolytic cleavage. J. Cell Biol *178*, 757-764.

Griparic,L., van der Wel,N.N., Orozco,I.J., Peters,P.J., and van der Bliek,A.M. (2004). Loss of the intermembrane space protein Mgm1/OPA1 induces swelling and localized constrictions along the lengths of mitochondria. J. Biol. Chem. *279*, 18792-18798.

Gross,A., Yin,X.M., Wang,K., Wei,M.C., Jockel,J., Milliman,C., Erdjument,B.H., Tempst,P., and Korsmeyer,S.J. (1999). Caspase cleaved BID targets mitochondria and is required for cytochrome c release, while BCL-XL prevents this release but not tumor necrosis factor-R1/Fas death. J. Biol. Chem. *274*, 1156-1163.

Guillery,O., Malka,F., Landes,T., Guillou,E., Blackstone,C., Lombes,A., Belenguer,P., Arnoult,D., and Rojo,M. (2007). Metalloprotease-mediated OPA1 processing is modulated by the mitochondrial membrane potential. Biol. Cell.

Hackenbrock,C.R. (1966). Ultrastructural bases for metabolically linked mechanical activity in mitochondria. I. Reversible ultrastructural changes with change in metabolic steady state in isolated liver mitochondria. J. Cell Biol. *30*, 269-297.

Hajek,P., Chomyn,A., and Attardi,G. (2007). Identification of a novel mitochondrial complex containing mitofusin 2 and stomatin-like protein 2. J. Biol. Chem. *282*, 5670-5681.

Hajek,P., Villani,G., and Attardi,G. (2001). Rate-limiting step preceding cytochrome c release in cells primed for Fas-mediated apoptosis revealed by analysis of cellular mosaicism of respiratory changes. J. Biol. Chem. *276*, 606-615.

Hales,K.G. and Fuller,M.T. (1997). Developmentally regulated mitochondrial fusion mediated by a conserved, novel, predicted GTPase. Cell *90*, 121-129.

Harder,Z., Zunino,R., and McBride,H. (2004). Sumo1 conjugates mitochondrial substrates and participates in mitochondrial fission. Curr. Biol. *14*, 340-345.

Hengartner,M.O. (2000). The biochemistry of apoptosis. Nature *407*, 770-776.

Herlan,M., Vogel,F., Bornhovd,C., Neupert,W., and Reichert,A.S. (2003). Processing of Mgm1 by the rhomboid-type protease Pcp1 is required for maintenance of mitochondrial morphology and of mitochondrial DNA. J. Biol. Chem. *278*, 27781-27788.

Hermann,G.J., Thatcher,J.W., Mills,J.P., Hales,K.G., Fuller,M.T., Nunnari,J., and Shaw,J.M. (1998). Mitochondrial fusion in yeast requires the transmembrane GTPase Fzo1p. J. Cell Biol. *143*, 359-373.

Hinshaw,J.E. (1999). Dynamin spirals. Curr. Opin. Struct. Biol *9*, 260-267.

Hitchcock,A.L., Auld,K., Gygi,S.P., and Silver,P.A. (2003). A subset of membrane-associated proteins is ubiquitinated in response to mutations in the endoplasmic reticulum degradation machinery. Proc. Natl. Acad. Sci. U. S. A. *100*, 12735-12740.

Hockenbery,D., Nunez,G., Milliman,C., Schreiber,R.D., and Korsmeyer,S.J. (1990). Bcl-2 is an inner mitochondrial membrane protein that blocks programmed cell death. Nature *348*, 334-336.

Hoffmann,B., Stockl,A., Schlame,M., Beyer,K., and Klingenberg,M. (1994). The reconstituted ADP/ATP carrier activity has an absolute requirement for cardiolipin as shown in cysteine mutants. J. Biol. Chem. *269*, 1940-1944.

Hudson,G., mati-Bonneau,P., Blakely,E.L., Stewart,J.D., He,L., Schaefer,A.M., Griffiths,P.G., Ahlqvist,K., Suomalainen,A., Reynier,P., McFarland,R., Turnbull,D.M., Chinnery,P.F., and Taylor,R.W. (2007). Mutation of OPA1 causes dominant optic atrophy with external ophthalmoplegia, ataxia, deafness and multiple mitochondrial DNA deletions: a novel disorder of mtDNA maintenance. Brain.

Huser,J., Rechenmacher,C.E., and Blatter,L.A. (1998). Imaging the permeability pore transition in single mitochondria. Biophys. J. *74*, 2129-2137.

Ishihara,N., Eura,Y., and Mihara,K. (2004). Mitofusin 1 and 2 play distinct roles in mitochondrial fusion reactions via GTPase activity. J. Cell Sci. *117*, 6535-6546.

Ishihara,N., Fujita,Y., Oka,T., and Mihara,K. (2006). Regulation of mitochondrial morphology through proteolytic cleavage of OPA1. EMBO J. *25*, 2966-2977.

Jacobs,E.E. and Sanadi,D.R. (1960). Reversible Removal of Cytochrome *c* from Mitochondria. J. Biol. Chem. *235*, 531-534.

Jagasia,R., Grote,P., Westermann,B., and Conradt,B. (2005). DRP-1-mediated mitochondrial fragmentation during EGL-1-induced cell death in C. elegans. Nature *433*, 754-760.

James,D.I., Parone,P.A., Mattenberger,Y., and Martinou,J.C. (2003). hFis1, a novel component of the mammalian mitochondrial fission machinery. J. Biol. Chem. *278*, 36373-36379.

John,G.B., Shang,Y., Li,L., Renken,C., Mannella,C.A., Selker,J.M., Rangell,L., Bennett,M.J., and Zha,J. (2005). The mitochondrial inner membrane protein mitofilin controls cristae morphology. Mol. Biol. Cell *16*, 1543-1554.

Jones,B.A. and Fangman,W.L. (1992). Mitochondrial DNA maintenance in yeast requires a protein containing a region related to the GTP-binding domain of dynamin. Genes. Dev. *6*, 380-389.

Ju,W.K., Misaka,T., Kushnareva,Y., Nakagomi,S., Agarwal,N., Kubo,Y., Lipton,S.A., and Bossy-Wetzel,E. (2005). OPA1 expression in the normal rat retina and optic nerve. J. Comp. Neurol. *488*, 1-10.

Jurgensmeier,J.M., Xie,Z., Deveraux,Q., Ellerby,L., Bredesen,D., and Reed,J.C. (1998). Bax directly induces release of cytochrome c from isolated mitochondria. Proc. Natl. Acad. Sci. U. S. A *95*, 4997-5002.

Kamei,S., Chen-Kuo-Chang,M., Cazevieille,C., Lenaers,G., Olichon,A., Belenguer,P., Roussignol,G., Renard,N., Eybalin,M., Michelin,A., Delettre,C., Brabet,P., and Hamel,C.P. (2005). Expression of the Opa1 mitochondrial protein in retinal ganglion cells: its downregulation causes aggregation of the mitochondrial network. Invest. Ophthalmol. Vis. Sci. *46*, 4288-4294.

Karbowski,M., Arnoult,D., Chen,H., Chan,D.C., Smith,C.L., and Youle,R.J. (2004a). Quantitation of mitochondrial dynamics by photolabeling of individual organelles shows that mitochondrial fusion is blocked during the Bax activation phase of apoptosis. J. Cell Biol. *164*, 493-499.

Karbowski,M., Jeong,S.Y., and Youle,R.J. (2004b). Endophilin B1 is required for the maintenance of mitochondrial morphology. J. Cell Biol. *166*, 1027-1039.

Karbowski,M., Lee,Y.J., Gaume,B., Jeong,S.Y., Frank,S., Nechushtan,A., Santel,A., Fuller,M., Smith,C.L., and Youle,R.J. (2002). Spatial and temporal association of Bax with mitochondrial fission sites, Drp1, and Mfn2 during apoptosis. J. Cell Biol. *159*, 931-938.

Karbowski,M., Norris,K.L., Cleland,M.M., Jeong,S.Y., and Youle,R.J. (2006). Role of Bax and Bak in mitochondrial morphogenesis. Nature *443*, 658-662.

Kay,B.K., Kasanov,J., Knight,S., and Kurakin,A. (2000). Convergent evolution with combinatorial peptides. FEBS Lett *480*.

Kerr,J.F., Cooksley,W.G., Searle,J., Halliday,J.W., Halliday,W.J., Holder,L., Roberts,I., Burnett,W., and Powell,L.W. (1979). The nature of piecemeal necrosis in chronic active hepatitis. Lancet *2*, 827-828.

Kerr,J.F., Wyllie,A.H., and Currie,A.R. (1972). Apoptosis: a basic biological phenomenon with wide-ranging implications in tissue kinetics. Br. J. Cancer. *26*, 239-257.

Kim,M.R., Jeong,E.G., Lee,J.W., and Lee,S.H. (2006). Absence of the BH3 domain mutation of proapoptotic Bcl-2 family gene BAD in serous and mucinous tumors of ovary. Gynecol. Oncol. *102*, 412-413.

Kim,P.K., Annis,M.G., Dlugosz,P.J., Leber,B., and Andrews,D.W. (2004). During apoptosis bcl-2 changes membrane topology at both the endoplasmic reticulum and mitochondria. Mol. Cell *14*, 523-529.

Kinnunen,P.K., Koiv,A., Lehtonen,J.Y., Rytomaa,M., and Mustonen,P. (1994). Lipid dynamics and peripheral interactions of proteins with membrane surfaces. Chem. Phys. Lipids. *73*, 181-207.

Kjer,P. (1959). Infantile optic atrophy with dominant mode of inheritance: a clinical and genetic study of 19 Danish families. Acta. Ophthalmol. Suppl. *164*, 1-147.

Klingenberg,M. (1973). The adenine nucleotide carrier in the mitochondrial membrane. Boll. Soc. Ital. Biol. Sper. *49*, 2pp.

Klingenberg,M. (1976). The state of ADP or ATP fixed to the mitochondria by bongkrekate. Eur. J. Biochem. *65*, 601-605.

Klingenberg,M. (1992). Structure-function of the ADP/ATP carrier. Biochem Soc Trans *20*.

Kluck,R.M., Esposti,M.D., Perkins,G., Renken,C., Kuwana,T., Bossy-Wetzel,E., Goldberg,M., Allen,T., Barber,M.J., Green,D.R., and Newmeyer,D.D. (1999). The pro-apoptotic proteins, Bid

and Bax, cause a limited permeabilization of the mitochondrial outer membrane that is enhanced by cytosol. J. Cell Biol. *147*, 809-822.

Koshiba,T., Detmer,S.A., Kaiser,J.T., Chen,H., McCaffery,J.M., and Chan,D.C. (2004). Structural basis of mitochondrial tethering by mitofusin complexes. Science *305*, 858-862.

Kuwana,T., Mackey,M.R., Perkins,G., Ellisman,M.H., Latterich,M., Schneiter,R., Green,D.R., and Newmeyer,D.D. (2002). Bid, Bax, and lipids cooperate to form supramolecular openings in the outer mitochondrial membrane. Cell *111*, 331-342.

Labrousse,A.M., Zappaterra,M.D., Rube,D.A., and van der Bliek,A.M. (1999). C. elegans dynamin-related protein DRP-1 controls severing of the mitochondrial outer membrane. Mol. Cell *4*, 815-826.

Lee,Y.J., Jeong,S.Y., Karbowski,M., Smith,C.L., and Youle,R.J. (2004). Roles of the mammalian mitochondrial fission and fusion mediators Fis1, Drp1, and Opa1 in apoptosis. Mol. Biol. Cell *15*, 5001-5011.

Legros,F., Lombes,A., Frachon,P., and Rojo,M. (2002). Mitochondrial fusion in human cells is efficient, requires the inner membrane potential, and is mediated by mitofusins. Mol Biol Cell *13*, 4343-4354.

Letai,A., Bassik,M.C., Walensky,L.D., Sorcinelli,M.D., Weiler,S., and Korsmeyer,S.J. (2002). Distinct BH3 domains either sensitize or activate mitochondrial apoptosis, serving as prototype cancer therapeutics. Cancer Cell *2*, 183-192.

Li,L.Y., Luo,X., and Wang,X. (2001). Endonuclease G is an apoptotic DNase when released from mitochondria. Nature *412*, 95-99.

Lindsten,T., Ross,A.J., King,A., Zong,W.X., Rathmell,J.C., Shiels,H.A., Ulrich,E., Waymire,K.G., Mahar,P., Frauwirth,K., Chen,Y., Wei,M., Eng,V.M., Adelman,D.M., Simon,M.C., Ma,A., Golden,J.A., Evan,G., Korsmeyer,S.J., MacGregor,G.R., and Thompson,C.B. (2000). The combined functions of proapoptotic Bcl-2 family members bak and bax are essential for normal development of multiple tissues. Mol. Cell *6*, 1389-1399.

Liu,X., Kim,C.N., Yang,J., Jemmerson,R., and Wang,X. (1996). Induction of apoptotic program in cell-free extracts: requirement for dATP and cytochrome c. Cell *86*, 147-157.

Lockshin,R.A. and Williams,C.M. (1965). Programmed cell death. V. Cytolytic enzymes in relation to the breakdown of the intersegmental muscles of silkmoths. J. Insect Physiol *11*, 831-844.

Lodi,R., Tonon,C., Valentino,M.L., Iotti,S., Clementi,V., Malucelli,E., Barboni,P., Longanesi,L., Schimpf,S., Wissinger,B., Baruzzi,A., Barbiroli,B., and Carelli,V. (2004). Deficit of in vivo mitochondrial ATP production in OPA1-related dominant optic atrophy. Ann. Neurol. *56*, 719-723.

Luo,X., Budihardjo,I., Zou,H., Slaughter,C., and Wang,X. (1998). Bid, a Bcl2 interacting protein, mediates cytochrome c release from mitochondria in response to activation of cell surface death receptors. Cell *94*, 481-490.

Mannella,C.A., Marko,M., Penczek,P., Barnard,D., and Frank,J. (1994). The internal compartmentation of rat-liver mitochondria: tomographic study using the high-voltage transmission electron microscope. Microsc. Res. Tech. *27*, 278-283.

Mannella,C.A., Pfeiffer,D.R., Bradshaw,P.C., Moraru,I.I., Slepchenko,B., Loew,L.M., Hsieh,C.E., Buttle,K., and Marko,M. (2001). Topology of the mitochondrial inner membrane: dynamics and bioenergetic implications. IUBMB. Life *52*, 93-100.

Marchbank,N.J., Craig,J.E., Leek,J.P., Toohey,M., Churchill,A.J., Markham,A.F., Mackey,D.A., Toomes,C., and Inglehearn,C.F. (2002). Deletion of the OPA1 gene in a dominant optic atrophy family: evidence that haploinsufficiency is the cause of disease. J. Med. Genet. *39*, e47.

Martins,L.M., Morrison,A., Klupsch,K., Fedele,V., Moisoi,N., Teismann,P., Abuin,A., Grau,E., Geppert,M., Livi,G.P., Creasy,C.L., Martin,A., Hargreaves,I., Heales,S.J., Okada,H., Brandner,S., Schulz,J.B., Mak,T., and Downward,J. (2004). Neuroprotective role of the Reaper-related serine protease HtrA2/Omi revealed by targeted deletion in mice. Mol. Cell Biol. *24*, 9848-9862.

Marzo,I., Brenner,C., Zamzami,N., Jurgensmeier,J.M., Susin,S.A., Vieira,H.L., Prevost,M.C., Xie,Z., Matsuyama,S., Reed,J.C., and Kroemer,G. (1998). Bax and adenine nucleotide translocator cooperate in the mitochondrial control of apoptosis. Science *281*, 2027-2031.

mati-Bonneau,P., Valentino,M.L., Reynier,P., Gallardo,M.E., Bornstein,B., Boissiere,A., Campos,Y., Rivera,H., de la Aleja,J.G., Carroccia,R., Iommarini,L., Labauge,P., Figarella-Branger,D., Marcorelles,P., Furby,A., Beauvais,K., Letournel,F., Liguori,R., La,M.C., Montagna,P., Liguori,M., Zanna,C., Rugolo,M., Cossarizza,A., Wissinger,B., Verny,C., Schwarzenbacher,R., Martin,M.A., Arenas,J.I., Ayuso,C., Garesse,R., Lenaers,G., Bonneau,D., and Carelli,V. (2007). OPA1 mutations induce mitochondrial DNA instability and optic atrophy 'plus' phenotypes. Brain.

Mattenberger,Y., James,D.I., and Martinou,J.C. (2003). Fusion of mitochondria in mammalian cells is dependent on the mitochondrial inner membrane potential and independent of microtubules or actin. FEBS Lett. *538*, 53-59.

McQuibban,G.A., Saurya,S., and Freeman,M. (2003). Mitochondrial membrane remodelling regulated by a conserved rhomboid protease. Nature *423*, 537-541.

Meeusen,S., DeVay,R., Block,J., Cassidy-Stone,A., Wayson,S., McCaffery,J.M., and Nunnari,J. (2006). Mitochondrial inner-membrane fusion and crista maintenance requires the dynamin-related GTPase Mgm1. Cell *127*.

Meeusen,S., McCaffery,J.M., and Nunnari,J. (2004). Mitochondrial fusion intermediates revealed in vitro. Science *305*, 1747-1752.

Minauro-Sanmiguel,F., Wilkens,S., and Garcia,J.J. (2005). Structure of dimeric mitochondrial ATP synthase: novel F0 bridging features and the structural basis of mitochondrial cristae biogenesis. Proc. Natl. Acad. Sci. U. S. A. *102*, 12356-12358.

Misaka,T., Miyashita,T., and Kubo,Y. (2002). Primary structure of a dynamin-related mouse mitochondrial GTPase and its distribution in brain, subcellular localization, and effect on mitochondrial morphology. J. Biol. Chem. *277*, 15834-15842.

Mitchell,P. and Moyle,J. (1965). Stoichiometry of proton translocation through the respiratory chain and adenosine triphosphatase systems of rat liver mitochondria. Nature *208*, 147-151.

Mootha,V.K., Wei,M.C., Buttle,K.F., Scorrano,L., Panoutsakopoulou,V., Mannella,C.A., and Korsmeyer,S.J. (2001). A reversible component of mitochondrial respiratory dysfunction in apoptosis can be rescued by exogenous cytochrome c. EMBO J. *20*, 661-671.

Moraru, I. I. Role of cristae morphology in regulating mitochondrial adenine nucleotide and H^+ dynamics. Biophys.J. [78], 194A. 2000.
Ref Type: Abstract

Muchmore,S.W., Sattler,M., Liang,H., Meadows,R.P., Harlan,J.E., Yoon,H.S., Nettesheim,D., Chang,B.S., Thompson,C.B., Wong,S.L., Ng,S.L., and Fesik,S.W. (1996). X-ray and NMR structure of human Bcl-xL, an inhibitor of programmed cell death. Nature *381*, 335-341.

Myung,J.K., Gulesserian,T., Fountoulakis,M., and Lubec,G. (2003). Deranged hypothetical proteins Rik protein, Nit protein 2 and mitochondrial inner membrane protein, Mitofilin, in fetal Down syndrome brain. Cell. Mol. Biol. (Noisy. -le. -grand.) *49*, 739-746.

Nakamura,N., Kimura,Y., Tokuda,M., Honda,S., and Hirose,S. (2006). MARCH-V is a novel mitofusin 2- and Drp1-binding protein able to change mitochondrial morphology. EMBO Rep. *7*, 1019-1022.

Narita,M., Shimizu,S., Ito,T., Chittenden,T., Lutz,R.J., Matsuda,H., and Tsujimoto,Y. (1998). Bax interacts with the permeability transition pore to induce permeability transition and cytochrome c release in isolated mitochondria. Proc. Natl. Acad. Sci. U. S. A *95*, 14681-14686.

Neuspiel,M., Zunino,R., Gangaraju,S., Rippstein,P., and McBride,H.M. (2005). Activated Mfn2 signals mitochondrial fusion, interferes with Bax activation and reduces susceptibility to radical induced depolarization. J. Biol. Chem. *280*, 25060-25070.

Neutzner,A. and Youle,R.J. (2005). Instability of the mitofusin Fzo1 regulates mitochondrial morphology during the mating response of the yeast Saccharomyces cerevisiae. J Biol Chem *280*.

Oakley,M.G. and Hollenbeck,J.J. (2001). The design of antiparallel coiled coils. Curr. Opin. Struct. Biol. *11*, 450-457.

Olichon,A., Baricault,L., Gas,N., Guillou,E., Valette,A., Belenguer,P., and Lenaers,G. (2003). Loss of OPA1 perturbates the mitochondrial inner membrane structure and integrity, leading to cytochrome c release and apoptosis. J. Biol. Chem. *278*, 7743-7746.

Olichon,A., Emorine,L.J., Descoins,E., Pelloquin,L., Brichese,L., Gas,N., Guillou,E., Delettre,C., Valette,A., Hamel,C.P., Ducommun,B., Lenaers,G., and Belenguer,P. (2002). The human dynamin-related protein OPA1 is anchored to the mitochondrial inner membrane facing the inter-membrane space. FEBS Lett. *523*, 171-176.

Ott,M., Robertson,J.D., Gogvadze,V., Zhivotovsky,B., and Orrenius,S. (2002). Cytochrome c release from mitochondria proceeds by a two-step process. Proc. Natl. Acad. Sci. U. S. A *99*, 1259-1263.

Pacher,P. and Hajnoczky,G. (2001). Propagation of the apoptotic signal by mitochondrial waves. EMBO J. *20*, 4107-4121.

Palade,G.E. (1952). The fine structure of mitochondria. Anat. Rec. *114*, 427-451.

Parone,P.A., James,D.I., Da,C.S., Mattenberger,Y., Donze,O., Barja,F., and Martinou,J.C. (2006). Inhibiting the mitochondrial fission machinery does not prevent Bax/Bak-dependent apoptosis. Mol. Cell. Biol. *26*, 7397-7408.

Pastorino,J.G., Chen,S.T., Tafani,M., Snyder,J.W., and Farber,J.L. (1998). The overexpression of Bax produces cell death upon induction of the mitochondrial permeability transition. J. Biol. Chem. *273*, 7770-7775.

Paumard,P., Vaillier,J., Coulary,B., Schaeffer,J., Soubannier,V., Mueller,D.M., Brethes,D., di Rago,J.P., and Velours,J. (2002). The ATP synthase is involved in generating mitochondrial cristae morphology. EMBO J. *21*, 221-230.

Pavlov,E.V., Priault,M., Pietkiewicz,D., Cheng,E.H., Antonsson,B., Manon,S., Korsmeyer,S.J., Mannella,C.A., and Kinnally,K.W. (2001). A novel, high conductance channel of mitochondria linked to apoptosis in mammalian cells and Bax expression in yeast. J. Cell Biol. *155*, 725-731.

Pelloquin,L., Belenguer,P., Menon,Y., Gas,N., and Ducommun,B. (1999). Fission yeast Msp1 is a mitochondrial dynamin-related protein. J. Cell Sci. *112*.

Perotti,M.E., Anderson,W.A., and Swift,H. (1983). Quantitative cytochemistry of the diaminobenzidine cytochrome oxidase reaction product in mitochondria of cardiac muscle and pancreas. J. Histochem. Cytochem. *31*, 351-365.

Pesch,U.E., Fries,J.E., Bette,S., Kalbacher,H., Wissinger,B., Alexander,C., and Kohler,K. (2004). OPA1, the disease gene for autosomal dominant optic atrophy, is specifically expressed in ganglion cells and intrinsic neurons of the retina. Invest. Ophthalmol. Vis. Sci. *45*, 4217-4225.

Pesch,U.E., Leo-Kottler,B., Mayer,S., Jurklies,B., Kellner,U., Apfelstedt-Sylla,E., Zrenner,E., Alexander,C., and Wissinger,B. (2001). OPA1 mutations in patients with autosomal dominant optic atrophy and evidence for semi-dominant inheritance. Hum. Mol Genet. *10*, 1359-1368.

Petronilli,V., Miotto,G., Canton,M., Colonna,R., Bernardi,P., and Di Lisa,F. (1999). Transient and long-lasting openings of the mitochondrial permeability transition pore can be monitored directly in intact cells by changes of mitochondrial calcein fluorescence. Biophys. J. *76*, 725-734.

Petrosillo,G., Ruggiero,F.M., and Paradies,G. (2003). Role of reactive oxygen species and cardiolipin in the release of cytochrome c from mitochondria. FASEB. J. *17*, 2202-2208.

Petrosillo,G., Ruggiero,F.M., Pistolese,M., and Paradies,G. (2004). Ca2+-induced reactive oxygen species production promotes cytochrome c release from rat liver mitochondria via mitochondrial permeability transition (MPT)-dependent and MPT-independent mechanisms: role of cardiolipin. J. Biol. Chem. *279*, 53103-53108.

Pfohler,C., Preuss,K.D., Tilgen,W., Stark,A., Regitz,E., Fadle,N., and Pfreundschuh,M. (2007). Mitofilin and titin as target antigens in melanoma-associated retinopathy. Int. J. Cancer. *120*, 788-795.

Praefcke,G.J. and McMahon,H.T. (2004). The dynamin superfamily: universal membrane tubulation and fission molecules? Nat Rev Mol Cell Biol *5*, 133-147.

Rak,M., Tetaud,E., Godard,F., Sagot,I., Salin,B., Duvezin-Caubet,S., Slonimski,P.P., Rytka,J., and di Rago,J.P. (2007). Yeast cells lacking the mitochondrial gene encoding the ATP synthase subunit 6 exhibit a selective loss of complex IV and unusual mitochondrial morphology. J. Biol. Chem. *282*, 10853-10864.

Rojo,M., Legros,F., Chateau,D., and Lombes,A. (2002). Membrane topology and mitochondrial targeting of mitofusins, ubiquitous mammalian homologs of the transmembrane GTPase Fzo. J. Cell Sci. *115*, 1663-1674.

Roucou,X., Montessuit,S., Antonsson,B., and Martinou,J.C. (2002). Bax oligomerization in mitochondrial membranes requires tBid (caspase-8-cleaved Bid) and a mitochondrial protein. Biochem. J. *368*, 915-921.

Rytomaa,M. and Kinnunen,P.K. (1995). Reversibility of the binding of cytochrome c to liposomes. Implications for lipid-protein interactions. J. Biol. Chem. *270*, 3197-3202.

Saito,M., Korsmeyer,S.J., and Schlesinger,P.H. (2000). BAX-dependent transport of cytochrome c reconstituted in pure liposomes. Nat. Cell Biol. *2*, 553-555.

Santel,A., Frank,S., Gaume,B., Herrler,M., Youle,R.J., and Fuller,M.T. (2003). Mitofusin-1 protein is a generally expressed mediator of mitochondrial fusion in mammalian cells. J. Cell Sci. *116*, 2763-2774.

Santel,A. and Fuller,M.T. (2001). Control of mitochondrial morphology by a human mitofusin. J. Cell Sci. *114*, 867-874.

Satoh,M., Hamamoto,T., Seo,N., Kagawa,Y., and Endo,H. (2003). Differential sublocalization of the dynamin-related protein OPA1 isoforms in mitochondria. Biochem. Biophys. Res. Commun. *300*, 482-493.

Schatz,G. (2007). The magic garden. Annu. Rev. Biochem. *76*, 673-678.

Schlame,M., Brody,S., and Hostetler,K.Y. (1993). Mitochondrial cardiolipin in diverse eukaryotes. Comparison of biosynthetic reactions and molecular acyl species. Eur. J. Biochem. *212*, 727-735.

Schmidt,A., Wolde,M., Thiele,C., Fest,W., Kratzin,H., Podtelejnikov,A.V., Witke,W., Huttner,W.B., and Soling,H.D. (1999). Endophilin I mediates synaptic vesicle formation by transfer of arachidonate to lysophosphatidic acid. Nature *401*, 133-141.

Scorrano,L., Ashiya,M., Buttle,K., Weiler,S., Oakes,S.A., Mannella,C.A., and Korsmeyer,S.J. (2002). A Distinct Pathway Remodels Mitochondrial Cristae and Mobilizes Cytochrome c during Apoptosis. Dev. Cell *2*, 55-67.

Scorrano,L. and Korsmeyer,S.J. (2003). Mechanisms of cytochrome c release by proapoptotic BCL-2 family members. Biochemical and Biophysical Research Communications *304*, 437-444.

Sesaki,H., Southard,S.M., Yaffe,M.P., and Jensen,R.E. (2003). Mgm1p, a dynamin-related GTPase, is essential for fusion of the mitochondrial outer membrane. Mol. Biol. Cell *14*, 2342-2356.

Shidoji,Y., Komura,S., Ohishi,N., and Yagi,K. (2002). Interaction between cytochrome c and oxidized mitochondrial lipids. Subcell. Biochem. *36*, 19-37.

Shimizu,S., Narita,M., and Tsujimoto,Y. (1999). Bcl-2 family proteins regulate the release of apoptogenic cytochrome c by the mitochondrial channel VDAC. Nature *399*, 483-487.

Smirnova,E., Griparic,L., Shurland,D.L., and van der Bliek,A.M. (2001). Dynamin-related protein Drp1 is required for mitochondrial division in mammalian cells. Mol. Biol. Cell *12*, 2245-2256.

Song,Z., Chen,H., Fiket,M., Alexander,C., and Chan,D.C. (2007). OPA1 processing controls mitochondrial fusion and is regulated by mRNA splicing, membrane potential, and Yme1L. J. Cell Biol *178*, 749-755.

Stojanovski,D., Koutsopoulos,O.S., Okamoto,K., and Ryan,M.T. (2004). Levels of human Fis1 at the mitochondrial outer membrane regulate mitochondrial morphology. J. Cell Sci. *117*, 1201-1210.

Sugioka,R., Shimizu,S., and Tsujimoto,Y. (2004). Fzo1, a protein involved in mitochondrial fusion, inhibits apoptosis. J. Biol. Chem. *279*, 52726-52734.

Sun,M.G., Williams,J., Munoz-Pinedo,C., Perkins,G.A., Brown,J.M., Ellisman,M.H., Green,D.R., and Frey,T.G. (2007). Correlated three-dimensional light and electron microscopy reveals transformation of mitochondria during apoptosis. Nat. Cell Biol. *9*, 1057-1065.

Susin,S.A., Lorenzo,H.K., Zamzami,N., Marzo,I., Snow,B.E., Brothers,G.M., Mangion,J., Jacotot,E., Costantini,P., Loeffler,M., Larochette,N., Goodlett,D.R., Aebersold,R., Siderovski,D.P., Penninger,J.M., and Kroemer,G. (1999). Molecular characterization of mitochondrial apoptosis-inducing factor. Nature *397*, 441-446.

Suzuki,M., Jeong,S.Y., Karbowski,M., Youle,R.J., and Tjandra,N. (2003). The solution structure of human mitochondria fission protein Fis1 reveals a novel TPR-like helix bundle. J. Mol. Biol. *334*, 445-458.

Suzuki,M., Youle,R.J., and Tjandra,N. (2000). Structure of Bax: coregulation of dimer formation and intracellular localization. Cell *103*, 645-654.

Szabadkai,G., Simoni,A.M., Chami,M., Wieckowski,M.R., Youle,R.J., and Rizzuto,R. (2004). Drp-1-dependent division of the mitochondrial network blocks intraorganellar Ca^{2+} waves and protects against Ca^{2+}-mediated apoptosis. Mol Cell *16*, 59-68.

Taguchi,N., Ishihara,N., Jofuku,A., Oka,T., and Mihara,K. (2007). Mitotic phosphorylation of dynamin-related GTPase Drp1 participates in mitochondrial fission. J. Biol. Chem. *282*, 11521-11529.

Thornberry,N.A. and Lazebnik,Y. (1998). Caspases: enemies within. Science *281*, 1312-1316.

Tondera,D., Czauderna,F., Paulick,K., Schwarzer,R., Kaufmann,J., and Santel,A. (2005). The mitochondrial protein MTP18 contributes to mitochondrial fission in mammalian cells. J Cell Sci *118*.

Tondera,D., Santel,A., Schwarzer,R., Dames,S., Giese,K., Klippel,A., and Kaufmann,J. (2004). Knockdown of MTP18, a novel phosphatidylinositol 3-kinase-dependent protein, affects mitochondrial morphology and induces apoptosis. J Biol Chem *279*.

Tuominen,E.K., Wallace,C.J., and Kinnunen,P.K. (2002). Phospholipid-cytochrome c interaction: evidence for the extended lipid anchorage. J. Biol. Chem. *277*, 8822-8826.

van,L.G., van,G.M., Depuydt,B., Srinivasula,S.M., Rodriguez,I., Alnemri,E.S., Gevaert,K., Vandekerckhove,J., Declercq,W., and Vandenabeele,P. (2002). The serine protease Omi/HtrA2 is released from mitochondria during apoptosis. Omi interacts with caspase-inhibitor XIAP and induces enhanced caspase activity. Cell. Death. Differ. *9*, 20-26.

Verhagen,A.M., Ekert,P.G., Pakusch,M., Silke,J., Connolly,L.M., Reid,G.E., Moritz,R.L., Simpson,R.J., and Vaux,D.L. (2000). Identification of DIABLO, a mammalian protein that promotes apoptosis by binding to and antagonizing IAP proteins. Cell. *102*, 43-53.

Vogel,F., Bornhovd,C., Neupert,W., and Reichert,A.S. (2006). Dynamic subcompartmentalization of the mitochondrial inner membrane. J. Cell Biol. *175*, 237-247.

Votruba,M., Aijaz,S., and Moore,A.T. (2003). A review of primary hereditary optic neuropathies. J. Inherit. Metab. Dis. *26*, 209-227.

Walensky,L.D., Pitter,K., Morash,J., Oh,K.J., Barbuto,S., Fisher,J., Smith,E., Verdine,G.L., and Korsmeyer,S.J. (2006). A stapled BID BH3 helix directly binds and activates BAX. Mol. Cell. *24*, 199-210.

Wang,J., Rosconi,M.P., and London,E. (2006a). Topography of the hydrophilic helices of membrane-inserted diphtheria toxin T domain: TH1-TH3 as a hydrophilic tether. Biochemistry *45*, 8124-8134.

Wang,J., Rosconi,M.P., and London,E. (2006b). Topography of the hydrophilic helices of membrane-inserted diphtheria toxin T domain: TH1-TH3 as a hydrophilic tether. Biochemistry *45*, 8124-8134.

Wang,L., Dong,J., Cull,G., Fortune,B., and Cioffi,G.A. (2003). Varicosities of intraretinal ganglion cell axons in human and nonhuman primates. Invest. Ophthalmol. Vis. Sci. *44*, 2-9.

Wei,M.C., Lindsten,T., Mootha,V.K., Weiler,S., Gross,A., Ashiya,M., Thompson,C.B., and Korsmeyer,S.J. (2000). tBID, a membrane-targeted death ligand, oligomerizes BAK to release cytochrome c. Genes Dev. *14*, 2060-2071.

Wei,M.C., Zong,W.X., Cheng,E.H., Lindsten,T., Panoutsakopoulou,V., Ross,A.J., Roth,K.A., MacGregor,G.R., Thompson,C.B., and Korsmeyer,S.J. (2001). Proapoptotic BAX and BAK: a requisite gateway to mitochondrial dysfunction and death. Science *292*, 727-730.

Wells,R.C., Picton,L.K., Williams,S.C., Tan,F.J., and Hill,R.B. (2007). Direct binding of the dynamin-like GTPase, Dnm1, to mitochondrial dynamics protein Fis1 is negatively regulated by the Fis1 N-terminal arm. J. Biol. Chem. *282*, 33769-33775.

Wojtczak,L., Zaluska,H., Wroniszewska,A., and Wojtczak,A.B. (1972). Assay for the intactness of the outer membrane in isolated mitochondria. Acta. Biochim. Pol. *19*, 227-234.

Wong,E.D., Wagner,J.A., Gorsich,S.W., McCaffery,J.M., Shaw,J.M., and Nunnari,J. (2000). The dynamin-related GTPase, Mgm1p, is an intermembrane space protein required for maintenance of fusion competent mitochondria. J. Cell Biol. *151*, 341-352.

Wong,E.D., Wagner,J.A., Scott,S.V., Okreglak,V., Holewinske,T.J., Cassidy-Stone,A., and Nunnari,J. (2003). The intramitochondrial dynamin-related GTPase, Mgm1p, is a component of a protein complex that mediates mitochondrial fusion. J. Cell Biol. *160*, 303-311.

Xie,J., Marusich,M.F., Souda,P., Whitelegge,J., and Capaldi,R.A. (2007). The mitochondrial inner membrane protein mitofilin exists as a complex with SAM50, metaxins 1 and 2, coiled-coil-helix coiled-coil-helix domain-containing protein 3 and 6 and DnaJC11. FEBS. Lett. *581*, 3545-3549.

Yoon,Y., Krueger,E.W., Oswald,B.J., and McNiven,M.A. (2003). The mitochondrial protein hFis1 regulates mitochondrial fission in mammalian cells through an interaction with the dynamin-like protein DLP1. Mol. Cell Biol. *23*, 5409-5420.

Youle,R.J. and Karbowski,M. (2005). Mitochondrial fission in apoptosis. Nat Rev Mol Cell Biol *6*, 657-663.

Zha,J., Weiler,S., Oh,K.J., Wei,M.C., and Korsmeyer,S.J. (2000). Posttranslational N-myristoylation of BID as a molecular switch for targeting mitochondria and apoptosis. Science *290*, 1761-1765.

Zhang,M., Mileykovskaya,E., and Dowhan,W. (2002). Gluing the respiratory chain together. Cardiolipin is required for supercomplex formation in the inner mitochondrial membrane. J. Biol. Chem. *277*, 43553-43556.

Zhang,Y. and Chan,D.C. (2007). Structural basis for recruitment of mitochondrial fission complexes by Fis1. Proc. Natl. Acad. Sci. U. S. A. *104*, 18526-18530.

Zhivotovsky,B., Orrenius,S., Brustugun,O.T., and Doskeland,S.O. (1998). Injected cytochrome c induces apoptosis. Nature *391*, 449-450.

Zhu,P.P., Patterson,A., Stadler,J., Seeburg,D.P., Sheng,M., and Blackstone,C. (2004). Intra- and intermolecular domain interactions of the C-terminal GTPase effector domain of the multimeric dynamin-like GTPase Drp1. J. Biol. Chem. *279*, 35967-35974.

Zoratti,M. and Szabo,I. (1995). The mitochondrial permeability transition. Biochim. Biophys. Acta *1241*, 139-176.

Zou,H., Henzel,W.J., Liu,X., Lutschg,A., and Wang,X. (1997). Apaf-1, a human protein homologous to C. elegans CED-4, participates in cytochrome c-dependent activation of caspase-3. Cell *90*, 405-413.

Zunino,R., Schauss,A., Rippstein,P., ndrade-Navarro,M., and McBride,H.M. (2007). The SUMO protease SENP5 is required to maintain mitochondrial morphology and function. J. Cell. Sci. *120*, 1178-1188.